Invited Speaker

589 Dynamics at phase boundaries of active catalyst studied by multi-scale operando EM
Prof. Dr. Marc Willinger[1]
[1]Department of Chemistry, School of Natural Sciences, TU Munich, Garching bei München, Germany
527 PVA/PEG-based nanofibers with Au nanoparticles for treatment of chronic woundss
Dr. Elena Filova[1], Prof. Petr Slepicka[2], Dr. Nikola Slepickova Kasalkova[2], Prof. Vera Jencova[3], Ing. Maxim Lisnenko[3], Ing. Sarka Hauzerova[3], Prof. David Lukáš[3], Dr. Jana Nebesarova[4], Dr. Silvie Rimpelova[5,6], Mrs. Yu-Chieh Wu[1], Prof. Lucie Bacakova[1]
[1]Laboratory of Biomaterials and Tissue Engineering, Institute of Physiology of the Czech Academy of Sciences, Prague, Czech Republic, [2]Department of Solid State Engineering, University of Chemistry and Technology Prague, Prague, Czech Republic, [3]Faculty of Science, Humanities and Education, Department of Chemistry, Technical University of Liberec , Liberec, Czech Republic, [4]Laboratory of Electron Microscopy, Faculty of Science, Charles University, Prague, Czech Republic, [5]Department of Biochemistry and Microbiology, University of Chemistry and Technology Prague, Prague, Czech Republic, [6]Department of Tissue Engineering, Institute of Experimental Medicine of the Czech Academy of Sciences, Prague, Czech Republic

Oral Presentation

224 Effect of the Applied Chemical Potential on Strong Metal-Support Interaction in Ni-TiO2 Catalysts
Min Tang[1], Matteo Monai[2], Angela Melcherts[2], Kellie Jenkinson[1], Bert Weckhuysen[2], Sara Bals[1]
[1]EMAT and NANOlab Center of Excellence, University of Antwerp, Antwerp, Belgium, [2]Inorganic Chemistry and Catalysis group, Institute for Sustainable and Circular Chemistry and Debye Institute for Nanomaterials Science, Utrecht University, Utrecht, Netherlands
474 In-situ/ Opernado (S)TEM on Mass Selected Pt Clusters Deposited on CeO2 for CO Oxidation Catalysis
Ajai Raj Lakshmi Nilayam[1], Ramin Shadkam[1], Dr. Carina Maliakkal[1], Mohana Veerraju Kante[1], Prof. Horst Hahn[1], Dr. Di Wang[1], Prof. Christian Kübel[1,2]
[1]Institute of Nanotechnology, Karlsruhe Institute of Technology, Eggenstein-Leopoldshafen, Germany, [2]Karlsruhe Nano Micro Facility, Karlsruhe Institute of Technology, Eggenstein-Leopoldshafen, Germany
560 Solid state diffusion as the driving force in the selective oxidation of 2-propanol
Dr. Thomas Götsch[1], Daniel Cruz[1], Patrick Zeller[1,2], Anna Rabe[3,4], Malte Behrens[3,4], Robert Schlögl[1,5], Axel Knop-Gericke[1,5], Thomas Lunkenbein[1]
[1]Fritz-Haber-Institut der Max-Planck-Gesellschaft, Berlin, Germany, [2]Helmholtz-Zentrum Berlin für Materialien und Energie GmbH, Berlin, Germany, [3]Christian-Albrechts-Universität zu Kiel, Kiel, Germany, [4]Universität Duisburg-Essen, Essen, Germany, [5]Max Planck Institute for Chemical Energy Conversion, Mülheim a. d. Ruhr, Germany
684 Reactivity of High Entropy Nanoalloys under O2 and CO Oxidation reaction studied by in-situ TEM
Syrine Krouna[1], Jaysen Nelayah[1], Christian Ricolleau[1], Guillaume Wang[1], Hakim Amara[2], Damien Alloyeau[1]
[1]Université Paris Cité, Paris, France, [2]ONERA, Châtillon , France
704 In situ ESEM study of supported noble metal nanoparticles dynamics under reaction conditions
Birger Holtermann[1], Jan-Christian Schober[2], Dr. Philipp N. Plessow[3], Prof. Dr. Andreas Stierle[2], Prof. Dr. Yolita M. Eggeler[1]
[1]Karlsruhe Institute of Technology (KIT), Laboratory of Electron Microscopy (LEM), Karlsruhe, Germany, [2]Centre for X-ray and Nano Science, Deutsches Elektronen-Synchrotron (DESY), Hamburg, Germany, [3]Karlsruhe Institute of Technology (KIT), Institute of Catalysis Research and Technology (IKFT), Karlsruhe, Germany

1079 Operando TEM Studies of Re@Cu2O-SnO2 catalysts during CO2 reduction reaction with optimized liquid flow configuration
Ms Cecilia Irene Gho[1,2], Dr Katarzyna Bejtka[1,2], Dr Marco Fontana[1,2], Dr Maria José López Tendero[3], Dr. Alberto Lopera López[3], Dr Roger Miro Serra[4], Dr Miriam Díaz de los Bernardos[4], prof Simelys Hernández[2], Dr Hilmar Guzmán[2], Dr Stefan Merkens[5], prof Andrey Chuvilin[5,6], prof Candido Fabrizio Pirri[1,2], Dr Angelica Chiodoni[1]
[1] Center for Sustainable Future Technologies @Polito, Istituto Italiano di Tecnologia, Via Livorno 60, 10144 , Torino, Itlay, [2]Department of Applied Science and Technology, Politecnico di Torino, Corso Duca degli Abruzzi 24, 10129 , Torino, Italy, [3]Laurentia Technologies Avda. Benjamin Franklin, 12 (CEEI) Parque Tecnológico/ 46980, Paterna (Valencia), Spain, [4]Centro Tecnológico de Catalunya, Eurecat, Campus Sescelades de la URV. Edifici N5 – Marcellí Domingo s/n - 43007, Tarragona, Spain, [5]Electron Microscopy Laboratory, CIC nanoGUNE BRTA, Tolosa Hiribidea 76, Donostia, San Sebastian, Spain, [6]Ikerbasque, Basque Foundation for Science, 48013 , Bilbao, Spain
124 Visualizing alloying in Au-Pd core-shell nanoparticles using in situ gas-phase transmission electron microscopy
Marta Perxés Perich[1], Christopher R. O'Connor[2], Koen M. Draijer[1], Nienke L. Visser[1], Nongnuch Artrith[1], Christian Reece[2], Petra E. de Jongh[1], Jessi E. S. van der Hoeven[1]
[1]Materials Chemistry and Catalysis, Debye Institute for Nanomaterials Science, Utrecht University, Utrecht, The Netherlands, [2]Rowland Institute at Harvard, Harvard University, Cambridge, USA
148 Characterization of functional nanoparticles applied in face masks by STEM-EDX
Charlotte Wouters[1], Marina Ledecq[1], Denrich Morales[1], Khariklia Tsilikas[1], François-Xavier Ouf[2], Eveline Verleysen[1], Jan Mast[1]
[1]Trace elements and nanomaterials, Sciensano, Brussels, Belgium, [2]Laboratoire national de métrologie et d'essais, Paris, France
181 Measuring the Interpretability of High-Resolution Transmission Electron Microscopy Images
William Bang Lomholdt[1], Matthew Helmi Leth Larsen[2], Cuauhtémoc Núñez Valencia[2], Jakob Schiøtz[2], Professor Thomas Willum Hansen[2]
[1]Nanolab, Technical University of Denmark, Kgs. Lyngby, Denmark, [2]Department of Physics, Technical University of Denmark, Kgs. Lyngby, Denmark
199 Surface facet-dependent redox dynamics in vanadium-oxide-based catalysts
Martin Ek[1], Dr. Anita Godiksen[2], Dr. Logi Arnarson[2], Dr. Poul Georg Moses[2], Dr. Søren Ramsussen[2], Prof. Magnus Skoglundh[3], Prof. Eva Olsson[3], Prof. Stig Helveg[4]
[1]Centre for Analysis and Synthesis, Lund University, Lund, Sweden, [2]Topsoe A/S, Kgs. Lyngby, Denmark, [3]Competence Centre for Catalysis, Chalmers University of Technology, Gothenburg, Sweden, [4]VISION, Technical University of Denmark, Kgs. Lyngby, Denmark
292 Atomic scale evolution of Ru nanoclusters on graphitic carbon nanofibers in NH3 decomposition reaction
Dr. Yifan Chen[1], Mr Benjamin Young[1], Dr Gazimagomed Aliev[2], Dr Emerson Kohlrausch[1], Dr Andreas Weilhard[1], Mr Thomas Liddy[1], Dr Wolfgang Theis[2], Prof Graham Hutchings[3], Dr Jesum Alves Fernandes[1], Prof Andrei Khlobystov[1]
[1]School of Chemistry, University of Nottingham, Nottingham, United Kingdom, [2]Nanoscale Physics Research Laboratory, School of Physics and Astronomy, University of Birmingham, Birmingham , United Kingdom , [3]Cardiff Catalysis Institute, Translational Research Hub, Cardiff University , Cardiff , United Kingdom
442 Direct observation of Ni nanoparticle growth in carbon supported nickel under carbon dioxide hydrogenation atmosphere
Nienke Visser[1], Savannah Turner[1], Joseph Stewart[2], Bart Vandegehuchte[2], Dr. Jessi Van Der Hoeven[1], Petra de Jongh[1]
[1]Utrecht University, Utrecht, Netherlands, [2]TotalEnergies OneTech Belgium, Seneffe, Belgium
192 TEM Exploration of High-Performance Non-Noble Metal Catalysts for OER

David Llorens Rauret[1], Mr. Ranit Ram[2], Dr. F. Pelayo García de Arquer[2], Dr. Alba Garzón Manjón[1], Prof. Jordi Arbiol[1,3]
[1]ICN2, CSIC and BIST, Bellaterra (Barcelona), Spain, [2]ICFO and BIST, Castelldefels (Barcelona), Spain, [3]ICREA, Barcelona (Barcelona), Spain

202 Microstructural evolution of zeolitic nanocrystals for CO2 capture by Environmental in-situ TEM

Dr. Simona Moldovan[1], Mr Edwin Clathworthy[2], Mrs. Kalthoum Nakouri[3], Mrs. Svetlana Mintova[2]
[1]CNRS, Rouen University, Groupe de Physique des Materiaux, Rouen, France, [2]Normandie University, ENSICAEN, Laboratoire de Catalyse et Spectrochimie, Caen, France, [3]TOTALEnergies, Solaize, France

273 Beam damage and dynamics modelled with equivariant neural networks

Cuauhtémoc Nuñez Valencia[1], Mathias Stokkebye Nissen[1], Patrick Giese[1], Stig Helveg[2], Thomas Willum Hansen[3], Jakob Schiøtz[1]
[1]Computational Atomic-scale Materials Design (CAMD), Department of Physics, Technical University of Denmark, Kongens Lyngby, Denmark, [2]Center for Visualizing Catalytic Processes (VISION), Department of Physics, Technical University of Denmark, Kongens Lyngby, Denmark, [3]National Center for Nano Fabrication and Characterization, Technical University of Denmark, , Denmark

547 In-situ STEM-EELS observations on heating TiO2-x nanoparticles for solar and electrocatalytic applications.

Dr Khalil El Hajraoui[1,2], Dr Leonardo Lari[2,3], Mrs Fayzah Talbi[2,3], Prof. Richard Douthwaite[4], Prof Quentin. M Ramasse[1,5], Prof Vlado. K Lazarov[2,3], Dr Demie Kepaptsoglou[1,2]
[1]SuperSTEM Laboratory, SciTech Daresbury, Daresbury, United Kingdom, [2]School of Physics, Engineering and Technology, University of York, York, United Kingdom, [3]Jeol York Nanocentre, University of York, York, United Kingdom, [4]Department of Chemistry, University of York, York, United Kingdom, [5]School of Chemical and Process Engineering & School of Physics and Astronomy, University of Leeds, Leeds, United Kingdom

590 Phenomenology of the dealumination in Faujasite Y zeolitic cataysts

Dr Valentina Girelli Consolaro[1], Dr Virgile Rouchon[2], Dr Walid Baaziz[1], Dr Sharmin Sharna[3], Dr Stefan Stanescu[3], Mme Anne-Lise Taleb[2], Dr Gerhard Pirngruber[2], Prof Ovidiu Ersen[1]
[1]Institut de Physique et Chimie des Matériaux de Strasbourg (IPCMS), UMR 7504 CNRS, Stasbourg, France, [2]IFP Energies Nouvelles (IFPEN), Etablissement de Lyon, Solaize, France, [3]Synchrotron SOLEIL, Gif-sur-Yvette, France

639 Quantitative analysis of single-atom support interactions by Deep Learning techniques

Paula Aniceto Ocaña[1], José Marqueses Rodríguez[1], José Antonio Pérez Omil[1], José Juan Calvino[1], Carmen Esther Castillo[1], Miguel López Haro[1]
[1]Departamento de Ciencias de los Materiales e Ingeniería Metalúrgica y Química Inorgánica. Facultad de Ciencias, Campus Rio San Pedro S/N. Puerto Real. 11510. Cádiz, Spain

1001 Dynamics of an industrial Cu/ZnO catalyst revealed by operando TEM

Maxime Boniface[1], Thomas Götsch[1], Jinhu Dong[1], Elias Frei[1], Annette Trunscke[1], Robert Schlögl[1,2], Beatriz Roldàn Cuenya[3], Thomas Lunkenbein[1]
[1]Fritz-Haber-Institut der Max-Planck-Gesellschaft, Department of Inorganic Chemistry, Berlin, Germany, [2]Department of Heterogeneous Reactions, Max-Planck-Institute for Chemical Energy Conversion, Mülheim, Germany, [3]Department of Interface Science, Fritz Haber Institute of the Max Planck Society, , Berlin, Germany

1046 Measurement of atom mobility of gold nanorods via coarse-sampling in quantitative 4D-STEM

Mr Cheng Zhao[1], Ms Zhi Tong Liew[2], Dr Bryan David Esser[3], Dr Alison Funston[2], Prof Joanne Etheridge[3,4]
[1]Department of Material Science and Engineering, Monash University, Clayton, Australia, [2]School of Chemistry, Monash University, Clayton, Australia, [3]Monash Centre for Electron Microscopy, Monash University, Clayton , Australia, [4]School of Physics and Astronomy, Monash University, Clayton , Australia

Poster Presentation

110 Confined single-molecule imaging by low-dose electron microscopy
Huiqiu Wang[1,2], Prof. Xiaodong Zou[1]
[1]Department of materials and environmental chemistry, Stockholm University, Stockholm, Sweden, [2]Department of chemical engineering, Tsinghua University, Beijing, China
127 Tri-layer graphene as membrane and electrode for liquid-phase electron microscopy studies of CO2 electroreduction nanocatalysts
Saltanat Toleukhanova[1], Dr. Tzu-Hsien Shen[1], Mr Chen Chang[1], Miss. Swathilakshmi Swathilakshmi[1], Miss. Tecla Bottinelli Montandon[1], Prof. Vasiliki Tileli[1]
[1]Institute of Materials, École Polytechnique Fédérale de Lausanne, Lausanne, Switzerland
179 Multimodal and multidimensional EELS and EDX for investigations of catalysts at the nanoscale
Dr Maria Meledina[1], Mr Dileep Krishnan[1], Mr Daen Jannis[2], Mr Maarten Wirix[1], Mr Xiaochao Wu[3], Mr Ulrich Simon[3], Mr Sorin Lazar[1], Mr Peter Tiemeijer[1], Mr Paolo Longo[1]
[1]Thermo Fisher Scientific, Eindhoven, Netherlands, [2]EMAT, University of Antwerp, Antwerp, Belgium, [3]Institute of Inorganic Chemistry, RWTH Aachen University, Aachen, Germany
213 Visualizing single-atom promotion of ultra-deep hydrodesulfurization catalysts (Pt-Co-Mo-S)
Principal Scientist Lars Pilsgaard Hansen[1], Mr. Christian F. Weise[1], Mrs. Hanne Falsig[1], Mr. Poul G. Moses[1], Mr. Stig Helveg[2], Mr. Michael Brorson[1]
[1]Topsoe A/S, DK-2800 Kgs. Lyngby, Denmark, [2]Center for Visualizing Catalytic Processes (VISION) Department of Physics Technical University of Denmark, DK-2800 Kgs. Lyngby, Denmark
282 Understanding Au cluster growth through electron microscopy
Tom Slater[1], Dr Malcolm Dearg[1,2], Mr Sean Lethbridge[3], Mr James McCormack[3], Dr Theo Pavloudis[3,4], Prof Joseph Kioseoglou[4], Prof Richard Palmer[3]
[1]School of Chemistry, Cardiff University, Cardiff, United Kingdom, [2]School of Physics, University of York, York, United Kingdom, [3]Nanomaterials Lab, Department of Mechanical Engineering, Swansea University, Swansea, United Kingdom, [4]Department of Physics, Aristotle University of Thessaloniki, Thessaloniki, Greece
295 η-Carbides (Co, Mo, or W) Nanoparticles from Octacyanometalates Precursors-Based Network
Dr Frédéric Fossard[1], Mr. Thomas Blin[2], Mrs Armelle Girard[1,3], Mrs Nathalie Guillou[3], Mrs Laure Catala[2], Mrs Annick Loiseau[1], Mr. Vincent Huc[2]
[1]Université Paris-Saclay, ONERA, CNRS, LEM, Châtillon, France, [2]ICMMO, CNRS, Université Paris-Saclay, Orsay, France, [3]ILV, UMR CNRS 8180, UVSQ, Université Paris-Saclay, Versailles, France
318 Atomic-scale model of the platinum (111)-water interface revealed by angstrom resolution off-axis phase shifting holography
Jonas Lindner[1], Dr. Ulrich Ross[1,2], Dr. Tobias Meyer[1], Dr. Sung Sakong[3], Prof. Dr. Axel Groß[3,4], Prof. Dr. Michael Seibt[2], Prof. Dr. Christian Jooß[1,5]
[1]Institute of Materials Physics, University of Goettingen, Göttingen, Germany, [2]4th Institute of Physics – Solids and Nanostructures, University of Goettingen, Göttingen, Germany, [3]Institute of Theoretical Chemistry, Ulm University, Ulm, Germany, [4]Helmholtz Institute Ulm (HIU) for Electrochemical Energy Storage, Ulm, Germany, [5]International Center for Advanced Studies of Energy Conversion (ICASEC), Göttingen, Germany
321 Nanoparticle formation mechanisms and molecular intermediates revealed by liquid phase EM and reaction pathway analysis
Ms. Jiayue Sun[1], Mr. Birk Fritsch[2], Mr. Andreas Körner[2], Ms. Lucia Morales[2], Mr. Chiwoo Park[3], Ms. Mei Wang[4], Dr. Andreas Hutzler[2], Mr. Taylor Woehl[4]
[1]Department of Chemistry and Biochemistry, University of Maryland, College Park, United States, [2]Helmholtz Institute Erlangen-Nürnberg for Renewable Energy, Erlangen, Germany, [3]Department of Industrial and Systems Engineering, University of Washington, Seattle, United States, [4]Department of Chemical Engineering, University of Maryland, College Park, United States

350 Detection of weak ELNES signals using dose-fractionated spectrum imaging combined with direct detection
Andrew Thron[1], Liam Spillane[1], Saleh Gorji[2], Ray Twesten[1]
[1]Gatan Inc., Pleasanton , USA, [2]Gatan GmbH, Unterschleissheim, Germany
380 Impact of oxidation state on copper nanoparticle stability in industrial Cu/ZnO/Al2O3 hydrogenation catalyst
Xiansheng Li[1], Henrik Eliasson[1], Rolf Erni[1]
[1]Empa-Swiss Federal Laboratories for Materials Science and Technology, Dübendorf, CH
394 Insights into the Structural Dynamics of Cu@Ag Core-Shell Nanoparticles during CO2 Reduction
Daniel Arenas Esteban[1], Dr. Lien Pacquets[1,2], Dr. Daniel Choukroun[2], Mrs. Saskia Hoekx[1,2], Dr. Ajinkya Kadu[1,3], Mr. Jonathan Schalck[2], Dr. Nick Daems[2], Prof. Tom Breugelmans[2], Prof. Sara Bals[1]
[1]Electron Microscopy for Materials Science (EMAT) and NANOlab Center of Excellence, University of Antwerp, Antwerp, Belgium, [2]Applied Electrochemistry and Catalysis (ELCAT), University of Antwerp, Antwerp, Belgium, [3]Centrum Wiskunde & Informatica (CWI), Amsterdam, The Netherlands
440 STEM-XEDS spectrokinetic analysis of oxygen: a tool to understand redox processes in nanostructured oxide catalysts
Professor José J. Calvino[1], Dr. Isabel Gómez-Recio[2], Dr. Huiyan Pan[1], Dr. Juan J. Delgado[1], Dr. Xiaowei Chen[1], Prof. Miguel A. Cauqui[1], Prof. José A. Pérez-Omil[1], Prof. María L. Ruiz-González[2], Dr. María Hernando[2], Prof. Marina Parras[2], Prof. José M. González-Calbet[2], Dr. Miguel López-Haro[1]
[1]Departamento de Ciencia de los Materiales e Ingeniería Metalúrgica y Química Inorgánica. Facultad de Ciencias, Universidad de Cádiz, Campus Rio San Pedro, Puerto Real, España, [2]Departamento de Química Inorgánica, Facultad de Química, Universidad Complutense de Madrid, Madrid, Spain
509 Cryo electron tomography of impregnated mesoporous catalyst supports
Jason Heinrichs[1,2], Mr. Rick Joosten[2,3], Ms. Jovana Zečević[4], Mr. Thomas Weber[1,4], Mr. Emiel Hensen[1], Mr. Heiner Friedrich[2,3]
[1]Laboratory of Inorganic Materials and Catalysis, Department of Chemical Engineering and Chemistry, Eindhoven University of Technology (TU/e), Eindhoven, The Netherlands, [2]Center for Multiscale Electron Microscopy, Department of Chemical Engineering and Chemistry, Eindhoven University of Technology (TU/e), Eindhoven, The Netherlands, [3]Laboratory of Physical Chemistry, Department of Chemical Engineering and Chemistry, Eindhoven University of Technology (TU/e), , The Netherlands, [4]Shell Projects and Technology, Energy Transition Campus Amsterdam (ETCA), Amsterdam, The Netherlands
510 Structure-activity relationship of Pt nanoparticles during the CO oxidation reaction
Christian Fink Elkjær[1], Ph.d. Sebastian Jespersen[1], Søren Vendelbo[2], Christian D. Damsgaard[3], Patricia Koymann[4], Ib Chorkendorff[3], Stig Helveg[3]
[1]Topsoe A/S, Kgs. Lyngby, Denmark, [2]Technological Institute, Taastrup, Denmark, [3]Technical University of Denmark, Kgs. Lyngby, Denmark, [4]University of Cape Town, Rondebosch, South Africa
524 Elucidation of Structure-catalytic Activity of Nickel-based Nanomaterial for Electrocatalytic Water Splitting
Dr. Jean Marie Vianney Nsanzimana[1], Charles Otieno Ogolla[1], Max Kasper[1], Prof. Manuela Killian[2], Prof. Butz Benjamin[1]
[1]Micro- and Nanoanalytics Group, University of Siegen, Siegen, Germany, [2]Chemistry and Structures of Novel Materials, University of Siegen, Siegen, Germany
539 Characterization of inorganic food additives and pearlescent pigments in sprays for food decoration by STEM-EDX
Noa Olluyn[1,2], Dr. Eveline Verleysen[1], Lisa Siciliani[1,2], Dr. Daniel Arenas Esteban[2], Dr. Stella Mathioudaki[1], Dr. Subhalakshmi Sharma[1], Joris Van Loco[1], Prof. Dr. Sara Bals[2], Dr. Jan Mast[1]
[1]Sciensano, Uccle, Belgium, [2]EMAT, University of Antwerp, Antwerp, Belgium
546 Leveraging gas-cell in situ electron microscopy to track atmosphere-dependent reversible transformations in reducible oxides

Postdoc Ramon Manzorro[1], Irene Piedra[1], Carmen Mora[1], Jose A. Perez-Omil[1], Jose J. Calvino[1], Miguel Lopez-Haro[1], Ana Hungria[1]
[1]Departamento de Ciencias de los Materiales e Ingeniería Metalúrgica y Química Inorgánica, Facultad de Ciencias, Universidad de Cádiz, Puerto Real, Spain

554 Direct Visualization of Temperature Induced Phase Separation of Completely Miscible Au-Pd Alloy by In-Situ TEM

Dr. Abhijit Roy[1,2], Dr. Simon Hettler[1,2], Dr. Raul Arenal[1,2,3]
[1]Instituto de Nanociencia y Materiales de Aragón (INMA), CSIC-Universidad de Zaragoza, Zaragoza, Spain, [2]Laboratorio de Microscopías Avanzadas (LMA), Universidad de Zaragoza, Zaragoza, Spain, [3]ARAID Foundation Zaragoza , Zaragoza, Spain

602 Understanding CuO/Al2O3 Interactions during Thermochemical Redox Reactions: TEM, X-ray Microscopy, and XAS Study

Dr Sharmin SHARNA[1,2,3], Dr Virgile Rouchon[2], Dr Christèle L Legens[2], Dr Arnold Lambert[2], Dr Stefan Stanescu[3], Dr Anne-Sophie Gay[2], Dr David Chiche[2], Dr Valérie Briois[3], Prof. Ovidiu Ersen[1]
[1]Institut de Physique et de Chimie des Matériaux de Strasbourg, Strasbourg, France, [2]IFP Energies nouvelles, Lyon, France, [3]Synchrotron Soleil, Saint-Aubin, France

623 New generation environmental in situ TEM holder for gas cell studies across multiple platforms

Dr. Yevheniy Pivak[1], Dr. Dan Zhou[2], MSc Christian Deen-van-Rossum[1], MSc Ronald Spruit[1], MSc Merijn Pen[1], Dr. Hongyu Sun[1], Dr. Hugo Perez[1]
[1]DENSsolutions BV, Delft, The Netherlands, [2]Leibniz-Institut für Kristallzüchtung (IKZ), Berlin, Germany

697 Operando TEM Reveals Oscillatory Surface and Bulk Dynamics of Nickel Nanoparticles in Ethylene Partial Oxidation

Dr. Claudiu Colbea[1,3], Prof. Jeroen Anton van Bokhoven[1], Prof. Marc-Georg Willinger[2,3], Dr. Milivoj Plodinec[1,3]
[1]Department of Chemistry and Applied Biosciences, ETH Zürich, Zürich, Switzerland, [2]Department of Chemistry, Technical University of Munich, Münich, Germany, [3]Scientific Center for Optical and Electron Microscopy, ETH Zürich, Zürich, Switzerland

762 Achieving methanol photo-oxidation to hydrogen and formaldehyde over lead-free halide perovskite

Mr Zhiyang Zhong[1,2], Prof Shik Chi Edman Tsang[2], Prof Angus Kirkland[1,3]
[1]Department of Materials, University of Oxford, Oxford, UK, [2]Department of Chemistry, University of Oxford, Oxford, UK, [3]Rosalind Franklin Institute, Harwell Campus, Didcot, UK

792 Restructuring of silver catalysts after oxidation reactions – looking beneath the surface

Dr Tina Bergh[1], Youri van Valen[1], Jia Yang[1], Ole H. Bjørkedal[2], Ann Kristin Lagmannsveen[3], Hilde J. Venvik[1]
[1]Department of Chemical Engineering, Norwegian University of Science and Technology (NTNU), Trondheim, Norway, [2]Dynea AS, Lillestrøm, Norway, [3]K.A. Rasmussen, Hamar, Norway

794 High quality graphene TEM supports for high-resolution transmission electron microscopy

Jenthe Verstraelen[1], Dr. Adrian Pedrazo Tardajos[1], Dr. Nathalie Claes[1], Dr. Tine Derez[1], Prof. Dr. Sara Bals[1]
[1]EMAT, university of Antwerp, Antwerp, Belgium

806 Multicore@shell nanoparticles synthesized from a multicomponent target by gas aggregation cluster source

Marie Elis[1], Dr. Amir Mohammad Ahadi[2], Tim Tjards[3], Dr. Alexander Vahl[3,4,5], Dr. Salih Veziroglu[3,4], Dr. Thomas Strunskus[3,4], Prof. Dr. Franz Faupel[3,4], Dr. Ulrich Schürmann[1,4], Prof. Dr. Lorenz Kienle[1,4]
[1]Chair for Synthesis and Real Structure, Department for Materials Science, Faculty of Engineering, Kiel University, Kiel, Germany, [2]Department of Physics, Faculty of Science, Shahid Chamran University of Ahvaz, Ahvaz, Iran, [3]Chair for Multicomponent Materials, Department for Materials Science, Faculty

of Engineering, Kiel University, Kiel, Germany, [4]Kiel Nano, Surface and Interface Science KiNSIS, Kiel University, Kiel, Germany, [5]Leibniz Institute for Plasma Science and Technology, Greifswald, Germany

810 Structure and Composition of High-Entropy-Alloy Nanoparticle synthesized by Pulsed Laser Ablation in Liquid

Felix Pohl[1], Robert Struckert[2], Dr. Ulrich Schürmann[1], Dr. Christoph Rehbock[2], Prof. Stephan Barcikowski[2], Prof. Lorenz Kienle[1]
[1]Institute for Material Science, Faculty of Engineering, Kiel University, Kiel, Germany, [2]Technical Chemistry I and Center for Nanointegration Duisburg-Essen (CENIDE), University of Duisburg-Essen, Essen, Germany

823 Charge density mapping of supported nanoparticle electrocatalysts by 4D STEM

Lazar Bijelic[1,2], Ana Rebeka Kamšek[1,3], Francisco Ruiz Zepeda[1], Goran Dražić[1], Nejc Hodnik[1,2]
[1]National Institute of Chemistry, Ljubljana, Slovenia, [2]University of Nova Gorica, Nova Gorica, Slovenia, [3]Faculty of Chemistry and Chemical Engineering, University of Ljubljana, Ljubljana, Slovenia

864 Oscillatory redox behavior of nickel catalysts observed by operando SEM

Ms. Sci. Alexander Nitsche[1], Ms. Sci. Nico Radde[1], Dr. Ali Rinaldi[1], Prof. Dr. Marc Willinger[1]
[1]Department of Chemistry, School of Natural Sciences, TU Munich, Garching bei München, Germany

938 In-situ observation and analysis of Ni-based catalysts for dry reforming of methane

Dr. Ayako Hashimoto[1,2], Mr. Yutain Han[1,2]
[1]National Institute for Materials Science, Tsukuba, Japan, [2]University of Tsukuba, Tsukuba, Japan

943 Advanced approaches for the analysis of micro- to nano-quartz particles using SEM, ESEM, FIB-SEM, SBF-SEM

Martin Olbert[1], Vilém Neděla[1], Josef Jirák[1], Jiří Hudec[1]
[1]Environmental electron microscopy group, Institute of Scientific Instruments of the CAS, v.v.i., Brno, Czech Republic

961 Chemical and morphological stability study of copper oxide nanocubes in controlled and non-controlled atmospheres

Irene Piedra[1], Ramon Manzorro[1], M. Jose Guerra[1], Jose J. Calvino[1], Miguel Lopez-Haro[1], Ana B. Hungria[1]
[1]Departamento de Ciencias de los Materiales e Ingeniería Metalúrgica y Química Inorgánica, Facultad de Ciencias, Universidad de Cádiz, Campus Río San Pedro S/N, Puerto Real, 11510 Cádiz, Spain, Cádiz, Puerto Real, Spain

975 Phase-controlled formation of NixPy catalyst using environmental TEM for potential application in CO2 reduction

Dr. Kshipra Sharma[1,2], Mr. Tianyi Hu[1,2], Prof. Kimberly A. Dick[1,2]
[1]Centre for Analysis and Synthesis, Lund University, Lund, Sweden, [2]Nanolund, Lund University, Lund, Sweden

1012 A validation methodology for size and shape measurement of nanoplastics by transmission electron microscopy

Charlotte Wouters[1], Denrich Morales[1], Khariklia Tsilikas[1], Eveline Verleysen[1], Jan Mast[1]
[1]Trace Elements and Nanomaterials, Sciensano, Brussels, Belgium

1017 IN-SITU SYNTHESIS OF FexPy NANOPARTICLES

PhD student Azemina Kraina[1,2], Tianyi Hu[1,2], Pau Ternero[2,3], Professor Kimberly A. Dick[1,2]
[1]Centre for Analysis and Synthesis, Lund University, Lund, Sweden, [2]NanoLund, Lund University, Lund, Sweden, [3]Solid State Physics, Lund University, Lund, Sweden

1036 Assessing feasibility of detecting photogenerated charge carriers in photocatalysts via transmission electron microscopy: simulation study

Monia Runge Nielsen[1,2], Shima Kadkhodazadeh[1,2], Michael S. Seifner[1,2]
[1]Nanolab - National Centre for Nano Fabrication and Characterization, Technical University of Denmark, Kongens Lyngby, Denmark, [2]NanoPhoton - Center for Nanophotonics, Technical University of Denmark, Kongens Lyngby, Denmark

1059 Investigation of self-assembly dynamics of magnetic nanoparticles in liquid phase by transmission electron microscopy
Dr Malika Khelfallah[1], Dr Claire Carvallo[2], Dr Amélie Juhin[2], Dr Govind Ummethala[1], Dr Amir Tavabi[1], Peng-Han Lu[1], Dr Thibaud Denneulin[1], Prof. Dr Rafal Dunin-Borkowski[1]
[1]Ernst Ruska-Centre for Microscopy and Spectroscopy with Electrons, Forschungszentrum Jülich GmbH, Jülich, Germany, [2]Institut de Minéralogie, de Physique des Matériaux et de Cosmochimie, Sorbonne Université, MNHN, CNRS, UMR 7590, Paris, France
1109 Physical and chemical parameters determining the formation of gold sp-metal (Al, Ga, In, Pb) nanoalloys
Prof Patrizia Canton[1], Prof Vincenzo Amendola[2], Dr Vito Coviello[2], Dr Daniel Forrer[3]
[1]Department of Molecular Sciences and Nanosystems, University Ca' Foscari of Venice, Venezia, Italy, [2]Department of Chemical Sciences, University of Padova, Padova, Italy, [3]CNR– ICMATE, Padova, Italy
1129 Tungsten nanoparticles generated in an atmospheric pressure plasma jet
Dr. Martin Müller[1], Maren Dworschak[2], Prof. Jan Benedikt[2], Prof. Lorenz Kienle[1]
[1]Faculty of Engineering, Kiel University, Kiel, Germany, [2]Faculty of Mathematics and Natural Sciences, Kiel University, Kiel, Germany
1132 Morphology evolution and phase transition of $Co(OH)_2$ and Co_3O_4 investigated with STEM-tomography and in-situ XRD
Olivia Kaya Gerds[1,2,3], Lars Fahl Lundegaard[3], Hanne Falsig[3], Christian Danvand Damsgaard[1,2,4], Lars Pilsgaard Hansen[3]
[1]Center for Visualizing Catalytic Processes (VISION), Department of Physics, Technical University of Denmark, Kgs. Lyngby, Denmark, [2]Surface Physics and Catalysis, Department of Physics, Technical University of Denmark, Kgs. Lyngby, Denmark, [3]Topsoe A/S, Kgs. Lyngby, Denmark, [4]National Center for Nano Fabrication and Characterization, Technical University of Denmark, Kgs. Lyngby, Denmark
1135 Synthesis and Characterization of Ultrathin Unconventional Mixed 2H-HCP/FCC Phase Au Nanowire
Dr. Abhijit Roy[1,2], Dr. Raul Arenal[1,2,3]
[1]Laboratorio de Microscopías Avanzadas (LMA), Universidad de Zaragoza, ZARAGOZA, SPAIN, [2]Instituto de Nanociencia y Materiales de Aragón (INMA), CSIC-Universidad de Zaragoza, ZARAGOZA, SPAIN, [3]ARAID Foundation Zaragoza , Zaragoza, Spain
1139 Studying nano-catalysts degradation with an identical location STEM approach
Dr. Francisco Ruiz Zepeda[1], Lazar Bijelić[1], Armin Hrnjić[1], Ana Rebeka Kamšek[1], Dr Andraž Pavlišič[1], Dr Marjan Bele[1], Dr Primož Jovanovič[1], Dr. Matija Gatalo[1], Dr Milutin Smiljanić[1], Prof. Nejc Hodnik[1]
[1]National Institute of Chemistry, Ljubljana, Slovenia
1141 TEM structural analysis of photocatalytically active mesoporous single crystalline LaTiO2N particles
Dr. Mont. Jakub Zalesak[1], MSc. Jakob Praxmair[1], MSc. Julian Hörndl[1], Univ.-Prof. Simone Pokrant[1]
[1]Chemistry and Physics of Materials, University of Salzburg, Salzburg, Austria

Late Poster Presentation

1228 Heterogeneous dissolution of Au nanoparticles under constant electrochemical potential as observed via in-situ liquid-cell TEM
Dr. Sorour Semsari Parapari[1], Layrton José Souza da Silva[1,2], Miguel Bernal[3], Daniel Torres[3], Dr. Miran Čeh[1,2], Dr. Kristina Žužek[1,2], Dr. Jon Ustarroz[3,4], Dr. Sašo Šturm[1,2]
[1]Jožef Stefan Institute, Department for Nanostructured Materials, Ljubljana, Slovenia, [2]Jožef Stefan International Postgraduate School, Ljubljana, Slovenia, [3]ChemSIN, Université libre de Bruxelles , Brussels, Belgium, [4]Electrochemical and Surface Engineering (SURF), Vrije Universiteit Brussel, Brussels, Belgium

1255 Observation of spontaneous fluctuations in product selectivity of the acetylene hydrogenation reaction in operando TEM
Dr. Christian Rohner[1], Mr Eugen Stotz[1], Dr. Alexander Steigert[2], Dr. Daniel Amkreutz[2], Prof. Dr. Rutger Schlatmann[2], Prof. Dr. Beatriz Roldan Cuenya[1], PD Dr Thomas Lunkenbein[1]
[1]Fritz Haber Institute of the Max Planck Society, Berlin, Germany, [2]Helmholtz-Zentrum Berlin für Materialien und Energie, Berlin, Germany
1259 Insights into the mechanisms of silver phase formation vial electrochemical liquid-cell TEM
Msc. Layrton José Souza Da Silva[1,2], Dr. Sorour Semsari Parapari[1], Monica Parpal Giménez[3], Mohammed El Marini[3], Prof. Dr. Jon Ustarroz[3,4], Prof. Dr. Sašo Šturm[1,2,5]
[1]Department for Nanostructured Materials, Jožef Stefan Institute, Ljubljana, Slovenia, [2]Jožef Stefan International Postgraduate School, Ljubljana, Slovenia, [3]ChemSIN – Chemistry of Surfaces, Interfaces and Nanomaterials, Université Libre de Bruxelles (ULB), , Brussels, Belgium, [4]SURF – Research Group Electrochemical and Surface Engineering, Vrije Universiteit Brussels, Brussels, Belgium, [5]Department of Geology, Faculty of Natural Sciences and Engineering, University of Ljubljana, Ljubljana, Slovenia
1286 SEM and mCT investigations on GDEs with Copper-Nafion coating for carbon dioxide reduction to ethylene
Dr. rer. nat. Lisa Christine Ehle[1], M. Sc. Vera Ubbenjans[2], Dr. rer. nat. Adrian Mikitisin[1], Prof. Dr. rer. nat. Joachim Mayer[1], Dr. Rer. Nat. Lisa Christine Ehle
[1]Central facility for electron microscopy (GFE), RWTH Aachen University, Aachen, Germany, [2]Chemical Engineering (AVT), RWTH Aachen University, Aachen, Germany
1291 3D Characterization of Pore Structures in Shaped Heterogeneous Catalysts Using FIB-SEM Tomography
Dr. Aram Yoon[1], Dr. Jaejin Kim[2], Dr. Xiaodan Chen[1]
[1]Shell Energy Transition Campus Amsterdam, Amsterdam, Netherlands, [2]Shell Technology Center Houston, Houston, USA
1307 Morphology-Driven Photothermal Efficiency in Nanostructured Semiconductors
Dr. Maibelin Rosales[1], Dr. Raynald Gauvin[2], Dr. Andreina García[3], Dr. Senentxu Lanceros-Méndez[1,4]
[1]BCMaterials, Basque Center for Materials, Applications and Nanostructures, Bilbao, Spain, [2]Mining and Materials Engineering Department, McGill University., Montreal, Canada, [3]Advanced Mining Technology Center (AMTC), Universidad de Chile, Santiago, Chile, [4]IKERBASQUE, Basque Foundation for Science, Bilbao, Spain
1340 Catalytically active MoS2 support for hydrogen generation from seawater
Soohyun Kwon[1], Doctor Ji-Hyung Han[2], Assistant professor Joohyun Lim[1]
[1]Department of Chemistry, Kangwon National University, Chuncheon, Republic of Korea, [2]Jeju Global Research Center, Korea Institute of Energy Research, Jeju, Republic of Korea

589

Dynamics at phase boundaries of active catalyst studied by multi-scale operando EM

Prof. Dr. Marc Willinger[1]
[1]Department of Chemistry, School of Natural Sciences, TU Munich, Garching bei München, Germany
PS-05 (1), Lecture Theater 1, august 28, 2024, 10:30 - 12:30

Catalysis is a highly complex phenomenon and intricately linked to the interplay between processes that dominate at different time and length scales. It is therefore impossible to understand the emergence of catalytic function solely based on the study of static atomic arrangements. Up to now, the full-scale complexity of catalysis is only poorly understood because the way in which atomic-scale processes influence the behavior and dynamics at larger scale is not well documented experimentally. The result is that we still, to a large extent, develop new catalysts on the basis of iterative trial-and-error approaches. Elucidating the link between atomic-scale structural dynamics, feedback mechanisms, and collective behaviour is the key to a deeper understanding and further optimisation of catalysts and processes. From imaging of quasi-static low- energy configurations through gas-phase-induced state switching to observation of complex non-equilibrium dynamics and oscillatory behaviour (Figure 1), electron microscopy has provided novel insights across several length and time scales and has meanwhile matured from a service tool for catalyst researchers to a driving force in catalysis research [1,2]. In my presentation, I will show that consideration of dynamics and processes taking place at different time and lateral scales as well as the consideration of non-linear and complex behaviour is essential for our understanding of working catalyst.

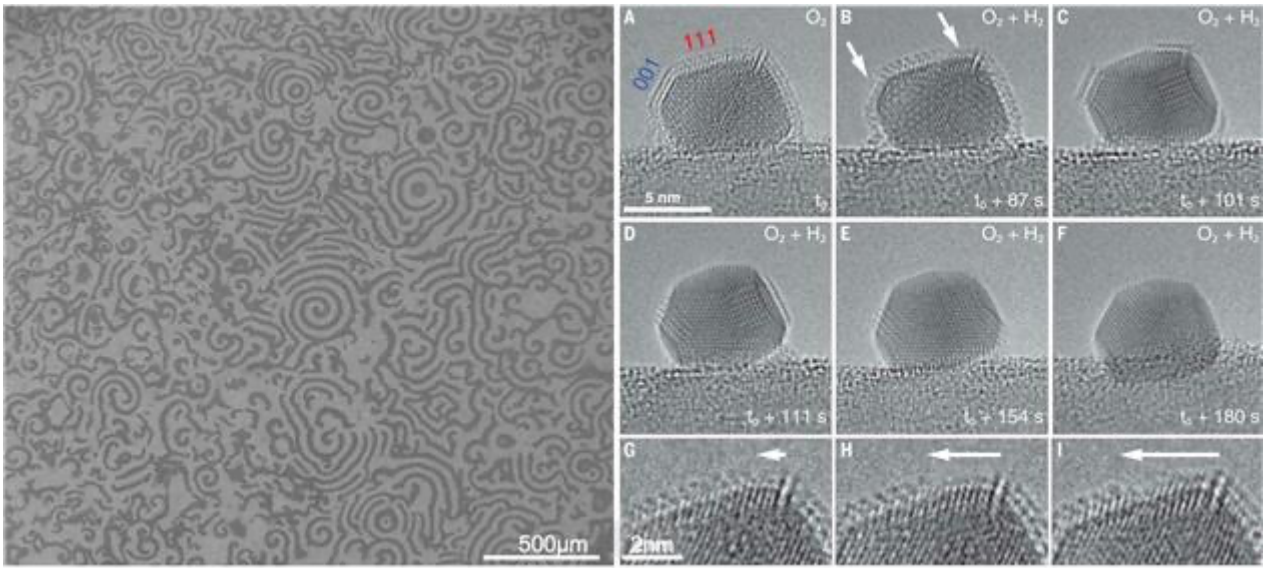

Keywords:

catalysis, non-equilibrium dynamics, multi-scale

Reference:

[1] Hansen, T.W., Willinger, M. From atomistic to collective dynamics: Bridging gaps in gas-phase electron microscopy for catalysis. MRS Bulletin 48, 842–851 (2023)
[2] H. Frey, A. et al., Science 376, 982-987 (2022).

527

PVA/PEG-based nanofibers with Au nanoparticles for treatment of chronic woundss

Dr. Elena Filova[1], Prof. Petr Slepicka[2], Dr. Nikola Slepickova Kasalkova[2], Prof. Vera Jencova[3], Ing. Maxim Lisnenko[3], Ing. Sarka Hauzerova[3], Prof. David Lukáš[3], Dr. Jana Nebesarova[4], Dr. Silvie Rimpelova[5,6], Mrs. Yu-Chieh Wu[1], Prof. Lucie Bacakova[1]
[1]Laboratory of Biomaterials and Tissue Engineering, Institute of Physiology of the Czech Academy of Sciences, Prague, Czech Republic, [2]Department of Solid State Engineering, University of Chemistry and Technology Prague, Prague, Czech Republic, [3]Faculty of Science, Humanities and Education, Department of Chemistry, Technical University of Liberec , Liberec, Czech Republic, [4]Laboratory of Electron Microscopy, Faculty of Science, Charles University, Prague, Czech Republic, [5]Department of Biochemistry and Microbiology, University of Chemistry and Technology Prague, Prague, Czech Republic, [6]Department of Tissue Engineering, Institute of Experimental Medicine of the Czech Academy of Sciences, Prague, Czech Republic

PS-05 (2), Lecture Theater 1, august 28, 2024, 14:00 - 16:00

Background incl. aims
Chronic wounds are a healthcare problem both for patients and for society. They are often contaminated with bacteria, and the infection impacts the healing of the wounds. Therefore, a tremendous effort has been made to develop wound dressings supporting wound healing and preventing or even eliminating bacterial infection. Due to increasing bacterial resistance to antibiotics, other research approaches are used [1]. The aim of this study was to prepare polyvinyl alcohol (PVA)/polyethylene glycol (PEG) – based wound dressing doped with gold nanoparticles, to analyze their physical and chemical properties, cytocompatibility, and antibacterial properties.
Methods
Sputtering of Au for nanoparticle preparation was carried out at 20 °C by the sputter coater device SCD 050 (Baltec, argon pressure of 8 Pa), with the current of 30 mA, sputtering time of 500 s, and the electrode distance of 50 mm. Immediately after deposition of the metal nanoparticles into PEG (polyethylene glycol, Mw 600), the mixture was diluted with 18 mL of distilled water. The ratio of PEG/H2O in this case was 1:9. PVA-based nanofibrous materials were prepared by DC electrospinning. Solution of nanoparticles (AuNPs) was added into a 10 % PVA solution; the ratio of PVA:PEG was 9:1 or 6:4. Electrospinning was carried out on a needleless electrospinning device NS 1WS500U (Elmarco, CZ) using high voltage on electrodes 40 and 10 kV. The temperature was set to 21 °C and the relative humidity was of 21 %. Some of the samples underwent heat treatment (HT) at 150 °C for 1 h. The presence, size and homogeneity of the AuNPs in nanofibers was proven by JEOL JSM-IT800 scanning electron microscope by the analyses of backscattered electrons. The theoretical Au concentration was 111 and 666 µg/g for 9:1 and 6:4 PVA:PEG ratio, respectively. The nanofibers were analyzed by energy dispersive spectroscopy, atomic force microscopy, scanning electron microscopy (VEGA Easy Probe (TESCAN, CR) as well. The PVA:PEG membranes with/without Au, with/without heat treatment and at both ratios (9:1, 6:4), 1 cm2 in size, were added into the culture of normal human dermal fibroblasts (NHDFs) or human umbilical vein endothelial cells (HUVECs), which were seeded at the density of 20 000 cells/well in a glass-bottom 24-well dish. Cell morphology was assessed by immunofluorescence staining of vinculin and F-actin staining using phalloidin-TRITC. Cell metabolic activity/viability was analyzed using resazurin assay on days 1, 3, and 7 after seeding. HUVECs were stained for von Willebrand factor, and NHDFs for type I collagen production on day 7. Antimicrobial properties of the prepared materials were characterized by contact tests of the materials with two environmental bacterial strains of Gram-positive S. epidermidis and Gram-negative E. coli. The number of colony-forming units of both bacterial strains after contact tests were calculated using ImageJ. As a control, bacteria incubated in a physiological solution were used.

Results

Scanning electron microscopy revealed different surface morphology of the prepared nanofibers for particular PVA:PEG mixtures, i.e. 6:4 and 9:1 as well as the presence and relatively homogeneous distribution of Au on/inside the nanofibers. The density of nanofibers, and more importantly the intensity of so-called “clusters”, were different; the PVA:PEG nanofibers had a narrow distribution of thickness with small or large drops inside membranes. The EDX analysis exhibited different surface chemistry of the prepared samples based on the amount of added nanoparticles and PEG in the solution. Atomic force microscopy was used for the determination of surface roughness, morphology and effective surface area both on the fiber (detailed scan), and also generally over the surface (larger scan above 30x30 µm). The heat treatment also affected both the surface morphology and chemistry of the prepared samples as was revealed by SEM, EDX and AFM techniques. Heat treatment decreased both the dissolution and shrinkage of the nanofibers in the cell culture medium. On day 1 after seeding, both HUVECs and NHDFs were well spread, and in the following days, they proliferated in the presence of all tested nanofibers with/without Au. Metabolic activity/cell viability of the cells was similar to that growing on the control tissue culture polystyrene surface. The HUVECs were positively stained for von Willebrand factor and NHDFs were proven to produce collagen on day 7. The analysis of material antimicrobial properties showed a partial inhibition of bacterial growth, presented as a lower number of colony-forming units.

Conclusions

The PVA:PEG–based nanofibers with homogeneously dispersed AuNPs at different Au concentrations were prepared and some of them were further stabilized by heat treatment.

The material physical and chemical properties were evaluated by various physical methods, their cytocompatibility was proven in vitro culture using both HUVECs and NHDFs cells. The materials with higher Au content seem to be promising for the treatment of chronic wounds with/without bacterial infection.

Acknowledgements: Supported by Project No CZ.02.01.01/00/22_008/0004562 of the Ministry of Education, Youth and Sports, which was co-funded by the European Union, by the Praemium Academiae grant (No. AP2202) provided by the Czech Academy of Sciences, and by the European Union—Next Generation EU, the project National Institute for Research of Metabolic and Cardiovascular Diseases, Programme EXCELES, ID Project No. LX22NPO5104.

Graphics

Fig. 1. A. Immunofluorescence staining of von Willebrand factor in HUVECs cultured in medium with added PVA:PEG_6:4_Au_HT nanofibers on day 7 of culture, Olympus IX71 epifluorescence microscope, obj. × 20, B. SEM image of the same sample, JEOL JSM-IT800 microscope, magnif. × 60,000.

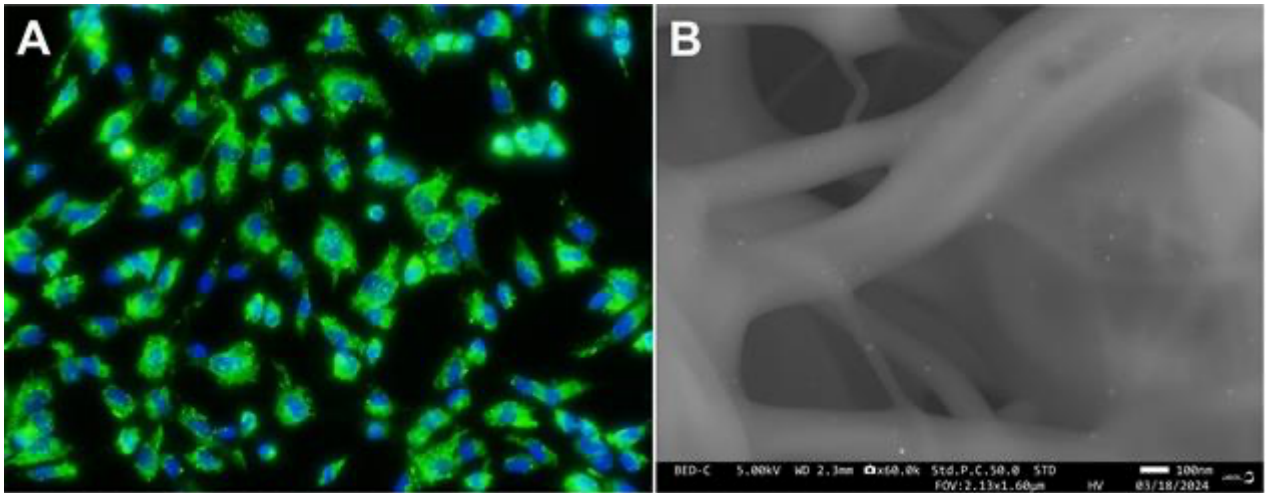

Keywords:

Gold nanoparticles, antimicrobial properties, cytocompatibility

Reference:

1. Chandrashekhar Singh et al. Molecules 2022, 27, 7059. https://doi.org/10.3390/molecules27207059.

224

Effect of the Applied Chemical Potential on Strong Metal-Support Interaction in Ni-TiO2 Catalysts

Min Tang[1], Matteo Monai[2], Angela Melcherts[2], Kellie Jenkinson[1], Bert Weckhuysen[2], Sara Bals[1]
[1]EMAT and NANOlab Center of Excellence, University of Antwerp, Antwerp, Belgium, [2]Inorganic Chemistry and Catalysis group, Institute for Sustainable and Circular Chemistry and Debye Institute for Nanomaterials Science, Utrecht University, Utrecht, Netherlands

PS-05 (1), Lecture Theater 1, august 28, 2024, 10:30 - 12:30

Background incl. aims
Strong metal–support interaction (SMSI) refers to metal nanoparticle coverage by suboxides that are generated from the support under reducing conditions. SMSI may serve as a powerful tool to tune the activity, selectivity, and stability of a catalyst in diverse reactions. Since the pioneering work of Tauster et al. on SMSI in Pt group nanoparticles (NPs) supported on a TiO2 support,1 there have been plenty of studies about SMSI for different catalyst systems, pretreatments and conditions. Recent studies showed that SMSI depends on many parameters, such as temperature and gas composition. For example, Matsubu et al. found that after treatment in 5% H2/N2 at 550 °C for 10 min, a TiOx SMSI crystalline bilayer was formed for Rh-TiO2, while after treatment in 20CO2:2H2 at 250 °C for 3 h, an amorphous SMSI overlayer was induced.2 Frey and co-workers reported that SMSI-induced encapsulation of Pt-TiO2 observed under reducing conditions is lost once the system is exposed to a redox-reactive environment containing O2 and H2.3 Very recently, Monai et al. found that thin TiOx bilayers formed on 111 facets of Ni-TiO2 catalysts during 400 °C reduction, which were completely removed under 1CO2:3H2. Conversely, after 600 °C reduction, the amorphous TiOx overlayers was only partially removed under 1CO2:3H2.4 It is currently still unknown how overlayers evolve with temperature. Moreover, it is yet to be studied systematically how the applied chemical potential affects the SMSI. Herein, through in situ ambient pressure TEM, we studied the effect of the applied chemical potential, including partial pressure of H2, temperature, and temperature rate, on SMSI in Ni-TiO2 catalyst systems.

Methods
Ni catalysts supported on TiO2 (Degussa P25, S.A. = 60 m2/g) were prepared by homogeneous deposition precipitation (HDP) with urea. The system was kept at 95 °C for 20 h under vigorous stirring to induce Ni precipitation via the hydrolysis of urea. Then, the system was washed by centrifugation with water until the pH of the supernatant was neutral. The resulting powders were dried at 60 °C overnight, followed by further drying at 120 °C for 24 h. In situ scanning transmission electron microscopy (STEM) studies were carried out using an aberration-corrected ThermoFisher Scientific Titan Cubed electron microscope operating at 300 kV. The gas and heating nanoreactor comprised two electron-transparent Si3N4 windowed chips and a gas cell holder (climate G+, DENSsolutions). The prepared powder Ni(OH)x/TiO2 was dispersed in ethanol and deposited on the lower climate chip before constructing the climate holder and sealing the nanoreactor. The reduction was performed for 4 h in a 5% H2/He, 50%H2/He or 100% H2 at 400 °C and following the increasing temperature step by step to 600 °C.

Results
The reduction process in 5% H2/Ar is shown in Figure 1a-c. Almost no changes were observed after more than 3 h reduction at 400 °C. When the temperature was raised to 600 °C and held for 48 min, Ni(OH)x was reduced to Ni (as shown in the red dashed square in Figure 1c). Some of the TiO2 support decomposed to small TiOx NPs. Figure 1d-f showed the reduction in 50% H2/He. Ni NPs were obvious at 400 °C only for 37 min. At 600 °C, the Ni NPs sintered significantly and the TiO2 support

was not stable (marked by red dashed square in Figure 1f). These results indicate the importance of the partial pressure of H2 during the reduction and SMSI formation in supported Ni catalysts. Atomic resolution HAADF-STEM images are shown in Figure 1g-j. As we increased the temperature step by step from 400 °C to 600 °C, TiOx bilayers survived at even 600 °C. These results demonstrated that the temperature ramp also has significant effect on the structure of SMSI layers in Ni-TiO2.

Conclusions

Using in situ ambient STEM, we studied the effect of the applied chemical potential, including partial pressure of H2, temperature, and temperature rate, on SMSI in Ni-TiO2 catalyst systems. We found that partial pressure of H2 affects the reduction of Ni(OH)x and the type of the SMSI encapsulation. Although SMSI bilayers survived with temperature increasing, Ni NPs still sintered.

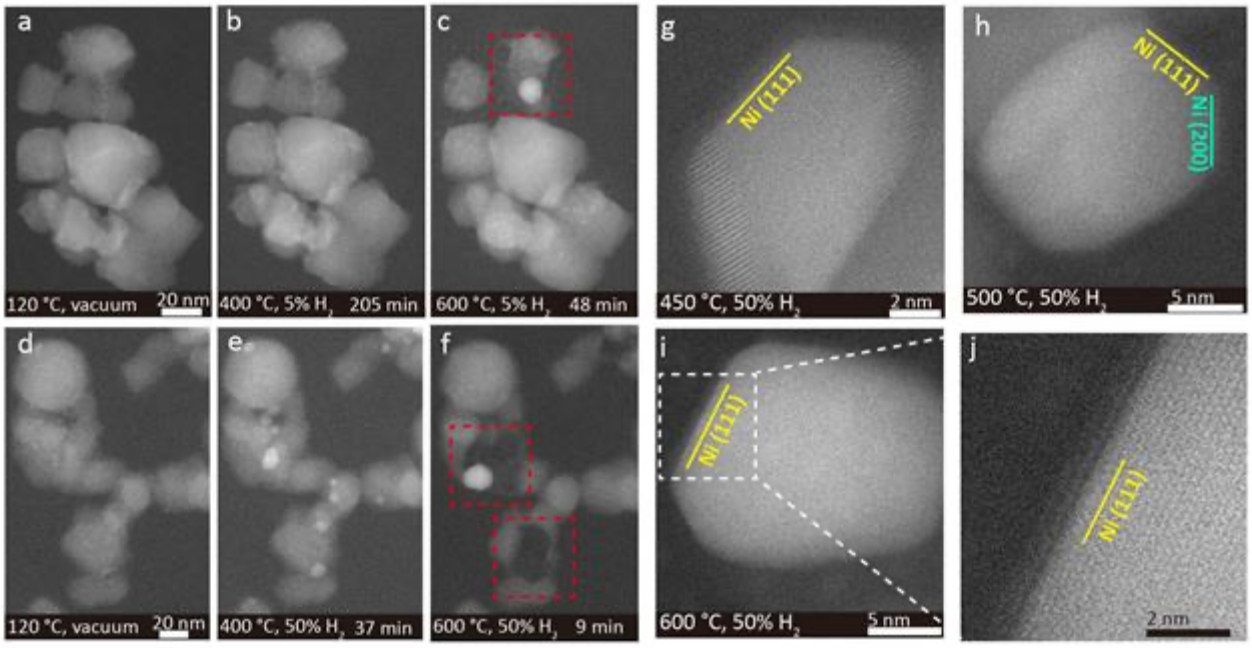

Figure 1. In situ STEM to monitor the reduction and SMSI of a Ni-TiO_2 catalyst in a-c) 5% H_2 and d-f) 50% H_2. HAA-DF-STEM images showing the SMSI at g) 450 °C, h) 500, i) 600 °C and magnified area j) in (i). Ni(111) and Ni(200) facets are indicated by yellow and green, respectively.

Keywords:

SMSI, Ni-TiO2, sinter-resistant, chemical potential

Reference:

1. S. J. Tauster et al., J. Am. Chem. Soc. 1978, 100, 170.
2. J. C. Matsubu et al., Nat. Chem. 2017, 9, 120.
3. H. Frey et al., Science 2022, 376, 982.
4. M. Monai et al., Science 2023, 380, 644.

474

In-situ/ Opernado (S)TEM on Mass Selected Pt Clusters Deposited on CeO2 for CO Oxidation Catalysis

Ajai Raj Lakshmi Nilayam[1], Ramin Shadkam[1], Dr. Carina Maliakkal[1], Mohana Veerraju Kante[1], Prof. Horst Hahn[1], Dr. Di Wang[1], Prof. Christian Kübel[1,2]
[1]Institute of Nanotechnology, Karlsruhe Institute of Technology, Eggenstein-Leopoldshafen, Germany, [2]Karlsruhe Nano Micro Facility, Karlsruhe Institute of Technology, Eggenstein-Leopoldshafen, Germany

PS-05 (1), Lecture Theater 1, august 28, 2024, 10:30 - 12:30

The study of model catalyst systems with mass selected Pt, Pd and Pt-Pd clusters on nanostructured metal oxide supports like CeO2, Al2O3 in exhaust gas environments can be helpful to understand the fundamental processes in catalytic reactions of exhaust gases, to unravel the complex relationship between the structure and the catalytic properties. During a catalytic reaction, the active metal clusters/ particles dynamically change their structure due to the interaction with the gas environment at elevated temperatures. In-situ TEM can be of aid to track the dynamic transient stages involved such as structural or morphological changes of clusters under catalytic reaction conditions. In this work the behavior of size selected Pt clusters (50-200 atoms) deposited on CeO2 support are studied using advanced scanning transmission electron microscopy (STEM) techniques, under pure gas environments (H2, Ar, O2, CO, CO2) and during CO oxidation (with CO and O2 as input gases).

Size selected Pt clusters are deposited using an ultra high vacuum (UHV) cluster ion beam deposition (CIBD) system on top CeO2 thin films, which is deposited on in-situ TEM nanoreactors[1]. Pt clusters are characterized calculating the pair distribution function from 4D-STEM datasets. The morphology changes in the clusters, cluster-support interaction, cluster-gas interaction etc. are studied realtime in pretreatment and exhaust gas environments using in-situ STEM imaging & spectroscopy. The CO2 generation and the level of conversion at different temperatures can be qualitatively studied using high sensitivity residual gas analyzer (RGA).

Figure 1(a) shows the 4D-STEM image of Pt55 deposited directly onto Si3N4. In order to calculate the PDF, it is necessary to substract the background signal of Si3N4 in the reciprocal space. The PDF is calculated by averaging the signal from the whole particle and compared with one another. The integrated PDF of all Pt55 clusters is comapred to the neighbouring distances expected for Pt FCC (Fig. 1). Additionally PDFs are obtained from multislice simulations of Pt55 icosahedra for comparison with experimental PDFs from individual clusters[2].

In-situ (S)TEM on Pt200 supported on CeO2 at pretreatment conditions (oxidation and reduction cycles at 300-500°C) are done and the clusters are found stable at both reducing and oxidative atmospheres. The clusters dynamics under catalytic reaction conditions (in CO & O2 atmospheres) are tracked in-situ at different temperatures from 200-700°C. The RGA showed a constant CO2 partial pressure at all the reaction temperatures, over a conversion of 15%. With continuous imaging, the clusters are found hopping through CeO2, sintering only at 200-300°C. The movement is not identified at higher temperatures when tracked with the electron beam. Clusters in the areas which are not tracked with e- beam are found coalesced, moved to other locations at higher temperatures. This shows that the effect of the electron beam on the reaction sites are inevitable and has to be taken into account during acquisition.

To summarize, the study concentrates on the structural characterization of Pt clusters using 4D-STEM PDF. The results show clear differences from bulk FCC-Pt but resemble towards isomeric shapes. Comparison of PDFs of Pt55 icosahedron at various orientations confirms shift of pair distances and intensity variations according to the changes in diffraction intensities with different orientation. Additionally, in-situ evaluation of the model catalyst system shows changes in the morphology as well as movement and sintering of the clusters on CeO2 under catalytic reaction conditions.

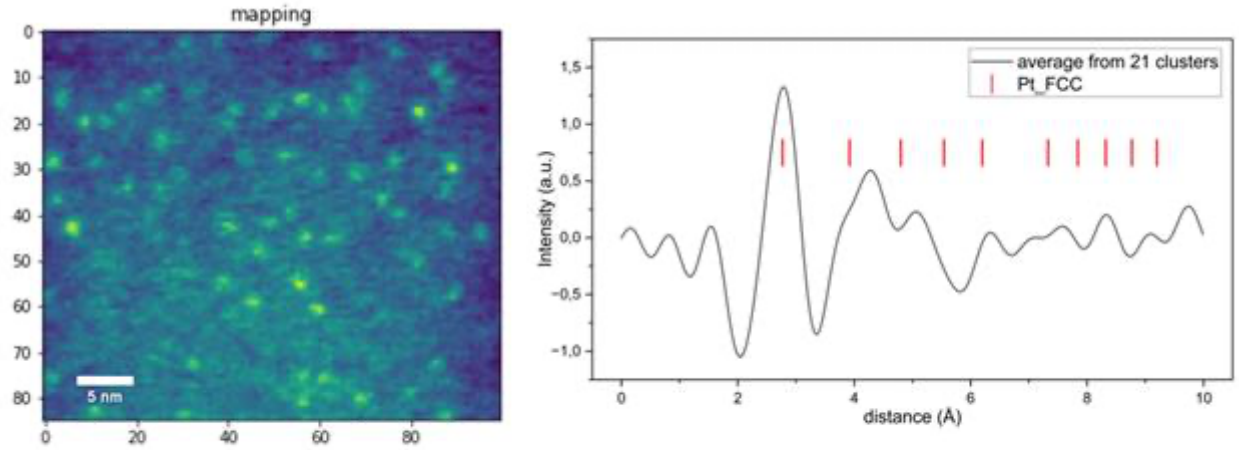

Fig 1: a) 4D-STEM map of Pt_{55} clusters on Si_3N_4, b) Comparison of background subtracted Pt_{55} PDF with Pt-FCC neighbour distances

Keywords:

In-situ, Catalysis, 4D-STEM, CO oxidation

Reference:

1. A. Fischer, R. Kruk, H. Hahn, Rev Sci Instrum 2015, 86, (2), 023304.
2. K. E. A. Batista, M. J. Piotrowski, A. S. Chaves, J. L. F. D. Silva, J. Chem. Phys. 2016, 144, 054310

560

Solid state diffusion as the driving force in the selective oxidation of 2-propanol

Dr. Thomas Götsch[1], Daniel Cruz[1], Patrick Zeller[1,2], Anna Rabe[3,4], Malte Behrens[3,4], Robert Schlögl[1,5], Axel Knop-Gericke[1,5], Thomas Lunkenbein[1]
[1]Fritz-Haber-Institut der Max-Planck-Gesellschaft, Berlin, Germany, [2]Helmholtz-Zentrum Berlin für Materialien und Energie GmbH, Berlin, Germany, [3]Christian-Albrechts-Universität zu Kiel, Kiel, Germany, [4]Universität Duisburg-Essen, Essen, Germany, [5]Max Planck Institute for Chemical Energy Conversion, Mülheim a. d. Ruhr, Germany

PS-05 (1), Lecture Theater 1, august 28, 2024, 10:30 - 12:30

Transition metal oxides are excellent catalysts for the industrially relevant selective oxidation reactions, particularly of alcohols,[1] In the selectively catalyzed oxidation of 2-propanol to form acetone, the spinel cobalt(II, III) oxide (Co_3O_4) exhibits a peculiar behavior, which is expressed by changing the catalytic properties significantly. The changes depend on the temperature: below 200 °C, the catalyst shows high acetone selectivity, but deactivates rapidly, while above 200 °C, stable conversions and steady-state conditions can be reached, at the expense of lowered selectivity due to total oxidation (to form H_2O and CO_2).[2] In addition, once the high-temperature regime has been reached, the low-temperature region gets deactivated completely, but can be recovered by re-oxidation. Thus, it would be beneficial to stabilize the low-temperature regime. However, a prerequisite for being able to accomplish this challenging task is gaining an understanding of the underlying processes. As many phases and states formed during the reaction are metastable, this understanding can only be obtained when the sample is investigated under reaction conditions, i.e. operando methodologies are of great importance. In an operando experiment, the system is exposed to reaction conditions and its performance is measured simultaneously.[3]
Here, we use a combination of operando TEM (OTEM), as well as (operando) near-ambient pressure X-ray photoelectron spectroscopy (NAP-XPS) and near-edge X-ray absorption fine structure (NEXAFS) spectroscopy, combining the spatial resolving power of OTEM with the surface-sensitivity and energy-resolution of X-ray techniques. We employ this multimodal approach to elucidate a network of interconnected diffusional solid-state processes governing the catalytic activity of Co_3O_4 in the selective oxidation of 2-propanol towards acetone.
OTEM was performed on an image-corrected ThermoFisher Scientific Titan 80-300 instrument operated at 300 keV, equipped with a TVIPS TemCam-XF 416R CMOS camera. A DENSsolutions climate in situ holder, connected to a custom gas feeding and detection system,[4] was used. Using a gas saturator filled with anhydrous 2-propanol, and subsequent mixing it with oxygen in a 1:1 ratio, a total reactant pressure of 13.5 hPa was obtained inside the nanoreactor, which was, filled to 450 hPa with helium.
NAP-XPS and NEXAFS measurements were performed at the CAT endstation at the BESSY II electron storage ring operated by the Helmholtz-Zentrum Berlin für Materialien und Energie using the UE48-PGM (soft X-ray) and CPMU17-DCM (tender X-ray) branches of the EMIL beamline.[5] The chamber was backfilled with a 1:1 mixture of 2-propanol and O_2 to a total pressure of 0.5 hPa and photoelectrons were detected using a differentially pumped Specs Phoibos 150 NAP hemispherical analyzer.
The reductive chemical potential of the reaction feed (isopropanol/O2 1:1) induces the exsolution of amorphous CoOx nanoparticles from the spinel, which is already significantly reduced at room temperature. This leaves behind cation vacancies, which cause strong distortions of the Co_3O_4 lattice. The exsolution is self-limiting as both the number of nanoparticles and the lattice parameter remain constant above 100 °C.
Increasing the temperature further causes the vacancies to collapse to voids inside the spinel particles, restoring the (mostly) undistorted lattice, as seen by the linear behavior of the lattice

parameter above 200 °C. The exsolved nanoparticles also start crystallizing as rock-salt-structured CoO at temperatures above 200 °C, as evidenced by SAED and HRTEM. Furthermore, NAP-XPS and NEXAFS measurements reveal a maximum in the cobalt oxidation state at this temperature. Thus, the catalyst is in a frustrated state at 200 °C: at this temperature, the system transits from the low-temperature to the high-temperature activity regime and exhibits the highest selectivity towards acetone. Moreover, cobalt is in its highest oxidation state, the exsolved particles start to crystallize and the cation vacancies coalesce to voids. If the system is cooled down again and a second catalytic run is started, the exsolved and crystallized particles remain, but they are dissolved again during reoxidation.
Using a combined operando microscopic and spectroscopic investigation, it could be shown that the selective oxidation of 2-propanol on Co_3O_4 is accompanied by severe morphological changes and restructuring, which already start at room temperature. Furthermore, the catalyst is strongly controlled by solid state processes such as exsolution, vacancy agglomeration and crystallization. All together, they determine the catalytic properties and are responsible for the transition between the low and high temperature activity regimes.

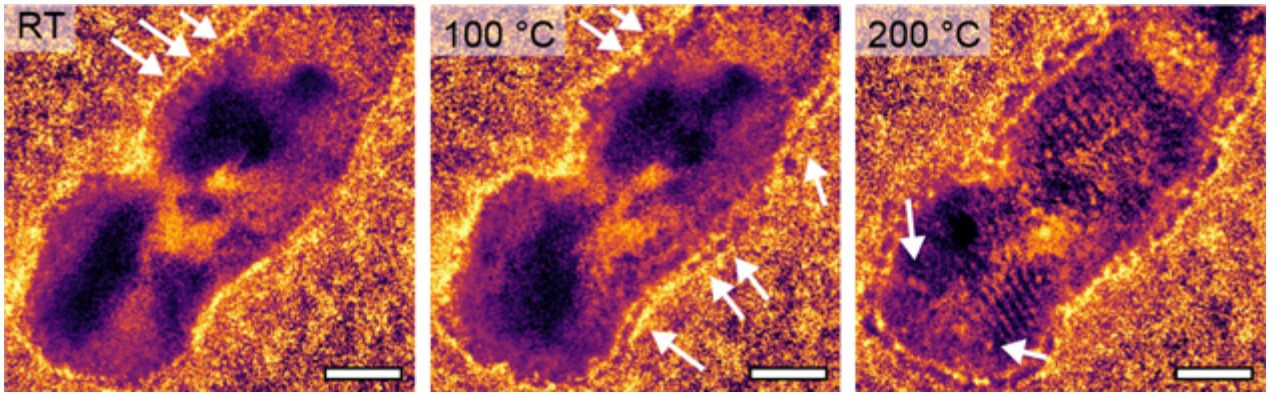

Keywords:

operando; catalysis; cobalt; diffusion; exsolution

Reference:

[1] Najafishirtari et al. Chemistry A European J 2021, 27 (68), 16809–16833
[2] Anke et al. ACS Catalysis 2019, 9 (7), 5974–5985
[3] Bañares, Wachs J. Raman Spectrosc. 2002, 33 (5), 359–380
[4] Plodinec et al. Microsc. Microanal. 2020, 26 (2), 220–228
[5] Hendel et al. AIP Conference Proceedings 2016, 1741 (1), 030038

684

Reactivity of High Entropy Nanoalloys under O2 and CO Oxidation reaction studied by in-situ TEM

Syrine Krouna[1], Jaysen Nelayah[1], Christian Ricolleau[1], Guillaume Wang[1], Hakim Amara[2], Damien Alloyeau[1]
[1]Université Paris Cité, Paris, France, [2]ONERA, Châtillon , France

PS-05 (1), Lecture Theater 1, august 28, 2024, 10:30 - 12:30

Carbon monoxide (CO) contamination has a major input in climate change. An efficient way to reduce its contribution is to oxidize CO into CO2. Therefore, heterogenous catalysis of CO oxidation reaction has been widely studied and many noble metal nanoparticles has been proposed as efficient catalysts. However, considering the price increase of noble metals and their rarity, there is a need to come up with new catalysts that involve less of noble metals. In this perspective, High Entropy NanoAlloys (HENA) represent a new class of catalysts with promising tunable properties. The presence of 5 metals or more crystalized in a solid solution and the mix of noble and non-noble metals allow easily tuning the reactivity and significantly reducing the cost. Moreover, the existence of different reaction sites on the same NP allows HENA to simultaneously activate CO and O2 molecules. Thanks to the synergy of the different elements, these NPs seem to be active at low temperatures but the relation between their complex atomic structure and their reactivity under O2 and CO remains unknown.

In this contribution, we exploit aberration-corrected in situ STEM investigations to reveal the structural and chemical evolution of single CoNiCuPtAu NPs between 100°C and 600° C under O2. The HENA were directly synthesized on the silicon nitride membrane of a MEMS-based gas cell, using pulsed laser deposition, allowing control of both particle composition and size1. Our in-situ gas experiments performed at atmospheric pressure combined atomic-scale STEM imaging with chemical analysis performed by STEM-EDS in an aberration-corrected JEOL ARM 200F TEM, using a Protochips Atmosphere gas/heating holder.

In comparison with our previous in-situ heating experiments of the same HENA performed under vacuum, gas in-situ experiments show that the NP growth, that is governed by coalescence, is slowed down with the presence of O2 and that the NPs are more stable. Unlike NPs annealed under vacuum, under O2 no evaporation was observed and the 5 elements remain in the NPs at high temperature. Nevertheless, we reported structural and morphological changes of the NPs. At 100°C and under 1 atm of O2, we can see reshaping of NP facets as shown in figure 1a. The NPs keep their CFC structure in the core and only the external layer will be oxidized (figure 1a) but, interestingly, at higher temperatures (up to 600°C), the oxide layer will disappear (see figure 1b). The oxidation of HENA also causes the formation of nanovoids in NPs, phenomena known as Kirkendall effect, that we can see in figure 1d. This effect will still be present at higher temperatures and for some NPs, even the coalescence would not allow refilling the holes.

These preliminary results allow us to identify that 100°C is the efficient working temperature of HENA under O2 and showcase that the oxidation occurs only on the external layer of the NPs.
Besides the unexpected Kirkendall effect has motivated an ongoing study of the influence of nanovoids on NPs' reactivity towards CO oxidation.

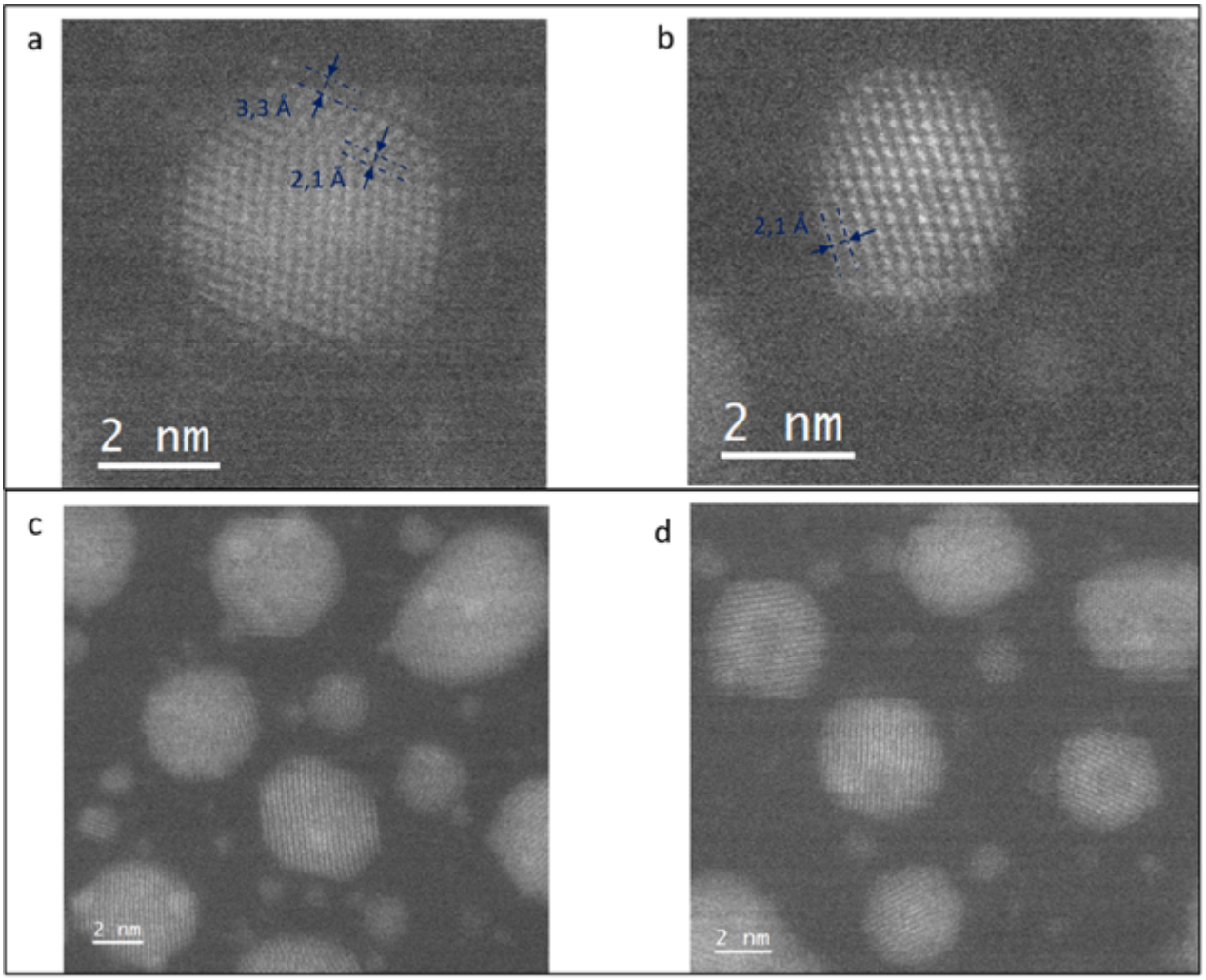

Figure 1 STEM HAADF image showing the morphological and structural changes under O_2 at (a) 100°C and (b) 300°C and the formation of voids in the NPs' core under O_2 : NPs (c) under Ar at 200°C and (d) under O_2 at 300°C

Keywords:

Oxidation, in-situ microscopy, kirkendall effect

Reference:

1. A. Barbero, C. Moreira Da Silva, N. O. Peña, N. Kefane, A. Jaffar, M. Thorey, H. Bouaia, J. Nelayah, G. Wang, H. Amara, C. Ricolleau, V. Huc and D. Alloyeau, Faraday Discuss., 2022

704

In situ ESEM study of supported noble metal nanoparticles dynamics under reaction conditions

Birger Holtermann[1], Jan-Christian Schober[2], Dr. Philipp N. Plessow[3], Prof. Dr. Andreas Stierle[2], Prof. Dr. Yolita M. Eggeler[1]
[1]Karlsruhe Institute of Technology (KIT), Laboratory of Electron Microscopy (LEM), Karlsruhe, Germany, [2]Centre for X-ray and Nano Science, Deutsches Elektronen-Synchrotron (DESY), Hamburg, Germany, [3]Karlsruhe Institute of Technology (KIT), Institute of Catalysis Research and Technology (IKFT), Karlsruhe, Germany

PS-05 (1), Lecture Theater 1, august 28, 2024, 10:30 - 12:30

Supported noble metal nanoparticles (NPs), including Pt, Pd, and PtPd alloys on Al2O3 or CeO2, are pivotal in heterogeneous catalysis for processes like the water gas shift reaction, methanation, and hydrocarbon oxidation/partial oxidation. Maximizing the economic efficiency of these costly metals necessitates catalysts with high activity over their lifetime. A primary challenge to maintaining activity is thermal deactivation via sintering. Two fundamental sintering mechanisms, namely Oswald ripening (OR) and particle migration and coalescence (PMC), have already been identified in the literature. However, recently there has been an ongoing debate about surface vs gas-phase mediated sintering pathways [Ple-16][Oh-23]. To help address this open question we aim to capture real-time, statistically significant data to provide insights into the dynamics of chosen NP/support systems under reactive conditions on a broad micrometer scale using electron microscopy.

While in situ catalysis experiments using electron microscopy were previously carried out only in transmission electron microscopes (TEM) equipped with special holders for heating or gas experiments, allowing the study of single nanoparticles with atomic resolution, recently environmental scanning electron microscopes (ESEM) have become a popular tool to study dynamic catalytic behavior on a broader micrometer scale [Bar-19].
In this work we will introduce our novel in situ experimental setup inside an ESEM using a heating stage, capable of temperatures of up to 1000°C and a self-build gas injection system, thereby enabling the study of large populations of supported NPs and their reaction to experimental stimuli. This experimental setup coupled with an automatic post-processing routine based on computer vision algorithms allows the analysis of long time series of recorded images and permits a statistical evaluation of the NP motion trajectories, thus providing insight into the sintering behavior of these NPs as a function of temperature and gas atmosphere.

Figure 1 shows the main steps of our post-processing routine, which is based on computer vision algorithms and an approach developed by Faraz et al [Far-22] for the environmental transmission electron microscope (ETEM). After acquiring long time series in step 1, NPs are detected in each frame and segmented in step 2. To overcome signal-to-noise limitations, the shape and center of mass of the nanoparticles are approximated in step 3 to better compute motion trajectories by comparing differences in nanoparticle positions from frame to frame in step 4. Not only the motion trajectories can be analyzed in step 5, but also the evolution of the NP size distribution over time.
In contrast to the work of Faraz et al., our routine works on a larger length scale and processes more nanoparticles under the additional constraint that the nanoparticle support has a more homogeneous contrast, making drift compensation based on background registration more difficult.

We will present the first preliminary results of our experimental setup under simplified oxidation conditions of 10mol-% O2 in N2, as well as reduction conditions of 5mol-% H2 in N2 at various temperatures for different NP/support systems. Following up from a previous study in which we

analyzed the redispersion mechanism of Pt/CeO2 under alternating oxidation/reduction cycles ex situ, we will present the results of this redispersion experiment in our new ESEM setup, as well as ex situ characterization of the CeO2 support substrates used in this work [Sch-24]. In addition, we will present our data post-processing routines and discuss some challenges.

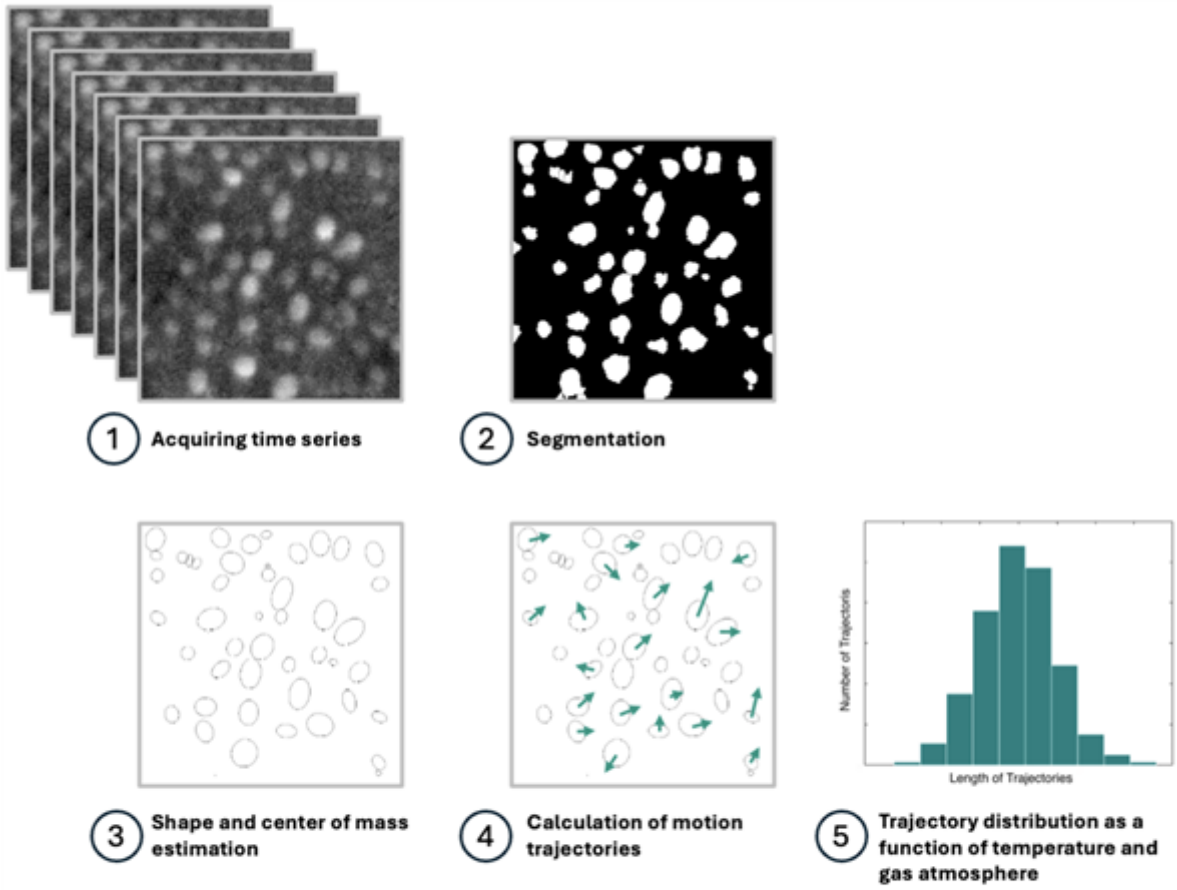

Figure 1: Main steps 1-5 of the post-processing routine. Step 1 shows the acquisition of images as a long time series during the in situ ESEM experiment. In step 2, each acquired image undergoes a segmentation process to separate nanoparticles from the background. Step 3 estimates the nanoparticle shape and center of mass based on the segmented nanoparticle. Step 4 compares each image and calculates motion trajectories for each nanoparticle based on changing nanoparticle position. Step 5 uses the distribution of motion trajectories or particle size distributions as a function of temperature and gas atmosphere to compare experiments.

Keywords:

In situ, ESEM, Sintering, post-processing

Reference:

[Oh-23] J. Oh, A. Beck, E. D. Goodman, L. T. Roling, A. Boucly, L. Artiglia, F. Abild-Pedersen, J. A. Van Bokhoven, M. Cargnello, ACS Catal. 2023, 13 (3), 1812–1822. DOI: 10.1021/acscatal.2c04683.
[Bar-19] C. Barroo, Z.-J. Wang, R. Schlögl, M.-G. Willinger, Nat. Catal. 2019, 3 (1), 30–39. DOI: 10.1038/s41929-019-0395-3.
[Far-22] K. Faraz, T. Grenier, C. Ducottet, T. Epicier, Sci. Rep. 2022, 12 (1), 2484. DOI: 10.1038/s41598-022-06308-2.
[Ple-16] P. N. Plessow, F. Abild-Pedersen, ACS Catal. 2016, 6 (10), 7098–7108. DOI: 10.1021/acscatal.6b01646.
[Sch-24] J.-C. Schober, E. E. Beck, M.-C. Kao, M. Kohantorabi, M. Creutzburg, D. Novikov, B. Holtermann, N. Firman, L. Caulfield, E. Sauter, V. Vonk, C. Wöll, Y. Wang, H. Noei, Y. Eggeler, A. Stierle, March 26, 2024. DOI: 10.26434/chemrxiv-2024-r58cx.

1079

Operando TEM Studies of Re@Cu2O-SnO2 catalysts during CO2 reduction reaction with optimized liquid flow configuration

Ms Cecilia Irene Gho[1,2], Dr Katarzyna Bejtka[1,2], Dr Marco Fontana[1,2], Dr Maria José López Tendero[3], Dr. Alberto Lopera López[3], Dr Roger Miro Serra[4], Dr Miriam Díaz de los Bernardos[4], prof Simelys Hernández[2], Dr Hilmar Guzmán[2], Dr Stefan Merkens[5], prof Andrey Chuvilin[5,6], prof Candido Fabrizio Pirri[1,2], Dr Angelica Chiodoni[1]

[1] Center for Sustainable Future Technologies @Polito, Istituto Italiano di Tecnologia, Via Livorno 60, 10144 , Torino, Itlay, [2]Department of Applied Science and Technology, Politecnico di Torino, Corso Duca degli Abruzzi 24, 10129 , Torino, Italy, [3]Laurentia Technologies Avda. Benjamin Franklin, 12 (CEEI) Parque Tecnológico/ 46980, Paterna (Valencia), Spain, [4]Centro Tecnológico de Catalunya, Eurecat, Campus Sescelades de la URV. Edifici N5 – Marcellí Domingo s/n - 43007, Tarragona, Spain, [5]Electron Microscopy Laboratory, CIC nanoGUNE BRTA, Tolosa Hiribidea 76, Donostia, San Sebastian, Spain, [6]Ikerbasque, Basque Foundation for Science, 48013 , Bilbao, Spain

PS-05 (1), Lecture Theater 1, august 28, 2024, 10:30 - 12:30

Background

The energy transition is nowadays a topic of huge attention, as a measure to face the global energy crisis and the more and more impacting climate change. In this framework, the production of carbon-based chemicals and fuels by exploiting anthropogenic CO2 is nowadays considered a way-out to leave the traditional oil-based technology. In fact, renewable and green approaches to CO2 valorisation are aimed at minimizing the worrying impact of its emission to the environment, and to drive the transition to a new circular economy approach in chemistry and energy production. A strategic method to reduce CO2 concentration in the atmosphere is to consider it as a valuable raw material, collecting it from industrials point sources and electrochemically reducing it into value-added products. This green approach can contribute to the development of alternative energetic vectors, or organic molecules normally derived from fossil resources. Among many products that can be obtained, which depend on the catalyst characteristics, reaction conditions and electrolyte, the CO2 reduction reaction (CO2RR) to carbon monoxide (CO) or formic acid (HCOOH) are up to now the most economically viable processes and can challenge conventional production routes [1]. In order to design efficient catalysts for CO2RR with high activity, selectivity and stability, it is important to understand the fundamental mechanisms involved in the electrochemical processes. In this context, in situ / operando characterization techniques provide insight into the correlation between physical-chemical properties and the electrochemical performance. Specifically, electrochemical liquid phase transmission electron microscopy (EC-LPTEM) yields temporally and spatially resolved morphological, structural and chemical information regarding catalytic materials under electrochemical stimulation [2]. Within this framework, in this paper, EC-LPTEM experiments on molecular Re@Cu2O/SnO2 catalysts for CO2RR are presented and compared to the lab-scale experiments.

Methods

EC-LPTEM experiments are typically carried out in miniaturized liquid cell TEM holders with controlled liquid flow, where the electrochemical functionality may be provided with different technological approaches. Poseidon liquid phase TEM holder and related electrochemical commercial and modified chips have been used to perform EC-LPTEM on a FEI TECNAI F20ST microscope. Molecular Re@Cu2O/SnO2 catalysts for the CO2 electroreduction to syngas have been prepared by wet precipitation of Cu2O/SnO2 followed two functionalization steps with vinyltriethoxysilane (VTES), to form stable surface Si-O bonds, with electropolymerizations on the silanized Cu2O/SnO2-VTES NPs with vinyl-tagged Re complex.

For the EC-LPTEM, a dispersion of the catalyst in ethanol is drop casted on a Glassy Carbon working electrode in a microchip-based electrochemical set-up. This chip, together with an optimized prototype chip, provided by Protochips, are used to compose the electrochemical cell. The catalyst was studied in 0.1M KHCO3 saturated with CO2. The electrochemical activity for the CO2RR was tested by means of CV and Chrono Potentiometry (CP) analyses.

Results

One major challenge in conventional liquid cell TEM setups for CO2RR operando experiments in aqueous electrolyte is that the evolution of gaseous products at the electrodes causes the formation of gas bubbles. Due to the miniaturized volume of the liquid cell, in few seconds the cell is completely filled with gas, in electrochemical conditions which are relevant for CO2RR. Once the cell is filled with gas, the electrolyte-electrode interface is dramatically affected, resulting in uncontrollable experimental conditions and elusive data interpretation. In this work, we use a customised liquid cell geometry with optimized liquid flow configuration, which minimizes the formation of gas bubbles in the liquid cell and concurrently removes the gaseous products more efficiently in electrochemical conditions relevant for operando CO2RR studies in aqueous electrolyte [3], [4].
With this improved experimental capability, we investigated the morphological dynamics during the life cycle of Re@Cu2O/SnO2 catalysts for the CO2 electroreduction to syngas. What emerged is that the catalyst during electrochemical activity experiences dissolution and re-crystallization phenomena, that partially change the particle size and in turn can possibly change the catalytic performance.

Conclusion

In-situ EC-LPTEM helped to shed light on the changes the material undergoes during electrocatalytic activity, and thanks to improved cell we have been able to study this catalyst at relatively wide range of potentials for prolonged periods of time, which are close to those of interest for the applications. The obtained results on the catalysts hold significance from the fundamental point of view, and, in addition, the optimised design of the LP flow TEM cell allowed to perform stability tests, which are of huge interest for the future application of these catalysts in real devices.

Ackowledgements

This work has received funding from the European Union's Horizon 2020 Research and Innovation Action programme under the Project SunCoChem (Grant Agreement No 862192).
The authors gratefully acknowledge Protochips Inc. for providing protype small chips and glass chips to perform the experiments.
This article was also funded under the National Recovery and Resilience Plan (NRRP), Mission 4 "Education and Research" - Component 2 "From research to business" - Investment 3.1 "Fund for the realization of an integrated system of research and innovation infrastructures" - Call for tender No. n. 3264 of 28/12/2021 of Italian Ministry of Research funded by the European Union – NextGenerationEU - Project code: IR0000027, Concession Decree No. 128 of 21/06/2022 adopted by the Italian Ministry of Research, CUP: B33C22000710006, Project title: iENTRANCE.
This study was carried out within the Ministerial Decree no. 1062/2021 and received funding from the FSE REACT-EU - PON Ricerca e Innovazione 2014-2020.

Keywords:

Operando EC-LPTEM, CO2RR, Cu-based catalyst

Reference:

1. Jouny, M. et al. “General Techno-Economic Analysis of CO2 Electrolysis Systems”. DOI: 10.1021/acs.iecr.7b03514
2. Shen T. et al., “Considerations of Liquid-Phase Transmission Electron Microscopy Applied to Heterogeneous Electrocatalysis”, Journal of The Electrochemical Society, 2023 170 056502, DOI 10.1149/1945-7111/acced4
3. Merkens S. et al., “Towards sub-second Solution Exchange Dynamics in Liquid-Phase TEM Flow Reactors”, under revision on Nature Communications, Nature Communications (2024) 15:2522, DOI 10.1038/s41467-024-46842-3
4. Bejtka K. et al., “Electrochemical liquid phase TEM in aqueous electrolytes for energy applications: the role of liquid flow configuration”, under review on Nature Communications, pre-print available on Research Square DOI 10.21203/rs.3.rs-3660145/v1

124

Visualizing alloying in Au-Pd core-shell nanoparticles using in situ gas-phase transmission electron microscopy

Marta Perxés Perich[1], Christopher R. O'Connor[2], Koen M. Draijer[1], Nienke L. Visser[1], Nongnuch Artrith[1], Christian Reece[2], Petra E. de Jongh[1], Jessi E. S. van der Hoeven[1]
[1]Materials Chemistry and Catalysis, Debye Institute for Nanomaterials Science, Utrecht University, Utrecht, The Netherlands, [2]Rowland Institute at Harvard, Harvard University, Cambridge, USA
PS-05 (2), Lecture Theater 1, august 28, 2024, 14:00 - 16:00

Background

The catalytic and optical properties of bimetallic gold-palladium (Au-Pd) nanoparticles (NPs) critically depend on the atomic distribution of the Au and Pd atoms [1]. Under operating conditions, the atomic distribution is highly dynamic. Analyzing gas induced redistribution kinetics at operating temperatures is key in understanding the behavior of Au-Pd nanoparticles but requires advanced in situ characterization strategies. In situ transmission electron microscopy (TEM) allows direct visualization of changes in metal nanoparticles at elevated temperatures and/or upon exposure to reactive gases. So far, several TEM studies on alloying dynamics of core-shell nanoparticles under high vacuum have been reported using EDX (energy-dispersive X-ray) mapping, fast tomography, and atomic resolution imaging [2]. However, these methods are difficult to utilize in the presence of a gas atmosphere because 1) EDX is time consuming and requires a high electron dose rate, which can lead to undesired beam effects, 2) the fast tomography approach is not possible with the current in situ TEM holder technologies, which do not allow tilting at the needed range, and 3) high resolution studies are often limited to only one nanoparticle. Assessing the effect of a gas atmosphere on the alloying dynamics of NPs has therefore remained unexplored and requires new methodologies for extracting the alloying kinetics from in situ gas-phase TEM data.
In this work, we use in situ gas-phase TEM to directly observe the effect of a reducing or oxidizing gas atmosphere on the surface and bulk alloying kinetics of Au-Pd nanoparticles [3]. We developed a methodology to quantify the alloying dynamics of core-shell NPs from high angular annular dark field scanning transmission electron microscopy (HAADF-STEM) images acquired at atmospheric pressure without the need of EDX, fast tomography or atomic resolution imaging, imaging around 35 nanoparticles per gas atmosphere. Using this approach, we assess the NP bulk alloying dynamics from the in situ TEM data and show that the observed alloying dynamics can be predicted using a simple diffusion model based on Fick's second law.

Materials and Methods

The in situ gas-phase HAADF-STEM measurements were performed using a Protochips Atmosphere system and a Talos F200x microscope operated at 200 kV. Prior to beam exposure, the sample was heated to 250 °C in 5% H_2 in Ar for 45 minutes to ensure the removal of water and reduction of oxidized species. During the experiment, the gases (H_2 or O_2, 10% diluted in Ar) were introduced at 1 bar and 0.1 sccm flow rate. The sample was heated to 375 °C for a total amount of time of 1 h, being paused at 18 time points to perform imaging at room temperature. The impact of the temperature on the alloying kinetics was assessed by conducting an additional experiment at 350 °C. The temperature ramp was 10 °C/s and the beam was always blanked at high temperatures. The data were analyzed using custom made python scripts quantifying the intensity decrease of the Pd-shell related grey values over time, thereby indicating progress in the alloying. After the experiment, the Au-Pd NPs were analyzed using EDX mapping in vacuum.

Results and Discussion

The alloying kinetics of the Au-core Pd-shell NPs were monitored through in situ TEM in oxidizing and reducing gas atmosphere. HAADF-STEM images of around 20-25 core-shell Au-Pd NPs (23.8 ± 1.3 nm diameter, 36 ± 5 atomic % Pd) were taken in the course of 1 h exposure at 375 °C under a H_2 or O_2 atmosphere. At time = 0 min, the core-shell structure with the light grey Pd-shell and white Au-core is visible due to the different Z-contrast of Au and Pd, which is lost upon alloying (Figure 1a,b). By monitoring the intensity decrease of the grey values related to the Pd-shell (Figure 1c) and normalizing it over all NPs, we obtain an indication of the kinetics of the alloying process of the whole NP. To validate this approach, we performed an in situ heating experiment under vacuum to be able to follow the alloying process both by EDX and HAADF-STEM imaging. This confirmed that our HAADF-STEM based data analysis correctly quantified the alloying process.
We find that the temperature impacts the alloying kinetics more strongly than a change in gas atmosphere. We verified that the electron beam did not affect the alloying kinetics by imaging 10-15 NPs less frequently, and by performing EDX mapping of irradiated and non-irradiated areas after the experiment. The temperature dependence of the alloying process can be described by a simple model based on Fick's second law. The modeled diffusion behavior at 350 and 375 °C shows good agreement with datapoints derived from the in situ TEM data (Figure 1d). This validates our in situ TEM approach, and it also shows that the modeled diffusion behavior is accurate for nanoparticle systems.

Conclusions

In this work, we quantified the alloying dynamics of bimetallic nanoparticles with in situ gas-phase TEM for the first time. To do so, we followed the loss of the core-shell structure of ~35 Au-Pd core-shell nanoparticles using their difference in Z-contrast in the HAADF-STEM images. The alloying kinetics were highly impacted by a change of temperature and to a lower extend by the gas atmosphere. Quantitative insight such restructuring phenomena at elevated temperatures and in catalytically relevant gasses is critical in understanding changes in the behavior of nanoparticle catalysts under operating conditions.

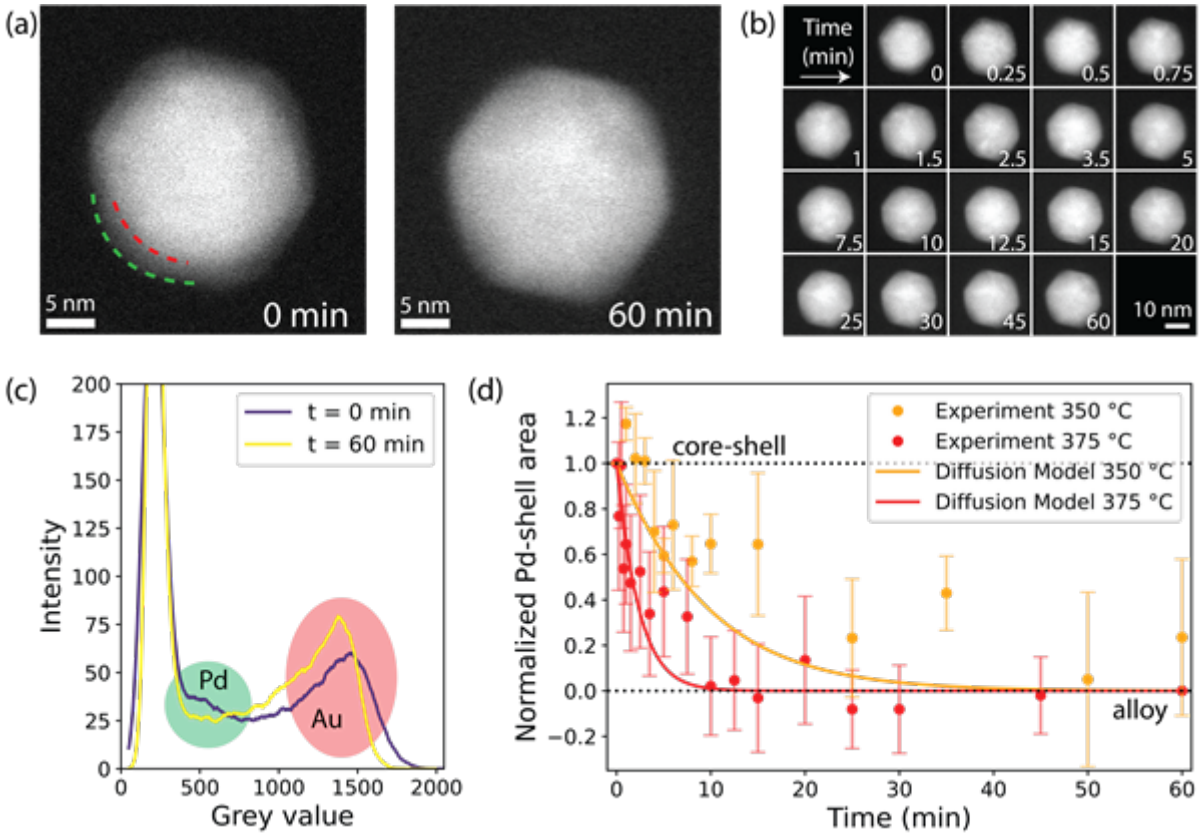

Figure 1. *In situ* STEM visualizing the alloying of Au-Pd core-shell NPs in H_2 (10% H_2 in Ar, 375 °C). (a) Example HAADF-STEM image of a NP at t = 0 min (left), with the red and green dashed lines highlighting the interface between the Au-core and the Pd-shell and the nanoparticle surface, respectively, and at t = 60 min (right), with the alloying process completed. (b) Images of the same NP obtained at different total time at 375 °C (min). (c) Grey-value histograms of the NP in (a) at t = 0 (purple) and t = 60 minutes (yellow), with the Pd and Au-related grey-values marked in green and red, respectively. (d) Normalized Pd-shell area decrease in a 10% H_2 in Ar at 1 bar at 350 °C (orange circles) and 375 °C (red circles), indicating a shift from a core-shell structure to an alloy. The solid lines show the alloying kinetics over time calculated from Fick's diffusion law model at 350 °C (orange) and 375 °C (red). The diffusion coefficients at t = 0 are 3.18×10^{-21} m^2s^{-1} and 1.30×10^{-20} m^2s^{-1} for the diffusion of Pd into Au and 1.73×10^{-26} m^2s^{-1} and 1.11×10^{-25} m^2s^{-1} for the diffusion of Au into Pd, at 350 and 375 °C, respectively.

Keywords:

in-situ-TEM, alloy, core-shell, Au-Pd, bimetallics

Reference:

M. Perxés Perich, et al. ChemRxiv. 2024 (preprint);
J. E. S. van der Hoeven, et al. Nat. Mater., 2021 20, 9, 1216–1220;
J. E. S. van der Hoeven, et al. ACS Nano 2018, 12, 8, 8467–8476;

148

Characterization of functional nanoparticles applied in face masks by STEM-EDX

Charlotte Wouters[1], Marina Ledecq[1], Denrich Morales[1], Khariklia Tsilikas[1], François-Xavier Ouf[2], Eveline Verleysen[1], Jan Mast[1]
[1]Trace elements and nanomaterials, Sciensano, Brussels, Belgium, [2]Laboratoire national de métrologie et d'essais, Paris, France

PS-05 (2), Lecture Theater 1, august 28, 2024, 14:00 - 16:00

Background incl. aims
The unique properties of nanomaterials are being leveraged to create textiles with enhanced fabric properties, a trend exemplified within the production of face masks since the onset of the Covid-19 pandemic. The use of silver (Ag) is advertised in several commercially available face masks because of its biocidal properties, claiming a higher form of protection to the wearer. The silver biocide can present itself either in ionic form, nanoparticle (NP) form or as part of a composite material, however, this is not always correctly advertised[1]. In addition, the presence of titanium dioxide (TiO_2) nanoparticles, acting as a whitening and mattening agent, in synthetic fibres applied in face masks has been demonstrated[2], even when no specific information was provided on their packaging. Since TiO_2 is a suspected carcinogen (IARC 2B) and potential negative health effects are reported for nano-silver[3], their use in masks raises health concerns because of the potential inhalation exposure to nanoparticles. This emerging area of concern lacks methodological development regarding the assessment of inhalation exposure to nanoparticles during mask use. To assess the potential of particle release and associated risks, at first a detailed characterization of the localization and the form of nanomaterials within the mask is necessary. This work applies scanning transmission electron microscopy (STEM) coupled with energy-dispersive x-ray spectroscopy (EDX) on a set of 10 face masks. The method is evaluated in terms of ability to distinguish different nanoforms, to measure particle properties (size/shape/agglomeration state) important in the context of risk assessment in line with the European Union's regulatory framework and to assess potential release of NP.

Methods
A set of 10 face masks, including community, surgical and FFP2 masks, was characterized. 6 masks, where the application of biocides (5 Ag, 1 unspecified) was advertised, and 4 masks, demonstrated to contain TiO_2 (2 of them also had Ag advertised) were selected to assess the form, localization and measurement of Ag (and other possible biocides) and TiO_2, respectively. Since the masks usually consist of multiple layers of fabric, at first the layer with the highest Ag or TiO_2 content was identified using inductively coupled plasma assisted optical emission spectroscopy or mass spectroscopy and selected for subsequent STEM analysis. The mask was disassembled and a piece of 1 mm x 5 mm was cut from the selected layer. The preparation of TEM specimens from the pieces of mask followed the methodology described in Wouters et al.[4] Ultra-thin sections of the textiles were prepared by embedding them in epoxy resin, followed by ultra-thin sectioning using ultramicrotomy. Subsequent STEM-EDX analysis was carried out on a Talos F200S transmission electron microscope equipped with a high angle annular dark field detector and a Super-X EDX detector (Thermo Fisher Scientific, Eindhoven, The Netherlands). Imaging and image analysis was done using Velox software (V3.11, Thermo Fisher Scientific).

Results
In 5 face masks, a form of (nano)silver could be identified. In each of those masks, the silver biocide presents itself under a different form: (i) a silver-silica NP composite, (ii) a reaction mass of silica,

titanium dioxide and silver chloride NP (see graphic), (iii) a silver-zincoxide NP composite, (iv) nanoscale silver precipitation on a mineral complex and (v) NP containing a combination of silver and sulfur or silver and tin. In 4 out of 5 cases, the identified biocide form is not matching the advertized description, which is often ambiguously reported or lacks the mention of a 'nanoform'. In cases (i) and (iii) the silver biocide is embedded within the fibres, while in the other three cases it is at least partly present on the surface of fibres. The amount of silver-containting particles detected in each sample is too low to build a statistically relevant size distribution but their sizes range from 5-200 nm and they have a spheroidal shape.
Even though only 4 masks were selected for evaluation of incorporated TiO_2 particles, TiO_2 was detected innine masks. This was notmentionedon the packaging or in the provided technical information. The TiO_2 appears in the form of aggregates and agglomerates of spheroidal (nano)particles which are embedded within the fibres, and some are also present on the edge of fibres. A preliminary quantitative analysis of TiO_2 in selected samples, reveals an average aggregate/agglomerate size of 186 nm and an average constituent particle size of 100 nm in terms of the minimum Feret diameter, in agreement with the typical textile grade TiO_2[5].
Three masks are found to consist of fibres with a (partial) coating of NP. In one mask this coating consists of a mix of TiO_2 and AgCl NPs embedded within silica (see graphic). The mask with unspecified biocide consists of fibres with a partial coating of agglomerated silica NP with constituent particle sizes on the order of a few tens of nm. And lastly, one mask, which applies a photocatalytic activation of the biocide, consists of a mix of polymer fibres and silica-containing, fibre-like structures. The latter ones have agglomerated TiO_2 particles attached to them, with constituent particle sizes varying from approximately 10 to 50 nm, i.e. smaller than the textile grade TiO_2 reported before. These three masks are considered to be most prone to partice release, based on the localization and amount of observed nanomaterial.

Conclusion
STEM-EDX proves itself as a valuable methodology to allow identification of the type of biocide, the localisation of the (nano)particles and their size measurement within fibres of face masks. Our analyses reveal that packaging labels are often not accurately reporting the type of biocide or nanoparticles applied within the product, highlighting the need for regulatory control. The presence of NP on the fibre's surface presses for investigations of potential release of particles under realistic usage conditions, which will be explored in the next stage of the project.

This project is funded by the ANSES National Environmental Health-Work Research Program with the support of the ministries responsible for the environment, agriculture and labor (ANSES-22-EST-023).

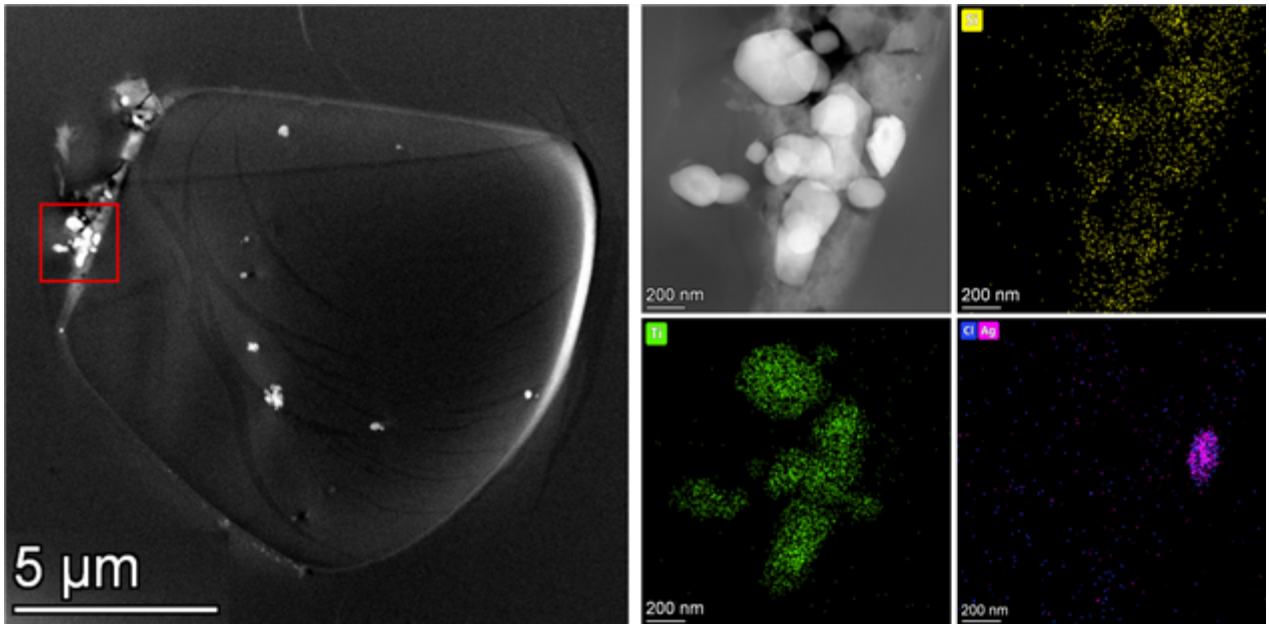

Keywords:

Nanoparticles, biocide, masks, ultramicrotomy, STEM-EDX

Reference:

[1]J. Mast et al., Science of The Total Environment 870, 161889 (2023)
[2]E. Verleysen et al., Scientific Reports 12, 1, 2529 (2022)
[3]Z. Ferdous and A. Nemmar, International Journal of Molecular Scienses 21, 7, 2375 (2020)
[4]C. Wouters, et al., May 2022, PROTOCOL (Version 1) available at Protocol Exchange
[5]Shanghai Liangjiang Titanium Chemical Co., Ltd, http://www.liangjiangchem.com/e25.htm

181

Measuring the Interpretability of High-Resolution Transmission Electron Microscopy Images

William Bang Lomholdt[1], Matthew Helmi Leth Larsen[2], Cuauhtémoc Núñez Valencia[2], Jakob Schiøtz[2], Professor Thomas Willum Hansen[2]
[1]Nanolab, Technical University of Denmark, Kgs. Lyngby, Denmark, [2]Department of Physics, Technical University of Denmark, Kgs. Lyngby, Denmark

PS-05 (2), Lecture Theater 1, august 28, 2024, 14:00 - 16:00

Background
Nanoparticles find uses in a plethora of applications ranging from food preservation and pharmacology to industrial catalysts. Obviously, the first question which is asked when it comes to nanoparticles is the size. However, several aspects of nanoparticles dictate their shape and function. This includes morphology, chemistry, crystallography, oxidation state and environment.
When it comes to providing answers on these topics, transmission electron microscopy (TEM) has been the go-to tool. Modern microscopes easily provide answers on all these topics. However, there are three main challenges. 1) the structure of nanoparticles is not always unaffected by the exposure to high-energy electron beams; 2) to provide statistically relevant information, a large number of nanoparticles should be analyzed; 3) the environment inside the TEM is most often not the same as that where the nanoparticles are used. To accommodate the beam sensitivity, we can lower the electron dose rate to levels where the effect is negligible or otherwise easy to accommodate for. To improve the statistical significance, we can count large numbers of particles and use automated data analysis approaches. Lastly, to image the particles under realistic conditions, we can control the environment in which we image them.

Methods
Here we use environmental transmission electron microscopy to monitor the size, shape and dynamics of nanoparticles relevant for catalytic applications. We focus particularly on gold nanoparticles on cerium dioxide which catalyzes the oxidation of carbon monoxide. Using a CMOS based OneView camera from Gatan, we have acquired data series at varying electron dose rate and under different environments. Using these datasets, we evaluate the signal to noise ratio (SNR) based on different models. Furthermore, we estimate the usability of the structure similarity index measure (SSIM) to detect structural changes of the gold nanoparticles and how prefiltering and adjusting can help our data analysis. We compare these results to measurements performed using data analysis by convolutional neural networks trained on simulated data [1, 2].

Results
Using three models of the signal-to-noise ratio we estimate the interpretability of HRTEM images and rate the measured SNR against the output of data analysis based on convolutional neural networks. SNR(I) is the traditional method of calculating SNR. SNR(II) uses the standard deviation of the nanoparticle and background region separately. SNR(III) takes the high intensity variation of phase contrast images into account. Figure 1 top pane shows images extracted from sequence acquired at increasing dose rate. The bottom pane shows the SNR calculated based on different models showing data from the entire image series. We have further pursued the analysis of Au nanoparticle structure as a function of the environment.

Conclusions
Determining the SNR of an image can tell us something about the interpretability and if it makes statistical sense to continue a more thorough analysis. Here we have attempted alternatives to the

traditional method of determining SNR which may not be well-suited to estimate the interpretability of HRTEM images. We have correlated this with data analysis based on convolutional neural networks.

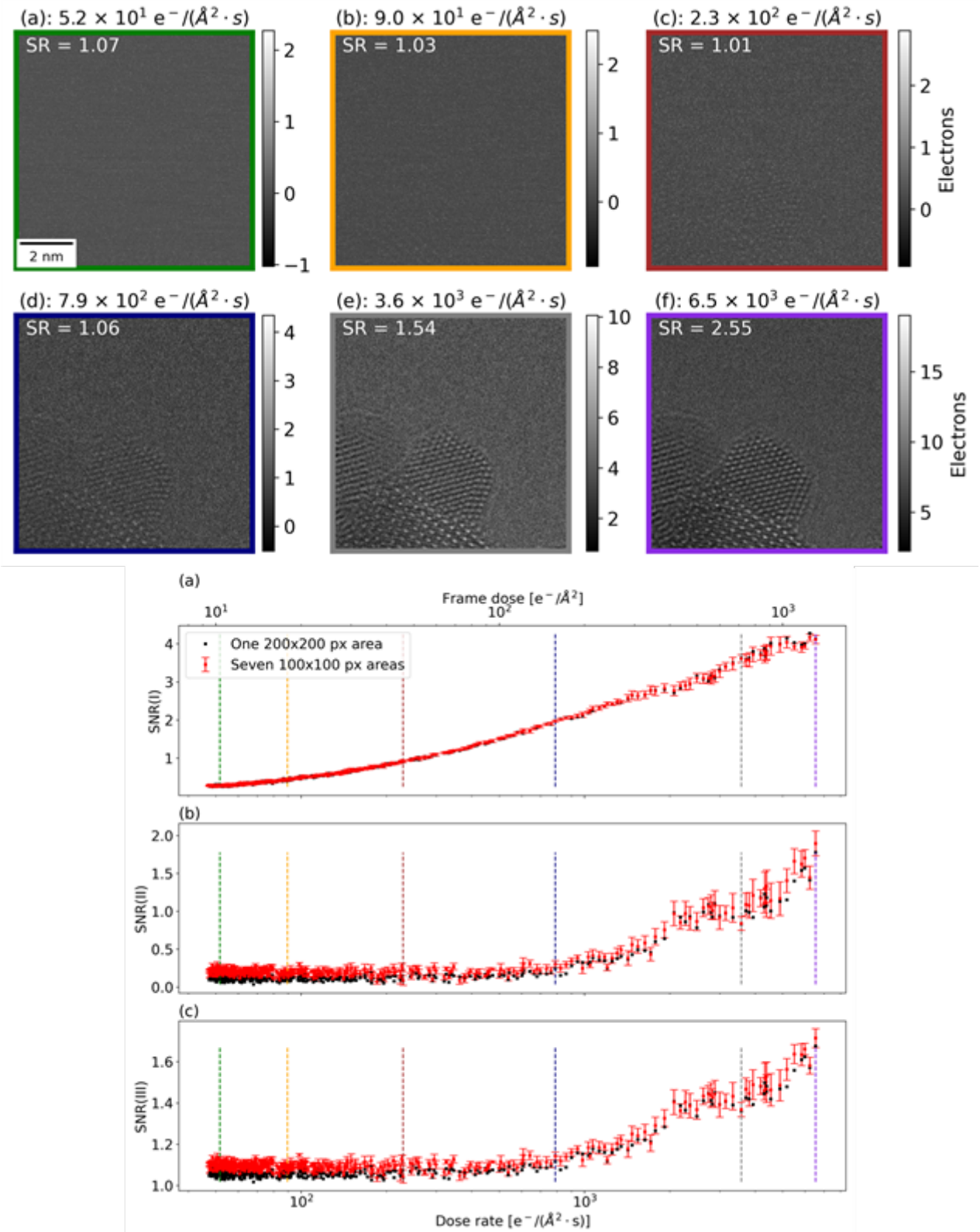

Keywords:

Nanopareticles, TEM, Interpretability, Low-dose

Reference:

1. Madsen, J., et al., A Deep Learning Approach to Identify Local Structures in Atomic-Resolution Transmission Electron Microscopy Images. Advanced Theory and Simulations, 2018. 1(8): p. 12.
2. Leth Larsen, M.H., et al., Quantifying noise limitations of neural network segmentations in high-resolution transmission electron microscopy. Ultramicroscopy, 2023. 253: p. 113803.

199

Surface facet-dependent redox dynamics in vanadium-oxide-based catalysts

Martin Ek[1], Dr. Anita Godiksen[2], Dr. Logi Arnarson[2], Dr. Poul Georg Moses[2], Dr. Søren Ramsussen[2], Prof. Magnus Skoglundh[3], Prof. Eva Olsson[3], Prof. Stig Helveg[4]
[1]Centre for Analysis and Synthesis, Lund University, Lund, Sweden, [2]Topsoe A/S, Kgs. Lyngby, Denmark, [3]Competence Centre for Catalysis, Chalmers University of Technology, Gothenburg, Sweden, [4]VISION, Technical University of Denmark, Kgs. Lyngby, Denmark

PS-05 (2), Lecture Theater 1, august 28, 2024, 14:00 - 16:00

Background incl. aims
Oxide materials play an important role in heterogeneous catalysis, either as functional nanomaterials in their own rights or as supports for other active nanostructures. The reactivity of oxide materials is often attributed to oxygen deficient surface sites. However, the surface motifs can undergo substantial rearrangements that are difficult to predict. A prototypical example of such complex behaviour is VOx/TiO2 catalysts, which are widely used for e.g. selective catalytic reduction (SCR) of NOx emissions. VOx undergoes a redox cycle during the SCR reaction [1], where the possible effect of the supporting TiO2 surface has been much debated. The debate reflects that earlier investigations have not provided definite information on local variations in structure and oxidation state of VOx under catalytic reaction conditions. To overcome this challenge, we present in situ atomic-resolution electron microscopy and spectroscopy observations of VOx/TiO2 catalysts under reducing and oxidizing reactions conditions.

Methods
The investigations focus on a VOx/TiO2 catalyst prepared by impregnation of commercially available TiO2 nanoparticles [2]. The morphology of a single catalyst particle is shown in Figure 1a. The catalyst was investigated using a Titan ETEM instrument [3]. High-resolution transmission electron microscopy (HRTEM) and electron energy loss spectroscopy (EELS) data, for structural and oxidation state analysis respectively, were recorded using low-dose-rate approaches [2,3]. The oxidation states were measured both as an average over multiple particles [2] and locally at individual facets by means of scanning TEM (STEM) [4].

Results
The integrated oxidation state of the VOx/TiO2 catalyst could be reversibly tuned in situ through the V(V)-V(II) range by suitable choice of gaseous environment. For conditions relevant to the SCR reaction (excess O2 with traces of NH3 and NO) an average oxidation state between V(V) and V(IV) was measured, consistent with operando spectroscopic and theoretical investigations [1]. However, the STEM-EELS measurements illustrated in Figure 1b,c revealed that the {001} facets retained oxidation states closer to V(V), whereas {101} facets on the same nanoparticle were almost fully reduced to V(IV). This difference rationalizes previous suggestions of enhanced reactivity for the {001} facets. The difference was consistently found for all nanoparticles investigated [4].

Increasing the reducing potential of the gaseous environment further revealed also reversible structural alterations in the outermost atomic layers of the VOx/TiO2 catalyst; the VOx surface transformed from an ordered to a disordered state concomitant with a reduction to the V(IV)-V(III) range in response to oxygen exchange at the surface. Surprisingly, the restructuring was found to depend on the supporting facet, with {001} facets demonstrating a greater ability to accommodate large changes in oxidation state through its high surface cation mobility, as shown by the changing contrast at the marked atomic columns in Figure 1d [2]. The high-index {10l} showed even more

extensive restructuring, forming rock-salt VO with V(II); this localized highly reduced phase must be accounted for to understand the overall redox behaviour of the supported VOx.[5]

Conclusion

The enhanced reactivity of the (001) facet terminations of anatase TiO2 have been extensively studied for photocatalytic reactions. Whether such properties extend to VOx/TiO2 catalysts, e.g. in relation to low temperature NH3-SCR of NO is addressed here for the first time at the atomic level. Varying cation coordination and density were found to be important factors for explaining differences between facets. This work shows that ETEM/STEM/EELS can be used as a unique tool to discriminate between different structural motifs at the atomic level, even on commercial catalysts.

Graphic

Figure 1. A) TEM overview image of VOx/TiO2 particle. B) EELS show that {001} facets better retain V(V) states. C) HRTEM shows distinct structural rearrangements for the facets.

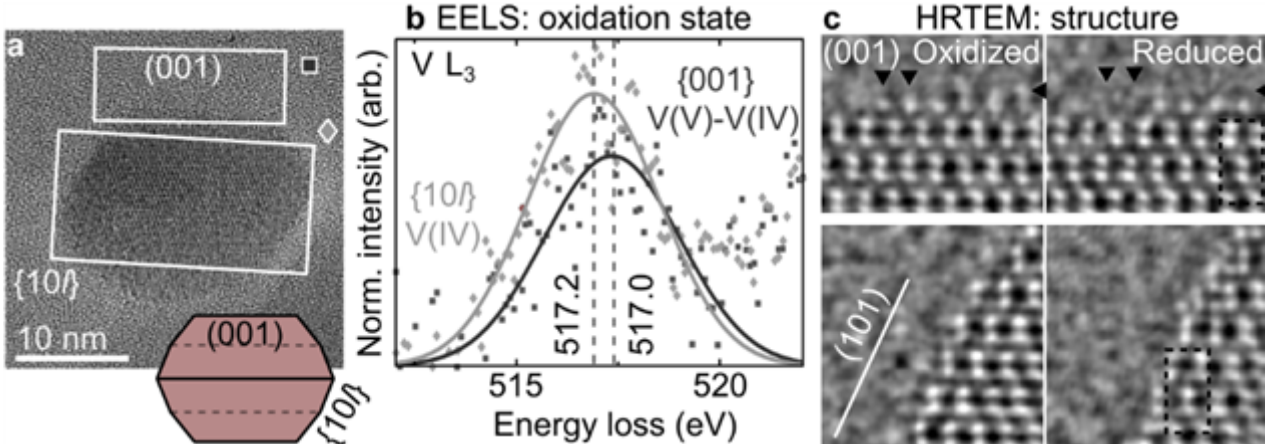

Keywords:

ETEM; catalysis; SCR; vanadia; anatase

Reference:

[1] L. Arnarson et al. J. Catal. 346, 188 (2017)
[2] M. Ek et al. Nat. Commun. 8, 305 (2017)
[3] S. Helveg et al. Micron 68, 176 (2014)
[4] M. Ek et al. Nanoscale 13, 7266 (2021)
[5] M. Ek, A.L. Godiksen, L. Arnarson, P.G. Moses, S.B. Rasmussen, M. Skoglundh, E. Olsson, S. Helveg, Nanoscale 15 (2023) 9503 https://doi.org/10.1039/d2nr07067g.

292

Atomic scale evolution of Ru nanoclusters on graphitic carbon nanofibers in NH3 decomposition reaction

Dr. Yifan Chen[1], Mr Benjamin Young[1], Dr Gazimagomed Aliev[2], Dr Emerson Kohlrausch[1], Dr Andreas Weilhard[1], Mr Thomas Liddy[1], Dr Wolfgang Theis[2], Prof Graham Hutchings[3], Dr Jesum Alves Fernandes[1], Prof Andrei Khlobystov[1]
[1]School of Chemistry, University of Nottingham, Nottingham, United Kingdom, [2]Nanoscale Physics Research Laboratory, School of Physics and Astronomy, University of Birmingham, Birmingham , United Kingdom , [3]Cardiff Catalysis Institute, Translational Research Hub, Cardiff University , Cardiff , United Kingdom

PS-05 (2), Lecture Theater 1, august 28, 2024, 14:00 - 16:00

Abstract
Background incl. aims
Ammonia dehydrogenation is the key process for completing the ammonia-based clean energy production-utilization cycle, and Ru/CeO2 has been known as one of the most active catalysts for ammonia decomposition reaction. Here, the catalytic activity of Ru/graphitic carbon nanofibers (GNFs) not only shows higher activity compared with Ru/CeO2 under the identical condition, but also continues to increase gradually over the time. Understanding the evolution of Ru nanocluster on GNFs (Ru/GNFs) is necessary for developing highly active and durable catalysts for ammonia decomposition reaction.

Methods
Loading of the catalyst onto the Transmission Electron Microscopy (TEM) grid for the Identical Location Scanning TEM (IL-STEM) experiments was carried out as follows: suitable GNFs was drop-cast on a holey carbon-coated Au grid (Agar scientific, H7 finder grids), where Ru nanoclusters were then deposited onto GNFs coated Au grid by magnetron sputtering. Samples are imaged by a JEM-2100F TEM (JEOL, Japan) operated at 200 kV, which is equipped with a spherical aberration (Cs) probe corrector for STEM (CEOS, Germany). The probe convergence angle is 19 mrad and the collection angle range of the annular dark field (ADF) detector is set from 31 to 82 mrad. aberration-corrected STEM (AC-STEM) images are captured with an electron probe size of 8 C and a pixel dwell time of 38 µs with a scanning area of 1024 × 1024 pixel. The bright field (BF) detector is also used in parallel. X-ray photoelectron spectroscopy (XPS) data was collected using a Kratos AXIS Ultra DLD instrument using monochromated aluminium Kα emission at 120 W and a Thermo Scientific K-Alpha X-ray spectrometer with a monochromated aluminium source at 1486 eV.

Results
A series of AC-STEM images of Ru nanoclusters at the identical location GNFs under different conditions have been recorded to track the evolution of the Ru nanoclusters. It clearly shows the sizes of Ru nanoclusters are relatively small and there are some single atoms exist in as-prepared material. After reduction process, the fraction of single atom increased, and the nanoclusters grown with increased size variation. After 3 hours of the ammonia decomposition reaction, the single atoms seem absorbed into clusters. To quantify the evolution of Ru nanoclusters, the images have been analysed with a custom python program. The average size of the Ru nanoclusters increases after the reduction process, from around 1.04 (as prepared) to 1.34 nm, and after 3 hours of the ammonia decomposition catalysis it still maintains around 1.34 nm. The size evolution suggests that the Ru nanoclusters agglomerate during reduction process to reduce the surface energy. Additionally, the nearly identical size of Ru nanoclusters after reduction and under ammonia decomposition reaction indicates that the Ru nanoclusters are stabilized by GNFs.

After reduction, the Ru nanoclusters show hexagonal close-packed (hcp) structure, which is maintained after 3 hours catalytic process. The development of the crystallinity of the Ru nanoclusters during the heating treatment is also validated by IL-STEM observation. The crystallinity of diffuse, almost amorphous Ru nanoclusters increases only slightly after the reduction process, and significantly more after 3 hours of catalysis. To quantify the crystallinity of the clusters, relative intensities of the strongest reflection spots in FFT of the images of different nanoclusters are analysed. The intensity is found to be the strongest for the crystalline, medium for semi-crystalline and low for amorphous forms of the clusters. The crystallinity of Ru nanoclusters during the reduction treatment has shown a general tendency of increasing and further enhancement after 3 hours of catalysis.
As the catalysis of the ammonia decomposition reaction proceeds for a longer period (12 hours), the ratio of single atom decreases further compared with 3 hours, while the average diameter of nanoclusters has not increased further after a longer catalysis time. The development of the hcp structure of the Ru nanoclusters after 12 hours is also validated by AC-STEM observation.
The strong binding energy of nitrogen on metals means that the rate-determining step in the ammonia decomposition reaction is recombination N atoms to N2, while the hcp Ru exhibits the lowest activation energy for the N2 desorption reaction, so it possesses the highest activity compared to other structures for low temperatures ammonia decomposition reaction. By activating the Ru/GNFs catalyst during the reaction process, the Ru nanoclusters evolve into faceted hcp structures, which lead to increased density of B5 sites (catalytic active sites with favourable electronic and geometric properties for rate-determining step). The electronic density on the Ru nanoclusters also increases during the catalysis, which has been indicated by the clear evidence of N present in the spent catalysts.

Conclusions

The Ru/GNFs, where Ru nanoclusters are deposited onto GNFs by magnetron sputtering, has shown as a highly active and self-improving catalytic behaviour for low-temperature ammonia decomposition reaction. A series of AC-STEM images of Ru nanoclusters at the identical location GNFs at different stages of the reaction process have been recorded to track the evolution of the Ru nanoclusters at the atomic level. The data shows that activation of the as-prepared Ru nanoclusters on GNFs at 450 °C induces a structural change from amorphous nanoclusters to the faceted hcp morphology, increasing the density of B5 sites, which are known to serve as active sites and exhibit high activity in ammonia decomposition reaction. This study demonstrates that GNFs stabilize the Ru nanoclusters and B5 sites in hcp structure which is crucial role for the enhanced catalytic activity. These results may open a path for designing highly active and durable catalysts for ammonia decomposition reaction.

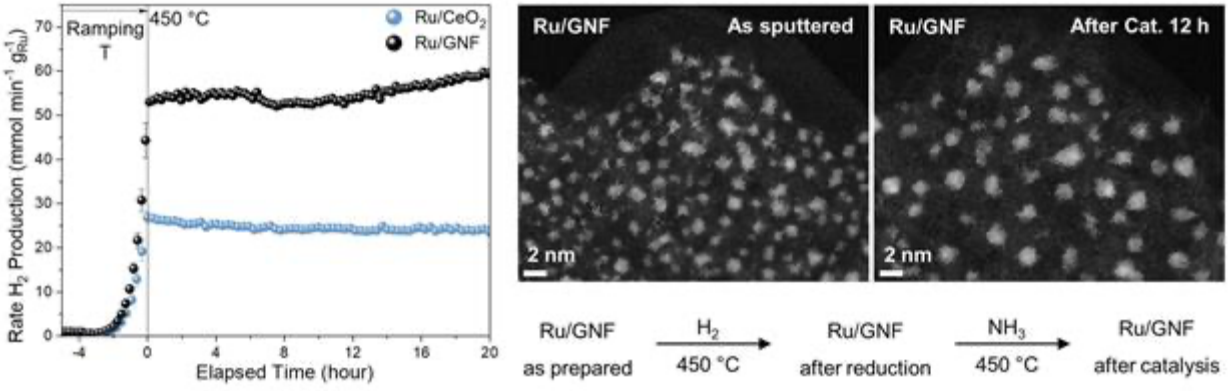

Keywords:

STEM; Ruthenium; Nanoparticles; Catalysis; Carbon.

Reference:

a. Nano Lett. 2023, 23, 17, 8006-8012
b. J. Mater. Chem. A, 2021, 9, 26676-26679
c. Nat. Chem. 2020, 12, 921-928
d. Appl. Catal. A, General 2022, 632, 118484

442

Direct observation of Ni nanoparticle growth in carbon supported nickel under carbon dioxide hydrogenation atmosphere

Nienke Visser[1], Savannah Turner[1], Joseph Stewart[2], Bart Vandegehuchte[2], Dr. Jessi Van Der Hoeven[1], Petra de Jongh[1]
[1]Utrecht University, Utrecht, Netherlands, [2]TotalEnergies OneTech Belgium, Seneffe, Belgium
PS-05 (2), Lecture Theater 1, august 28, 2024, 14:00 - 16:00

Background:
Understanding nanoparticle growth is crucial to increase the lifetime of supported metal catalysts. The recent advances in in situ transmission electron microscopy (TEM) using closed cell nanoreactors, in which samples can be exposed to gas or liquid phase environments, allow the visualization of nanoparticle catalysts under 1 bar gas. This enables the analysis of changes in nanoparticle morphology, size, composition and shape of metal nanoparticles under reaction conditions, which is highly relevant to the field of catalysis.[1]
Nickel-based catalysts are of interest for the conversion of CO2 and renewable H2 into synthetic natural gas (Power-to-Gas process). The catalytic performance in terms of activity is controlled by the available surface area of the metal nanoparticles. The exposure of nanoparticles to reaction atmospheres and elevated temperatures can result in nickel particle growth and activity loss. In this study,[2] in situ gas phase TEM is employed to visualize the movement and growth of ensembles of tens of nickel nanoparticles supported on carbon for CO2 hydrogenation at atmospheric pressure in real time.

Methods:
Carbon supported nickel catalysts were prepared via incipient wetness impregnation using an aqueous Ni(NO3)2 precursor solution, followed by a heat treatment under H2 atmosphere. In situ gas phase TEM was performed at 450 °C under 1 bar H2:CO2 (4:1) atmosphere using a Protochips Atmosphere holder. The results were compared to ex situ experiments, amongst others in a catalytic setup, to study the influence of beam dose, which was kept at a maximum of 20 e- A-2 s-1.

Results:
Various movement and growth mechanisms of a supported Ni catalyst were directly observed in real time under CO2 hydrogenation conditions, using in situ gas cell TEM at 1 bar and 450 °C. During 50 min under reaction conditions, the average Ni particle diameter grew from d = 5.7 ± 1.4 nm to d = 7.7 ± 1.9 nm, while the number of particles decreased from 72 at t = 2 min to 34 at t = 50 min. This correlated to a decrease in specific Ni active surface area from 105 to 78 m2 gNi-1. Comparison of the averaged particle growth within a nickel on carbon catalyst in situ and ex situ validated the relevance of the in situ obtained results.
Furthermore, the in situ TEM experiments enabled the analysis of individual nanoparticles in real time. We observed two modes of particle movement with an order of magnitude difference in velocity: fast, intermittent movement (vmax = 0.7 nm s-1) and slow, gradual movement (vaverage = 0.05 nm s-1). Two distinct particle growth mechanisms were visualized: diffusion and coalescence, and Ostwald ripening. Figure 1A shows the electron microscopy images of particles at selected times with the projected areas of the four particles highlighted in Figure 1B. Figures 1C-F show the evolution of the projected areas of the four particles over time. Particle 2 and particle 3 disappeared due to coalescence with particle 1, highlighted in the purple regions. Interestingly, particle 4 showed different growth behavior. After the first 20 minutes in which particle 1 had grown to ~60 nm2, particle 4 started shrinking, until it completely disappeared after 50 minutes. Hence a striking

interplay between the two mechanisms was observed: first coalescence took place, followed by Ostwald ripening, caused by the increased difference in particle size.

Conclusions:
Our direct visualization of the complex nanoparticle growth mechanisms highlights the relevance of studying nanoparticle growth in supported nanoparticle ensembles under reaction conditions, and contributes to the fundamental understanding of the stability in supported metal catalysts.

Figure 1 - Direct observation of particle growth via coalescence (purple) and Ostwald ripening (green). A) In situ transmission electron microscopy images of carbon supported nickel nanoparticles acquired at t = 2, 20, 22, 24 and 70 min. B) Analysis of the projected areas of individual particles overlayed on the original EM images. The bottom row shows the evolution of the projected area versus time of C) particle 1, where the arrows indicate coalescence with particles 2 and 3, D) particle 2, E) particle 3 and F) particle 4.

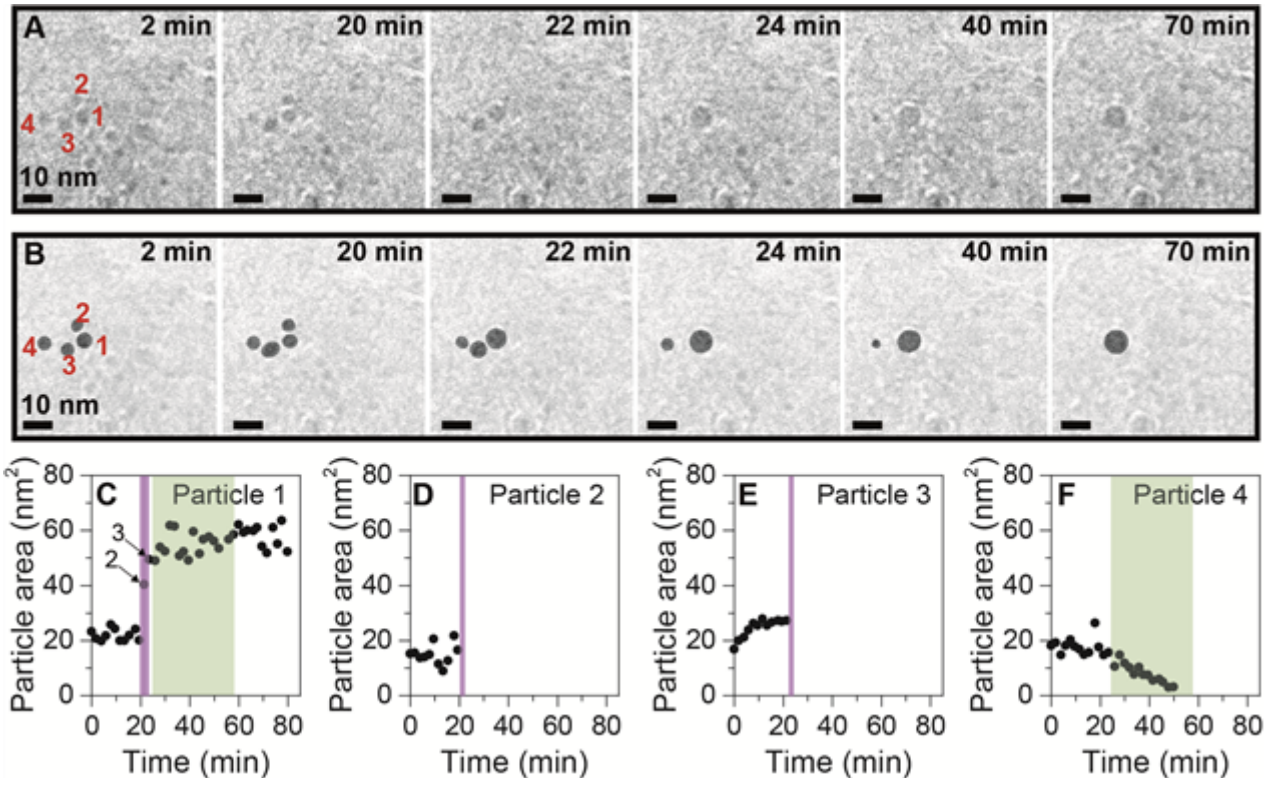

Keywords:

in situ TEM, catalysis, nanoparticle-growth

Reference:

1. L. I. van der Wal, S. J. Turner, J. Zečević, Catal. Sci. Technol. 2021, 11, 3634
2. N.L. Visser, S.J. Turner, J.A. Stewart, B.D. Vandegehuchte, J.E.S. van der Hoeven, P.E. de Jongh, ACS Nano, 2023, 17, 14963–14973

192

TEM Exploration of High-Performance Non-Noble Metal Catalysts for OER

David Llorens Rauret[1], Mr. Ranit Ram[2], Dr. F. Pelayo García de Arquer[2], Dr. Alba Garzón Manjón[1], Prof. Jordi Arbiol[1,3]
[1]ICN2, CSIC and BIST, Bellaterra (Barcelona), Spain, [2]ICFO and BIST, Castelldefels (Barcelona), Spain, [3]ICREA, Barcelona (Barcelona), Spain

PS-05 (3), Lecture Theater 3, august 30, 2024, 10:30 - 12:30

Within the current global energy crisis scenario, the oxygen evolution reaction (OER) has emerged as a pivotal process in vital systems for sustainable energy generation, conversion and storage. However, the demanding 4-electron transfer mechanism of the reaction requires exceptionally high activity levels, currently only achieved by noble metal-based nanocatalysts (1). This limitation impedes the widespread economic adoption of OER systems, restraining advancements in green energy technologies. Consequently, recent research has focused on non-noble metal-based systems such as cobalt tungstate ($CoWO_4$). $CoWO_4$ has emerged as promising and cost-effective noble metal-free catalyst for OER, thanks to its remarkable physicochemical properties (2). Nevertheless, a profound up to the atomic scale comprehension of the catalytic system's structure, underlying reaction mechanisms, and potential degradation and alterations in composition and morphology under harsh OER conditions, requires the use of powerful and sophisticated characterization tools (3).

In that regard, (scanning) transmission electron microscopy ((S)TEM) stands out as an outstanding solution, integrating high spatial resolution imaging with spectroscopy techniques for chemical analysis. Moreover, TEM can be adapted for in-situ experiments, allowing the direct observation of dynamical effects in catalytic systems within their natural or operational environment. Furthermore, additional synchrotron X-ray absorption spectroscopy (XAS) served as a powerful complement to the comprehensive (S)TEM characterization.

In this work, (S)TEM was employed to effectively examine the catalyst's structural and compositional changes during activation, such as the formation of vacancies on its surface. These vacancies are crucial contributors to the observed high activity and stability of the system (4). The results yielded unique information about the catalyst's morphology, which would have been inaccessible through other methods. Furthermore, employing in-situ TEM allowed for initial observations of the catalyst's response to electrochemical bias. Finally, XAS helped to establish a cohesive correlation with the insights gained from TEM analysis.

In summary, the exploration of highly active catalysts for the OER not only unlocks valuable insights into catalyst activity and stability but also correlates it to the system's morphology and composition. This structure-property relationship is crucial for advancing the development of catalytic materials with exceptional efficiency and enduring stability in OER applications, contributing significantly to the progress of cost-effective green energy technologies.

Keywords:

(S)TEM, OER, nanoparticles, catalysis, noble-metal-free

Reference:

1. Y. Wen et al., Nat Commun. 13, 1–11 (2022).
2. P. P. Bagwade et al., Int J Hydrogen Energy. 48, 8465–8477 (2023).
3. L. Liu, A. Corma, Nat Rev Chem. 5, 256–276 (2021).
4. R. Ram (2024) [Submitted].

202

Microstructural evolution of zeolitic nanocrystals for CO2 capture by Environmental in-situ TEM

Dr. Simona Moldovan[1], Mr Edwin Clathworthy[2], Mrs. Kalthoum Nakouri[3], Mrs. Svetlana Mintova[2]
[1]CNRS, Rouen University, Groupe de Physique des Materiaux, Rouen, France, [2]Normandie University, ENSICAEN, Laboratoire de Catalyse et Spectrochimie, Caen, France, [3]TOTALEnergies, Solaize, France
PS-05 (3), Lecture Theater 3, august 30, 2024, 10:30 - 12:30

In the current context of demographic evolution resulting in the considerable increase in greenhouse gas emissions, the academic and industrial community allocates more and more resources to the development of new solutions for capturing, storage and recovery of these undesirable products, the main component of which is carbon dioxide (CO2). Micronsized zeolites such as FAU, LTA or TiSi are currently the most widely used for CO2/CH4 separation, but they have disadvantages such as reduced accessibility of pore volume, slow CO2 kinetics, low regeneration and low cycling, and high costs of organic templates used for their synthesis. In this context, functionalized nanosized zeolites (RHO type) with fully accessible active internal and external surfaces and high crystalline yields were synthesized [1]. Considering the ultimate atomic resolutions (<1 Å) achieved in a TEM, and the in-situ capabilities available nowadays, the in-situ environmental TEM is the only approach able to allow the real-time exploration of the impact of specific parameters such as the gas flow, pressure, temperature on the nanosized crystals evolution upon reactions. It allows the real-time analysis of parameters such as crystal size, the proportion of open/closed pores and/or crystalline facets.
In this study, we focus on and the microstructural changes of nanosized RHO zeolites analyzed by the MET in-situ Environmental under a CO2 flux under high temperatures and pressures.

The STEM-HAADF 2D and 3D observations were carried out on a double corrected Analythical JeolARM 200CF equipped with a Jeol Centurio EDS detector and a Quantum GIF. The in-situ experiments were performed by using an Environmental-Cell from Protochips [2] which has been employed under 1 bar of CO2 flow and for temperature increased from 25 to 900 °C with a heating rate of 10 °C/min. Owing to the high sensitivity of zeolites upon electrons irradiation, the STEM observations were carried out at well-defined temperatures (the beam was turned off during the heating steps).

The RHO nanozeolite was initially heated under Ar at 200 °C, and images under these conditions were taken as references. Maintaining the temperature at 200 °C, CO2 was then contacted with the sample followed by heating and imaging at 700°C, 800 °C and 900 °C. No significant lattice expansion occurs between 200 and 700 °C, when the RHO nanosized zeolite is exposed to CO2. However, the visible expansion of the crystals at 800 °C is consistent with the structural flexibility behavior under air where we observed a substantial increase of the lattice parameter (0.2221 Å) from 700 to 800 °C due to the change in symmetry of the crystalline structure from non-centrosymmetric to centrosymmetric [1]. Superposition of the very same nanozeolite crystals recorded at different temperatures revealed distinct differences in the size of the discrete nanocrystallites. Specifically, the images recorded at 800 °C [3] and 900 °C superimposed with the reference images taken at 200 °C under CO2 show a clear difference in the size of the nanosized crystals, corresponding to an expansion of the particle-matrix by 3 nm and 4.8 nm, or 9% and 15% of the average particle size, respectively. The increase in the volume of RHO crystals was evaluated on the basis of 2D micrographs and corroborated with the exploration of the volume of nanocrystals obtained by electron tomography. The particle expansion between 800°C and 900°C is accompanied by a sharp change of the nanocrystal's microstructure. The crystals morphology remains stable up to 1000°C.

This original study highlights for the first time the flexibility and the microstructural stability of RHO nanosized zeolite at high temperatures under CO2 exposure by in situ HRTEM.

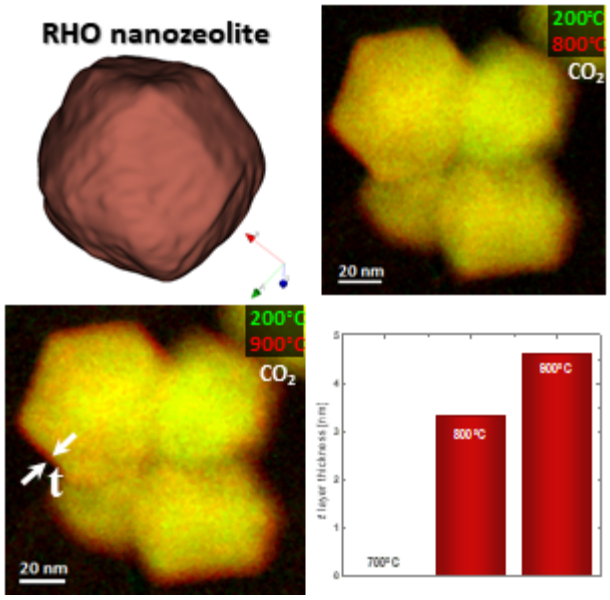

Keywords:

In-situ ETEM-CO2, Flexible RHO zeolites,

Reference:

[1] E. Clathworthy et al., ACS Appl. Energy Mater. (2022), 5, 6032−6042.
[2] https://www.protochips.com/solutions/in-situ-tem-solutions/in-situ-gas-cell/
[3] E. Clathworthy et al., J. Am. Chem. Soc. 2023, 145, 28, 15313–15323.

273

Beam damage and dynamics modelled with equivariant neural networks

Cuauhtémoc Nuñez Valencia[1], Mathias Stokkebye Nissen[1], Patrick Giese[1], Stig Helveg[2], Thomas Willum Hansen[3], Jakob Schiøtz[1]
[1]Computational Atomic-scale Materials Design (CAMD), Department of Physics, Technical University of Denmark, Kongens Lyngby, Denmark, [2]Center for Visualizing Catalytic Processes (VISION), Department of Physics, Technical University of Denmark, Kongens Lyngby, Denmark, [3]National Center for Nano Fabrication and Characterization, Technical University of Denmark, , Denmark
PS-05 (3), Lecture Theater 3, august 30, 2024, 10:30 - 12:30

Background incl. aims
Molecular Dynamics (MD) simulations require a model for the interatomic interactions that is both accurate and computationally inexpensive. Density Functional Theory (DFT) offers good accuracy and decent computational performance for small systems, and ab-initio molecular dynamics (AIMD) is now possible based on DFT. However, many simulations require system sizes and/or simulation times that makes AIMD impossible.

Machine learning potentials can be used to generate inter-atomic potentials for specific systems, with accuracy close to that of DFT and computational efficiency close to that of classical interatomic potentials [1]. While such machine learning potentials have been used to extend the size and time scale of MD simulations to obtain adequate sampling of structures and thermodynamical properties, they suffer from the need of very large training sets and depend on the quality of the rotationally invariant descriptors used as input to the neural networks [2]. Equivariant Neural Networks change this dramatically [3], cutting down the amount of training data by several orders of magnitude while giving better accuracy. In an equivariant network, vector quantities can be used directly as input to the network and are then processed in a rotationally equivariant way.

We apply these methods to two different scientific problems. The first is heating of supported metallic nanoparticles by the electron beam in HR-TEM. The second is thermal vibrations in supported 2D nanoparticles, where recent HR-TEM studies show significantly increased vibrations near the edges of the nanoparticles [4].

Methods
We develop a simulation protocol for training Equivariant Neural Network Potentials (ENNPs) on a limited number of DFT simulations, based on the NequIP package [3]. We gradually expand the training set based on Molecular Dynamics simulations, where we use an ensemble of ENNPs to identify configurations where the uncertainty is large. DFT calculations are then added to the training data, gradually improving the ENNPs. After a few generations, we have a stable ENNP, but can still use the ensemble method to monitor the accuracy, also when simulating systems beyond the size limitations of DFT.

We simulate the heat transport between gold nanoparticles and TiO_2 support. From this we make a simple model for the temperature of the nanoparticle based on the heat deposited by the electron beam and the heat transport into the substrate. Parameters for the energy deposition by the beam are extracted from electron energy-loss spectroscopy (EELS), whereas the heat transport parameters come from the MD simulation.

Results

We simulate the heat transport between gold nanoparticles and TiO_2 support with molecular dynamics and ENNP potentials. We see that thermal transport is limited by the interface between nanoparticle and support, due to the mismatch in phonon frequencies. From this we make a simple model for the temperature of the nanoparticle based on the heat deposited by the electron beam and the heat transport into the substrate. Parameters for the energy deposition by the beam are extracted from EELS data, whereas the heat transport parameters come from the MD simulation [5].

We also simulate thermal vibrations in nanoparticles of the two-dimensional material MoS_2, supported on graphite. We use the simulated vibrational amplitudes as input to HR-TEM image simulations using the multislice algorithm and the frozen phonon formalism for vibrations. We find that edge phonon states significantly increase the vibrational amplitude not just at the edge of the nanoparticle, but several lattice constants away from the edge. This matches well what has been found experimentally by Chen et al. [4], where exit wave reconstructions were used to gauge vibrational amplitudes in HR-TEM image series of supported MoS_2 nanoparticles.

Conclusion
Equivariant Neural Network Potentials make it possible to use molecular dynamics simulations on systems with tens to hundreds of thousands of atoms, with accuracy close to that of DFT, but without the computational cost of DFT, where even a thousand atoms are a challenge. The accuracy of the potentials can be monitored with ensemble methods, and problematic configurations can be used to retrain the ENNP. The method can be directly applied to study effects of the electron beam in HR-TEM, and the role of realistic atomic vibrations in imaging.

Keywords
Equivariant Neural Network Potentials, HR-TEM, image simulation, molecular dynamics, nanoparticles.

Keywords:

Molecular Dynamics, HR-TEM, Machine Learning

Reference:

[1] J. Behler and M. Parrinello, Generalized Neural-Network Representation of High-Dimensional Potential-Energy Surfaces, Phys. Rev. Lett. 98, 146401 (2007).

[2] A. E. G. Mikkelsen et al. Is the water/Pt(111) interface ordered at room temperature? J Chem Phys 155, 224701 (2021).

[3] S. Batzner et al. E(3)-equivariant graph neural networks for data-efficient and accurate interatomic potentials. Nat. Commun. 13, 2453 (2022).

[4] F.-R. Chen et al. Probing atom dynamics of excited Co-Mo-S nanocrystals in 3D. Nat. Commun. 12, 5007 (2021).

[5] C. Nuñez Valencia et al. Beam induced heating in electron microscopy modeled with machine learning interatomic potentials. Nanoscale, 16, 5750 (2024).

547

In-situ STEM-EELS observations on heating TiO2-x nanoparticles for solar and electrocatalytic applications.

Dr Khalil El Hajraoui[1,2], Dr Leonardo Lari[2,3], Mrs Fayzah Talbi[2,3], Prof. Richard Douthwaite[4], Prof Quentin. M Ramasse[1,5], Prof Vlado. K Lazarov[2,3], Dr Demie Kepaptsoglou[1,2]
[1]SuperSTEM Laboratory, SciTech Daresbury, Daresbury, United Kingdom, [2]School of Physics, Engineering and Technology, University of York, York, United Kingdom, [3]Jeol York Nanocentre, University of York, York, United Kingdom, [4]Department of Chemistry, University of York, York, United Kingdom, [5]School of Chemical and Process Engineering & School of Physics and Astronomy, University of Leeds, Leeds, United Kingdom

PS-05 (3), Lecture Theater 3, august 30, 2024, 10:30 - 12:30

Background incl. aims
Titanium dioxide (TiO2) nanoparticles (NPs) are extensively studied due to their versatile applications ranging from photocatalysis [1] and photovoltaics [2] to incorporation into food items as additives [3] . The reduction of these NPs to sub-stoichiometric TiO2-x, e.g., by solar light irradiation, exposure to inert or reducing atmospheres, or doping is garnering significant interest due to the reaction products superior physical properties compared to the unprocessed NPs. For instance, the introduction of Ti3+ species has been shown to prevent the recombination of photogenerated electron-hole pairs in TiO2 resulting in improved photoelectric properties. Similarly, Magneli TixOy based phases are highly desirable as electron transport layer (ETL) in dye-sensitised solar cells thanks to their high electrical conductivity, and chemical stability [4]. Here, we use state of the art in-situ electron microscopy to elucidate the evolution of the atomic structure, chemistry, and electronic structure of TiO2 anatase nanoparticles for ETL and photocatalysis applications.

Methods
We investigate at the atomic scale, the evolution of the microstructure in single-crystal anatase NPs, under variable temperature and in ultra-high vacuum environment, in an aberration-corrected monochromated Nion UltraSTEM100MC – Hermes Scanning Transmission Electron Microscope (STEM) operated at 60kV. The instrument is equipped with a cold field emission source, and can be monochromated down to an energy spread of around 6meV. STEM bright field (BF) and high-angle annular dark field (HAADF) images were acquired by rastering a 1Å corrected probe with a beam convergence half-angle of 30 mrad across the interfaces. The electron energy loss spectroscopy (EELS) spectrum images (SI) were acquired with a probe with an energy spread of 150 meV with a collection half-angle of 22 mrad using a Nion EEL spectrometer equipped with a Dectris ELA hybrid-pixel direct electron detector optimized for EELS acquisition at low acceleration voltages. The in-situ heating experiments were performed using a Protochips Fusion in-situ heating biasing adapter for Nion, and the temperature calibrated thermal E-chips from Protochips.

Results
STEM BF and HAADF imaging was used to observe the formation of extended defects during the annealing process of [111] oriented TiO2 NPs for which the {111} facets are known to exhibit high photocatalytic activity [5]. We observe the continuous growth of Ti2O3 trigonal structures (Fig.1) forming via Σ3 grain boundaries (yellow line) in the three corners of the {111} TiO2 anatase facet and between the Ti2O3 grains at a temperature as low as 300 ^{o}C. The formation of the Ti2O3 trigonal structures was further confirmed by spatially resolved monochromated electron energy loss spectroscopy (EELS) measurements of the Ti L2,3 and O K edges at each stage of the annealing process. Specifically, we observed the change on the Ti L2,3 fine structure in the new domains, with the four characteristic multiplet peaks of the anatase near-edge structure (ELNES) broadening into

two peaks more characteristic of a Ti2O3 trigonal structure alongside a shift toward a lower energy loss position: see Fig.(1,d-e). This ELNES change is known as a fingerprint of a Ti4+ to Ti3+ transition, confirming the imaging observations and the assignment of the newly formed domains to a Ti2O3 phase.

Conclusion

These observations are used to create realistic atomic models of the reduced and anatase phases, and of transitional structures observed during the experiments, which will be critical to develop a more fundamental understanding of possible unique electronic states forming at the Σ3 boundaries and their effect on the electron transport, including charge trapping, and other phenomena.

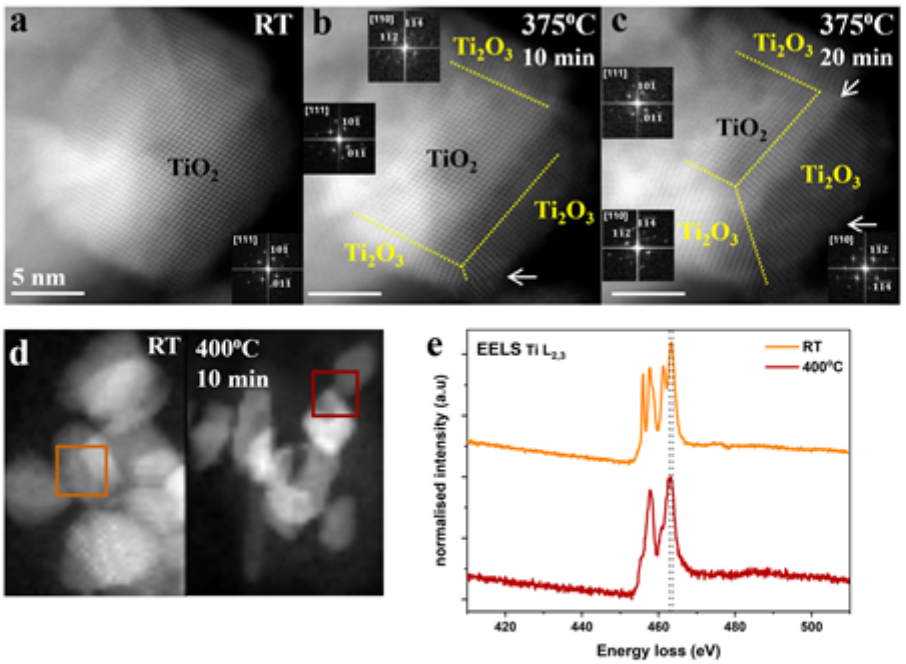

Fig. 1: High resolution HAADF and EELS spectra showing the TiO_{2-x} NP formation below 400 °C. (a) HAADF image of a TiO_2 anatase NP observed along the [111] zone axis as confirmed by the diffractogram (FFT), inset. (b), (c) HAADF images show the coexistence of TiO_2 and Ti_2O_3 domains, separated by Σ3 grain boundaries (yellow line) and between the Ti_2O_3 grains. The Ti_2O_3 grains are oriented along the [110] zone axis as indexed in the FFTs inset. (d), (e) HAADF images of TiO_{2-x} NPs and the EELS spectra of the Ti $L_{2,3}$ fine near-edge structure at room temperature and 400°C, respectively.

Keywords:

EELS, Photocatalysis, Photovoltaic, In-situ

Reference:

[1] J. Schneider et al., “Understanding TiO2 Photocatalysis: Mechanisms and Materials,” Chem. Rev., vol. 114, no. 19, pp. 9919–9986, Oct. 2014, doi: 10.1021/cr5001892.

[2] B. O’Regan and M. Grätzel, “A low-cost, high-efficiency solar cell based on dye-sensitized colloidal TiO2 films,” Nature, vol. 353, no. 6346, pp. 737–740, 1991, doi: 10.1038/353737a0.

[3] U. Blaznik, S. Krušič, M. Hribar, A. Kušar, K. Žmitek, and I. Pravst, “Use of Food Additive Titanium Dioxide (E171) before the Introduction of Regulatory Restrictions Due to Concern for Genotoxicity,” Foods, vol. 10, no. 8. 2021, doi: 10.3390/foods10081910.

[4] W. Fang, M. Xing, and J. Zhang, “Modifications on reduced titanium dioxide photocatalysts: A review,” J. Photochem. Photobiol. C Photochem. Rev., vol. 32, pp. 21–39, 2017, doi: https://doi.org/10.1016/j.jphotochemrev.2017.05.003.

[5] H. Xu et al., “Anatase TiO2 Single Crystals Exposed with High-Reactive {111} Facets Toward Efficient H2 Evolution,” Chem. Mater., vol. 25, no. 3, pp. 405–411, Feb. 2013, doi: 10.1021/cm303502b.

590

Phenomenology of the dealumination in Faujasite Y zeolitic cataysts

Dr Valentina Girelli Consolaro[1], Dr Virgile Rouchon[2], Dr Walid Baaziz[1], Dr Sharmin Sharna[3], Dr Stefan Stanescu[3], Mme Anne-Lise Taleb[2], Dr Gerhard Pirngruber[2], Prof Ovidiu Ersen[1]
[1]Institut de Physique et Chimie des Matériaux de Strasbourg (IPCMS), UMR 7504 CNRS, Stasbourg, France, [2]IFP Energies Nouvelles (IFPEN), Etablissement de Lyon, Solaize, France, [3]Synchrotron SOLEIL, Gif-sur-Yvette, France

PS-05 (3), Lecture Theater 3, august 30, 2024, 10:30 - 12:30

Background incl. aims
The dealumination is one of the most efficient strategies for designing optimized catalysts of zeolite-type [1]. In aluminosilicates such as the zeolite Y, which is a widely employed material in the field of the heterogeneous catalysis, the dealumination involves the removal of Al atoms in the 4-fold coordination (with oxygen) from the crystalline zeolitic framework thus leading to an acquired hydrothermal stability and an interconnected hierarchical porosity [2], which are both beneficial properties in catalytic reactions. Although, the mechanism of structural rearrangement after the extraction of the framework Al atoms (FAL) from their tetrahedral sites turning into extra-framework Al atoms (EFAL), the evolution of the mesopores (pores from 2 to 50 nm of diameter), the elemental distribution of Si and Al as well as the chemical speciation between the FAL and EFAL are still considered as hot topics in the subject [3]. Our study aims indeed to provide an understanding of the phenomenology of the dealumination at the nanometric space resolution by combining different TEM-based approaches.

Methods
For this research work, a series of 4 zeolites Y at subsequent stages of a multi-step dealumination process, mainly obtained by alternating thermal treatments under steam and chemical treatments, was considered. A first hydrothermal treatment (steaming 1, 620°C and 80% humidity) is performed on the commercial CBV300 (Zeolyst) zeolite Y in a reactor and followed by a NH4 ionic bath, a second hydrothermal treatment (steaming 2, 700°C and 80% humidity) and a HNO3 (1M) leaching. These zeolites undergoing such protocol were characterized by Electron Tomography, STEM EDX, STEM EELS together with synchrotron STXM XAS in order to locate the chemical signatures of Si and Al within the grain and correlate with morphological modifications.

Results
The results of the electron tomography highlight the presence of a well developed system of mesopores that is structured in cavities and channels converging towards the core of the grains of zeolites. The facets of the zeolites Y are mainly belonging to the {111} smmetry and the results show the preferential elongation of the mesopores parallelly to the basal facets. Moreover, most of the channeling mesopores propagate at the intersection between two plans of the {111} simmetry. At more advanced steps of the dealumination, the mesoporous network is observed in conjunction with some extra material on the edges of the zeolite, inside its microporous matrix and into the mesopores. This extra-framework material, that is suspected to be amorphous, is associated to a phase enriched in Al as it is observed with the STEM EDX analysis. The characterization by STEM EELS on the K-edge of Al and Si reveals the gradient of these two elements on the edge of the grain and at the mesopore mouth. The Si/Al ratio is provided for this extra-framework material, that we consider as EFSiAl (Extra-Framework Silica Alumina) and, for the first time, related to morphological aspects at the nanometric scale. Moreover, the analysis by STXM XAS on the Al K-edge shows that the signal arising from such areas is mainly tetrahedral, in contrast with the current idea that the EFAl sites are octahedral α-alumina type. These findings could be interpreted by assuming the flexibility of the the

framework and its reversibility to 4-fold Al under experimental vacuum conditions. Although, small traces of 6-fold Al persist in the XAS spectrum and might provide a proof of the difference in terms of structure and stochiometry of the EFSiAl phase.

Conclusion

This study has evidenced the role of the {111} family of plans as preferential symmetry for the development of the mesoporous network within Faujasite Y zeolites during dealumination treatments. At the single crystal scale, the removal of material inside the grain is coupled in parallel with the presence of areas enriched in Al. This is termed as the EFSiAl phase, and it is considered as a collateral product of the dealumination. The EFSiAl is mainly observed at the edges of the grain and inside the mesopore. Contrarily to the expectations arising from the literature which tend to assign to the Al sites of the extra-framework material the 6-coordination, our results show a principal tetrahedral signal even for the Al on the EFSiAl phase.

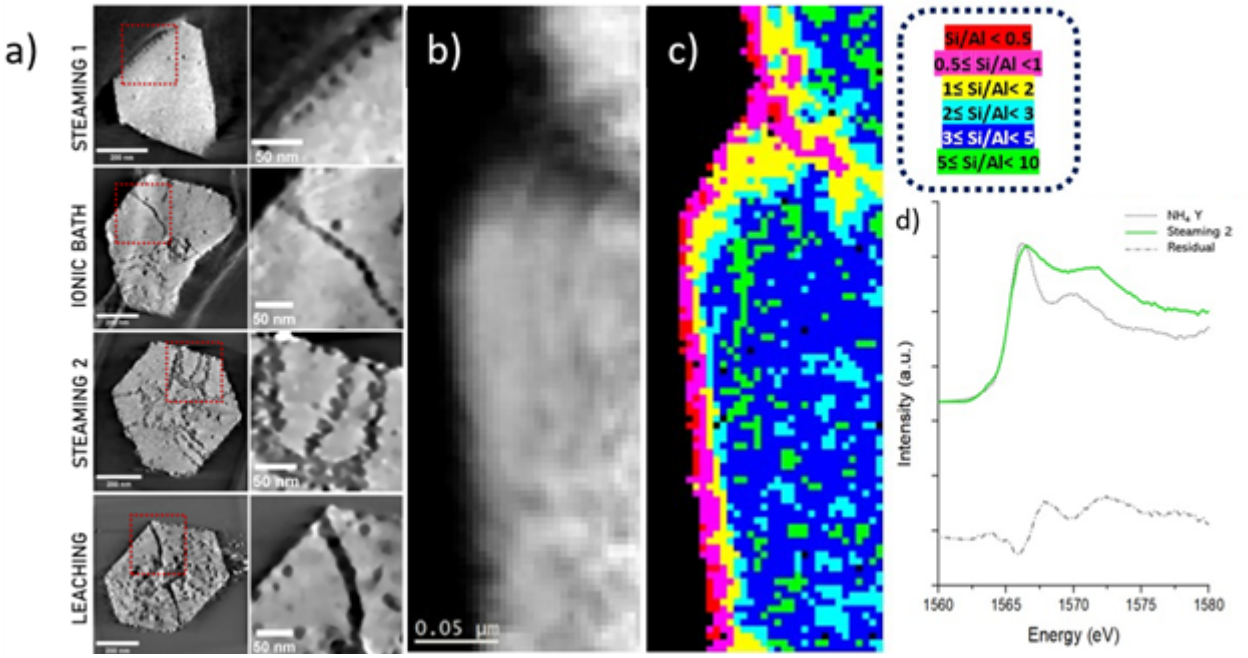

Keywords:

Zeolites, Hierarchical porosity, 3D-TEM, Spectro-Microscopy

Reference:

[1] Verboekend, D., Vilé, G., & Pérez-Ramírez, J. (2012). Hierarchical Y and USY zeolites designed by post-synthetic strategies. Advanced functional materials, 22(5), 916-928. https://doi.org/10.1002/adfm.201102411

[2] Scherzer, J. (1984). The Preparation and Characterization of Aluminum-Deficient Zeolites. In T. E. Whyte, R. A. Dalla Betta, E. Derouane, & R. T. Baker (Eds.), Catalytic Materials: Relationship between Structure and Reactivity 248, 157-200. https://doi.org/10.1021/bk-1984-0248.ch010

[3] Van Bokhoven, J. A., Nabi, T., Sambe, H., Ramaker, D. E., & Koningsberger, D. C. (2001). Interpretation of the Al K- and LII/III-edges of aluminium oxides: Differences between tetrahedral and octahedral Al explained by different local symmetries. Journal of Physics Condensed Matter, 13(45), 10247–10260. https://doi.org/10.1088/0953-8984/13/45/311

639

Quantitative analysis of single-atom support interactions by Deep Learning techniques

Paula Aniceto Ocaña[1], José Marqueses Rodríguez[1], José Antonio Pérez Omil[1], José Juan Calvino[1], Carmen Esther Castillo[1], Miguel López Haro[1]
[1]Departamento de Ciencias de los Materiales e Ingeniería Metalúrgica y Química Inorgánica. Facultad de Ciencias, Campus Rio San Pedro S/N. Puerto Real. 11510. Cádiz, Spain

PS-05 (3), Lecture Theater 3, august 30, 2024, 10:30 - 12:30

Background
The utilization of single atom catalysts (SACs) has captured significant interest due to their superior reactivity compared to nanoparticle counterparts, especially in Environmental Catalysis and Clean Energy applications [1].
SACs can be supported on non-porous structures like oxides or carbon-based materials, or within crystalline porous materials such as zeolites or metal-organic frameworks (MOFs). Their performance is heavily influenced by the local atomic environment and structural characteristics, particularly notable in non-porous materials where surface heterogeneity and defects offer diverse anchoring sites with distinct catalytic performances. Tailoring these characteristics is essential for modulating catalyst reactivity, prompting significant efforts in synthetic methods development and characterization techniques advancement [2]. Notably, High Resolution High Angle Annular Dark Field Scanning Transmission Electron Microscopy (HR HAADF-STEM) emerges as a crucial tool for directly visualizing single metal atoms. However, while its qualitative usage is widespread, quantitative extraction of structural features remains limited [3].
This gap motivates the integration of deep learning algorithms, particularly convolutional neural networks (CNNs), with DFT calculations for a comprehensive and quantitative assessment of metal-support interactions in SACs. In this study, we focus on Pd SACs anchored onto MgO (100) nanoplates, aiming to provide a detailed understanding of their structural features and interactions with the support, crucial for advancing heterogeneous catalysis knowledge and applications in Environmental Catalysis.

Methods
The synthesis of morphology-controlled MgO nanoplates involved a hydrothermal method followed by thermal treatment, resulting in $Mg(OH)_2$ nanoplates that were subsequently heated in a H_2(5%)/Ar flow. Pd-based catalysts were synthesized using two precursors: $Pd(NO_3)_2$ in acetone and an aqueous solution of the coordination complex $[H_3PdL]^{5}$+, with both catalysts prepared via semi-wetness impregnation methods and treated to remove nitrates. Macroscopic characterization included X-ray diffraction using a Bruker D8 Advanced A25 diffractometer, X-ray photoelectron spectroscopy analysis using a Kratos Axis Ultra DLD spectrometer, and electron tomography experiments conducted on a Talos FX200 G2 microscope operated at 200 kV. Transmission and Scanning Transmission Electron Microscopy measurements were carried out on a FEI Titan3 Themis 60-300 double aberration-corrected microscope operated at 200 kV. In particular, HR-HAADF images were acquired with a beam current of 30 pA and a dwell time of 1.25 µs. The Deep Learning algorithm, implemented using Tensor Flow and Keras, involved segmentation using a residual U-net structure for HR-HAADF STEM image analysis. Additionally, DFT calculations using Quantum Espresso with Perdew-Burke-Ernzerhof functional and Hubbard U parameter were performed to assess structural properties

Results

Figure 1a illustrates a representative HR-HAADF STEM images acquired on the Pd catalyst supported on MgO {001} nanoplates, recorded along <211> zone axis. In this orientation, the atomic columns comprise only either Mg or O atoms, allowing to distinguish the nature of the interaction at play.
To precisely quantify these interactions, a smart segmentation procedure leveraging Deep Learning techniques was developed, enabling the accurate discrimination of atomic columns containing Pd single atoms from those containing only Mg. The segmentation process, guided by convolutional neural networks employing the U-net architecture, effectively separates contrasts in HR-HAADF images, Figure 1b. In particular, 900 Pd-support interactions, revealing Pd species adjacency to cationic columns, suggesting substantial interaction with Mg. XPS signals indicate Pd^{2}+ oxidation state, implying Pd species may substitute Mg^{2}+ ions on {001} surfaces, contrasting previous reports of Pd atoms stabilizing on oxygen vacancies.
To unravel the mechanisms underlying Pd-support interactions, we conducted density functional theory (DFT) calculations. These calculations provide an energy differences which suggest a sequence wherein Pd first interacts with V-centers (Mg-vacancies), then likely occupies F-centers (O-vacancies), and finally resides atop the surface, aligning with experimental observations, indicating Pd species localized within Mg atomic columns.
Detailed structural analysis of relaxed models reveals that Pd atoms tend to move slightly into the surface or outside the center in the case of F-centers, while in V-centers, the displacement is subtler, highlighting distinct behaviors in Pd localization within defects. A method, using AtomSegNet, achieves sub-pixel precision, measuring displacements accurately. This approach maps displacement vectors and modulus, enabling precise measurement of shifts from 0.1 to 0.6 Å, Figure 1c. The histogram fitting reveals peaks at 0.17±0.07 Å and 0.45±0.12 Å, matching DFT-calculated values for V and F centers. A 3:1 ratio in Gaussian curve areas indicates more atoms with smaller displacement, consistent with theoretical predictions. Considering MgO support properties, metal loading, and V-to-F ratio, an estimated 1% cationic vacancies align with literature findings for powder MgO.

Conclusion

The methodology's strong validation is evidenced by the close agreement between experimental image analysis and computational predictions, providing unprecedented insights into metal-support interactions in high-surface area powder catalysts. Direct imaging reveals that Pd species preferentially stabilize within surface-located V-centers on MgO supports, a significant advancement in SAC structural analysis. The method's robustness is further underscored by alignment with macroscopic techniques like XPS, enhancing confidence in conclusions drawn from the synergistic integration of advanced AC-STEM, AI analysis, and computational approaches. Its application to diverse catalytic materials promises to uncover general principles governing metal-support interactions, advancing both fundamental and applied catalysis research.

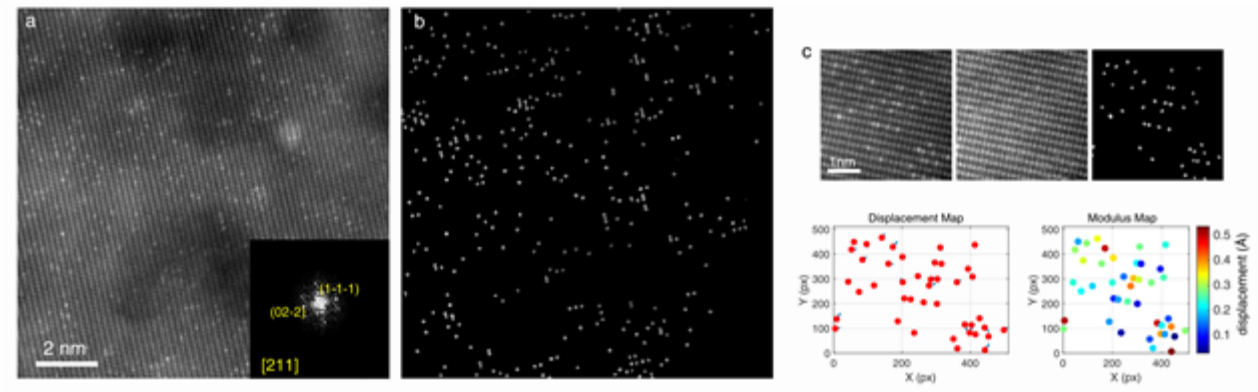

Keywords:

Single-atoms, HR-HAADF, Deep Learning, DFT

Reference:

1. Ding, S. P., Hülsey, M. J., Pérez-Ramírez, J. & Yang, N. Transforming energy with single-atom catalysts. Joule 3, 2897-2929 (2019).
2. Mitchell, S. & Pérez-Ramírez, J. Atomically precise control in the design of low-nuclearity supported metal catalysts. Nat. Rev. Mater. 6, 969-985 (2021).
3. Liu, L. C. & Corma, A. Metal catalysts for heterogeneous catalysis: From single atoms to nanoclusters and nanoparticles. Chem. Rev. 118, 4981-5079 (2018).

1001

Dynamics of an industrial Cu/ZnO catalyst revealed by operando TEM

Maxime Boniface[1], Thomas Götsch[1], Jinhu Dong[1], Elias Frei[1], Annette Trunscke[1], Robert Schlögl[1,2], Beatriz Roldàn Cuenya[3], Thomas Lunkenbein[1]
[1]Fritz-Haber-Institut der Max-Planck-Gesellschaft, Department of Inorganic Chemistry, Berlin, Germany, [2]Department of Heterogeneous Reactions, Max-Planck-Institute for Chemical Energy Conversion, Mülheim, Germany, [3]Department of Interface Science, Fritz Haber Institute of the Max Planck Society, , Berlin, Germany

PS-05 (3), Lecture Theater 3, august 30, 2024, 10:30 - 12:30

Introduction
Cu/ZnO catalysts have been used since the mid-1960s for both the water-gas shift (WGS) reaction and methanol synthesis. The key to understanding the activation, performance and deactivation of this catalyst system seems to lie in the delicate interplay between the formation of a CuZn alloy phase and the wetting of Cu nanoparticles by ZnOx after partial reduction through strong metal-support interactions (SMSI) [2,3]. The highly dynamic nature of the catalyst requires the use of in situ techniques. Using operando transmission electron microscopy (TEM), we aim to provide unprecedented insight into the morphological and structural evolution of an industrial catalyst during reductive activation and in CO2 hydrogenation conditions. These results are compared to model Cu/ZnO thin film heterostructure and Cu2O nanocube catalysts.

Materials and Methods
The catalyst (Cu/ZnO/Al2O3) was synthesized by calcination of a zincian malachite precursor with a Cu:Zn ratio of 70:30 and 3 mol % Al, following a protocol published previously. A sample was mounted in a DENS Climate environmental TEM holder, which was connected to our homebuilt gas feed setup. Selected area electron diffraction (SAED) temperature series were corrected for astigmatism [5], enabling us to track small lattice parameter changes and phase fractions from Rietveld refinement with the fast time resolution of SAED.

Results
The calcined sample is first activated (pH2 = 79 mbar, 10% H2, 4K.min-1) during a 2-step process involving the segregation of CuO NPs from a decomposing (Cu,Zn) carbonate phase from 110°C to 200°C, then reduction and sintering of these NPs from CuII to Cu0. A CuI intermediate is detected as well between 200°C and 250°C, with all 3 oxidation states co-existing at these temperatures until only Cu0 remains after 2h at 250°C. The final morphology consists of a network of Cu metallic nanoparticles linked by wurtzite ZnO. This was confirmed by in situ STEM-EELS measurements. A ZnOx overlayer, is sporadically observed after the reduction is complete after 2h at 250°C. Cooling the sample to 50°C then reveals a much fuller coverage, indicating that the overlayer is not stable at high temperatures and forms reversibly.

Observations in MeOH synthesis conditions (H2:CO2:He = 3:1:0.5) and reverse water gas shift (rWGS) conditions (H2:CO2:He = 1:1:0.5), shed tremendous insight into how Cu wetting by ZnOx is mediated by temperature as well as H2 and CO2 partial pressures through a delicate balance of Cu-Zn alloy formation and reoxidation on Cu NPs surfaces [5]. rWGS products (CO and H2O) were detected alongside these observations.

Increasing the temperature to 400°C showed a sudden increase of the Cu lattice parameter above the thermal expansion baseline, indicating CuZn alloy formation. Remarkably the lattice parameters

then levels off over 30 minutes. This corresponds to a delayed increase of the water content in the reactor, suggesting that water plays a critical role in the reoxidation of Zn in the catalyst, and demonstrating the transient nature of CuZn alloys in this system.

Conclusion

In summary, extensive operando TEM experimental capabilities were leveraged to shed unprecedented insight into the morphological and structural evolution of Cu/ZnO catalysts during CO2 hydrogenation. Coupling mass spectrometry, electron diffraction and imaging yields a comprehensive description of the activation and reaction process. Altogether our results suggest that a frustrated phase transition between CuZn alloy and Cu-ZnO surface states, rather than one of the two being more active, could be key to the high performance of CZA catalysts for methanol synthesis.

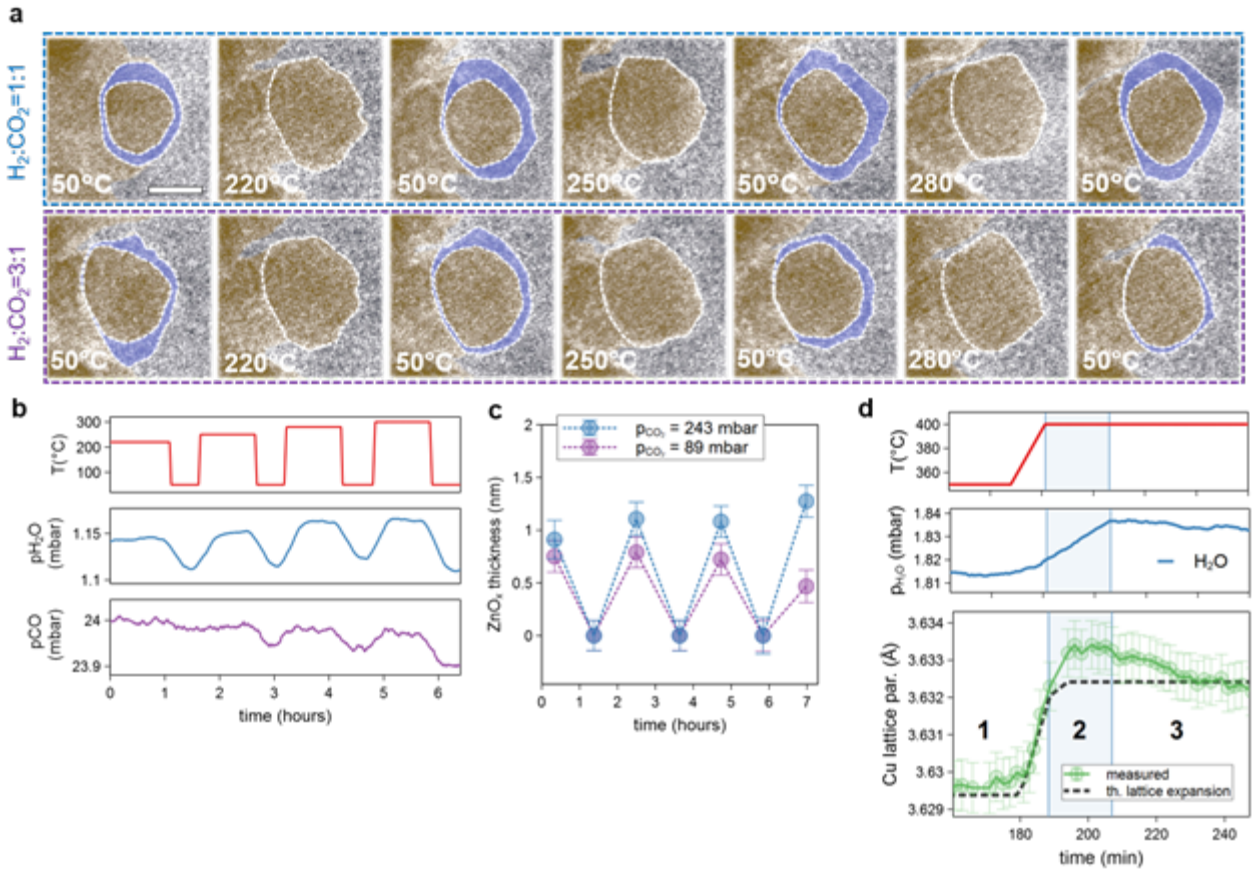

Keywords:

Operando; catalysis; SAED; diffraction; EELS

Reference:

1. A. Olah, A. Goeppert, G. K. Surya Prakash, in “Beyond Oil and Gas: The Methanol Economy”, Wiley-VCH, Weinheim, 2006.
2. Lunkenbein, T., Schumann, J. et al., Angewandte Chemie 54, 15 (2015).
3. Amann, P., Klötzer, B. et al., Science 376, 6593 (2022).
4. Schumann, J., Lunkenbein, T. et al. ChemCatChem 6, 10 (2014).
5. Frisch, B., Wu, M., Ultramicroscopy 235 (2022)

1046

Measurement of atom mobility of gold nanorods via coarse-sampling in quantitative 4D-STEM

Mr Cheng Zhao[1], Ms Zhi Tong Liew[2], Dr Bryan David Esser[3], Dr Alison Funston[2], Prof Joanne Etheridge[3,4]
[1]Department of Material Science and Engineering, Monash University, Clayton, Australia, [2]School of Chemistry, Monash University, Clayton, Australia, [3]Monash Centre for Electron Microscopy, Monash University, Clayton , Australia, [4]School of Physics and Astronomy, Monash University, Clayton , Australia

PS-05 (3), Lecture Theater 3, august 30, 2024, 10:30 - 12:30

Metal nanoparticles have attracted significant interest due to their distinctive properties which show significant potential in applications including drug delivery, chemical sensing, and biological imaging. A common method for synthesizing such nanoparticles is wet chemical synthesis; however, despite decades of development in synthetic methodologies, the precise mechanisms governing symmetry breaking and shape modification of these particles remains ambiguous and subject to debate. It is widely recognized that the introduction of different surfactants affects nanoparticle morphology.

In this work, we aim to study the influence of surfactants on the surface energies of nanoparticle facets. Our approach uses quantitative scanning transmission electron microscopy (STEM) to obtain a measure of surface mobility — as a proxy to estimate surface stability and hence energy [3]. We investigate the optimum set of parameters, including course sampling, for acquisition of a four-dimensional STEM dataset, such that the location and number of atoms in each atom column can be accurately determined while minimizing the electron dose. We quantify dose versus accuracy across these different parameter sets.

We apply these parameters to investigate the relationship between dose and atom mobility on a gold nanoparticle, with the use of double aberration-corrected microscopes (FEI Titan3 80-300 FEG TEM and a newly installed Thermo Fisher Scientific Spectra ϕ FEG TEM) (see Fig.1). We further apply this to measure surface mobilities on different gold nanoparticle morphologies.

This approach aims to offer insights into the fundamental processes underlying nanoparticle synthesis and shape evolution, paving the way for tailored nanoparticle design and optimization in various applications.

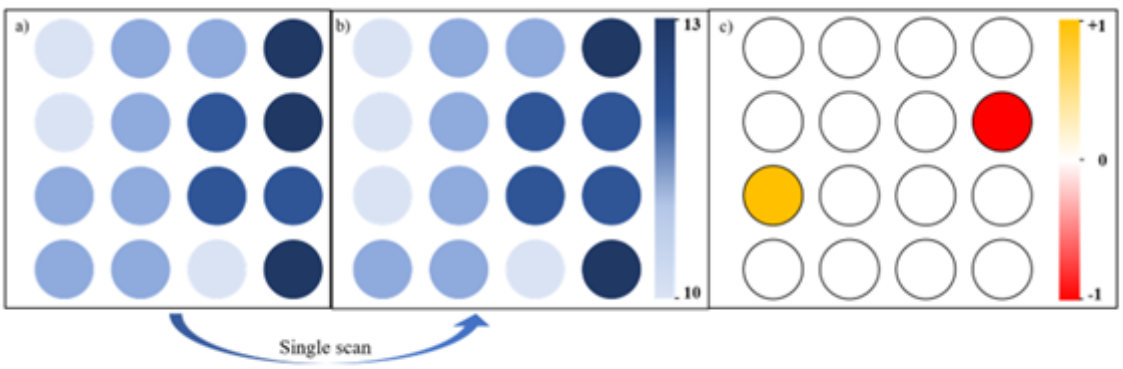

Figure 1. ***Schematics for the determination of facet mobility****. a) and b) two consecutive 4D-STEM scans with known electron doses, and c) difference in number of atoms in each atom column. The mobility of the atoms on this facet can be measured as the energy of one scan under which one atom movement can be detected.*

Keywords:

4D-STEM, nanoparticles, surface mobility

Reference:

[1] Luis M. Liz-Marzán. (2024). Materials Today, 7 (2), 26–31.
[2] Ophus, C. (2019). Microscopy and Microanalysis, 25(3), pp. 563-582.
[3] H. Katz-Boon, et al. (2015). Nano Letters, 15, 1635.

110

Confined single-molecule imaging by low-dose electron microscopy

Huiqiu Wang[1,2], Prof. Xiaodong Zou[1]
[1]Department of materials and environmental chemistry, Stockholm University, Stockholm, Sweden,
[2]Department of chemical engineering, Tsinghua University, Beijing, China

Poster Group 2

Single-molecule imaging with atomic resolution is a notable method to study various molecular behaviors and interactions. Although low-dose electron microscopy has been proven effective in observing small molecules., it has not yet helped us achieve an atomic understanding of the basic physics and chemistry of single molecules in porous materials, such as zeolites. The configurations of small molecules interacting with acid sites determine the wide applications of zeolites in catalysis, adsorption, gas separation, and energy storage. Here we report the atomic imaging of single pyridine and thiophene confined in the channel of zeolite ZSM-5. Based on integrated differential phase contrast scanning transmission electron microscopy (iDPC-STEM), we directly observe pyridines or thiophenes' adsorption and desorption behaviors in ZSM-5 under the in situ atmosphere. The adsorption configuration of a single pyridine or thiophene is atomically resolved and the S atoms in thiophenes are located after comparing imaging results with calculations. The strong interactions between molecules and acid sites can be visually studied in real-space images.

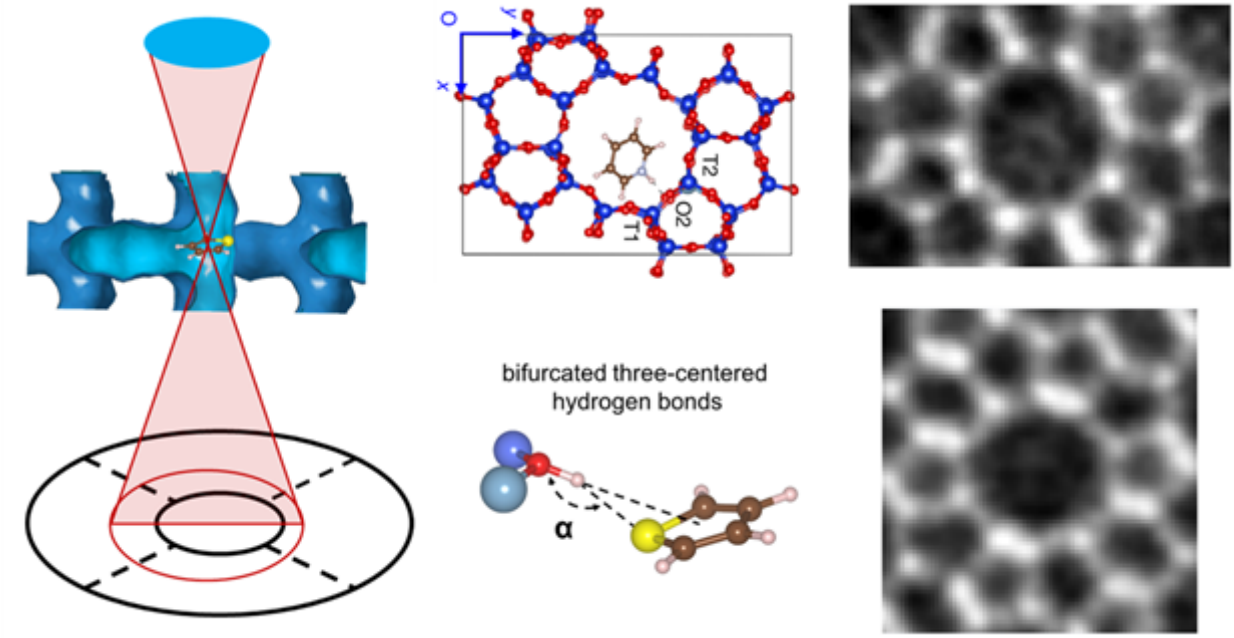

Keywords:

Single-molecule imaging, iDPC-STEM, zeolites

Reference:

[1] Wang HQ, et al. Atomic imaging of zeolite-confined single molecules by electron microscopy. Nature 607, 703-707 (2022).
[2] Wang HQ, et al. Imaging of Single Molecular Behaviors Under Bifurcated Three-Centered Hydrogen Bonding. Angew. Chem. Int. Ed. e202308675, (2023).

127

Tri-layer graphene as membrane and electrode for liquid-phase electron microscopy studies of CO2 electroreduction nanocatalysts

Saltanat Toleukhanova[1], Dr. Tzu-Hsien Shen[1], Mr Chen Chang[1], Miss. Swathilakshmi Swathilakshmi[1], Miss. Tecla Bottinelli Montandon[1], Prof. Vasiliki Tileli[1]
[1]Institute of Materials, École Polytechnique Fédérale de Lausanne, Lausanne, Switzerland

Poster Group 2

Electrochemical liquid-phase electron microscopy (ec-LPEM) has been successfully applied to understand catalyst degradation during CO2 electroreduction (CO2ER).[1] However, to be able to fully reproduce full cell conditions at these highly cathodic potentials, further advances in imaging and electrode configuration are required. Herein, we have integrated tri-layer graphene to serve as a liquid-sealing membrane and a substrate electrode material and tested its applicability for studying nanocatalysts at realistic CO2ER potentials.[2]
All experiments were carried out in a dedicated scanning electron microscopy (SEM) stage that is equipped with bulk reference and counter electrodes. The fabrication of the working electrode started by patterning a single Pt electrical pad on a Si/SiNx electrochemical chip with an electron transparent window. Holes were perforated onto the 50 nm thick SiNx membrane in a cleanroom. Tri-layer graphene was obtained via PMMA-assisted wet transfer of monolayer graphene sheets. The final tri-layer graphene was wet transferred on the electrochemical chip, ensuring the coverage of the electrical contact and membrane area. To assemble the graphene electrochemical microcell, the graphene chips were treated with H2 plasma to ensure their hydrophilicity. Subsequently, Cu nanocubes (NCs) were drop-casted on the graphene region overlapping with the perforated SiNx support membrane.
First, we evaluated the inert potential range and stability of the graphene cells and the results showed that the graphene electrode has a wider inert potential range in the cathodic region than the conventionally used glassy carbon electrode. Graphene was also found to have a stable current profile for up to 10 min at a cathodic potential of -1.1 V vs RHE, which is common for bulk cell CO2ER studies. In addition, cyclic voltammetry tests with Cu2O NCs loaded on graphene allowed for the investigation of Cu oxide reduction and oxidation peaks, confirming a good charge transfer between graphene and catalyst. Overall, the bench-top experiments demonstrate the suitability of graphene as a substrate electrode for CO2ER studies. Furthermore, in situ SEM control experiments showed improved spatial resolution with the graphene membrane and also demonstrated reduced electron beam induced damage in the bare graphene region compared to the SiNx region. However, in situ SEM electrochemical tests indicated the presence of adverse synergistic effects of e-beam and applied cathodic potential on the electrochemical stability time window of graphene electrodes. These effects are shown to be mitigated by minimizing the electron beam dose (i.e. probe current) or avoiding high cathodic potentials. Optimized in situ SEM experiments on Cu NCs, performed at -1.1 V vs RHE, a probe current of 16 pA and a duration of 3 min, revealed that their degradation proceeds via a subtle dissolution and redeposition mechanism during CO2ER.
In conclusion, this work demonstrates that graphene can play the dual role of membrane and electrode for investigating the degradation mechanisms of CO2ER catalysts under realistic potentials, while increasing the spatial resolution for ec-LPEM studies.
Acknowledgment
This work was supported by NCCR Catalysis (grant number 180544), a National Center of Competence in Research funded by the Swiss National Science Foundation.

Keywords:

CO2_electroreduction, Cu_nanocubes, liquid-phase_electron_microscopy, graphene, microcells

Reference:

[1] J. Vavra, T. Shen, D. Stoian, V. Tileli, R. Buonsanti, Angew. Chem. Int. Ed. 2021, 60, 1347.
[2] S. Toleukhanova, T.-H. Shen, C. Chang, S. Swathilakshmi, T. Bottinelli Montandon, V. Tileli, Adv. Mater. n.d., n/a, 2311133.

179

Multimodal and multidimensional EELS and EDX for investigations of catalysts at the nanoscale

Dr Maria Meledina[1], Mr Dileep Krishnan[1], Mr Daen Jannis[2], Mr Maarten Wirix[1], Mr Xiaochao Wu[3], Mr Ulrich Simon[3], Mr Sorin Lazar[1], Mr Peter Tiemeijer[1], Mr Paolo Longo[1]
[1]Thermo Fisher Scientific, Eindhoven, Netherlands, [2]EMAT, University of Antwerp, Antwerp, Belgium, [3]Institute of Inorganic Chemistry, RWTH Aachen University, Aachen, Germany

Poster Group 2

Ceria-based materials find their applications in various fields. Due to their oxygen deficiency at the surface the ceria nanoparticles are especially attractive catalysts [1]. By introduction of dopants into the ceria lattice the catalytic performance of ceria nanoparticles can be even further increased. To fine-tune the catalytic performance though the insights into the structural-properties relationships in the materials advanced TEM with spectroscopy should be applied. 2D and 3D multimodal STEM is of crucial importance to understand the structure and chemistry of doped catalysts at the nanoscale and to enable the targeted approach to the materials development.

In this work we combined EDX, EELS and electron tomography to investigate the local chemistry of Cu-doped ceria (Cu:CeOx) catalyst exhibiting superior performance for low temperature CO oxidation with respect to the undoped CeOx material. EELS both in 2D and 3D evidenced the elegant double core-shell structure of the undoped CeOx nanorod (see the figure), most likely related to the large amount of voids inside the particle: a shift of the Ce M4,5 edge onset as well as the white line ratio variation was clearly observed in the EELS spectrum allowing to distinguish between Ce4+ and Ce3+. In contrast to the previous work [1] where to gain the similar insights the monochromated 120kV setting was applied in the present study the experiment did not require the use of the excited monochromator and the lowered HT making the experimental work easier. Simultaneous EELS-EDX investigation was performed to study the Cu:CeOx material. Even though the CuL2,3 edge is visible in the EELS spectrum, its overlap with the fine structure of Ce inhibits the reliable STEM-EELS mapping of Cu in Cu:CeOx. EDX in this case clearly located Cu locations within the nanorod while STEM-EELS evidenced the Ce3+ oxidation state of cerium, highlighting the high amount of oxygen vacancies which can be correlated to the superior performance of the doped ceria catalyst.
To sum up, both EELS and EDX giving the access to the local chemical information, in combination with the electron tomography, giving the access to the 3D information, are of great help while investigating catalytic nanoparticles. We highlighted here the unique insights of the multimodal and multidimensional approach by an example of doped ceria catalyst investigation.

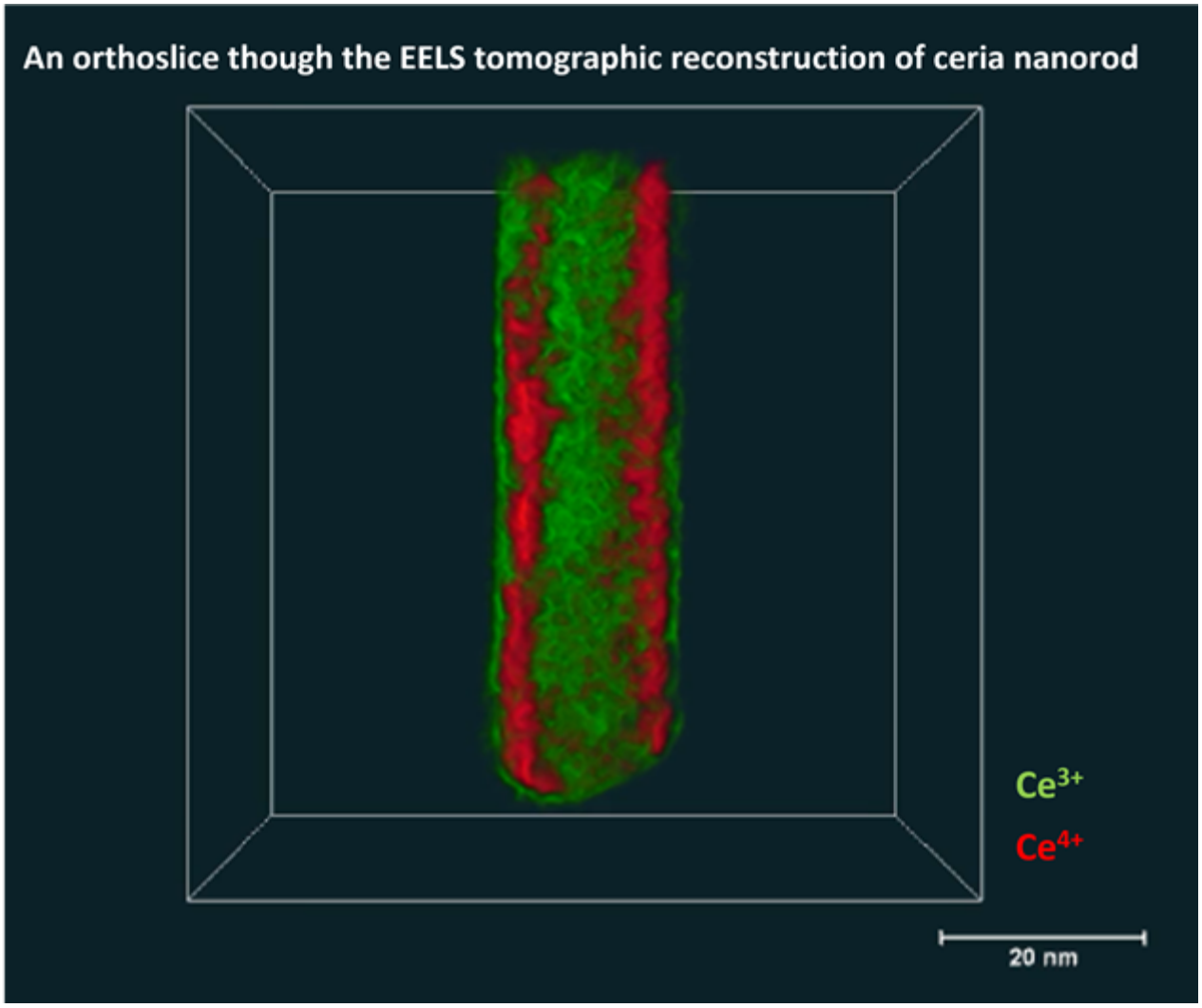

Keywords:

EELS, EDX, Multimodality, Catalysis

Reference:

[1] Maria Meledina, Stuart Turner, Vladimir V Galvita, Hilde Poelman, Guy B. Marin, Gustaaf Van Tendeloo F, Nanoscale 7 (2015), p. 3196-3204. https://doi.org/10.1039/C4NR06060A

213

Visualizing single-atom promotion of ultra-deep hydrodesulfurization catalysts (Pt-Co-Mo-S)

Principal Scientist Lars Pilsgaard Hansen[1], Mr. Christian F. Weise[1], Mrs. Hanne Falsig[1], Mr. Poul G. Moses[1], Mr. Stig Helveg[2], Mr. Michael Brorson[1]
[1]Topsoe A/S, DK-2800 Kgs. Lyngby, Denmark, [2]Center for Visualizing Catalytic Processes (VISION) Department of Physics Technical University of Denmark, DK-2800 Kgs. Lyngby, Denmark

Poster Group 2

Background incl. aims

The shift towards environmentally friendly fuels has led to stricter regulations on transportation fuel purity, necessitating more efficient catalysts for high-quality, low-sulfur diesel from both fossil and renewable sources. Co-Mo catalysts, supported on alumina, are used to remove sulfur from organosulfur molecules in mineral oil in industrial processes conducted under high hydrogen pressure. However, a significant challenge remains in extracting sulfur atoms from certain sulfur compounds, such as 4,6-dimethyldibenzothiophene (4,6-DMDBT), due to steric hindrance in the molecular reaction pathway.

Over the last four decades, our understanding of Co-Mo catalysts has greatly improved, largely thanks to the Co-Mo-S model introduced by Dr. Henrik Topsøe and his team [1]. According to this model, the active phase of the catalyst is MoS_2 nanocrystals with Co atoms attached at the edges [1,2]. Similar detailed atomic-level imaging of industrial catalysts has remained a challenge since the catalysts are prepared by incipient wetness methods on high-surface area (oxide) supports. However, recent advancements in aberration-corrected electron microscopy, which now allow for single atom detection, have extended this understanding to industrial-grade catalysts supported on high-surface area (conducting) materials, such as graphite, by imaging atom-by-atom the Co-Mo-S structure, even in 3D [3,4]. This has been available due to a combination of ultra-thin supports for single atom contrast optimization and low-voltage (60kV) and low-dose imaging schemes to suppress beam damage.

These breakthroughs provide a powerful set of tools for designing and characterize new active edge and corner structures in hydrotreating catalysts. Here, we present such an approach to enhance a commercial alumina-supported Co-Mo catalyst with small amounts of Pt [5]. This has significantly increased the catalyst's hydrodesulfurization (HDS) activity, boosting the process of removing sulfur from diesel distillates, including 4,6-DMDBT molecules, by +46% in a pilot test unit under industrial conditions. The tested catalysts are analyzed using atomically resolved scanning transmission electron microscopy (STEM) to precisely pinpoint the location of the Pt promoter atoms. These findings are compared to DFT studies based on the well-established Co-Mo-S model. Furthermore, the desulfurization process of 4,6-DMDBT molecules will be modeled to shed light on the catalytic role of Pt.

Methods

The Pt-Co-Mo catalysts were synthesized by incipient wetness impregnation on a mesoporous shaped alumina carrier, resulting in catalysts with metal loads of 16 wt% Mo, 3.5 wt% Co, and between 0 and 1.9 wt% Pt [5]. The catalysts were tested for their HDS activity in a pilot unit using a diesel oil feed containing 1.22 wt% sulfur. After the HDS process, the catalysts were cleaned with the solvent dichloromethane to remove any remaining oil residues. The catalysts were then characterized by scanning transmission electron microscopy (STEM) using two different microscopes; a FEI Talos F200X for element mapping (EDX), and a probe-corrected JEOL ARM-200F for high resolution imaging, operated at 200kV with a probe size of ~1Å for single-atom detection. The interpretation of these results was aided by STEM image simulations conducted in QSTEM, and

density functional theory (DFT) calculations of Pt and Co-Mo-S interactions to visualize edge motifs of the Pt-Co-Mo-S catalyst. The nature of Pt was further justified by Pt L-edge X-ray absorption near edge structure (XANES).

Results

Here we present the synthesis of platinum-cobalt-molybdenum (Pt-Co-Mo) catalysts and their application in the hydrodesulfurization (HDS) process. The resulting catalysts showed a significant increase of +46% in HDS activity when tested in a pilot unit under industrial conditions. Surface science studies using scanning tunneling microscopy (STM) and density functional theory (DFT) have provided a detailed understanding of the catalysts' edge-motifs in Co-Mo-S structures at the atomic level [2]. These model studies, prepared on planar Au substrates under ultra-high vacuum levels, suggest that the cobalt atoms act to increase the concentration of sulfur vacancies on the MoS_2 edges and that corner sites provide favorable geometries for adsorption of specifically the sterically hindered 4,6-DMDBT molecules. Therefore, we focus on characterizing the Pt-Co-Mo catalysts at the atomic level using Pt L-edge XANES and high-resolution STEM. The results revealed a tertiary transition metal sulfide nanostructure, Pt-Co-Mo-S, with Pt attached to edges and corner sites of the Co-Mo-S structure. The study also utilize DFT calculations to further understand the catalytic working principle and the promotional role of Pt in ultra-deep hydrodesulfurization, especially the desulfurization of refractory 4,6-DMDBT molecules.

Conclusion

This study reveals that a Pt-Co-Mo-S nanostructure, with Pt strategically positioned at the edges and corners of the Co-Mo-S structure, significantly enhances the desulfurization process, particularly for bulky 4,6-DMDBT molecules. The introduction of Pt in these tertiary structures appears to break the conventional scaling relations, modifying the behavior of corner and edge sites in the Co-Mo-S catalyst. These single-atom level insights into complex edge motifs in industrial catalysts elucidate the role of promoter elements and provide a new perspective on how to tailor nanostructures for more efficient catalysts in the future.

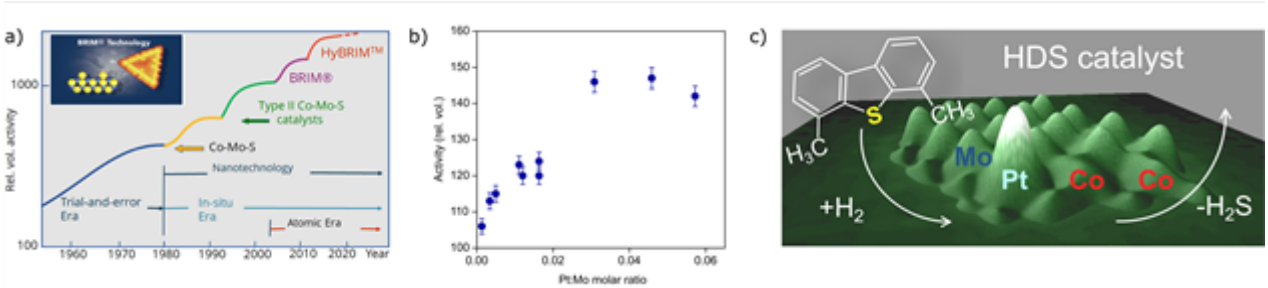

Keywords:

HDS catalyst, single-atom promotion, HRSTEM

Reference:

[1] Topsøe, H. et al. J. Catal. 68, 433 (1981)
[2] Besenbacher, F. et al., Catal. Today, 130, 86 (2008)
[3] Hansen, L.P. et al., Angew Chem Int. Ed, 50, 10153 (2011)
[4] Chen, F.R. et al. Nat Commun, 12, 5007 (2021)
[5] Weise, C. F. et al., J. Catal., 403, 74 (2021)

282

Understanding Au cluster growth through electron microscopy

Tom Slater[1], Dr Malcolm Dearg[1,2], Mr Sean Lethbridge[3], Mr James McCormack[3], Dr Theo Pavloudis[3,4], Prof Joseph Kioseoglou[4], Prof Richard Palmer[3]
[1]School of Chemistry, Cardiff University, Cardiff, United Kingdom, [2]School of Physics, University of York, York, United Kingdom, [3]Nanomaterials Lab, Department of Mechanical Engineering, Swansea University, Swansea, United Kingdom, [4]Department of Physics, Aristotle University of Thessaloniki, Thessaloniki, Greece

Poster Group 2

Background incl. aims
Metal nanoparticles are the key active component in a wide array of heterogeneous catalysts. Specifically, Au nanoparticles are highly active catalysts for oxidation reactions, most notably the oxidation of CO [1]. The structure of Au nanoparticles in the size range less than 5 nm is crucial for their catalytic performance, with specific facets and edge-sites key to maximizing activity and selectivity. Understanding the formation of different Au nanoparticle morphologies is therefore highly important to predicting and controlling their use at catalysts.
In this study we have employed aberration-corrected scanning transmission electron microscopy to observe the structure of Au nanoparticles formed via growth from individual sputtered atoms on amorphous carbon films. Understanding of the specific structures formed from surface-growth at different nanoparticle sizes is vital to predict catalytic performance. We aim to determine whether structures are two-dimensional or three-dimensional, whether they are spherical or hemi-spherical and whether they are amorphous or take on a distinct crystalline morphology (e.g. single crystal fcc or a twinned structure such as icosahedra or decahedra).
Methods
Gold atoms were sputtered onto a carbon film using a sputtered atom source (SAS), which produces an Ar+ beam using a cold cathode ion gun (Scienta Omicron ISE 5) typically operated at 5 keV. The ion beam strikes the gold target (99.999% pure gold) at 45 degrees, producing a secondary flux of gold atoms onto the holey amorphous TEM carbon substrate. The gold atoms were deposited at thermal energies, thus ensuring surface deposition, not implantation. Subsequently, the sputtered atoms form gold clusters on the surface of a holy carbon film (on a copper TEM grid). Enough material was sputtered to observe a wide range of cluster sizes, from single atoms to clusters consisting of >1000 atoms.
High-angle annular dark field (HAADF) images were acquired on a probe-corrected JEOL Grand ARM scanning transmission electron microscope (STEM) operated at 300 kV at the ePSIC facility at Diamond Light Source. A convergence semi-angle of 26 mrad, a beam current of 25 pA and a detector inner semi-angle of 58 mrad were used for all the data collection. Quantification of numbers of atoms in each nanoparticle was performed using a calibrated intensity measurement for single Au atoms.
Results
Au nanoparticles of size < 100 atoms were found to contain a mixture of 2D and 3D structures. In sizes < 50 atoms, approximately one third of structures were two-dimensional. This is contrary to structure predictions from DFT simulations of free-standing nanoparticles (i.e. without the influence of any support), which typically predicts three-dimensional structures are energetically favourable in structure of size > 15 atoms [2]. In novel DFT simulations of Au structures supported on a 2D carbon support, we find that 2D structures compete in energy with 3D structures up to approximately 60 atoms in size. This cut-off size of 60 atoms from DFT simulation corresponds well with our experimental data, where the largest 2D structure observed was approximately 80 atoms in size.

As nanoparticles grow to larger sizes (between 100 and 1000 atoms), they all adopt a three-dimensional morphology. This morphology was found to be approximately spherical in shape, indicating a weak interaction between the Au nanoparticle and the carbon film. The sphericity of the nanoparticles was determined through plotting of number of atoms vs diameter (as shown in the attached Figure). This result is in contrast to previous results that indicated a mixture of spherical and hemispherical structures of Au nanoparticles on a carbon film [3], which we hypothesize may be due to differences in growth rates due to different atomic deposition fluxes.

In the surface-grown nanoparticles of size 100 – 1000 atoms, we also determine the proportion of amorphous and crystalline structures at different sizes. The proportion of amorphous/glassy structures decrease as the size of nanoparticle increases (79% in the range 100-228 atoms, 54% in the range 229-435 atoms, reaching 0% in sizes above 700 atoms). The proportion of different crystalline structures also varies with size of nanoparticle, with icosahedral structures preferred at small sizes but a clear increase in the proportion of decahedral and single-crystal structures as nanoparticle size increases. The proportion of each crystalline structural isomer at different sizes closely matches previous studies of nanoparticles produced from gas-condensation cluster sources [4,5], demonstrating that nanoparticles produced using these two different methodologies are highly comparable.

Conclusion

Nanoparticles grown from single sputtered atoms on an amorphous carbon film show clear trends in morphology. 2D structures are supported up to sizes of approximately 80 atoms due to interactions between nanoparticles and support. At sizes greater than 100 atoms, nanoparticles form approximately spherical structures with no clear influence of support interactions. Surface-grown nanoparticles in the size range 100 – 1000 atoms show a distribution of crystalline structures that closely matches the distribution found in nanoparticles produced using a gas-condensation cluster source, although greater proportions of amorphous nanoparticles are observed in surface-grown samples.

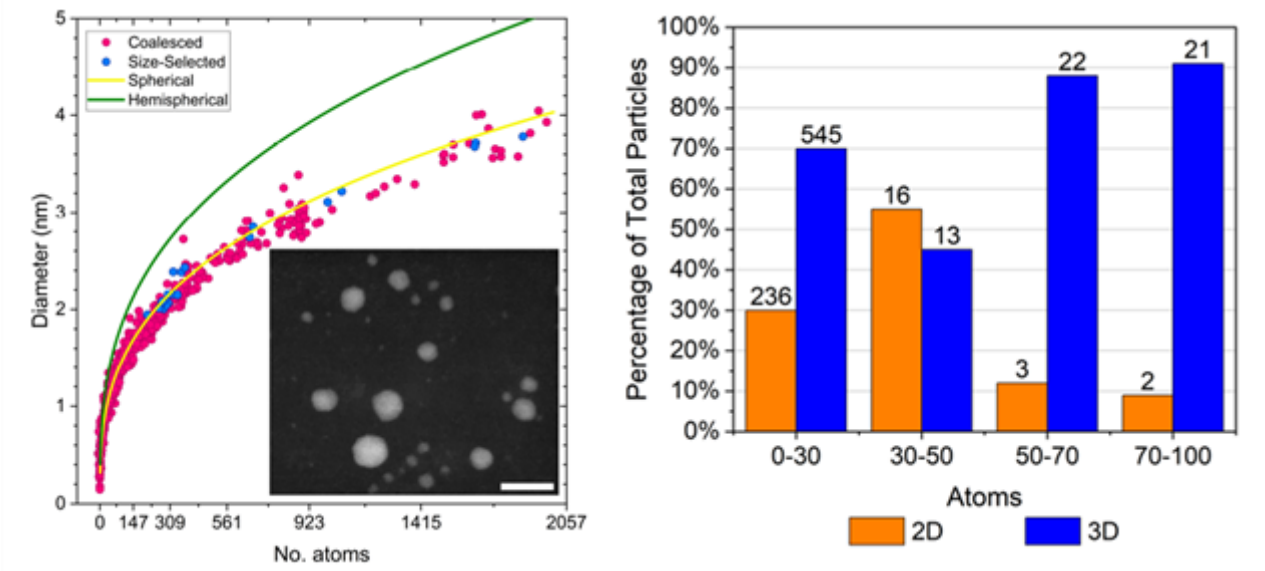

Keywords:

Gold nanoparticles, AC-STEM, nanoparticle growth

Reference:

1. Kung M. C. et al. Understanding Au-Catalyzed Low-Temperature CO Oxidation. J. Phys. Chem. C 2007, 111, 32, 11767-11775.

2. Xing X. et al. Structural evolution of Au nanoclusters: From planar to cage to tubular motifs. Phys. Rev. B 2006, 74, 165423.

3. Young N. P. et al, Weighing Supported Nanoparticles: Size-Selected Clusters as Mass Standards in Nanometrology. Phys. Rev. Lett. 2008, 101, 246103.
4. Li Z. Y. et al. Three-dimensional atomic-scale structure of size-selected gold nanoclusters. Nature 2008, 451, 46-48.
5. Wells D. M. et al. Metastability of the atomic structures of size-selected gold nanoparticles. Nanoscale 2015, 7, 6498-6503.

295

η-Carbides (Co, Mo, or W) Nanoparticles from Octacyanometalates Precursors-Based Network

Dr Frédéric Fossard[1], Mr. Thomas Blin[2], Mrs Armelle Girard[1,3], Mrs Nathalie Guillou[3], Mrs Laure Catala[2], Mrs Annick Loiseau[1], Mr. Vincent Huc[2]
[1]Université Paris-Saclay, ONERA, CNRS, LEM, Châtillon, France, [2]ICMMO, CNRS, Université Paris-Saclay, Orsay, France, [3]ILV, UMR CNRS 8180, UVSQ, Université Paris-Saclay, Versailles, France

Poster Group 2

Noble metal nanoparticles such as Au and Pt are well known and widely used for their catalytic properties. Because of the cost of these noble metals, different strategies are pursued to find surrogates to noble metals in catalysis. Emerging and promising approach is to play with NPs of transition metal carbides. Among the candidates for these substitutions are WC NPs [1] ,Mo2C nanoparticles [2] or Co6Mo6C2 combined with graphitic carbon for oxygen reduction. The aim of this study was to develop a route for synthesizing bimetallic carbides NPs in two-step process and the originality of this approach lies in the choice of the metallic precursors.
Octacyanometalate-based networks (OCMs) are 3D metal networks in which the metals are linked together by CN bridges. A water-based surfactant-free synthesis was shown to be applicable for the synthesis of PBAs [3]. It is versatile enough to get networks composed of the combination of any transition metals of our choice. The desired 3D compounds are obtained by mixing a solution of cyanometallates involving one kind of metal (M' = Mo or W) with a solution of another metallic salt of the second metal (M = Co). To turn the metalate network into metallic carbide, the OCMs undergo heat treatment, under inert atmosphere as the procedure used by Aparicio et al [4].
In bimetallic particles, different types of η-carbides-type structures were evidenced in our sample. Co3Mo3C, Co6Mo6C, and Co2Mo4C from the Co-Mo-C system. Co3W3C (fig 1), Co6W6C, Co4W2C, and Co2W4C from the CO-W-C system. These compounds were identified by combination of Transmission Electron Microscopy, high resolution STEM/HAADF imaging of individual NPs (fig A), EDS analysis (fig B-C), and compared simulated (fig D) and experimental HAADF-STEM image (fig E). The size of these carbide nanoparticles is 5 nm in average. Along with η-carbides, the presence of monometallic carbide nanoparticles such as Mo2C and WC has also been observed. The pyrolysis temperature is an important factor in the formation of nanoparticles. Indeed, a treatment at a too low temperature, < 700 °C for Co-Mo system and 800 °C for Co-W system will not enable the complete transformation of the precursors. Beyond these temperatures, η-carbide nanoparticles account for the majority of the nanoparticles observed (> 60%).
Co3M'3C, Co6M'6C, Co2M'4C (M' = Mo or W), and Co4W2C, metallic carbide nanoparticles were successfully synthesized by thermal decomposition of Cs-Co-M' precursor octacyanometalate networks. Their presence in significant proportions in a definite temperature range attests for the efficiency of the synthesis route by thermal decomposition of OCM. The strength of this method also lies in the wide choice of metals that can be used to fabricate octacyanometalate-based networks and thus potentially the wide choice of carbides nanoparticles that could be made easily and rapidly accessible

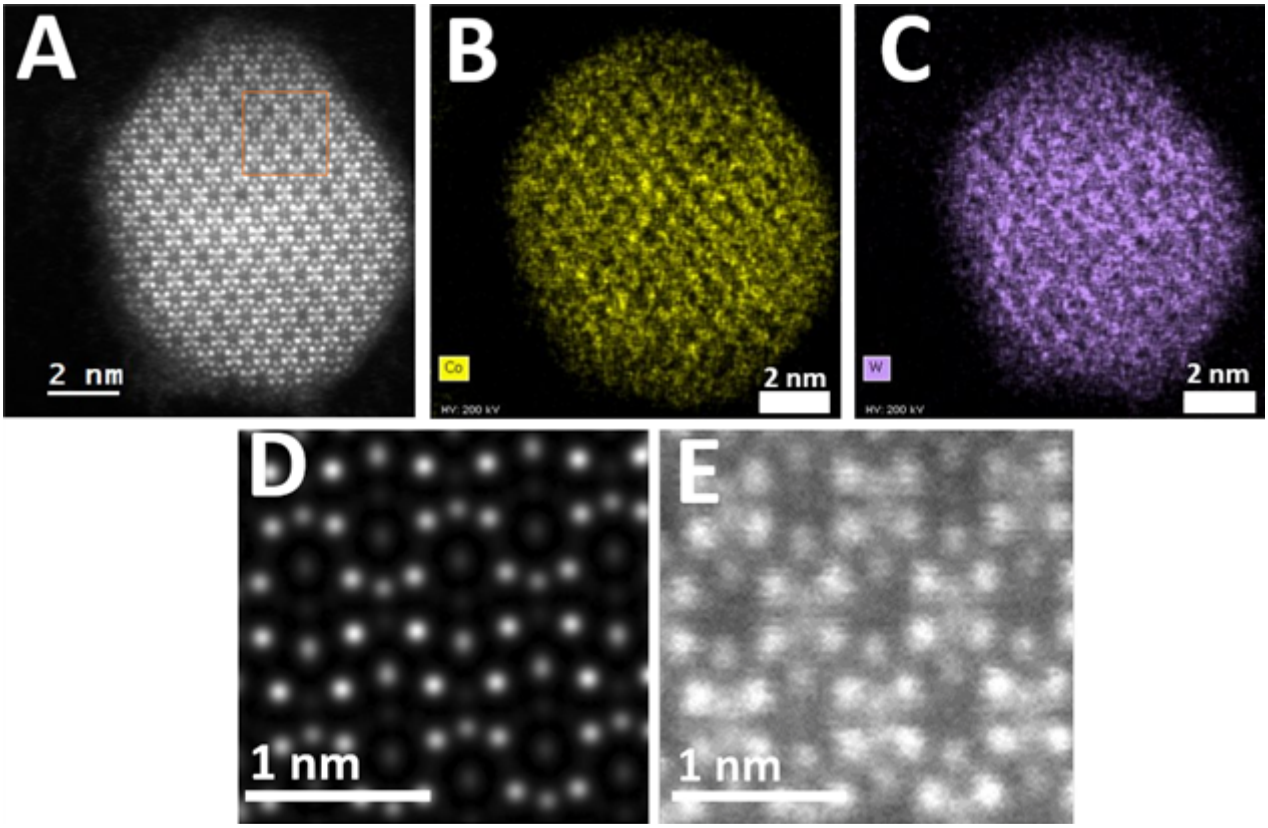

Keywords:

eta-carbides, STEM/HAADF, catalysts

Reference:

[1] L. H. Bennett et al., Science 1974, 184, 563.
[2] Z. Zhou et al., Small 2019, 15, 1900358.
[3] X. Ma et al., J. Am. Chem. Soc. 2012, 134, 1954.
[4] C. Aparicio et al. J. Therm. Anal. Calorim. 2012, 110, 661.

318

Atomic-scale model of the platinum (111)-water interface revealed by angstrom resolution off-axis phase shifting holography

Jonas Lindner[1], Dr. Ulrich Ross[1,2], Dr. Tobias Meyer[1], Dr. Sung Sakong[3], Prof. Dr. Axel Groß[3,4], Prof. Dr. Michael Seibt[2], Prof. Dr. Christian Jooß[1,5]
[1]Institute of Materials Physics, University of Goettingen, Göttingen, Germany, [2]4th Institute of Physics – Solids and Nanostructures, University of Goettingen, Göttingen, Germany, [3]Institute of Theoretical Chemistry, Ulm University, Ulm, Germany, [4]Helmholtz Institute Ulm (HIU) for Electrochemical Energy Storage, Ulm, Germany, [5]International Center for Advanced Studies of Energy Conversion (ICASEC), Göttingen, Germany

Poster Group 2

Background
The colossal challenge against climate change highlights the necessity of scaling up renewable energy storage capacity and enhancing green hydrogen production by electrocatalysis. However, developing stable and high-performance electrocatalysts for hydrogen production using abundant materials requires a further fundamental atomic-scale understanding of the charge transfer process at the catalytic interfaces.
Although the metal-water interface is the preeminent part of interest for a basic understanding of electrocatalysis and has become an extensively discussed topic in current catalysis research, the atomic structure of the electrolyte, the active sites of the reactions, and the role of single atoms and step edges on the catalyst surfaces remain elusive.
Environmental TEM research enables atomic-scale assessments of metal-water interfaces. We present an open-cell in-situ study of the interface between catalytically active platinum (111) and water vapor under experimentally feasible pressures. Under a water ambient condition, we measure the projected potential across the interface using the angstrom-resolution electron holography method. The results obtained at various external bias conditions are compared to the atomic structures from ab initio molecular dynamics (AIMD) simulations. We will discuss the metal-water interface structures and their natures from experiment and theory.

Methods
A two-electrode MEMS setup is exposed to 50 microbar water vapor, which forms an ultrathin condensed water layer at the Pt electrode surfaces. An in situ analysis is carried out by employing an image-aberration-corrected Titan environmental TEM. Off-axis phase-shifting electron holography is used in conjunction with an improved drift-correction scheme to reconstruct the exit-wave with a spatial resolution up to the information limit of the microscope (<1.0 Å).

Results
The in-situ HRTEM image series and phase reconstructions identify dynamic platinum adatoms at the metal-water interface. The adatoms are residues of the metal-water interface formation and appear only after the electrode is exposed to the water. The existence of the adatoms may depend on the preparation procedures of the metal electrode. By comparing the quantitative frozen-lattice multi-slice simulations, we retrieve the specimen thickness at the edge and, subsequently, the coverage of the dynamic platinum adatoms. At the metal-water interface, the oscillations of the projected potential up to 5 Å above the platinum adatoms are monitored. We interpret the oscillations as preferential orientations of the water molecules in the first water layer with the help of predicted holography data from multi-slice simulations using the AIMD trajectories of the model interface configurations. Furthermore, we provide an outlook on the influence of external bias on the potential profiles and expectations based on AIMD-simulation for different surface conditions.

Conclusions

In conclusion, we identify the dynamic platinum adatoms at the platinum- (111) interface to water in an open cell ETEM experiment under in-situ conditions. Applying the angstrom resolution phase shifting off-axis electron holography captures the signatures in the projected potential of the first water layers. Based on the multi-slice simulations derived from AIMD trajectories, we attribute these signatures as the preferential ordering of the interfacial water. First experimental indications of the influence of external an bias on the water layer are discussed with respect to AIMD predictions.

Keywords:

metal-water interface, atomic-scale, holography, environmental-TEM

Reference:

Lindner, J., Ross, U., Meyer, T., Boureau, V., Seibt, M., & Jooss, C. (2024). Reconstruction of Angstrom resolution exit-waves by the application of drift-corrected phase-shifting off-axis electron holography. Ultramicroscopy, 256, 113880.

Huang, J., Zhang, Y., Li, M., Groß, A., & Sakong, S. (2023). Comparing Ab Initio Molecular Dynamics and a Semiclassical Grand Canonical Scheme for the Electric Double Layer of the Pt (111)/Water Interface. The Journal of Physical Chemistry Letters, 14(9), 2354-2363.

Barthel, J. (2018). Dr. Probe: A software for high-resolution STEM image simulation. Ultramicroscopy, 193, 1-11.

321

Nanoparticle formation mechanisms and molecular intermediates revealed by liquid phase EM and reaction pathway analysis

Ms. Jiayue Sun[1], Mr. Birk Fritsch[2], Mr. Andreas Körner[2], Ms. Lucia Morales[2], Mr. Chiwoo Park[3], Ms. Mei Wang[4], Dr. Andreas Hutzler[2], Mr. Taylor Woehl[4]
[1]Department of Chemistry and Biochemistry, University of Maryland, College Park, United States, [2]Helmholtz Institute Erlangen-Nürnberg for Renewable Energy, Erlangen, Germany, [3]Department of Industrial and Systems Engineering, University of Washington, Seattle, United States, [4]Department of Chemical Engineering, University of Maryland, College Park, United States

Poster Group 2

Classical nucleation theory (CNT) is used to describe the growth of metal nanoparticles by seed formation from insoluble metal atoms generated by chemical reduction of precursors containing metal ions. It involves a nucleation step, and subsequent monomer attachment on the seeds which is limited by diffusion of metal atoms.

In contrast, liquid phase transmission electron microscopy (LPTEM) has revealed that nanoparticles do not form by the above-mentioned process but via cluster-cluster aggregation instead.[1] Although this non-classical growth of nanoparticles has been observed frequently, precise knowledge about atomic and cluster species remains concealed. Mechanisms comprising thermodynamically preferred cluster sizes have been suggested in prior studies. However, these magic clusters cannot explain formation mechanisms involving strong reductants at room temperature where kinetics are dominated by the reaction.

In LPTEM, reaction kinetic modeling has been shown to facilitate uncovering reaction conditions in irradiated solutions and how to tailor redox chemistry [2] and acidity [3] in precursor solutions with radiation.

Unraveling ionic precursor species guiding the formation pathways of metallic nanoparticles would enable to specifically design synthesis routes and thus to deliberately adjust their nanostructure properties.

Herein we correlate liquid phase electron microscopy with reaction throughput analysis to demonstrate that nucleation and growth of silver nanoparticles is based on aggregation and attachment of various metal clusters and ions. Therefore, we utilize LPTEM to study nucleation and growth rate of silver nanoparticles induced by radiolysis of aqueous silver nitrate solution. [4] Observations are complemented by a time dependent radiolysis model of the precursor solution (Figure 1a and 1b) illustrating the concentration of most silver species being directly proportional to electron dose rate (Figure 1c).

LPTEM measurements revealed a nearly invariant nanoparticle growth rate with increasing electron dose rate and a decreasing nucleation rate (Figure 1d and 1e). Furthermore, our reaction kinetic model suggests that Ag_4 and Ag- have steady state concentrations orders of magnitude larger than those of the other species which are also almost invariant with dose rate. Experimental dose rate dependent growth and nucleation rates were fitted by power laws yielding growth exponents of $(2.5 \pm 7.5) \cdot 10^{-2}$ and -0.17 ± 0.07, respectively (Figure 1d and e, red lines). The large concentrations of Ag_4 and Ag- in combination with their dose rate dependent power law exponents of $(-7.5 \pm 1.0) \cdot 10^{-3}$ and $(6.5 \pm 2.6) \cdot 10^{-3}$ indicated by our kinetic model and located within the error margin of the experimentally obtained data, suggest a nanoparticle growth by attachment of Ag_4 and Ag- to the

silver seeds. However, the nucleation rate exponent did not match any of the simulation results. Furthermore, CNT evaluation yields very high supersaturation values suggesting unrealistically small critical radii of no more than a single atom.

The inconsistency of the dose rate dependency of the observed nucleation rate with that of all silver species and CNT suggests a silver nanoparticle growth via a non-classical pathway. Our results provide evidence, that nucleation rather takes place in a millisecond time scale which is dominated by Ag_4^{2}+ cluster-cluster aggregation. Overall, this work showcases the power of quantitative LPTEM combined with transient reaction kinetic modeling for disentangling which chemical processes are involved in nanoparticle formation.

Figure caption
Figure 1. (a) and (b) Radiolysis model for a dose rate of 0.56 MGy/s and 5.6 MGy/s. (c) Steady state concentration of silver species as a function of dose rate. (d) Growth rate multiplied by the squared particle size as a function of dose rate. The blue symbols represent experimental measurements. The red line is a fit assuming diffusion limited growth to the Lifshitz-Slyozov-Wagner (LSW) model. (e) Nucleation rate as a function of the dose rate fitted by a power law. Green symbols are experimental nucleation rates and the red line a power law fit. The green shaded region represents the 3σ confidence interval for the fits.

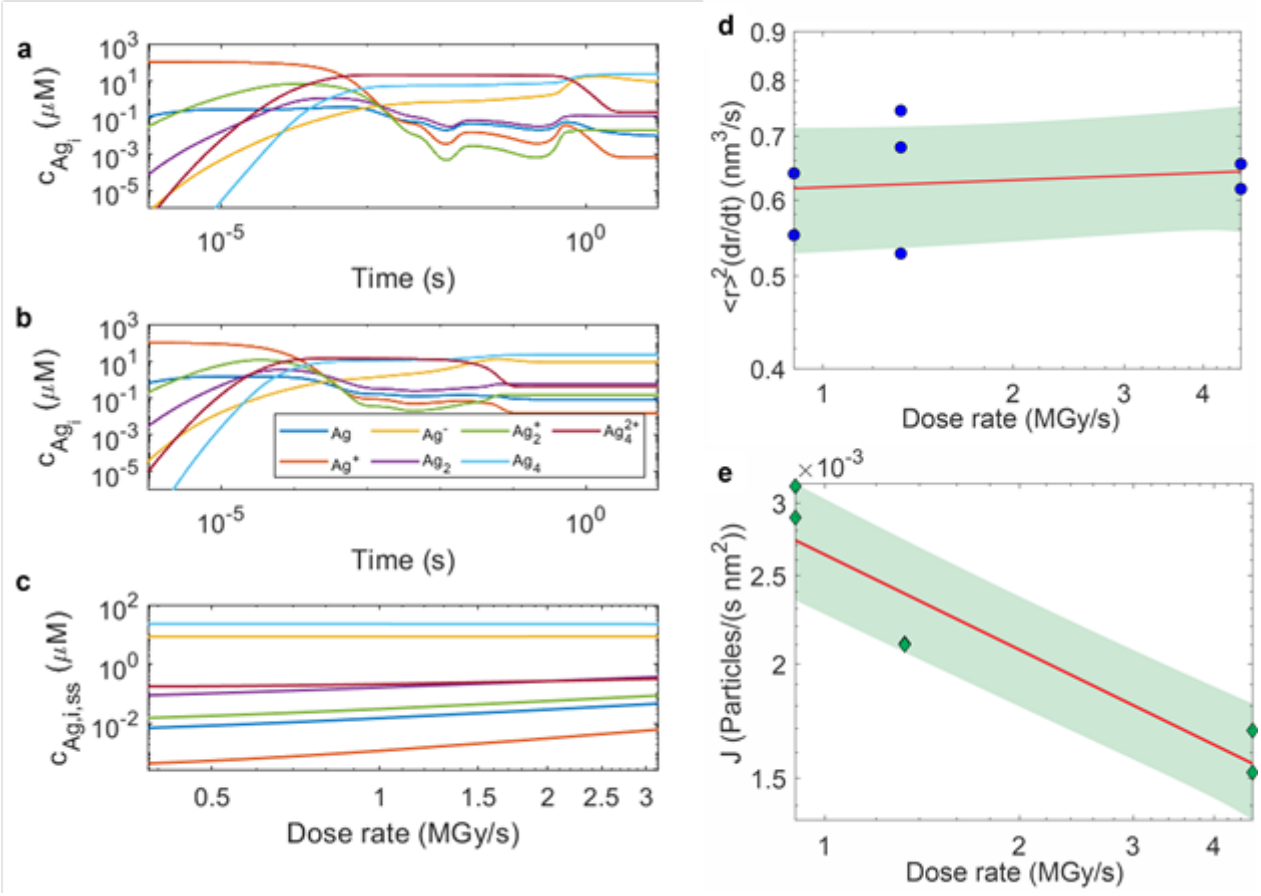

Keywords:

LPTEM; nucleation; growth; silver; nanoparticles

Reference:

[1] J. De Yoreo et al., Science 349, 2015, aaa6760, DOI: 10.1126/science.aaa6760
[2] B. Fritsch et al., Adv. Sci. 9, 2022, 2202803, DOI: 10.1002/advs.202202803
[3] B. Fritsch et al., J. Phys. Chem. Lett. 14, 2023, 4644–4651, DOI: 10.1021/acs.jpclett.3c00593

[4] M. Wang, C. Park, T. J. Woehl, Chem. Mater. 30, 2018, 7727, DOI: 10.1021/acs.chemmater.8b03050

350

Detection of weak ELNES signals using dose-fractionated spectrum imaging combined with direct detection

Andrew Thron[1], Liam Spillane[1], Saleh Gorji[2], Ray Twesten[1]
[1]Gatan Inc., Pleasanton , USA, [2]Gatan GmbH, Unterschleissheim, Germany

Poster Group 2

Background:
Recent studies showed that mixed Fe-Co oxide nanoparticles could replace more expensive Ir oxide and Ru oxide for the oxygen evolution reaction for water electrolysis [1]. Acquiring spectra at a high resolution is especially advantageous for understanding how the valence state of Fe and Co changes across the nanoparticles and potentially influences their catalytic behavior. EELS combined with STEM has proven effective at studying chemical changes at the sub-nm level [2]. Previous studies systematically characterized how the Fe L2,3 edge changes with changes in local symmetry based on the phase of Fe oxide [3]. The L2,3 edges of the first-row transition metals probe the unoccupied 3d states, which are sensitive to spin-orbit coupling, linking local symmetry changes to oxidation state. However, the transition metal K-edges probe unoccupied 4p states and are more sensitive to nearest neighbor distances, bonding angles, and the onset of the K edge undergoes measurable shifts with changes in oxidation state. Characterizing the Fe K edge at the sub-nm scale could add more profound insight into changes in structure and chemistry.
The cross-section of the transition metal K edges is ~3 orders of magnitude smaller than the corresponding L2,3 edge. This requires increased acquisition times and the likelihood that radiolysis and sample drift will compromise the measurement. It was shown in polymer blends that the performance of the microscope does not limit the resolution of an EELS spectrum image. Instead, the resolution is limited by a critical dose above which the polymer structure changes [4]. Gatan recently implemented new software and hardware tools that acquire and analyze weaker signals without compromising the sample. Using direct detection cameras for EELS on the GIF Continuum increases the detection efficiency needed to collect weaker, higher-energy K-edges, mitigating radiolysis by reducing acquisition times [5]. Upgrades to DigiScan 3 enable continuous in-line drift correction, where features in the simultaneously acquired ADF image are used to monitor drift, reducing latency during the drift measurement. Coupled with the fast, sub-millisecond frame rate of these direct detection cameras, accurate and frequent drift correction is critical in ensuring no spatial blurring of the spectrum image during long acquisition times. Finally, the in-situ spectrum imaging in DigitalMicrograph allows tracking and monitoring of the experiment over time and the total dose to be fractionated over multiple, individually saved passes. This enables integration or removal of passes after acquisition, enabling the enhancement of the SNR or removal of passes that may be compromised by sample damage or contamination.
In this study, we demonstrate why it is critical to combine the sensitivity and speed of direct detection with the ability to fractionate the dose over several passes using in-situ spectrum imaging when acquiring weaker ionization edges. We show how these tools can be utilized to study the spatial resolution limits based on the dose threshold of Fe oxide and mixed Fe-Co oxide nanoparticles. Ultimately, we explore how the material's interaction with the electron beam limits the resolution of the measurement and how this compares to analogous techniques such as scanning XAS.

Methods:
A JEOL F200 with a cold-FEG with a post-column Gatan Continuum Spectrometer was used to acquire EELS spectrum images (SI) at 200 kV. The spectrometer is fitted with single electron counting (K3, Gatan) and hybrid pixel thresholding (Stela, Gatan/Dectris) cameras, and were used to collect SI

datasets targeting the Fe K edge (7112 eV). DigitalMicrograph's Elemental Quantification tool and concurrent standards were used to study the reduction of the Fe oxide particles as a function of applied dose. The linear-least squares tool in DigitalMicrograph was used to measure the shift in the Fe K-edge across the nanoparticles by fitting Gaussian functions to the pre-peak and main peak after the edge onset.

Results :
An EELS spectrum image acquired from a cluster of Fe¬2O3 nanoparticles is shown in the ADF image in Figure 1a. The spectrum image was acquired using multi-pass spectrum imaging. A step size of 5 nm and a pixel dwell time of 330 µs was used to minimize the total dose per pass while being able to resolve individual particles in the SI. The short pixel dwell time combined with inline drift correction enabled frequent and accurate drift correction to minimize drift artifacts during the measurement. In Figure 1b, an elemental map was created from the integrated intensity of the Fe K-edge, and the smaller particles can be resolved in the cluster. The Fe K-edge ELNES extracted from the Fe¬2O3 particles is plotted in Figure 1c, along with the fitted Gaussian functions of the pre-peak and the main peak of the K-edge. Shifts in the pre-peak and the main peak were measured by mapping the position of the fitted Gaussian in Figure 1e and 1f, respectively. The pre-peak originates from a weak 1s to 3d quadrupole transition. As a result, the SNR is lower than the main peak, producing a larger variability in the fit in Figure 1e. The main peaks in the Fe K ELNES originate from a stronger 1s to 4p dipole transition, resulting in a signal that is an order of magnitude larger than the pre-peak. A shift in the main peak is observed in Figure 1f, from 7130 eV in the smaller particles to 7132 eV in the larger particles. To confirm this trend, further measurements are needed from well-separated particles.

Conclusion:
Detailed analysis of the weaker Fe K-edge is possible across individual particles. However, further experiments are needed to determine why the main peak of the Fe K edge shifts with changes in particle size. In-situ experiments fractionating the dose over several individually acquired passes are needed to confirm that the shift in the main peak is caused by radiolysis. We will apply this workflow to a mixed Fe-Co oxide system to study how the oxidation state changes with the concentration of Fe and Co, by examining changes to the ELNES of the Fe and Co K-edges. Finally, we aim to study how radiolysis limits the spatial resolution of weaker ionization edges.

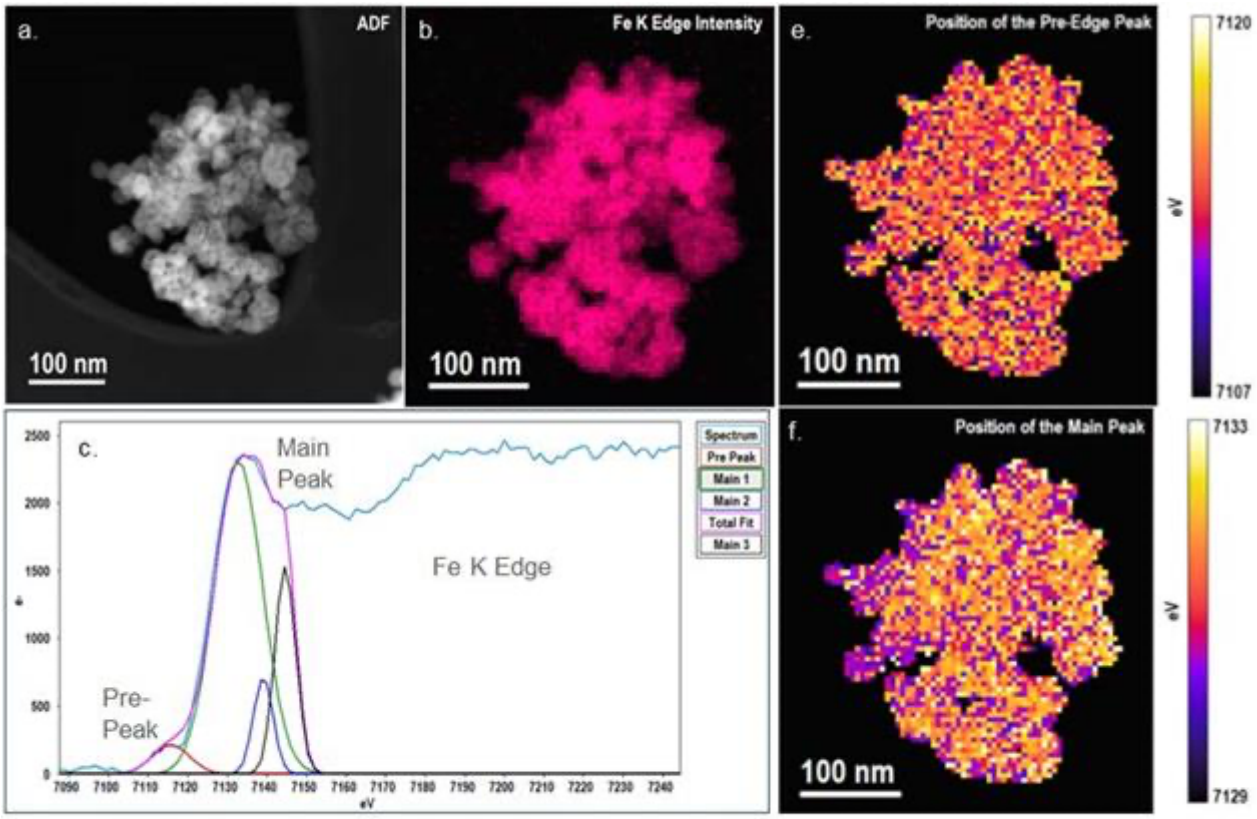

Figure 1. (a) ADF image of the Fe_2O_3 particle cluster. **(b)** Integrated Fe K Intensity **(c)** Extracted Fe K ELNES with Gaussian functions fitted to the pre-peak and the main peak. Shifts in the **(e)** pre-peak and the **(f)** main peak were observed by plotting the position of the fitted Gaussians.

Keywords:

Dose Fractionated EELS, ELNES, Catalyst

Reference:

[1] W. Xiang et al., 3D Atomic-Scale Imaging of Mixed Co-Fe Spinel Oxide Nanoparticles during Oxygen Evolution Reaction, Nat Commun 13, (2022).

[2] N. D. Browning, M. F. Chisholm, and S. J. Pennycook, Atomic-Resolution Chemical Analysis Using a Scanning Transmission Electron Microscope, Nature 366, 143 (1993).

[3] P. A. Van Aken and B. Liebscher, Quantification of Ferrous/Ferric Ratios in Minerals: New Evaluation Schemes of Fe L23 Electron Energy-Loss near-Edge Spectra, Phys Chem Miner 29, 188 (2002).

[4] R. Colby, R. E. A. Williams, D. L. Carpenter, N. Bagués, B. R. Ford, and D. W. McComb, Identifying and Imaging Polymer Functionality at High Spatial Resolution with Core-Loss EELS, Ultramicroscopy 246, (2023).

[5] J. L. Hart, A. C. Lang, Y. Li, S. Shahrezaei, D. D. Alix-Williams, M. L. Falk, S. N. Mathaudhu, A. I. Frenkel, and M. L. Taheri, Revealing Local Order via High Energy EELS, Mater Today Nano 21, (2023).

380

Impact of oxidation state on copper nanoparticle stability in industrial Cu/ZnO/Al2O3 hydrogenation catalyst

Xiansheng Li[1], Henrik Eliasson[1], Rolf Erni[1]
[1]Empa-Swiss Federal Laboratories for Materials Science and Technology, Dübendorf, CH

Poster Group 2

Background
The escalating concentrations of atmospheric CO2 represent an urgent challenge for the global climate system, driving intensive research efforts aimed at mitigating this trend through innovative strategies for CO2 reduction, conversion, and sequestration. The catalytic conversion of CO2 into liquid fuels and high-value chemicals emerges as a pivotal area of focus within the realm of environmental stewardship and energy efficiency. Among these strategies, the hydrogenation of CO2 to methanol stands out as a particularly promising avenue for the effective large-scale deployment of CO2 utilization technologies. The production of methanol through the conversion of CO2 using green hydrogen obtained from sustainable energy sources like wind, solar, and biomass, serves the dual purpose of CO2 utilization and the storage of renewable energy into chemical compounds.
The standard methanol catalyst Cu/ZnO/Al2O3 has been industrially applied for more than 50 years. Still, its efficacy is marred by exceeding 50% decline in activity within the initial weeks of operation, primarily due to thermal sintering and structural reconfigurations. It underscores the critical need for an in-depth exploration into the mechanisms underlying catalyst deactivation, with the ultimate goal of engineering more resilient catalyst systems. Previous studies attribute this deactivation to the sintering of copper, a process intimately linked to the dynamics and stability of Cu nanoparticles (NPs).
In the quest to elucidate the dynamic behaviors and migration patterns of NPs, electron microscopy stands as the method of choice. Specifically, in situ Transmission Electron Microscopy (TEM) offers unparalleled insights into catalyst structures under near-industrial operational conditions, including the intricate dynamics of nanoparticulate entities. This study, therefore, harnesses the power of in situ TEM to meticulously examine the behaviors of Cu NPs on industrial Cu/ZnO/Al2O3 catalysts throughout the entire CO2 hydrogenation lifecycle, spanning activation, steady-state operation, and eventual deactivation. By focusing on the oxidation state of copper under varying operational conditions, this investigation seeks to unravel the complex interplay between the chemical state and the mobility of Cu NPs, with the overarching aim of fostering advancements in catalyst design and CO2 conversion technologies.
Methods
In situ TEM experiments were carried out using a windowed gas cell nanoreactor (Climate, DENS solutions) comprising of two electron-transparent Si3N4 windowed chips. Commercial Cu/ZnO/Al2O3 catalyst (Alfa Aesar, 45776) was dispersed in ethanol and deposited on the bottom climate chip before constructing the climate holder and sealing the nanoreactor. The nanoreactor consists of a top and bottom chip of 50 nm and 30 nm thickness respectively. The internal temperature of the microreactor was accurately controlled by a 4-point probe method.
Microscopy measurements were conducted using a probe aberration-corrected FEI Titan Themis microscope operating at 300 kV. The beam convergence angle was set to approximately 26 mrad. EEL spectra were recorded with an ELA hybrid pixel direct electron detector from Dectris that was retrofitted with a CEFID energy filter from CEOS. The energy dispersion of the ELA detector was 0.747 eV per channel, and the dwell time was set to 1 s.
Results

Upon careful reduction following standard industrial procedures, the catalyst was activated, demonstrating significant changes in the behavior of Cu NPs across various stages of treatment, as monitored by in situ STEM and complemented by EDS and EELS analyses.
Initially, under high vacuum at room temperature, Cu NPs exhibited stability with no discernible movement; the only observable change was the slight contraction of the overall catalyst structure. EELS indicated a pronounced white line, suggesting an oxidized state of copper.
Heating to 180°C under a 1 bar N2 atmosphere triggered dynamics within Cu NPs, extending them towards the sample's edge to form larger entities. EDS data revealed Cu's segregation from Zn, highlighting Cu's higher mobility. This segregation could contribute to deactivation, as the Cu-Zn synergy is deemed crucial for catalytic activity. Notably, areas not subjected to electron beam exposure did not exhibit similar changes, suggesting that temperature or gas composition, in conjunction with beam interaction, might facilitate these dynamics. Post-sintering, EELS data suggested a reduction in Cu, with a diminished white line intensity and reduced mobility.
At 260°C in a 1 bar H2 atmosphere, Cu NPs demonstrated sintering with no alteration in the white line intensity of Cu EELS before and after observation, indicating a stable oxidation state that was reduced compared to the initial state but more oxidized than beam-induced sintered NPs. Some level of dynamic behavior was still observed, albeit less than in N2. Significant movements, such as approaching beyond the edge of the specimen, are indiscernible, suggesting that the beam-demage is minimized in H2 atmosphere.
Exposure to a 1 bar CO2+H2 atmosphere at 260°C resulted in immediate stabilization of Cu NPs, with EELS revealing a lower white line intensity, approaching that of beam induced sintered NPs.
Finally, under a 1 bar O2 atmosphere at 260°C, Cu NPs were re-oxidized, regaining high mobility. The presence of O2 also facilitates the redispersion of Cu NPs.
Conclusions
The comprehensive investigation delineates the nuanced mobility hierarchy within the catalytic system, conclusively establishing that the mobility of copper is positively related to its oxidatino state. The discovery holds significant importance within the realm of Cu/ZnO/Al2O3 deactivation, as corroborated empirically that deactivated Cu/ZnO/Al2O3 catalysts exhibit the presence of partially oxidized copper. The study further corroborates the role of oxygen in facilitating the reoxidation of Cu to CuO, a process that significantly contributes to the sintering, underscoring the detrimental impact of oxidation processes on catalyst longevity and performance. The mobility difference between copper and zinc could potentially cause their segregation and contribute to deactivation, as the Cu-Zn synergy is deemed crucial for catalytic activity. Moreover, the addition of CO2 to the hydrogen flow enhances the reduction power, likely through the formation of CO by Reverse water gas shift. Collectively, these insights not only advance our understanding of the dynamic interplay between catalytic components under varying environmental conditions but also pave the way for the development of more resilient and robust hydrogenation catalyst systems.

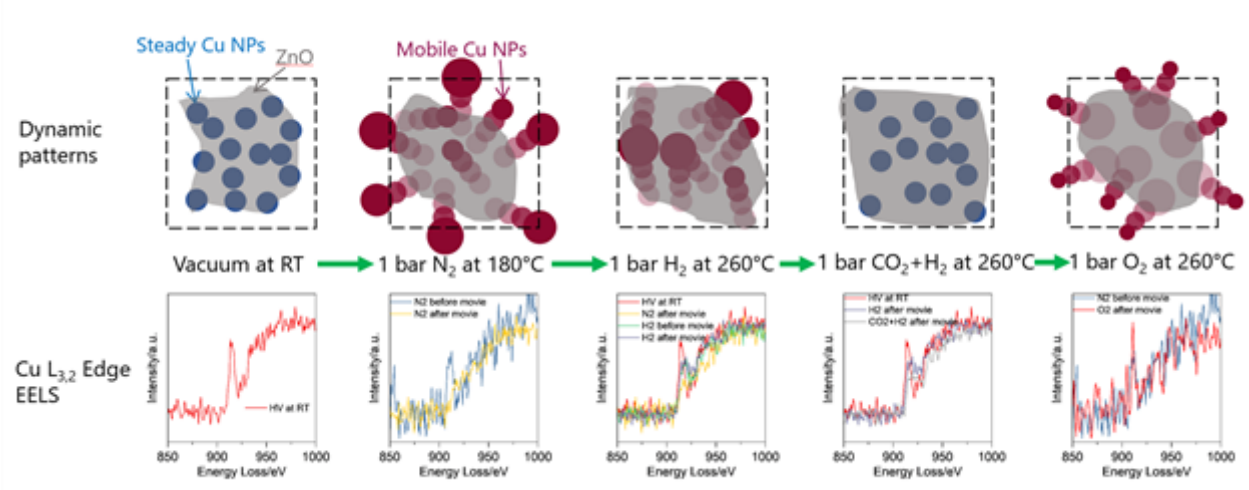

Keywords:

Cu/ZnO/Al2O3, In-situ-TEM, Gas-Cell, Sintering, Stability

Reference:

Nat Catal 4, 488–497 (2021).
Angew. Chem. Int. Ed. 2016, 55, 12708.
Nanoscale, 2021,13, 9747-9756
Ind. Eng. Chem. Res. 2019, 58, 21, 9030–9037
ChemCatChem 2022, 14, e202201280.

394

Insights into the Structural Dynamics of Cu@Ag Core-Shell Nanoparticles during CO2 Reduction

Daniel Arenas Esteban[1], Dr. Lien Pacquets[1,2], Dr. Daniel Choukroun[2], Mrs. Saskia Hoekx[1,2], Dr. Ajinkya Kadu[1,3], Mr. Jonathan Schalck[2], Dr. Nick Daems[2], Prof. Tom Breugelmans[2], Prof. Sara Bals[1]
[1]Electron Microscopy for Materials Science (EMAT) and NANOlab Center of Excellence, University of Antwerp, Antwerp, Belgium, [2]Applied Electrochemistry and Catalysis (ELCAT), University of Antwerp, Antwerp, Belgium, [3]Centrum Wiskunde & Informatica (CWI), Amsterdam, The Netherlands

Poster Group 2

Electrochemical CO2 reduction reaction (eCO2RR) is one of the most promising and sustainable approaches to CO2 conversion to reduce atmospheric CO2 concentrations and mitigate the impacts of climate change [1]. For this purpose, the use of metallic nanoparticles (NPs) as electrocatalysis is on the rise, with Cu/Ag bimetallic interfaces being particularly popular for enhancing the eCO2RR towards CO and C2 products [2]. However, the electrochemical performance and product distribution of Cu@Ag core-shell configurations can change drastically under reaction conditions, particularly during the first few minutes of the reaction. In this study, our goal is to reveal the underlying structural changes these NPs experience at the critical first steps of the eCO2RR to understand their structure-properties relationship.

In this study, we utilized EDS analysis and high-resolution electron tomography to characterize the evolution of the Cu@Ag core-shell NP structure. The electrochemical measurements were performed in a homemade two-compartment, three-electrode cell, where the TEM grid was used as the working electrode, allowing for direct observation of the NPs before and immediately after the crucial first minutes of the reaction.

The Cu@Ag core-shell NPs used were found to be oblate and not homogeneously covered by Ag, with atomic-sized pinholes that expose the Cu core. Based on 3D characterization of various nanostructures found after current application, we hypothesized a transformation pathway. We observed an enlargement of these pinholes, most likely caused by the catalytic activity of the Ag shell, resulting in Cu leaching and, subsequently, a complete structural transformation of the NPs. Remarkably, the transformed Cu-Ag core-shell structure almost doubles the production of CO, presumably due to the combined effect of the different structures at various stages of transformation, as these transformations do not occur simultaneously [3].

Through the combined use of electrochemistry and advanced electron microscopy techniques, we have gained a better understanding of the relationship between the structure and electrochemical properties of Cu@Ag core-shell NPs, and how this affects their electrocatalytic performance. This research enhances our knowledge of Cu@Ag core-shell configurations and provides insights into other largely immiscible metal combinations. The study emphasizes the significance of the crystallinity of the central metal nanoparticle in deciding the formation of a complete and uniform second metal shell, which will be the key parameter towards nanoparticle stability.

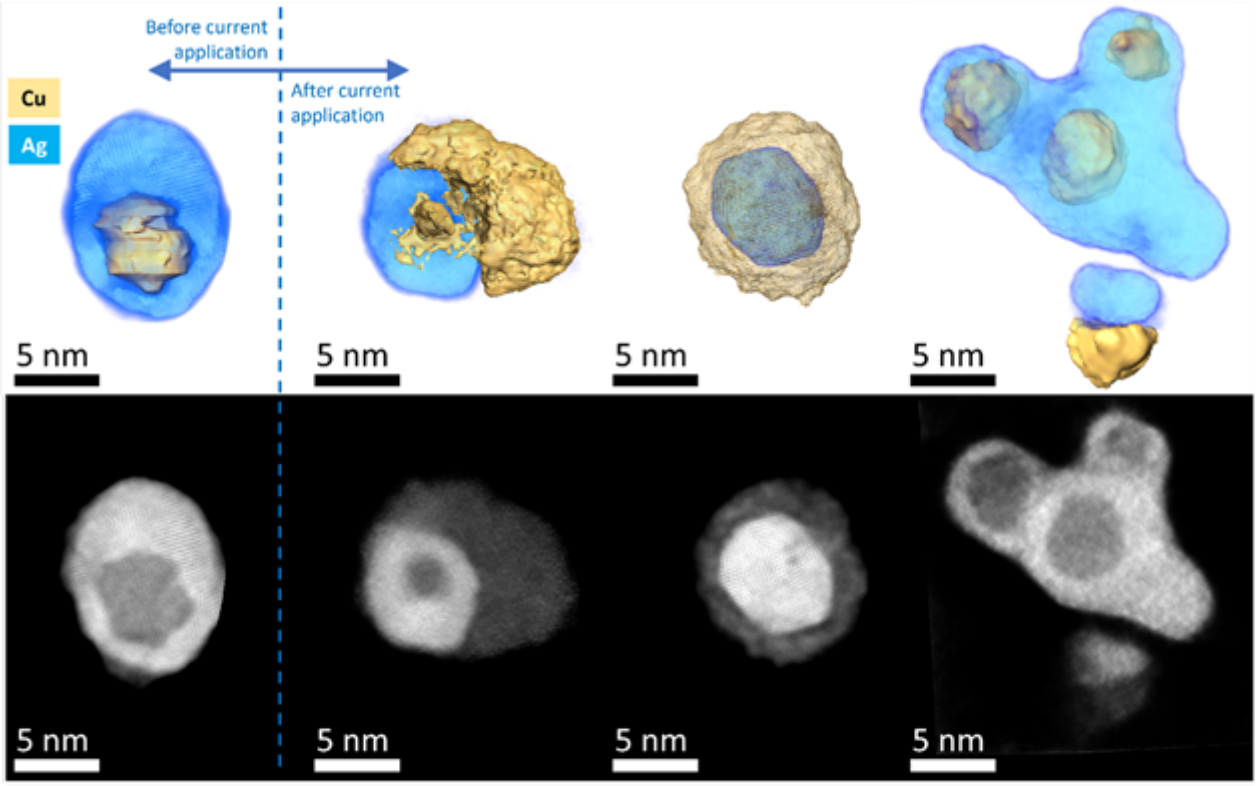

Figure 1. 3D reconstructions and their respective orthoslices through the reconstructed volume for the nanoparticles found before and after the CO2 reduction reaction.

Keywords:

Cu@Ag core-shell, CO2 reduction, Tomography

Reference:

[1] Garg, S. et al. Journal of Materials Chemistry A vol. 8 1511–1544 (2020).
[2] Chen, C. et al. Cu-Ag. Joule 4, 1688–1699 (2020).
[3] Huang, J., Mensi, M., Oveisi, E., Mantella, V. & Buonsanti, R. J Am Chem Soc 141, 2490–2499 (2019).

440

STEM-XEDS spectrokinetic analysis of oxygen: a tool to understand redox processes in nanostructured oxide catalysts

Professor José J. Calvino[1], Dr. Isabel Gómez-Recio[2], Dr. Huiyan Pan[1], Dr. Juan J. Delgado[1], Dr. Xiaowei Chen[1], Prof. Miguel A. Cauqui[1], Prof. José A. Pérez-Omil[1], Prof. María L. Ruiz-González[2], Dr. María Hernando[2], Prof. Marina Parras[2], Prof. José M. González-Calbet[2], Dr. Miguel López-Haro[1]
[1]Departamento de Ciencia de los Materiales e Ingeniería Metalúrgica y Química Inorgánica. Facultad de Ciencias, Universidad de Cádiz, Campus Rio San Pedro, Puerto Real, España, [2]Departamento de Química Inorgánica, Facultad de Química, Universidad Complutense de Madrid, Madrid, Spain

Poster Group 2

Background

Understanding the details of oxygen exchange processes becomes key to understand the performance of catalysts used in redox processes as well as to fix the most convenient pretreatment conditions to activate the catalyst prior to reaction. At macroscopic level, hydrogen temperature programmed experiments (H_2-TPR) are the most commonly used tool to propose the different phases and processes resulting from this activation step. Nevertheless, the interpretation of these TPRs becomes cumbersome and most of the times rather speculative.

A reliable determination of the actual phases appearing during the different oxygen evolution processes involved in these TPRs requires a precise quantification of the oxygen content of the materials at different steps of the reduction process. Such information, combined with structural analysis at local level provides the necessary information to interpret the H_2-TPR trace at quantitative level on solid backgrounds.

Regarding the compositional aspects. STEM-XEDS stems as a possible technique to face the quantification of the oxygen content at nanoscale in oxides with interest in redox catalysis. However, such approach requires to overcome two major difficulties: (a) dealing with absorption effects in the quantification of the oxygen signal; (b) disentangling the influence of beam reduction effects, which are particularly relevant in the case of high surface area, beam sensitive oxide nanostructures.

This contribution illustrates how combining time-resolved STEM XEDS experiments recorded during the in-situ reduction under the electron-beam performed on an aberration-corrected microscope equipped with large area detectors; an O-quantification scheme based on the use of the so-called ζ-factors method [1] and modeling of the kinetics of oxygen evolution, it is possible to determine with high accuracy the composition of the intermediate phases involved in the oxygen exchange processes of oxide nanostructures. In particular, the methodology is applied to the quite challenging case of nanorods of a complex, extremely beam sensitive, multicationic K-modified manganese oxide with hollandite type structure highly active in CO oxidation.

Methods

The starting K0.11MnO2-δ nanoxide was prepared from Mn(SO4)2, HNO3 and KMnO4 solutions under reflux over 24 h. This oxide was characterized at microscopic and macroscopic levels by Electron Probe Microanalysis (EPMA) and Neutron Diffraction (ND). The implementation of the ζ-factors method was done starting from Electron Tomography experiments performed in a Titan Themis 60-300 microscope operated at 80 kV. For reconstruction, a methodology based on TVM3D algorithms was employed to ensure high accuracy in the determination of local thickness values the oxide nanostructures [2]. XEDS maps were acquired with a Super-X G2 detector, using a beam current ranging between 135 and 145 pA. Maps were recorded in both single and multiple frames modes setting a pixel dwell time between 0.128 and 5.000 ms respectively. These conditions result in a frame acquisition time of approximately 3-100s, after which the drift was corrected using cross

correlation. XEDS line profiles were extracted using Velox 3.1 and the quantification was carried out using home-made scripts coded in Matlab.
Hydrogen temperature-programmed reduction (H_2-TPR) experiments were performed in an AutoChem II 2920 automated characterization system, equipped with a calibrated thermal conductivity detector (TCD).

Results

The quantitative analysis of XEDS spectra recorded at different irradiation times under the electron beam allowed us tracking the evolution of the O/Mn molar ratio of different oxide nanostructures, Figure 1 (left). Extrapolation to t=0 of the O/Mn ratio vs t plot provided an estimate of K0.13MnO1.98 stoichiometry for the pristine material. Full agreement with the K/Mn ratio determined by EPMA (K/Mn=0.125) and with the composition obtained by ND (K0.11MnO1.96) and H_2-TPR (K0.13MnO1.99) validated the oxygen quantification procedure proposed by us.
Formation of K0.13MnO1.61 as steady-state product of the electron-beam reduction process, which could be perfectly fitted to a contracting-volume kinetics, suggested that oxygen evolution proceeds in steps of 1/3 of the oxygen located at the O1 or O2 positions of the unit cell.
Taking this experimental observation into account and analysing in quantitative terms the deconvolution of the H_2-TPR experiments, Figure 1 (middle), all the steps involved in the reduction under hydrogen of this type of oxides could be perfectly interpreted and the corresponding intermediate phases proposed (Figure 1, right).
Combination of these results with those coming from DFT calculations allowed us confirming that the usual pre-reduction procedures used to activate these oxides lead to the elimination of all the oxygen residing at the O2 sites of the hollandite structure, rather than just all the oxygen sites (O1 and O2) at the surface of the oxide nanorods, as it has been proposed on speculative basis in the existing literature.
Likewise, it was possible to determine that the formation of MnO concludes at 553°C after the so-called δ step, rather than after the γ one, just at 423°, as it has also been proposed in literature.
Moreover, it has been possible to clarify that the intensity of this δ step is totally determined by the initial K content of the hollandite, this suggesting that oxygen evolution in this peak is related to O at the interface between Mn and K.

Conclusions

A novel methodology to implement the ζ-factors scheme to quantify with high accuracy the oxygen content in multi-cationic, beam sensitive, materials has been developed [3]. This methodology has been fruitfully applied to analyse in full quantitative terms time-resolved STEM-XEDS experiments recorded during the in-situ e-beam irradiation of nanorods of a potassium-modified manganese oxide with hollandite-type structure.
The quantitative results obtained at nanoscopic level fully agree with reference data obtained at macroscopic level by EPMA, ND and H_2-TPR, which supports the reliability of the developed approach. Moreover, from the nanoscopic results and the deconvolution of the TPR diagram on the basis of α step processes, it has been possible to determine the composition of the different intermediate phases involved in the reduction of the oxide under hydrogen, avoiding erroneous assignments in the literature.

Acknowledgements

This work has received support from Projects: PID2020-113006-RB-I00 funded by MCIN/AEI/ 10.13039/501100011033, PID2019-110018GA-I00, PID2020-113753RB-I00 and PID2020- 113809RB-C33. TEM/STEM experiments were recorded using equipment and scientific support of the Spanish Singular Infrastructure for Electron Microscopy of Materials (ICTS ELECMI).

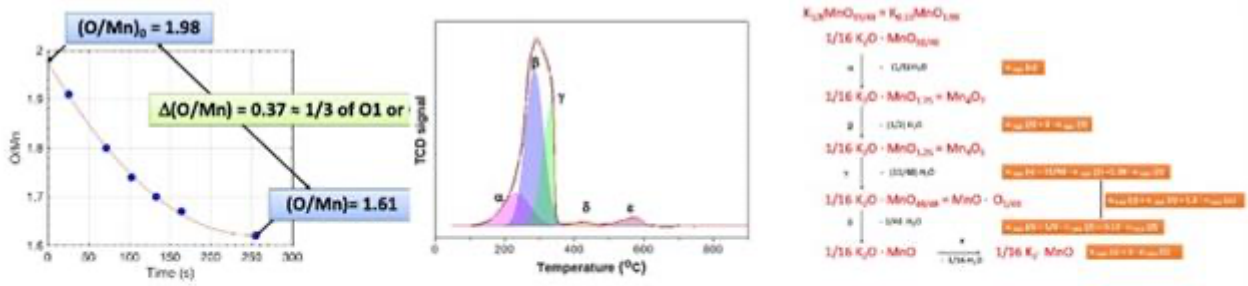

Figure 1. (left) O/Mn molar ratio vs t curve as determined from ζ-factors quantification of time-resolved STEM-XEDS in-situ e-beam reduction experiments; (middle) Deconvolution of the H_2-TRP diagrams of the hollandite oxide; (right) Scheme depicting the different oxygen evolution processes and intermediate phases during the reduction of the hollandite under hydrogen.

Keywords:

Time-resolved-STEM-XEDS, oxygen-stoichiometry, quantitative-XEDS-at-nanoscale, beam-sensitive-materials, ζ-factors

Reference:

1. Watanabe, M.; Williams, D. B., J. Microsc. 2006, 221, 89-109.
2. Van Aarle W., Palenstijn W. J., De Beenhouwer J., Altantzis T., Bals S., Batenburg K. J., Sijbers J., Ultramicroscopy 2015, 157, 35.
3. M. López-Haro, I. Gómez-Recio, H. Pan, J.J. Delgado, X. Chen, M.A. Cauqui, J.A. Pérez-Omil, M.L. Ruiz-González, M. Hernando, M. Parras, J.M. González-Calbet, J.J. Calvino, Microscopy & Microanalysis, 29 (3), 900-912.

509

Cryo electron tomography of impregnated mesoporous catalyst supports

Jason Heinrichs[1,2], Mr. Rick Joosten[2,3], Ms. Jovana Zečević[4], Mr. Thomas Weber[1,4], Mr. Emiel Hensen[1], Mr. Heiner Friedrich[2,3]
[1]Laboratory of Inorganic Materials and Catalysis, Department of Chemical Engineering and Chemistry, Eindhoven University of Technology (TU/e), Eindhoven, The Netherlands, [2]Center for Multiscale Electron Microscopy, Department of Chemical Engineering and Chemistry, Eindhoven University of Technology (TU/e), Eindhoven, The Netherlands, [3]Laboratory of Physical Chemistry, Department of Chemical Engineering and Chemistry, Eindhoven University of Technology (TU/e), , The Netherlands, [4]Shell Projects and Technology, Energy Transition Campus Amsterdam (ETCA), Amsterdam, The Netherlands

Poster Group 2

Background

Mesoporous materials are important for industry and society given their wide-ranging application areas including sorbents, separation, energy storage, biomedicine, or heterogeneous catalysis. Particularly heterogeneous catalysts have played a major role in our fossil-based society but they are also facilitating the transition towards a sustainable chemical industry based on renewable feedstocks and energy. One of the most commonly used methods to prepare a supported heterogeneous catalyst is incipient wetness impregnation (IWI). In IWI, the mesopores of the support material (e.g. silica, titania and alumina) are filled with a metal-salt solution that matches the volume of available pore space. Subsequently, the impregnated material is dried, calcined, and reduced yielding supported metallic catalyst particles within the mesopore network of the support. However, fundamental aspects of IWI such as pore filling, solute-support interactions, solid precipitation and/or (re-)deposition are still not fully understood. Furthermore, the corrugated surface and typically disordered mesopore structure of supports, both before, during, and after liquid impregnation have remained unexplored so far.

Methods

We employed cryogenic electron tomography (cryo-ET) to quantitatively assess the 3D structure of wet impregnated and freeze-dried disordered mesoporous supports. To this end, alumina extrudates of a few mm in diameter and length were crushed into small particles and IWI was performed with either water or aqueous solutions containing different molarities of Mo and Ni. Impregnated support particles were deposited on TEM grids and vitrified in liquid nitrogen. In addition, to study the solid deposition upon drying, impregnated support particles were freeze-dried by equilibrating the TEM to room temperature overnight. To capture the liquid-filled and freeze-dried state of a particle in 3D, tomographic tilt series were acquired under cryogenic conditions. A low-dose acquisition scheme combined with a direct electron detector (Falcon 4i) were utilized to minimize electron beam induced damage to the samples. Tilt series alignment and reconstructions were performed in IMOD or Inspect3D. Image processing, segmentation and quantitative analysis were carried out using a combination of Ilastik, MATLAB and AMIRA3D. We quantitatively evaluated the pore size distribution (PSD), specific surface area (SSA), pore volume (PV), pore tortuosity, surface shape index, and surface curvature to explore the change in pore structure and support surface induced by impregnation and solid deposition after drying.

Results

The degree of mesopore filling by a liquid was assessed from tilt series acquired with a cumulative electron dose ranging from 200 to 300 e-/Å2 which prevents beam-induced damage such as liquid bubbling. Numerical slices extracted from the 3D reconstructed volume show good contrast between

water and the alumina support structure. However, the contrast decreases with increasing concentration of metal components in the solution (i.e., 1.3 M, 3.0 M, 5.1 M, 8.1 M of Ni andMo). The PSD, SSA, and PV derived from these cryo-ET measurements were close to the bulk values, as determined by N2 physisorption. The additional morphological information uniquely provided by cryo-ET are pore tortuosity, surface shape index, and surface curvature, which were comparable for all samples. However, the sample with the highest molality was an outlier, which we attribute to the much-reduced contrast between alumina and the impregnation solution, hampering precise segmentation.

To study solid deposition during the drying step, an impregnated support particle (5.1 M precursor solution) was 3D imaged in the wet state and after freeze drying. The sufficient contrast between the solution and the support in the wet state allows observing the removal of water after freeze drying. The surface of the dried impregnated particle is covered with precipitated solids, substantially impacting the morphology of some of the pores, while other pores remain unaffected. Due to the low contrast between the precipitated solids and the support, it is not possible to measure the thickness of the deposited layer. Nevertheless, the darker regions at the outer rim of the freeze-dried support particle suggest preferential solid deposition in the outer regions of the impregnated and dried particle. In this state, cryo-ET-derived PSD, SSA, and PV values were lower than those of the bare support. The less tortuous pore structure together with the decrease of the average solid surface shape index, corresponding to an average surface change from ridge-like to saddle-like, suggests preferential deposition in pockets with initially a high negative curvature.

Conclusion

We employed a cryo-ET workflow to study the impregnation and drying steps of IWI performed on disordered catalyst support particles. To this end, wet impregnated support particles were successfully vitrified and imaged in 3D under cryogenic conditions. Good contrast was obtained between liquids containing up to 5.1 M metal (Ni and Mo) precursor and the alumina support, demonstrating the potential of this cryo-ET approach to investigate different liquid-solid systems. Furthermore, solid deposition was evaluated by quantification of the pore network and particle surface before and after freeze drying. Although it was not possible to directly distinguish the deposited solids from the support particles after drying, the deposited solids affected the pore size and particle surface as probed by quantitative analysis of cryo-ET reconstructions. In conclusion, this study shows the potential of cryo-ET to explore the liquid impregnation and/or drying processes across a diverse range of mesoporous materials applications.

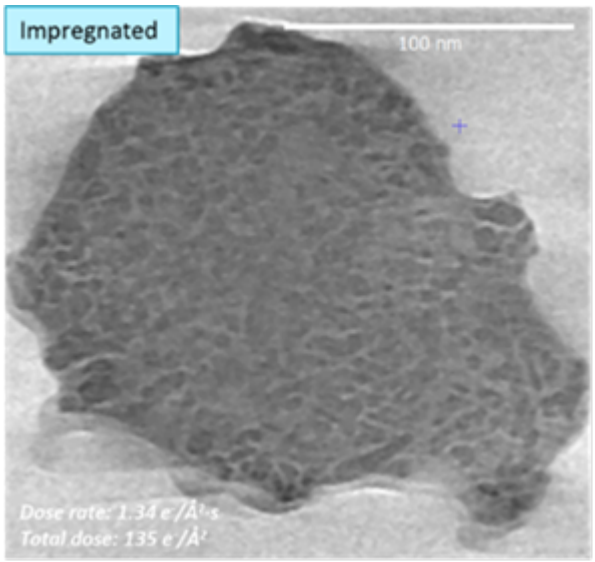

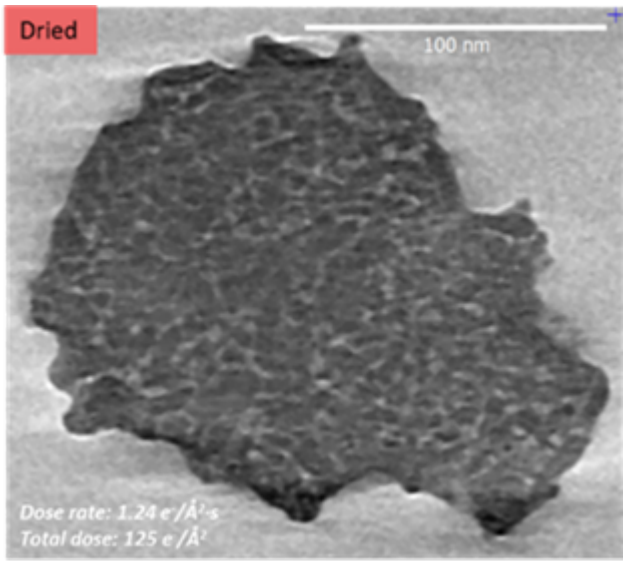

Keywords:

Cryo-ET
Quantitative analysis
Catalysts
Mesopores

510

Structure-activity relationship of Pt nanoparticles during the CO oxidation reaction

Christian Fink Elkjær[1], Ph.d. Sebastian Jespersen[1], Søren Vendelbo[2], Christian D. Damsgaard[3], Patricia Koymann[4], Ib Chorkendorff[3], Stig Helveg[3]
[1]Topsoe A/S, Kgs. Lyngby, Denmark, [2]Technological Institute, Taastrup, Denmark, [3]Technical University of Denmark, Kgs. Lyngby, Denmark, [4]University of Cape Town, Rondebosch, South Africa

Poster Group 2

Background incl. aims
The coupling between catalytic activity and the structure of supported nanoparticles under reaction conditions has been a significant driver for the development of in situ and operando characterization techniques in catalytic research. Traditional photon-techniques provide spatially averaged structural information of nanoparticle ensembles in miniaturized reactors, with conversion of reactants measured at the reactor exit by use of e.g. Mass Spectrometry (MS). To improve the spatial resolution of local structure and catalytic function of nanoparticle ensembles it is, however, beneficial using miniaturized reactors in conjunction with Transmission Electron Microscopy (TEM) [1,2,3,4].

Methods
Herein we focus on operando electron microscopy based on a nanoreactor. The nanoreactor is a Micro Electro-Mechanical System (MEMS) device equipped with a unidirectional and micrometer-sized gas channel, including a heating element, which facilitates MS of the exhaust gas from the nanoreactor as well as reaction calorimetry. With an array of electron transparent windows, the nanoreactor permits atomic-resolution TEM imaging of the nanoparticles under ambient pressure levels at different positions along the heated reactor zone [1,2,3]. Previously, we demonstrated how this system offered unprecedented insight into the oscillatory CO oxidation reaction catalyzed by an ensemble of Pt nanoparticles at ambient pressure levels by correlating high-resolution TEM of individual nanoparticles with global MS and calorimetry data. Moreover, a time-dependent first-principal reactor model was established that suggested marked gradients in the reactants along the gas flow channel under conditions of finite conversion levels.

Results
Herein, we will examine experimentally such gradients in the reaction environments by means of Electron Energy-Loss Spectroscopy (EELS). EELS offers sensitive detection of lighter elements in the gas phase with a special resolution defined by the area of illumination with the electron beam. EELS has therefore previously been used investigate gradients in temperature of heating devices [3] and gas composition[4]. Here we employ EELS for the first time to a gas flow reactor. By recording EELS at the Carbon K ionization edge, we examine the CO conversion profile along the nanoreactor and compare with mass-flow calculations through the nanoreactor and we relate the local structure and conversion to resolve spatially dependent structure-activity relationship during the Pt-catalyzed CO oxidation reaction.

Conclusion
In perspective, this operando electron microscopy and spectroscopy approach sets apart from the vast number of operando photon-techniques by the ability to relate nanoparticle structures with their catalytic activity, selectivity, and stability. However, such analyses take the reactor and mass-flow conditions into account conditions in order to develop chemical meaningful insight.

Keywords:

TEM, EELS, in-situ, Operando, Nanoreactor

Reference:

[1] S.B. Vendelbo, C.F. Elkjær, I. Puspitasari, P. Dona, L. Mele, B. Morana, B.J. Nelissen, R. van Rijn, J.F. Creemer, P.J. Kooyman, S. Helveg, Natur Materials, 13, 884-890 (2014)

[2] J.F. Creemer, S. Helveg, G.H. Hoveling, S. Ullmann, A.M. Molenbroek, P.M. Sarro and H.W. Zandbergen, Ultramicroscopy, 108, 993-998 (2008)

[3] S.B. Vendelbo, P.J. Kooyman, J.F. Creemer, B. Morana, L. Mele, P. Dona, B.J. Nelissen and S. Helveg, Ultramicroscopy, 133, 72-79 (2013)

[4] B.K. Miller and P.A. Crozier, Mircoscopy and Microanalysis, 20, 815-824 (2014)

524

Elucidation of Structure-catalytic Activity of Nickel-based Nanomaterial for Electrocatalytic Water Splitting

Dr. Jean Marie Vianney Nsanzimana[1], Charles Otieno Ogolla[1], Max Kasper[1], Prof. Manuela Killian[2], Prof. Butz Benjamin[1]
[1]Micro- and Nanoanalytics Group, University of Siegen, Siegen, Germany, [2]Chemistry and Structures of Novel Materials, University of Siegen, Siegen, Germany

Poster Group 2

Background

The lack of satisfactory and cheaper catalysts for hydrogen production by electrocatalytic water splitting and hydrogen utilization in fuel cells is the major challenge for this clean energy technology [1]. New advanced nanostructured materials with special properties for green H2 production by water splitting are needed to address this major and urgent challenge [2]. Nanostructured materials have shown promising catalytic performance that exceeds the sum of their individual components [3-4]. Thus, they contribute to the development of industrially applicable and sustainable materials for new alternative clean electrochemical energy technologies. For the discovery of novel advanced energy materials that meet the requirements of emerging clean electrochemical energy technologies, advanced tools for the elucidation of structural (electro)catalytic activity are at the heart of future and sustainable nanomaterial development. These advanced materials require advanced scale-bridge spectroscopic technics characterization to understand the chemistry and the elemental species of nanostructured materials at the nanoscale. We have developed a rational design of easily scalable nickel boride (NixB)-derived catalyst to correlate with optimized catalytic activity through metal elements incorporation in a one-pot synthesis method. Our method overcomes the challenge of conventional annealing-dependent processes which have limited applicability on a large scale since they also require an inert processing environment. Furthermore, we elucidate a structure-activity relationship by utilizing scale-bridging correlative microscopy techniques leveraging transmission electron microscopy coupled with electrochemical characterization.

Methods

To elucidate the structure-electrocatalytic activity functionality of these nanostructures, we conducted a thorough electrochemical and TEM investigation on binary nickel boride and quaternary nickel boride-derived catalysts.

Results & Conclusion

A one-pot synthesis method enabled a rational design of non-noble metal, highly efficient, and durable electrocatalysts for hydrogen production at low-temperature electrolysis in harsh alkaline solutions. This improved catalytic performance is further corroborated by microstructural investigations using TEM. The nanoparticles obtained have an improved porous structure compared to conventionally synthesized NixB (Figure 1), providing more available sites for surface reactions and catalytic performance of this nanostructured material. Furthermore, we demonstrate that activation enables morphological and structural changes, while some transition metal elements act as sacrificial elements to provide more accessible and stable sites for oxygen-forming centers. This paves the way for a better understanding of metal boride-derived electrocatalysts for electrocatalytic water splitting and contributes to future discoveries of non-noble metal catalysts, yet with highly efficient and stable nanostructured materials.

Acknowledgements:

This project has received funding from the European Union's Horizon 2020 research and innovation program under the Marie Skłodowska-Curie grant agreement No 945422. We acknowledge use of the DFG-funded Micro-and Nanoanalytics Facility (MNaF) at the University of Siegen (INST 221/131-1).

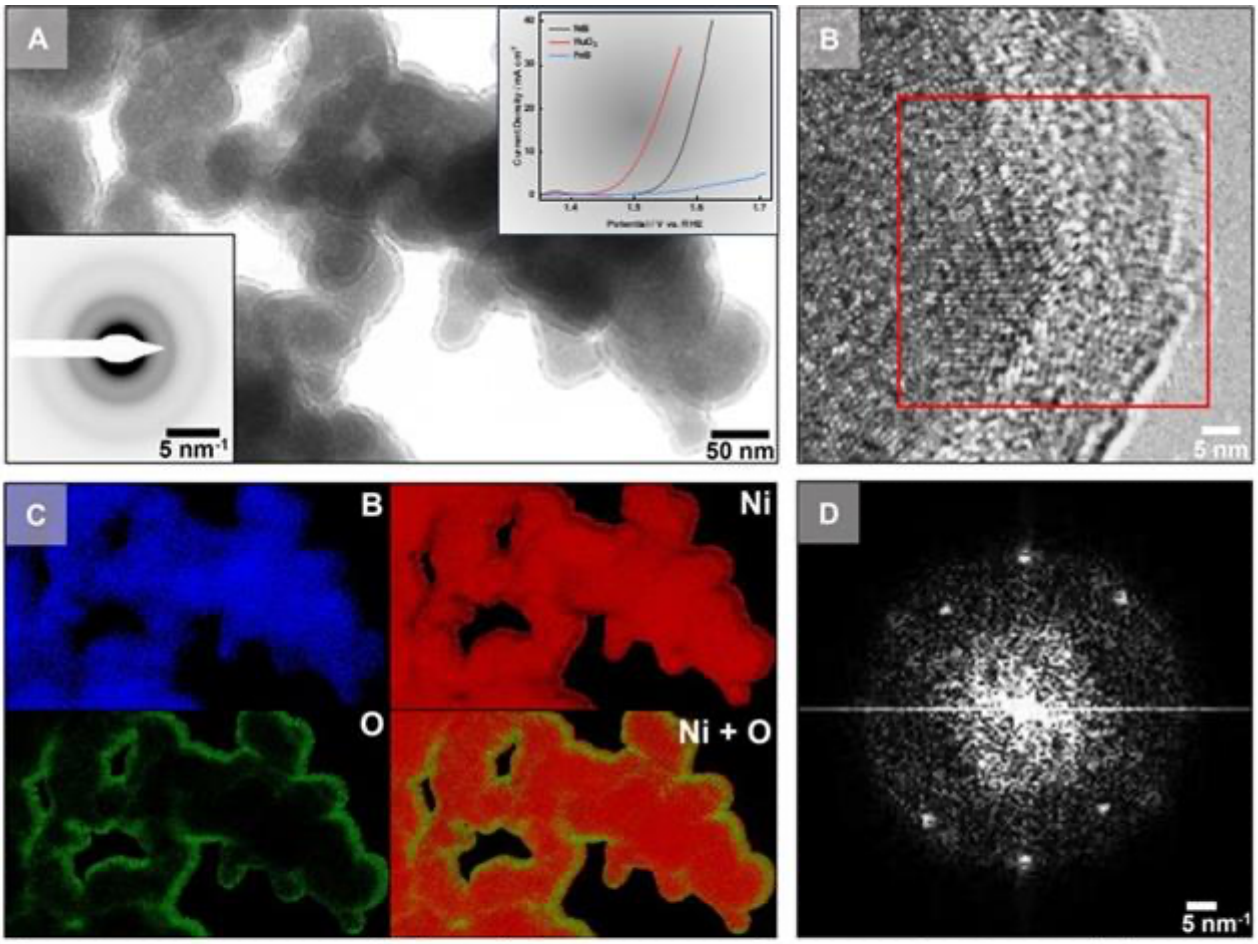

Figure 1. Microstructure and chemical characterization of as-prepared Ni_xB; A) well-dispersed material indicating shell outline and compound amorphous-crystalline heterostructure; B) HRTEM of shell indicating the nano crystalline domains; C) EDXS elemental distribution maps indicating localized enhanced oxidation along the shell structure; D) FFT of ROI (red square) in Ni_xB.

Keywords:

STEM-EELS, catalyst, nanoparticles, water electrolysis

Reference:

[1] A. Kazemi, et al. ACS Omega 2024, 9, 7310−7335
[2] J. Jayaprabakar, et al., Int. J. Hydrogen Energy., 2024, 52, 674-686
[3] JMV, Nsanzimana, et al., ACS applied materials & interfaces 2018, 11 (1), 846-855
[4] Z. Qin, Nanomaterials 2023, 13(13), 1980

539

Characterization of inorganic food additives and pearlescent pigments in sprays for food decoration by STEM-EDX

Noa Olluyn[1,2], Dr. Eveline Verleysen[1], Lisa Siciliani[1,2], Dr. Daniel Arenas Esteban[2], Dr. Stella Mathioudaki[1], Dr. Subhalakshmi Sharma[1], Joris Van Loco[1], Prof. Dr. Sara Bals[2], Dr. Jan Mast[1]
[1]Sciensano, Uccle, Belgium, [2]EMAT, University of Antwerp, Antwerp, Belgium

Poster Group 2

Background and aims:
Food colorants are applied to enhance the appearance of food. To obtain specific hues, inorganic food additives containing (nano)particles are mixed in varying concentrations, and pearlescent pigments, consisting of mica platelets coated with a layer of titanium dioxide and/or iron oxide particles, are applied to provide glitter effects [1]. For assessing potential risks of multi-constituent substances and mixtures, characterisation of the fraction of small particles, including the particle size distribution, is needed for each single constituent or each component in the mixture [2]. This is challenging for control laboratories and only limited guidance is currently available [3].
This study developed electron microscopy-based methods to identify and characterize the particles of individual components in 8 commercially available food-decoration sprays of different colours, containing mixtures of food additives and pearlescent pigments.

Methods:
To avoid altering the properties of the particles consumers are exposed to, no extensive dispersion protocols or purifications steps were applied. Samples were prepared by spraying 5 mL in a glass vial and coated on EM-grids using the grid-on-drop method. Scanning transmission electron microscopy (STEM) combined with energy dispersive X-ray spectroscopy (EDX) and EDX-tomography were applied to image the various components. Subsequently, image processing using the ImageJ software was performed to obtain quantitative results.

Results:
The various components were identified based on their elemental composition, including potassium aluminum silicate-based pearlescent pigments, vegetable carbon, rutile titanium dioxide, iron oxide and aluminum containing (nano)particles. Their presence, size, and relative concentration varied among the different spray colours. Often the layer of titanium dioxide particles detached from the mica substrate, and titanium dioxide particles were also observed forming near-spherical aggregates. STEM-EDX tomography allowed identifying particles of overlapping components and examining the structure of the pearlescent pigments in 3D. This way, all components in the mixtures could be successfully identified, and the particle size distributions of each components in all but the most challenging mixtures could be obtained.

Conclusion:
The developed electron microscopy-based methods allowed identifying the different components in the mixtures, and the presence of a fraction of nanoparticles in each component was demonstrated based on their number-based particle size distributions. The methods and findings support regulatory bodies in assessing the potential health risks of mixtures of (nano)particles used in food-related applications.

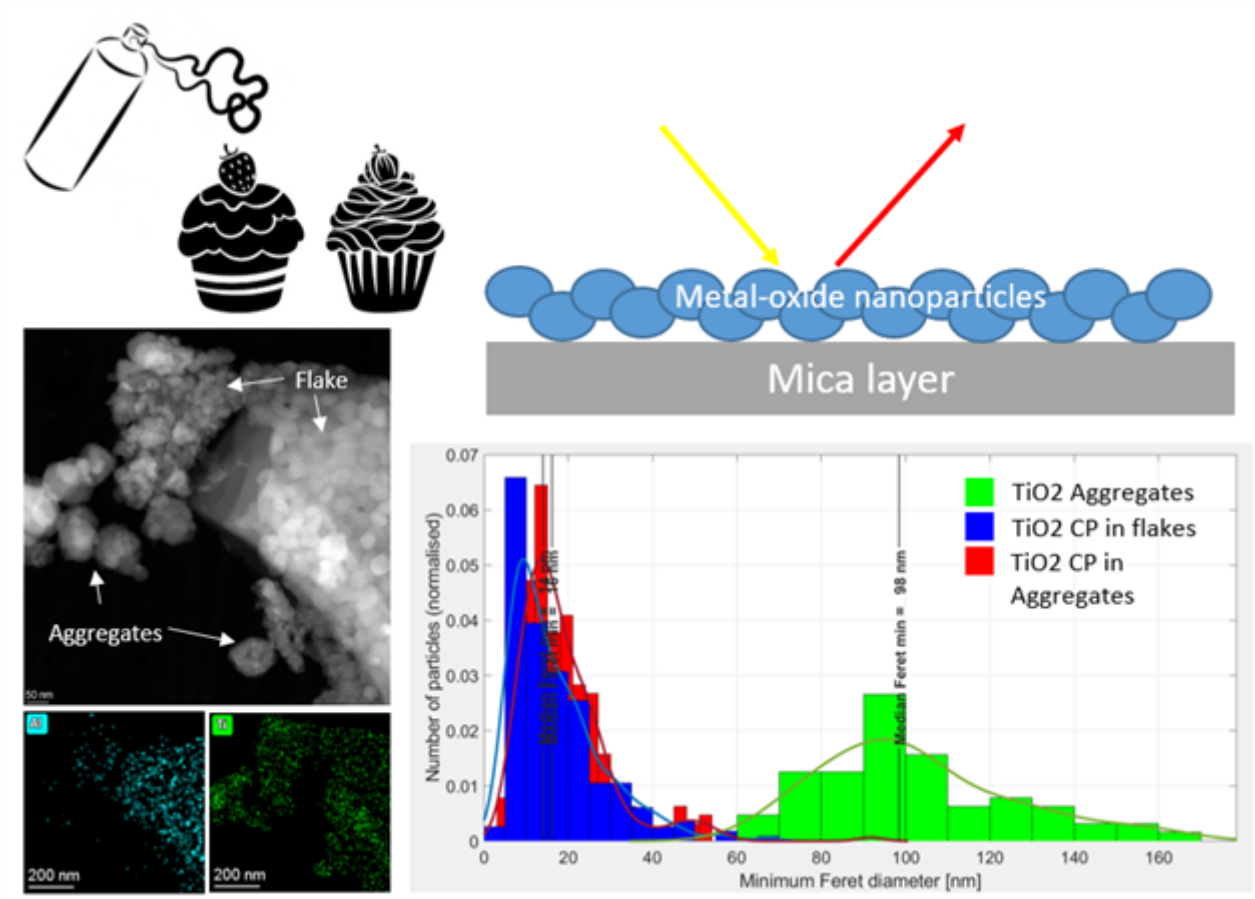

Keywords:

pearlescent pigments, STEM-EDX, nanomaterials

Reference:

(1) Joint FAO/WHO Expert Committee on Food Additives, Compendium of Food Additive Specifications; 77th Meeting 2013; FAO JECFA monographs; Rome, 2014.
(2) EFSA Scientific Committee; Guidance on Technical Requirements for Regulated Food and Feed Product Applications to Establish the Presence of Small Particles Including Nanoparticles. EFSA J. 2021, 19 (8). https://doi.org/10.2903/j.efsa.2021.6769.
(3) CEN. Nanotechnologies - Guidance on Detection and Identification of Nano-Objects in Complex Matrices. TC352 2018, TS17273.

546

Leveraging gas-cell in situ electron microscopy to track atmosphere-dependent reversible transformations in reducible oxides

Postdoc Ramon Manzorro[1], Irene Piedra[1], Carmen Mora[1], Jose A. Perez-Omil[1], Jose J. Calvino[1], Miguel Lopez-Haro[1], Ana Hungria[1]
[1]Departamento de Ciencias de los Materiales e Ingeniería Metalúrgica y Química Inorgánica, Facultad de Ciencias, Universidad de Cádiz, Puerto Real, Spain

Poster Group 2

Background
Environmental catalysis has long been a subject of significant interest, particularly given the pressing need for renewable, eco-friendly energy sources amid the current energy crisis. O2 and/or H2 are commonly involved in these processes, either as reactants or products, with redox reactions playing a pivotal role in understanding the reaction pathways and their mechanisms. The performance of catalysts is closely linked to these mechanisms, making an in-depth study of these systems vital for enhancing catalytic activity and selectivity. However, catalysts are dynamic entities prone to undergoing structural and chemical transformations during reactions. Traditional electron microscopy techniques are limited in their ability to capture these changes, typically providing insights only into the catalyst's initial and final states1. In response to this challenge, gas-cell in situ electron microscopy has emerged as a crucial tool. This cutting-edge technique allows for the direct visualization of phenomena occurring at the nano and even atomic scale during catalytic reactions. A better understanding of the materials and their functionality during reaction will aid in designing rational catalysts with improved performance.
Yet, there is a big scale gap between conventional catalytic reactors and the in situ nanoreactor affecting phenomena such as mass or heat transport that should be given more consideration2,3. Aiming to investigate the potential disparities emerging between the macro and nano scales, we propose to in situ characterize the chemical behavior of reducible oxides, while contrasting it with the results obtained in regular catalytic reactors.

Methods
To this end, two families of model catalysts have been picked to track their evolution during reduction/oxidation reactions. The systems consist of CeO2 and Cu2O oxides with nanocubes morphology. A well-defined surface crystallography will contribute to generalizing about the phenomena taking place. These samples have been submitted to temperature-programmed reductions/oxidations (TPR and TPO) monitoring their reducibility.
Similarly, in situ redox reactions under H2 or O2 atmospheres have been carried out in a DENS Solutions Climate holder, using a double-corrected FEI Titan Cubed at 200 kV. Pressure inside the nanoreactor was about 950 mbar and gas flow was set to 0.01 ml/min with 50% of reactive gas (either H2 or O2) balanced with N2. The phase transformations related to temperature and gas flow in electron-transfer reactions entail chemical changes, like a shift in the valence state, and structural changes triggering a modification in the crystal lattice. Electron diffraction and electron energy loss spectroscopy (Gatan Quantum 966 ERS) have allowed us therefore to trace the modifications on the model Cu2O and CeO2 catalysts.

Results
Prior to investigate controlled-morphology Cu2O and CeO2 catalysts, a reference CuO sample has been tested to compare reduction degree and temperature between in situ and ex situ redox cycles. Their correlation determines a shift of about 50 ºC towards higher temperatures in the reduction at the nano scale, spanning as well over a wider range. Deviations in the actual conditions of both

experiments may point out differences in their kinetics that should be further considered. From a structural point of view, Figure 1A shows the drastic change suffered in commercial CuO crystals after interaction with H2, splitting apart into way smaller nanoparticles. The interpretation of electron diffraction patterns unveils that, in line with the TPR results, the morphological transformation is linked with the transition to metallic Cu.
Moving forward with our target systems, we have first explored the reduction of CeO2 nanocubes, where the ex situ TPR is mainly defined by two reduction events separated by at least 300 ºC. Figure 1B follows the evolution of ceria nanocubes under H2 when the temperature increases up to 950 ºC. The elemental mapping has been extracted from Ce-M4,5 EELS fine structure, showing the spatial distribution of Ce3+ (red color) and Ce4+ (green color) at 450 ºC and 950 ºC. The in situ reduction triggers the formation of a reduced cerium-based shell which propagates towards the core of the nanocubes at elevated temperatures. The presence of two reduction peaks muddles the direct correlation between the ex situ and in situ experiments, demanding therefore a quantitative analysis of both processes to match the temperatures and defined each of the two reduction events.
To clear out the roots of these and further experiments, a deeper investigation on the reduction/oxidation of these oxides is required. In addition, the Cu2O nanocubes will also be addressed comparing the results with the CuO reference and the details determined in the reduction of the CeO2 nanocubes approach.

Conclusion

The relationship between conventional quartz reactors and Si3N4-membrane nanoreactors has inferred a temperature deviation in the in situ measurement, although further experiments are mandatory to determine if this departure is material-related or just a fixed value. Despite the reduction of CeO2 nanocubes has been captured with the surface-to-core spreading of a reduced phase, the nature of this shell still remains unclear. Future experiments based on Cu2O nanocubes will be used to cross-check this singular observation.

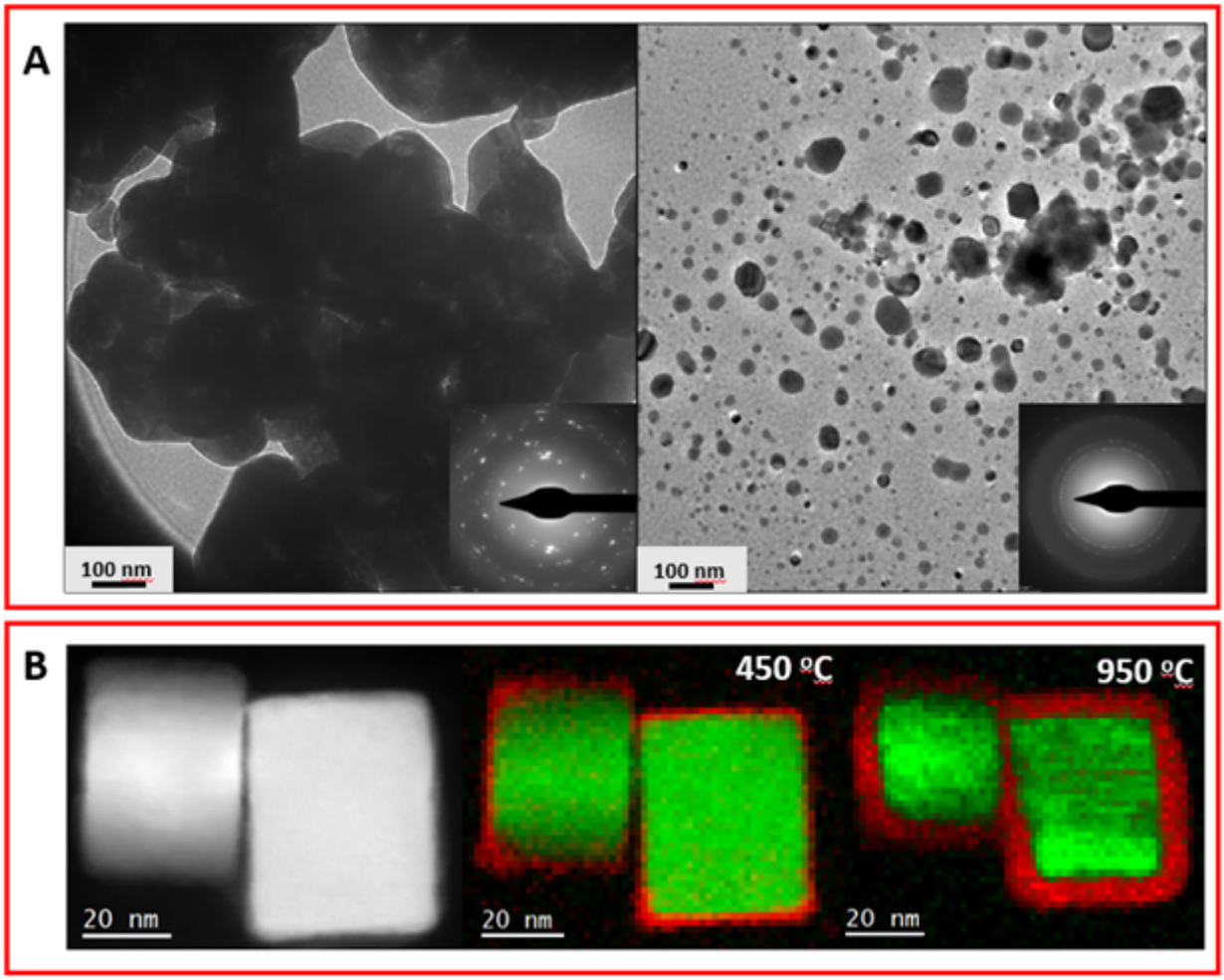

Keywords:

in-situ, EELS, diffraction, reducible-oxides, catalysts

Reference:

(1) Chinchilla, L.; Manzorro, R.; Olmos, C.; Chen, X.; Calvino, J. J.; Hungría, A. B. Temperature-Driven Evolution of Ceria–Zirconia-Supported AuPd and AuRu Bimetallic Catalysts under Different Atmospheres: Insights from IL-STEM Studies. Nanoscale 2024, 16 (1), 284–298. https://doi.org/10.1039/D3NR02304D.
(2) Beck, A.; Zabilskiy, M.; Newton, M. A.; Safonova, O.; Willinger, M. G.; van Bokhoven, J. A. Following the Structure of Copper-Zinc-Alumina across the Pressure Gap in Carbon Dioxide Hydrogenation. Nature Catalysis 2021, 4 (6), 488–497. https://doi.org/10.1038/s41929-021-00625-x.
(3) Vincent, J. L.; Vance, J. W.; Langdon, J. T.; Miller, B. K.; Crozier, P. A. Chemical Kinetics for Operando Electron Microscopy of Catalysts: 3D Modeling of Gas and Temperature Distributions during Catalytic Reactions. Ultramicroscopy 2020, 218, 113080. https://doi.org/10.1016/j.ultramic.2020.113080.

554

Direct Visualization of Temperature Induced Phase Separation of Completely Miscible Au-Pd Alloy by In-Situ TEM

Dr. Abhijit Roy[1,2], Dr. Simon Hettler[1,2], Dr. Raul Arenal[1,2,3]
[1]Instituto de Nanociencia y Materiales de Aragón (INMA), CSIC-Universidad de Zaragoza, Zaragoza, Spain, [2]Laboratorio de Microscopías Avanzadas (LMA), Universidad de Zaragoza, Zaragoza, Spain, [3]ARAID Foundation Zaragoza , Zaragoza, Spain

Poster Group 2

Background incl. aims
Very recently, bimetallic nanoparticles (NPs) are getting a lot of attentions due to their superior efficiency in heterogeneous catalysis and potential to replace conventional fossil fuels. Bimetallic systems showed superior stability, and superior activity compared to any of their individual metallic counterpart. In this aspect, Au@Pd core@shell NPs and recently Au-Pd nano-alloys has been used for electrocatalytic production hydrogen peroxide (H2O2), ethanol oxidation reactions and they observed to show much better catalytic activity compared to bare Pd nanoparticles. However, Au NPs are less efficient for oxygen reduction but highly efficient for conversion of alcohols to aldehyde, which is completely opposite to the catalytic activity of Pd. These limitations were repressed by alloying both systems (Au and Pd), but the lower electrochemical potential of the metal alloy contrast to the individual metals decreases its efficiency towards alcohol to aldehyde conversion reaction. Thus, it should be highly beneficial to construct a bi-metallic Au-Pd system where both the phases are separated from each other in a single nanoparticle. In such systems, the oxidation and reduction reactions will take place at totally different locations of the same nanoparticle, leading to more superior catalytic activity and stability. Such systems are unique in this sense, as they retain the individual properties of separate constituents and also provide physical, chemical, optical interaction between them due to the presence of a common interface [1]. However, obtaining bi-metallic nanoparticle based on phase separation method depends on the fact that the lattice mismatch between two constituent metals must be large (>5%, ex. Au-Ni, Au-Cu). Metals with lower lattice mismatch tend to create an alloy system due to complete miscibility in their all composition range at all the temperatures according to their bulk phase diagram (i.e. Au-Pd) [2]. Though theoretical researchers predicted a miscibility gap of an Au-Pd bimetallic system, the conversion of Au-Pd nanoalloy to phase separated Au/Pd bi-metallic system with annealing could not be observed till now. Okamoto et. Al. observed Au-Pd alloy formation in face centered cubic (fcc) structure at high temperature for all Pd composition range [3]. Wu et. Al. observed formation of an alloyed nanoparticle upon in-situ heating of a core@shell Au@Pd nanostructure up to 600°C [4]. Precot et. al. studied the annealing effect of Au-Pd nanoparticles deposited on amorphous carbon at 873K and observed bi-modal distribution of nanoparticle upon annealing, where small nanoparticle and big nanoparticles became Au-rich and Pd-rich, resulting a bi-modal distribution of nanoparticles driven by Ostwald ripening mechanism [5].
We have shown by in-situ vacuum annealing high-resolution transmission electron microscopy (HRTEM) study of the generation of phase separated Au-Pd bimetallic nanoparticles from an initial Au nanotriangle (AuNT)@Pd core@shell nanoparticle system. We have observed through extensive aberration-corrected HRTEM, high-resolution scanning TEM (HRSTEM) and energy-dispersive X-ray spectroscopy (EDS) that the core@shell Au@Pd nanostructure forms an Au-Pd alloy during in-situ heating at 400°C and is very much stable up to 800°C, which is a completely normal behavior. Upon further heating at 900°C-1000°C range, the Au and Pd phase surprisingly got separated from each other and the separation is observed to be much prominent for initial core@shell NPs with higher Pd loading.

Methods

Au nanotriangles (AuNT) were produced by a previously described seedless method. Thickness of Pd layer was controlled by controlling the amount of H2PdCl4 in the AuNT solutions. The nanoparticles were initially identified by UV-Visible and X-ray photoelectron spectroscopy (XPS) technique. The in-situ HRTEM and selected area diffraction (SAD) studies were performed in an image-corrected FEI TITAN operated at 300 kV. HRSTEM, energy dispersive X-ray spectroscopy (EDS) analyses were carried out in a probe-corrected FEI TITAN TEM equipped with high-brightness gun and an Oxford Instruments Ultim X-MaxN 100TLE detector for EDS measurements. A DENSsolutions Wildfire MEMS based double-tilt heating holders was used for the in-situ heating measurements. The heating circuits were fabricated on a SixNy membrane and it can measure temperature until 1300 °C. A very dilute solutions of the AuNT nanoparticles were drop casted on the heating chips and kept overnight for drying.

Results

We have extensively studied the interface and surface of bare AuNT and AuNT@Pd core@shell nanostructures and identified presence of number of defects at the Au/Pd interfaces (i.e. stacking-faulst, dislocation pair etc.). Also, the melting point of bare AuNT is observed to be lower compared to the Pd doped sample and the melting point seemed to be increasing with increase in Pd content. Besides that, the relative change in lattice parameter with in-situ heating was also studied for bare NT and AuNT@Pd with different Pd thickness using fast Fourier transform (FFT) method and we observed the change in lattice parameter of (220) plane is much lesser for Au-Pd alloy compared to bare AuNT. However, the most important observation was the phase separation of Au-Pd alloy triangular nanostructure producing distinctive Au and Pd region at higher temperature which was verified by HRTEM and EDS measurement. The Pd region increased in size with higher Pd loading. The in-situ microscopy reveals the Pd atoms outward movement from the core due to their higher mobility at high temperature while Au atoms move inwards to finally produce a phase separated structure. This structure was also observed to be very stable as the EDS spectra taken from the sample at room temperature after 7 days revealed that the nanoparticle still remains in the phase separated form.

Conclusion

We have done in-situ heating experiment on bare AuNT and AuNT@Pd core@shell nanostructure up to 1000°C. The Pd deposited AuNT showed much more stability in terms of structure and thermal resistance as observed. Most importantly, though Au and Pd are miscible in all temperature range and all compositions. We observed when Pd content is higher, it can produce phase separated region at High temperature which was observed to be very much stable in ambient atmosphere over a month. This result will be of very much important to understand not only the catalytic activity of Au-Pd alloy but also to produce phase separated bi-metallic nanostructure consisted of separated Au and Pd region for superior catalytic activity.

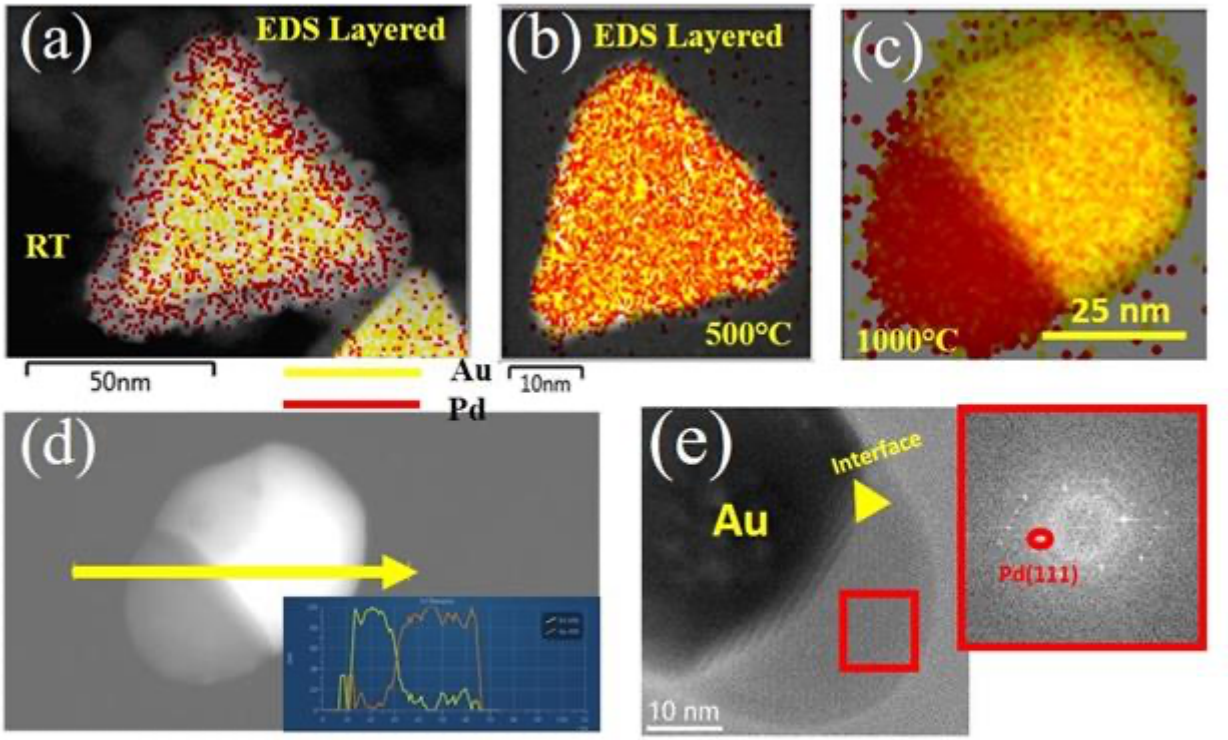

Fig. (a-c) EDS map of Au-Pd region at RT, 500°C and 1000°C, respectively showing complete phase separation at high T. (d) Line spectra (e) HRTEM image. The FFT [inset] taken from the Pd region [red square] showing lattice parameter corresponds to (111) planes of Pd.

Keywords:

Au-Pd alloy, Phase separation, in-situ

Reference:

Reference:
1. J. Qui, et. Al. Adv.Mater. 2022, 34, 2102591.
2. B. Lim, et. Al. Science 2009, 324, 1302-1305.
3. H. Okamoto, T. B. Massalski. Bulletin of Alloy Phase Diagrams 1985, 6, 229–235.
4. Z. Wu. et. Al. Phys. Chem. Chem. Phys., 2019,21, 3134-3139.
5. G. Prévot et. Al. ACS Nano 2016, 10, 4127–4133.

Funding : Research supported by the Spanish MICIU (PID2019-104739GB-100/AEI/10.13039/501100011033), the Government of Aragon (DGA) through the project E13_23R and by the European Union's Horizon Europe research and innovation programme under the Marie Sklodowska-Curie grant agreement No 101109165.

602

Understanding CuO/Al2O3 Interactions during Thermochemical Redox Reactions: TEM, X-ray Microscopy, and XAS Study

Dr Sharmin SHARNA[1,2,3], Dr Virgile Rouchon[2], Dr Christèle L Legens[2], Dr Arnold Lambert[2], Dr Stefan Stanescu[3], Dr Anne-Sophie Gay[2], Dr David Chiche[2], Dr Valérie Briois[3], Prof. Ovidiu Ersen[1]
[1]Institut de Physique et de Chimie des Matériaux de Strasbourg, Strasbourg, France, [2]IFP Energies nouvelles, Lyon, France, [3]Synchrotron Soleil, Saint-Aubin, France

Poster Group 2

Background

Chemical Looping Combustion (CLC) presents a midterm solution for fossil fuel utilization with inherent carbon dioxide capture, utilizing oxygen carrier materials. These carriers replace air to provide oxygen for combustion across a wide range of fuels, operating through reduction/oxidation cycles in a circulating fluidized bed reactor at high temperatures [1]. Copper oxide supported on alumina grain (CuO/Al2O3) is widely considered a promising oxygen carrier (OC) for industrial CLC use due to its benign nature and flexible redox behavior, ensuring high reactivity and oxygen transfer capacity. However, successive high-temperature (800-900°C) reduction (combustion) and oxidation (regeneration of oxide phase) cycles induce chemical and morphological changes in the material, leading to degradation in its oxygen-carrying properties. The evolution in the cycled material is attributed to the diffusion of Cu-phases at the grain scale [2]. Herein, we bridge the gap in understanding between the observed µm-scale migration of Cu-based phases and nanoscale transformations of Cu nanoparticles (NPs) by employing a multi-scale characterization approach, both temporally and spatially, using Scanning Transmission X-ray (STXM) and Scanning Transmission Electron (STEM) Microscopies, and operando Quick X-ray Absorption Spectroscopy.

Methods

We conducted a study on CuO supported on 50-100 µm sized γ-Al2O3 grains, synthesized via incipient wetness impregnation and calcined at 900°C. To replicate the cyclic nature of (CLC), we subjected the fresh samples to oxidation and reduction under air and H2 at 900°C using a thermogravimetric analyzer (TGA). Ultramicrotomy sections with a thickness of 100 nm were prepared for SEM, STXM, and TEM characterizations. Energy stacks and mappings were generated at the Cu L-edge and Al K-edge to identify specific spectral features of each compound. In situ TEM analysis was conducted using a probe Cs-corrected microscope equipped with closed-cell in situ gas setup featuring a sealed environmental cell (e-Cell), operating at atmospheric pressure. Finally, operando XAS measurements were performed in a capillary tube under identical reaction conditions as in the TGA. By acquiring relevant reference material spectra and utilizing chemometric data processing, we extracted chemical-structural phase distribution over the course of 50 redox cycles at 900°C.

Results

The microscopic study reveals significant transformations in the CuO/γ-Al2O3 system during redox cycling (Figure 1 a and b) [3]. Initially, fresh grains consist of γ-Al2O3 with uniformly dispersed CuO nanoparticles (10-20 nm). After 50 redox cycles, observation at the grain scale (µm) demonstrates the progression of the gamma to alpha reaction front within the solids. This front exhibits a distinct structural-chemical gradient, characterized by three zones: zone 1 displaying non-stoichiometric Cu (II) aluminate, zone 2 with an intermediate thin layer (< 200 nm) of Cu (II) aluminate enriched in Cu, and zone 3 composed of α-Al2O3 phase containing large CuO particles. The proportion of copper varies significantly across these zones, ranging from 10 wt% Cu in zone 1 to ~25 wt% at the edge of the reaction front in zone 2. In situ STEM observation at 900°C under H2-reduction reveals the

migration of copper, forming copper nanoparticles from a starting oxidized sample predominantly composed of homogeneous Cu (II) aluminate. This suggests that copper mobility during redox cycling is associated with the phase transition of γ to α-Al2O3.

Furthermore, the spectral evolution during oxidation and reduction reactions, depicted in Figure 1c, highlights changes in the concentration of different Cu-Al species [4]. The oxidized state initially consists of CuxAlyO4, gradually transforming into the metallic copper phase with increasing redox cycles. Notably, a threshold circa 25 cycles indicate a drastic conversion from the aluminate phase to copper oxide. At the end of the redox cycles, the oxygen carrier predominantly comprises α- Al2O3 and CuO. The transition point is linked to the growth and propagation of α- Al2O3, suggesting a mechanism involving particle size influencing the alpha alumina phase transition, proceeding through an initial slow seeding phase followed by rapid propagation.

Conclusion

The integration of spectroscopic and microscopic techniques, both in situ and post-mortem modes, provided a comprehensive understanding of the material evolution in terms of morphology and the diverse phase interactions across spatial dimensions and over extended reaction durations.

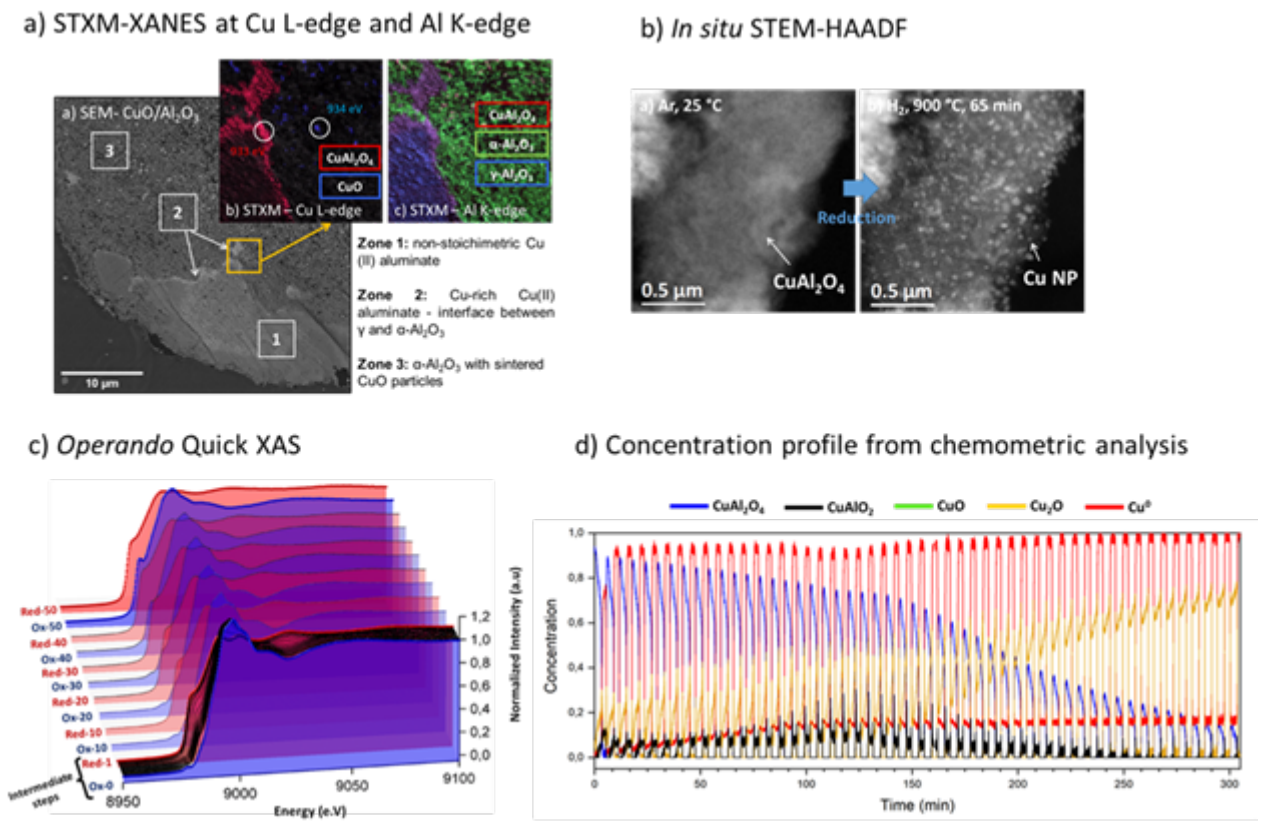

Keywords:

STEM, STXM, Quick XAS, Copper

Reference:

[1] Adanez et al., Progress in Energy and Combustion Science., 38, (2012), 215-282
[2] Lambert et al. Fuel., 216 (2018), 71–82
[3] S. Sharna, et al. ChemCatChem, 2023, 15, 4, e202201259
[4] S. Sharna. PhD thesis: Understanding the mechanisms leading to copper migration in supported oxygen carrier for chemical looping combustion. Theoretical and/or physical chemistry. Université de Strasbourg, 2021

623

New generation environmental in situ TEM holder for gas cell studies across multiple platforms

Dr. Yevheniy Pivak[1], Dr. Dan Zhou[2], MSc Christian Deen-van-Rossum[1], MSc Ronald Spruit[1], MSc Merijn Pen[1], Dr. Hongyu Sun[1], Dr. Hugo Perez[1]
[1]DENSsolutions BV, Delft, The Netherlands, [2]Leibniz-Institut für Kristallzüchtung (IKZ), Berlin, Germany

Poster Group 2

In situ (scanning) transmission electron microscopy ((S)TEM) experiments in gases became widely possible with the development of sandwiched MEMS-based samples carriers (e.g. Nano-Chips) – gas Nano-Reactors. Various stimuli like heating or biasing in gaseous environments have been employed to study materials synthesis [1], catalyst [2], ferroelectrics [3], resistive switching [4] and more. The majority of the commercial in situ (S)TEM sample holders, however utilize only four electrical contacts that limit the combination of stimuli that the user can simultaneously apply. Real life applications, like proton exchange membranes, fuel cells, and non-volatile memory, etc, on the other hand, require combined application of thermal and electrical stimuli at ambient environmental conditions and thus, higher number of electrical signals.

In this work we present our new platform for in situ and operando environmental (S)TEM experiments. The heart of this platform is a newly designed holder that has eight electrical connections and allows the application of thermal and electrical stimuli in ambient environmental conditions. This is achieved through a newly designed dual chip environmental cell with an increased number of contacts. Additional electrodes are used to characterize the electrical performance of a FIB lamella sample either in 2- or 4-contact mode. The holder has a removable tip that has generic design and fits different brands of TEM, which substantially improves the correlation of the same sample between different TEM platforms. Furthermore, the design of the holder allows to rotate the tip making it suitable to both, TEM and STEM operation.

Using the new holder, it is possible to achieve high resolution at ambient gas pressure as obvious from the TEM image below. When rotating the tip by 180 degrees, the sample will become on top, which is beneficial for the high resolution STEM imaging. Since the tip flipping is done without the Nano-Reactor disassembly, it is possible to observe the same sample in different modes and easily trace the same region of interest. We will also demonstrate the capability of the holder in terms of elemental analysis using EDS and EELS analysis. We will show a few experimental examples of the new environmental operando system and explain how our new platform can be used in correlative studies involving different experimental methods like in situ TEM, SEM and beamlines.

Graphic
During the in-situ experiments, the user has full flexibility to define if the sample should be on top (better for STEM imaging mode) or on the bottom (better for TEM imaging mode). Therefore, the user can simply flip the tip 180 degrees (as seen in Figure a-c). Despite the rotation of the tip, the user can always preserve the same environmental and stimuli conditions constant. Figures d-f) show that the same tip is mounted on Thermo Fisher and JEOL holder bodies. The high resolution image of a nano-particle at ambient pressure in TEM (left) and STEM(right) imaging modes. The inset in the TEM image correspond to the sample place of the sample imaged in the STEM mode.

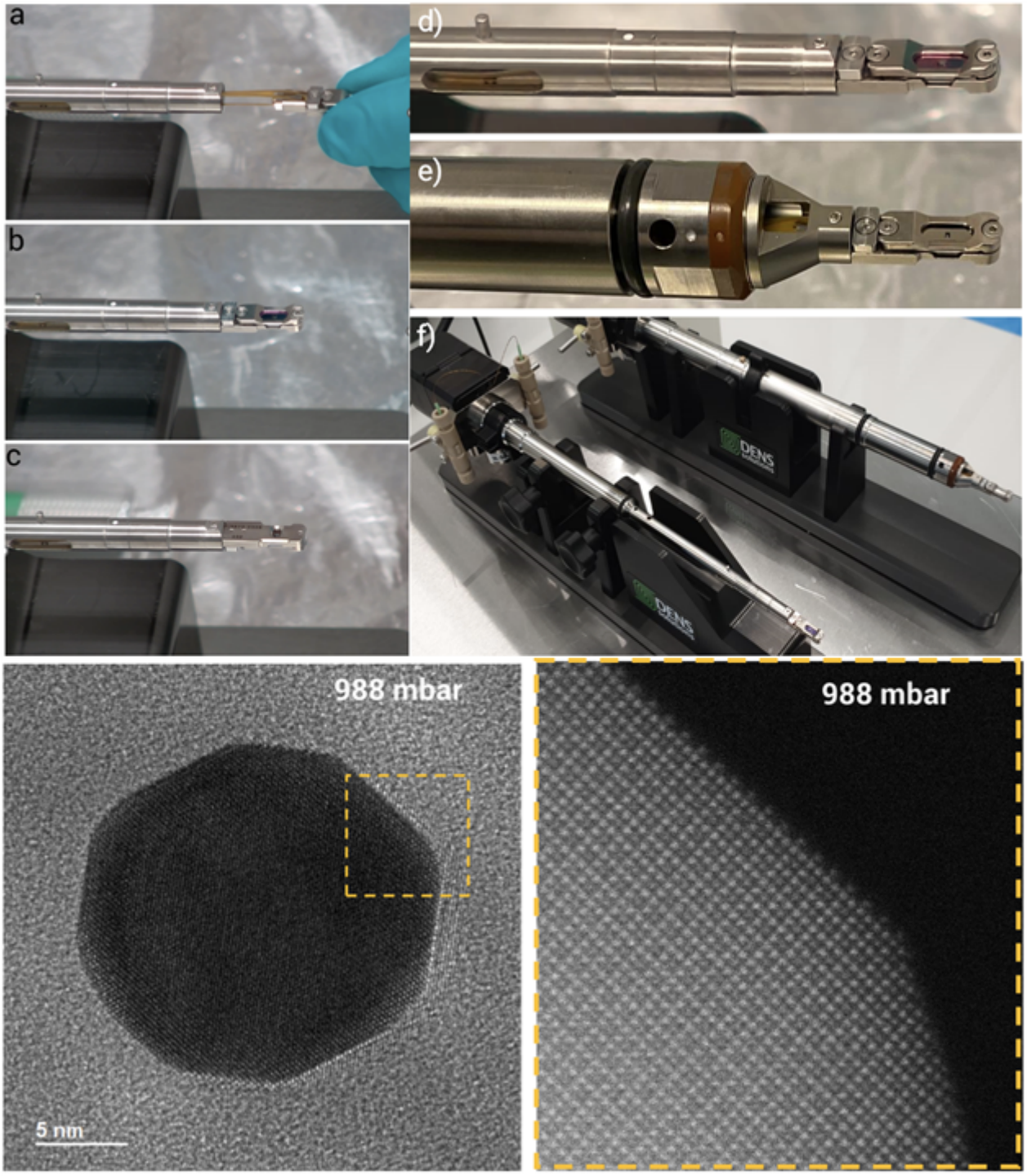

Keywords:

In situ, cross-platform, TEM, beamline

Reference:

1. Y. Wang et al., Sci. Adv. 8 (2022) ebabo5686.
2. J.H. Carter et al., ACS Nano 16 (2020) 15197.
3. T. O'Reilly et al., Adv. Sci. 10 (2023) 2303028.
4. O. Rescalde-Benitez et al., Microscopy & Microanalysis 00 (2024) 1-8

697

Operando TEM Reveals Oscillatory Surface and Bulk Dynamics of Nickel Nanoparticles in Ethylene Partial Oxidation

Dr. Claudiu Colbea[1,3], Prof. Jeroen Anton van Bokhoven[1], Prof. Marc-Georg Willinger[2,3], Dr. Milivoj Plodinec[1,3]
[1]Department of Chemistry and Applied Biosciences, ETH Zürich, Zürich, Switzerland, [2]Department of Chemistry, Technical University of Munich, Münich, Germany, [3]Scientific Center for Optical and Electron Microscopy, ETH Zürich, Zürich, Switzerland

Poster Group 2

Background

Heterogeneous catalysis, particularly employing transition metal nanoparticles as catalysts, has emerged as a promising avenue for facilitating the partial oxidation (POX) of hydrocarbons (methane, ethane, propane) to syngas.[1] Syngas, a mixture of carbon monoxide (CO) and hydrogen (H_2), serves as a crucial precursor for a wide range of industrial processes including the synthesis of methanol, ammonia, and various other essential carbon based chemicals.[2] Recent efforts have focused on unravelling the catalytic mechanisms at play in these reactions aiming to improve efficiency and selectivity while minimizing unwanted byproducts. One intriguing phenomenon observed in such catalytic systems is the self-sustained oscillatory behaviour, where the catalytic activity undergoes periodic fluctuations over time.[2] These oscillations can lead to enhanced reaction rates and selectivity, offering specific insights into the dynamic nature of catalytic processes. This phenomenon have been observed in many heterogenous catalytic systems including oxidation of hydrogen or ammonia, oxidation or reduction of carbon monoxide, dry reforming of methane, nitric oxide, various saturated and unsaturated hydrocarbons and alcohols.[2] In the context of transforming ethylene to syngas, POX presents one of possible pathways for production of valuable chemicals and fuels. Our study investigates the role of nickel nanoparticles (Ni NPs) as catalysts in the POX of ethylene, aiming to understand the oscillatory dynamics observed during the reaction. Utilizing operando transmission electron microscopy (TEM), we attempt to gain valuable insights into structural and morphological changes of catalyst at high spatial (sub-nm) and temporal resolution (milliseconds), thus contributing to the development of more efficient and sustainable catalytic systems.

Methods

For this study, Ni NPs were sputtered onto the heater of a Microelectromechanical Systems (MEMS) chip of the nanoreactor.[3] The operando TEM experiments were conducted using an aberration-corrected JEOL GRAND ARM Vortex TEM microscope, operating at 300 kV, combined with a DENSsolution Climate gas system and a HIDEN quadrupole mass spectrometer (QMS) 3F PIC for real-time gas analysis. Before the gas mixture for the POX of ethylene was introduced, the Ni NPs underwent reduction in a gas mixture of H_2:He (1:4 ratio) at 500°C for 3 hours. The POX of ethylene was then carried out at a pressure of 1 bar, with a gas ratio of C_2H_4:O_2 = 1:1, and at a temperature of 950°C.[4]

Results

Using operando TEM, we were able to directly observe the structural and morphological changes of Ni NPs in a self-sustained oscillatory regime during the POX of ethylene to syngas. Despite the Ni NPs varying in shape and size, ranging from several tens to up to 200 nm (Figure 1a), mass spectrometry

(MS) data have demonstrated that the vast majority of Ni NPs exhibited synchronized behaviour, oscillating between a high activity (metallic state) and a low activity regime (nickel-oxide state) shown in Figure 1b.[4] More importantly, the MS data allows direct correlations between the structural and morphological changes of the NPs and alterations in the gas phase, thus providing a comprehensive understanding of the catalytic process at play.[4]
Furthermore, the observed dynamics of Ni NPs, though some of them unsynchronized, can be categorized into two distinct types: bulk dynamics and surface dynamics.[4] In bulk dynamics, as depicted in the Figure 1c, the entire particle undergoes a structural transformation when transitioning between the high activity and low activity regimes. On the other hand, the nanoparticles that exhibit surface dynamic only show minor morphological changes to their overall shape.[4] The time-lapse series of TEM images (Figure 1c) showing a single Ni NP undergoing bulk dynamics under specific reaction conditions. The transition period between the Ni and NiO states varies, ranging from 2 to 100 seconds within a single cycle. The sequence initiates with the particle in a metallic, high activity regime. Within approximately 1 second, it swiftly transitions to the oxidic state, low activity regime, indicating a rapid structural change. Ultimately, as one cycle concludes, the particle returns to the high activity regime, during which it shifts from an irregular oxide shape to a more rounded, metallic configuration.[4]

Conclusions

In conclusion, our investigation into the POX of ethylene using Ni NPs as catalysts reveals intricate dynamics underpinning the catalytic process. Utilizing advanced operando TEM, we observed both the structural and morphological transformations of Ni NPs in a self-sustained oscillatory regime. Through detailed analysis and characterization by operando TEM, we pave the way for optimizing catalyst design and operational parameters, aiming for enhanced efficiency, selectivity, and a deeper mechanistic understanding of catalytic processes at the nanoscale.

Figure 1: Oscillatory dynamics of nickel nanoparticles during ethylene partial oxidation. (a) Overview TEM image highlighting size and shape variations of Ni NPs. (b) Mass Spectrometry (MS) data depicting a complete cycle, illustrating the catalyst's high and low activity regimes. (c) Time-lapse evolution showcasing morphological changes in a single Ni NP under reaction conditions: C_2H_4:O_2 gas mixture ratio of 1:1, at a pressure of 1 bar and a temperature of 950°C.

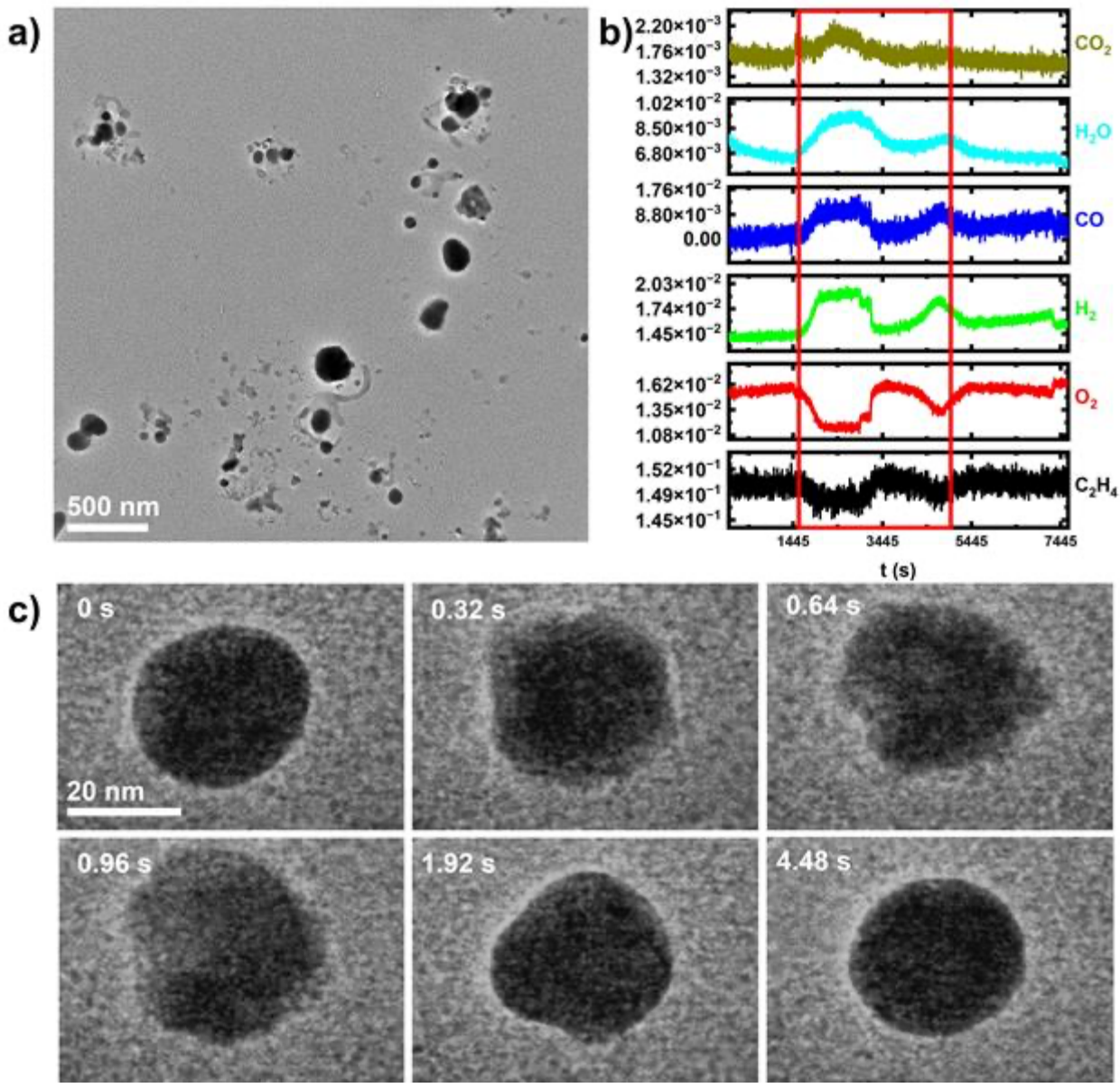

Keywords:

operando TEM, oscillations, catalysis, Nickel

Reference:

1. Ma, R. et al., “Catalytic partial oxidation (CPOX) of natural gas and renewable hydrocarbons/oxygenated hydrocarbons—A review “, Catalysis Today, 338(1), (2019), 18-30.
2. Schüth, F., et al., “Oscillatory reactions in heterogeneous catalysis.” Advances in Catalysis, 39, (1993), 51–127.
3. Plodinec, M. et al. “Deactivation Mechanism of Ni Nanoparticles in Dry Reforming of Methane Revealed by Operando TEM”, Microscopy and Microanalysis, 28(S1), (2022), 146–148.
4. Colbea, C. “Correlated operando electron microscopy and protoemission spectroscopy in partial oxidation of etylene over nickel”. Diss. ETH NO. 29751, (2023), ETH Zürich

762

Achieving methanol photo-oxidation to hydrogen and formaldehyde over lead-free halide perovskite

Mr Zhiyang Zhong[1,2], Prof Shik Chi Edman Tsang[2], Prof Angus Kirkland[1,3]
[1]Department of Materials, University of Oxford, Oxford, UK, [2]Department of Chemistry, University of Oxford, Oxford, UK, [3]Rosalind Franklin Institute, Harwell Campus, Didcot, UK

Poster Group 2

Background

Hydrogen can be a source of clean energy, but its production heavily relies on fossil fuels [1]. Methanol can be a good storage vessel for hydrogen, as each molecule contains four hydrogen atoms. Industrially, methanol can be decomposed into H_2, CO and/or CO_2, but high temperature and pressure are required [2]. Alternatively, at milder conditions such as room temperature photo-oxidation, it can be split into hydrogen and formaldehyde, but a suitable catalyst is required. In this research project, I have been studying $Cs_2AgBiBr_6$ (CABB) as a type of lead-free halide perovskite photocatalyst, which has been found to possess the ability to dehydrogenate methanol to acquire H_2. Multiple electron microscopy techniques have been used to examine the structures of CABB before and after reactions. As CABB degrades in methanol easily, the aims of this project are to keep the structure of CABB stable in the reactions, and to enhance hydrogen production rates.

Methods

Synthesis of bulk CABB: CsBr, AgBr and $BiBr_3$ were mixed with HBr, heated to 110°C, and kept for 2 hours. After cooling, CABB was collected by using centrifuge and dried in vacuum oven.
Synthesis of CABB nanocubes [3]: Cesium acetate, bismuth acetate and silver acetate were dissolved in oleylamine, oleic acid and 1-octadecene. The mixture was heated under vacuum, and then filled with argon at a higher temperature, where bromotrimethylsilane was rapidly injected. Next, the mixture was quenched in water bath, centrifuged and dried.
Synthesis of CABB nanosheets [4]: Cs_2CO_3 was dissolved in oleic acid by heating in vacuum followed by argon to prepare Cs-oleate. Separately, $BiBr_3$, $AgNO_3$, octadecene, HBr, oleic acid, oleylamine were mixed and heated in vacuum. The mixture was cooled to room temperature, and Cs-oleate solution was injected into the mixture. After that, the mixture was then heated in argon. Finally it was quenched in water bath, centrifuged and dried.
Photocatalytic tests: For reactions in liquid methanol, CABB was put into liquid methanol with or without bromide additives, and irradiated with 300W Xe lamp. For reactions in gaseous methanol, CABB was placed in the reactor but not in direct contact with liquid methanol, and irradiated with 300W Xe lamp.
Characterisations: Quantification of hydrogen was performed on Agilent 7890B Gas Chromatograph. Powder X-Ray (XRD) data were collected by Bruker D8 Advance Eco, using Cu Kα1,2 as source. Transmission electron microscope (TEM) images were obtained on a JEOL JEM-2100 at 200kV. Scanning transmission electron microscope (STEM) images were obtained using JEOL ARM-200F operated at 200kV.

Results

Without additional support, all three forms of CABB (bulk, nanocubes, nanosheets) degrade quickly in methanol. Adding bromide additives allows bulk CABB to remain stable during the photoreaction, and it showed an overall H_2 production rate of 167 µmol h-1 g-1. However, for nanosize CABB the protection given by bromide additives turned out to be inadequate, and CABB still degraded during the photoreaction. The H_2 generation rates were 76 µmol h-1 g-1 for CABB nanocubes, and 74 µmol h-1 g-1 for nanosheets. STEM images clearly showed their change in structures after reaction.

Reaction with methanol vapour is another approach to keep CABB stable in the photoreaction, without the need of bromide additives. XRD results demonstrated that the structure of bulk CABB was retained during the reaction. An overall H_2 generation rate of 524 µmol h-1 g-1 was achieved. Nanosize CABB will be tested and characterised using this method soon.

Conclusion

Both bromide additive method and methanol vapour method could prevent the structural degradation of halide perovskite CABB, and the results showed that photo-oxidation of methanol using CABB as photocatalyst is feasible. However, both methods has been proved to be useful on bulk CABB only, while for CABB nanocubes and nanosheets more research is needed.

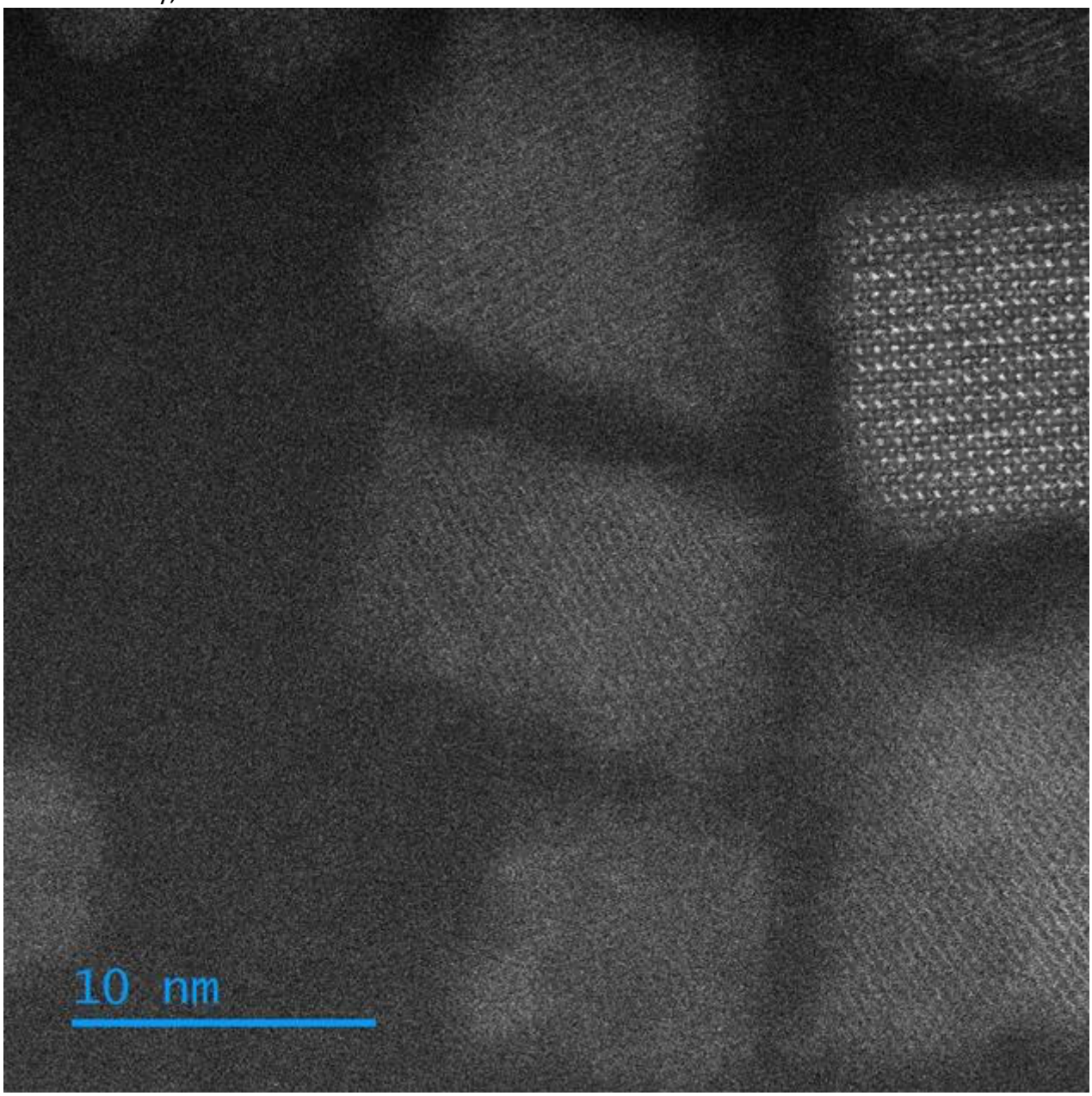

Keywords:

Microscopy, perovskite, photocatalyst, methanol oxidation

Reference:

[1] Liu, M. et al. Chemical Engineering Journal 461, 141918 (2023).
[2] Wang, H. et al. Nature Materials 22, 619-626 (2023).
[3] Sun, R. et al. ACS Appl. Nano Mater. 6, 16, 15247-15254 (2023).
[4] Liu, Z. et al. Nano Lett. 21, 4, 1620-1627 (2021).

792

Restructuring of silver catalysts after oxidation reactions – looking beneath the surface

Dr Tina Bergh[1], Youri van Valen[1], Jia Yang[1], Ole H. Bjørkedal[2], Ann Kristin Lagmannsveen[3], Hilde J. Venvik[1]
[1]Department of Chemical Engineering, Norwegian University of Science and Technology (NTNU), Trondheim, Norway, [2]Dynea AS, Lillestrøm, Norway, [3]K.A. Rasmussen, Hamar, Norway

Poster Group 2

Introduction

The silver catalysed partial oxidation of methanol is one of the most used industrial processes to produce formaldehyde globally [1]. The industrial catalysts take the form of unsupported silver particles, but it is not possible to run under differential conditions with a particle bed setup at a lab scale. Therefore, we instead use an annular reactor that enables operating at low oxygen and methanol conversions, isothermal conditions and suppressing unwanted gas phase reactions [2]. We study the methanol to formaldehyde reaction and its sub-reactions including oxidation of CO and H_2, with and without water in the feed. At elevated temperatures, oxygen dissolves into the silver, the silver restructures, and pinholes form [3]. Electron microscopy techniques enable us to get a complete view of the restructuring that extends beneath the silver surface. We aim to understand the structural changes as a function of the gas mixture and couple this to the kinetic studies.

Methods

Silver cylinders (Ø 10 mm, 10-20 mm length) were machined from rods (Goodfellow) and placed inside a narrow quartz tube reactor that extended upstream to ensure low path length and linear flow. Fresh silver catalysts were exposed continuously as they were heated up and held for 12, 36 and 84 h at furnace setpoints in the range of 620-650 °C. Gas chromatography enabled quantification of all products except for H_2O. Microstructural characterisation of the catalysts was done after subsequent cooling. For comparison, also fresh silver catalysts and catalysts heated in inert gas and air were characterised. Scanning electron microscopy (SEM) enabled studying large areas of the catalyst surfaces. Focused ion beam (FIB)-SEM tomography, slice-and-view, provided three-dimensional views of the silver grains and enclosed cavities beneath the surface. Further, we prepared cross-sectional lamellae using FIB, collected scanning precession electron diffraction (SPED) data in the transmission electron microscope and did orientation mapping using pyxem [4].

Results

The kinetic studies show that the conversion of CO is enhanced by H_2, while it is completely inhibited if H_2O is added to the feed. Moreover, the methanol conversion and selectivity towards formaldehyde increases with time if H_2O is added. The microstructural characterisation reveals that the fresh silver is decorated by surface scratches and has a nanocrystalline grain structure in the near-surface region. Drastic changes are seen after exposure to the various reaction atmospheres at elevated temperatures. All heated catalysts display larger grains with twins. Faceted pinholes and sub-surface cavities ($Ø \lesssim 10$ µm) appear after oxidation of H_2 and syngas (CO and H_2), also with H_2O in the feed. For several catalysts, smaller rounded cavities down to a few nanometres in diameter can also be seen. Most of the heated silver catalysts show surface faceting and preferential exposure of {111} surface planes. An exception is the catalyst after methanol oxidation, which displays rounded surface features and no distinct faceting.

Conclusions

Kinetic data obtained from an annular reactor setup with cylindrical silver catalysts show how the catalyst activity changes with time in various gas mixtures. Microstructural characterisation using primarily FIB-SEM and SPED discloses the silver catalyst restructuring that has occurred after the different oxidation reactions. Distinct changes were documented in terms of grain structure, surface faceting and (sub)-surface pores. By combining the results from the characterisation and the kinetic studies, we explain how the reaction mixture and resulting restructuring affect the catalyst activity.

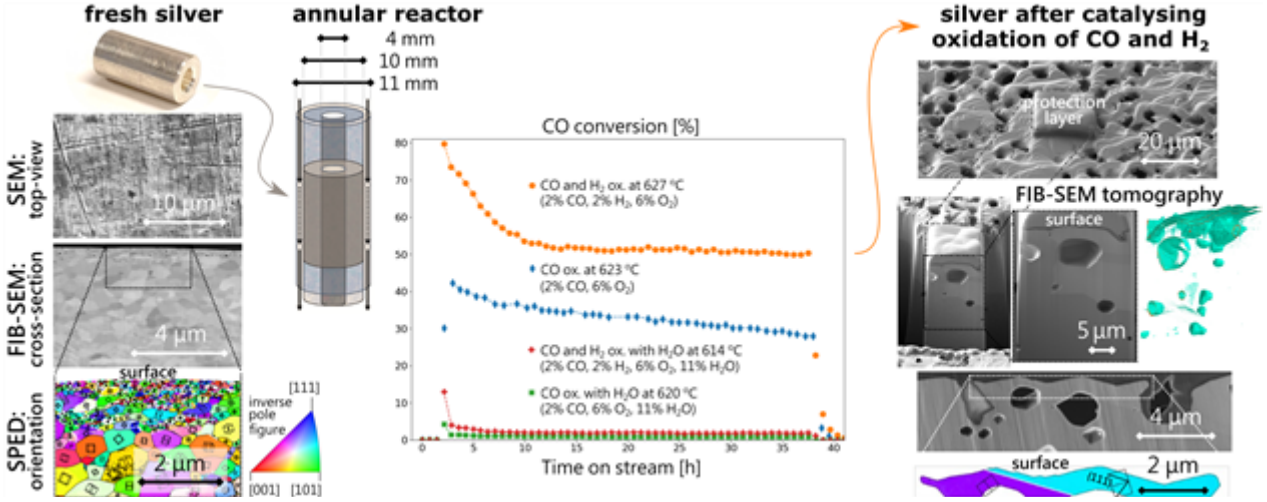

Keywords:

Silver catalyst; FIB-SEM tomography; SPED

Reference:

[1] Millar, G. J.; Collins, M. Ind. Eng. Chem. Res. 2017, 56, 9247.
[2] Lervold, S. et al. Chemical Engineering Journal 2021, 423, 130141.
[3] Waterhouse, G. I. N. et al. Applied Catalysis A: General 2004, 266, 257.
[4] Johnstone, D. N. et al. Zenodo, 10.5281/zenodo.2649351.

We acknowledge the financial support from the Research Council of Norway to the centre iCSI (grant no. 237922) and the infrastructures NORTEM (197405), NorFab (295864) and Smart-H (296197). We would like to thank Tomasz Skrzydło (IKP NTNU), Pio Gramazio (IKP NTNU) and Rune Lødeng (SINTEF Industry) for their contributions to the project.

794

High quality graphene TEM supports for high-resolution transmission electron microscopy

Jenthe Verstraelen[1], Dr. Adrian Pedrazo Tardajos[1], Dr. Nathalie Claes[1], Dr. Tine Derez[1], Prof. Dr. Sara Bals[1]
[1]EMAT, university of Antwerp, Antwerp, Belgium

Poster Group 2

Background incl. aims
Transmission electron microscopy (TEM) plays a critical role in the investigation of the atomic structure, morphology and chemical composition of nanomaterials. The field has significantly evolved during the last decade through the implementation of improved aberration correctors, novel detectors, more stable stages/holders and the implementation of many new low dose techniques. However, further progress in spatial resolution, contrast and potentially beam damage can still be achieved from improvements in sample preparation, particularly from the optimization of the TEM sample support.
The ideal sample support would be as thin and clean as possible in order to avoid interference with the sample signal, resulting in a background noise and a reduction of the contrast in the final (S)TEM image. Conventional grids consist of a fine metal mesh covered with an amorphous carbon layer (~20 nm), usually perforated with holes. For thin samples, this 20 nm is too thick to provide contrast, therefore a continuous support layer of 2 nm – 5 nm amorphous carbon is often used.
Graphene-based TEM grids have recently appeared as a promising alternative to the regular carbon coated TEM grids. Graphene, a monolayer of tightly bound carbon atoms, possesses exceptional properties. The monoatomic thickness of graphene minimizes the background signal, significantly improving signal to noise ratio which is crucial for high resolution imaging. Additionally, graphene's excellent electrical and thermal conductivity makes it an ideal candidate for dissipating excess heat and charge from the sample, mitigating electron beam induced damage.
However, to fully capitalize on the advantages of these new TEM grids, the graphene substrates need to be of exceptional quality. Therefore, we identify the current state of the art of the available graphene TEM substrates and discuss the existing problems with these grids and how these can be overcome.

Methods
Utilizing TEM and STEM, we evaluate key quality metrics of the currently available graphene TEM grids and discuss their relative importance. Based on these parameters, we compare the commercial grids with in-house made grids and discern their advantage in several advanced experiments.

Results
Unfortunately, depending on the transfer method and subsequent cleaning method, the graphene quality strongly fluctuates. Graphene grids are often plagued by cracks, folds, metal nanoparticles and polymer residues. Such impurities add background noise, introduce undesired obstructions in TEM images and degrade the conductive properties of the graphene. On the contrary, our in-house graphene grids alleviate some off these drawbacks, enabling previously unattainable experiments such as the visualization of surface ligands.

Conclusion
Current graphene TEM grids often lack the necessary quality for advanced experiments. Our in-house produced graphene TEM grids demonstrate significantly higher quality, enabling a set of previously unfeasible experiments.

Keywords:

Graphene TEM substrate

Reference:

[1] The authors acknowledge financial support by the ERC (Hypergraph - 101059468)

806

Multicore@shell nanoparticles synthesized from a multicomponent target by gas aggregation cluster source

Marie Elis[1], Dr. Amir Mohammad Ahadi[2], Tim Tjards[3], Dr. Alexander Vahl[3,4,5], Dr. Salih Veziroglu[3,4], Dr. Thomas Strunskus[3,4], Prof. Dr. Franz Faupel[3,4], Dr. Ulrich Schürmann[1,4], Prof. Dr. Lorenz Kienle[1,4]
[1]Chair for Synthesis and Real Structure, Department for Materials Science, Faculty of Engineering, Kiel University, Kiel, Germany, [2]Department of Physics, Faculty of Science, Shahid Chamran University of Ahvaz, Ahvaz, Iran, [3]Chair for Multicomponent Materials, Department for Materials Science, Faculty of Engineering, Kiel University, Kiel, Germany, [4]Kiel Nano, Surface and Interface Science KiNSIS, Kiel University, Kiel, Germany, [5]Leibniz Institute for Plasma Science and Technology, Greifswald, Germany

Poster Group 2

In nanoscience, the fabrication of multifunctional nanomaterials with unique properties as well as their optimization is an ongoing challenge. The synthesis by gas cluster aggregation source (GAS) offers the opportunity to fabricate a wide range of nanoparticles in terms of particle size, morphology and chemical composition in a single preparation step.
In this work, nanoparticles from titanium oxide (TiOx) and gold (Au) are fabricated by GAS from a single multicomponent target.
The morphology of the resulting particles is analyzed by bright field transmission electron microscopy (TEM) as well as high angle annular dark field (HAADF) scanning TEM (STEM). The crystal structures are determined by selected area electron diffraction (SAED), high resolution TEM (HRTEM) as well as high resolution STEM (HRSTEM). Energy dispersive X-ray spectroscopy (EDX) is combined with STEM to gain local information on the chemistry of the particles. X-ray photoelectron spectroscopy (XPS) as well as X-ray diffraction (XRD) are applied to confirm and complement the results from TEM.
In TEM, the nanoparticles were observed to consist of several Au cores embedded in a TiOx matrix, resulting in a multicore@shell (Au@TiOx) morphology. The Au was present in its standard cubic crystal phase while TiOx was found to be in the amorphous state. Changes in the GAS source pressure were applied to alter the particle size and deposition rate. Upon heat treatment for 1 h at 500 °C in air, the TiOx crystallized to anatase TiO2 while the Au partially formed larger particles and partially diffused to the surface of the nanoparticles.
The preparation of Au@TiOx nanoparticles by GAS gives the possibility to prepare nanoparticles of complex morphology. Heat treatment of the material can be applied to tailor the crystal structure of the TiOx as well as the distribution of the Au. This approach can solve the issue of poor adhesion of Au on TiO2 since Au nanoparticles are mechanically fixed in a TiO2 matrix. The approach of GAS preparation of multicomponent nanoparticles can in principle be applied to a broad variety of materials and material combinations.

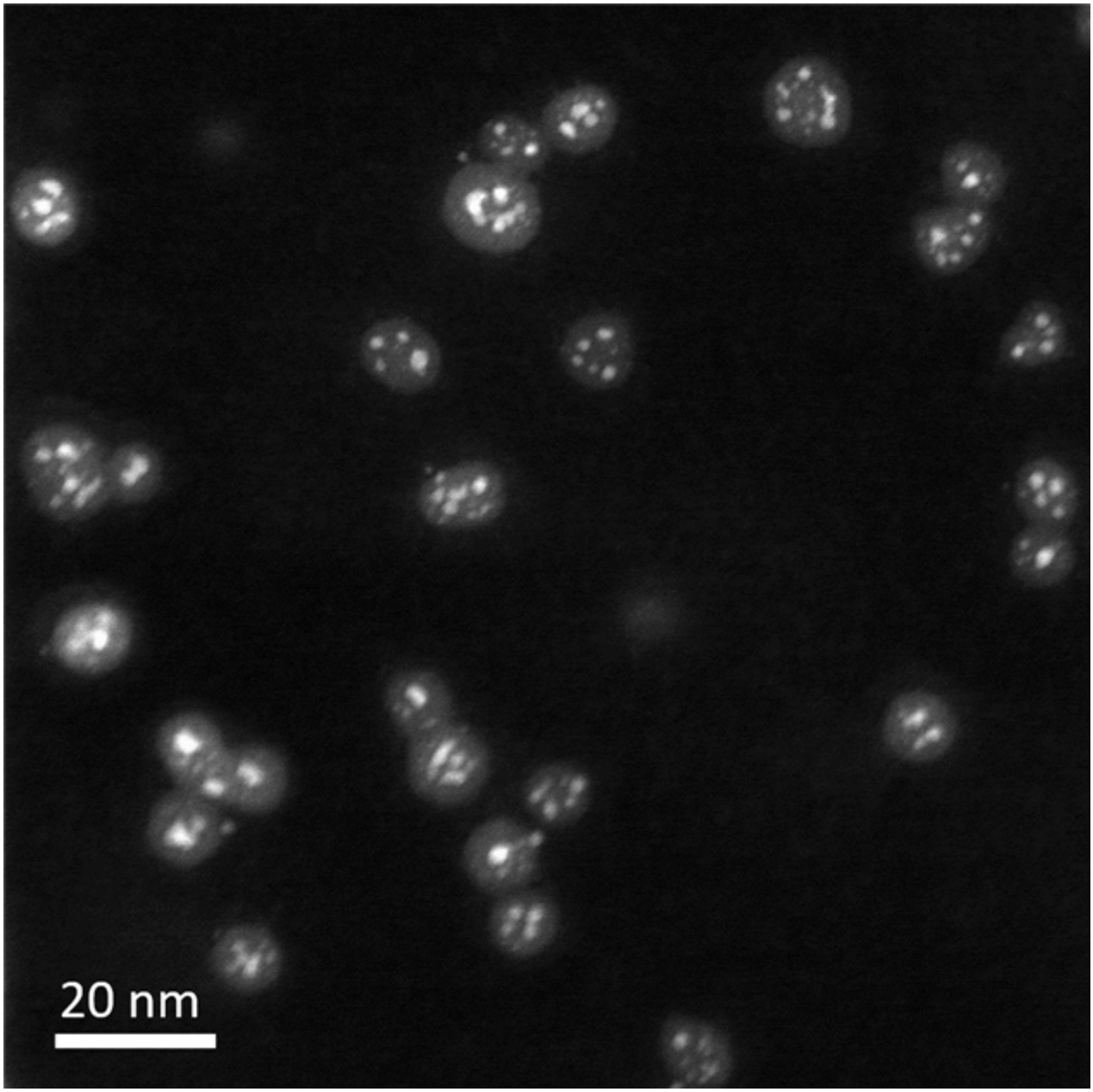

Keywords:

Multicomponent Nanoparticles, TiO2, Au, GAS

810

Structure and Composition of High-Entropy-Alloy Nanoparticle synthesized by Pulsed Laser Ablation in Liquid

Felix Pohl[1], Robert Struckert[2], Dr. Ulrich Schürmann[1], Dr. Christoph Rehbock[2], Prof. Stephan Barcikowski[2], Prof. Lorenz Kienle[1]
[1]Institute for Material Science, Faculty of Engineering, Kiel University, Kiel, Germany, [2]Technical Chemistry I and Center for Nanointegration Duisburg-Essen (CENIDE), University of Duisburg-Essen, Essen, Germany

Poster Group 2

Background incl. aims
Recently, synthesis of colloidal alloy nanoparticles (NPs) by pulsed laser ablation in liquid (LAL) was successfully transferred to high entropy alloy (HEA) systems. HEA NPs are particularly interesting for heterogenous catalysis and form a simple solid solution structure despite their high chemical complexity. In this work the influence of the target composition, solvent and laser pulse duration on the structure as well the chemical composition of these NPs is investigated. Two HEA systems are chosen: CoCrFeMnNi (Cantor) and AgAuCuPdPt (Noble metal). While in preliminary work crystalline and amorphous NPs with oxide-shells were found, it is unclear to what extent the excess of one element in the base target leads to elemental segregation not dominated by oxidation.
Methods
The nanoparticles were synthesized by LAL in a circulating solvent (Acetone vs. Ethanol) and NIR-laser pulse durations (10 ps vs. 10 ns pulse duration) and characterized in (S)TEM. For chemical analysis methods like Z-contrast imaging and nanoprobe elemental mapping were applied, while the structural analysis was performed using methods like TEM-high-resolution phase-contrast imaging (-HR imaging) and selected area electron diffraction (SAED).
Results
All Cantor alloy systems show a pulse energy dependency of the phase structure with fcc solid solution with ps-lasers and amorphous NPs with ns-lasers, while additional core-shell and multi-core structured NPs driven by Mn and Cr oxidation are also found. Further, oxide-core-multi-shell NPs were observed where localized target oxidation could provide nuclei for their formation. Interestingly, a predominant fcc-structure without pronounced elemental segregation was found upon enrichment of Mn or Cr in the system synthesized with the ps-laser. Further, NPs synthesized by the ns- laser maintained their amorphous structure upon enrichment of either Cr or Mn however additional crystalline oxides were detectable.
The noble metal systems showed no segregation into core-shell or multi-core structured NPs. Instead, two solid solution NP fractions appear, which are Ag-rich and Pt-rich. Contrary to the Cantor alloy systems and verified by HR-imaging the noble metal NPs retain their crystalline structure when synthesized with ns-lasers, although some hints on amorphous structures in Cu-rich and Ag-rich NPs based on SAED warrant further examination.
Conclusion
In conclusion, the Cantor alloy system shows the possibility of amorphous and crystalline solid solution NPs controlled by the laser pulse duration. Segregation into core-shell, multi-core or even oxide-core-multi-shell NPs is dominated by oxidation. The noble metal system displays de-mixing tendencies between Ag and Pt resulting in two solid solution NPs fractions. This could hint towards different cooling rates during particle formation offering insights into the HEA formation mechanism by LAL.

Keywords:

High-entropy-alloy, nanoparticle, pulsed-laser-ablation

Reference:

[1] F. Waag, Y. Li, A. R. Ziefuss, E. Bertin, M. Kamp, V. Duppel, G. Marzun, L. Kienle, S. Barcikowski and B. Gökce, Rsc Advances 2019, 9, 18547-18558.
[2] J. Johny, Y. Li, M. Kamp, O. Prymak, S. X. Liang, T. Krekeler, M. Ritter, L. Kienle, C. Rehbock, S. Barcikowski and S. Reichenberger, Nano Research 2022, 15, 4807-4819.

823

Charge density mapping of supported nanoparticle electrocatalysts by 4D STEM

Lazar Bijelic[1,2], Ana Rebeka Kamšek[1,3], Francisco Ruiz Zepeda[1], Goran Dražić[1], Nejc Hodnik[1,2]
[1]National Institute of Chemistry, Ljubljana, Slovenia, [2]University of Nova Gorica, Nova Gorica, Slovenia, [3]Faculty of Chemistry and Chemical Engineering, University of Ljubljana, Ljubljana, Slovenia

Poster Group 2

The negative impact of fossil fuel consumption on the environment, along with being a limited energy resource, makes fossil fuels unappealing from a standpoint of future-proof energy frameworks. Hydrogen fuel cells play an important role in such a system, mainly for energy storage and applications for transportation. Proton exchange membrane fuel cells are electrochemical devices which convert hydrogen and oxygen into water, generating electrical current. Platinum nanoparticles supported on carbon show very high activity towards the hydrogen oxidation reaction. On the other hand, the oxygen reduction reaction (ORR) proves to be more difficult in terms of finding a material with adequate performance, both in terms of activity as well as durability. The activity of electrocatalysts can be increased either by increasing their surface area, or by modifying the material composition such that the intrinsic activity is improved. However, the long term stability of fuel cells is hindered by degradation of the electrocatalyst during operation. One idea to tackle this issue is the use of catalyst supports which serve as more than just as a substrate. The metal-support interaction, in which the support influences the catalyst through strain or by changing the electronic structure, is a way of tuning performance of a nanocatalyst. At present, few methods are available that can directly characterize this interaction. A method for probing the catalyst-support interaction would be beneficial for accelerating the process of creating improved ORR catalysts. 4D scanning transmission electron microscopy (4D STEM) is a technique that can be utilized in order to locally probe and analyse the interaction between nanoparticles and their support. Namely, 4D STEM involves using a fast, pixelated electron detector which captures diffraction patterns at each probe position in a scan. The divergence of the center of mass (dCOM) of the electron probe is proportional to charge density. As such, charge redistribution occurring at the catalyst-support interface can be visualized. However, particle orientation and support thickness affect dCOM image contrast, and complicate the interpretation of dCOM directly as charge density. In the following research, a methodology for determining the charge density distribution of supported nanoparticle electrocatalysts is developed. As a model system, platinum supported on graphene was chosen for its simple composition and uniform thickness. After establishing the methodology, it is applied to platinum supported on titanium oxynitride and amorphous carbon, selected as a more complex catalyst-support system.

Keywords:

4D STEM, charge mapping, nanocatalyst

Reference:

1. Minhua Shao, Qiaowan Chang, Jean-Pol Dodelet, and Regis Chenitz. Recent Advances in Electrocatalysts for Oxygen Reduction Reaction. Chemical Reviews 116 (6), 3594-3657 (2016).

2. Zachman, M.J., Fung, V., Polo-Garzon, F. et al. Measuring and directing charge transfer in heterogenous catalysts. Nat Commun 13, 3253 (2022).

emc2024 COPENHAGEN

864

Oscillatory redox behavior of nickel catalysts observed by operando SEM

Ms. Sci. Alexander Nitsche[1], Ms. Sci. Nico Radde[1], Dr. Ali Rinaldi[1], Prof. Dr. Marc Willinger[1]
[1]Department of Chemistry, School of Natural Sciences, TU Munich, Garching bei München, Germany

Poster Group 2

Background

A catalytic cycle in heterogeneous catalysis involves the adsorption, reaction, and desorption of species on the surface of an active catalyst. This cycle repeats as long as the catalyst remains active and is inked to the concept of turnover frequency - defined by chemists to estimate the number of conversions per active site per unit of time. The cyclic behavior that occurs at the molecular or atomistic level involves catalyst restructuring and cannot be separated from the larger scale processes involving collective phenomena of heat and mass flow. Under reaction conditions, the coupling of processes dominating at different time and length scales can give rise to complex dynamics that are observable at both microscopic and macroscopic levels [1,2].
The aim of this work is to investigate how catalytic function emerges in the interplay between reactive species and catalyst. We employ operando scanning electron microscopy to study the simple model system of hydrogen oxidation. This reaction is known to exhibit oscillatory behavior characterized by periodic variations in the reaction rate [3]. This is primarily due to the dynamic and cyclic interplay between the adsorption of reactants, the formation of water, and the autocatalytic formation and reduction of nickel oxide.

Methods

The experiments were conducted using a FEI Quanta 600F Environmental Scanning Electron Microscope (ESEM) at pressures between 20 to 30 Pa. The instrument is attached to a home-built gas feeding system and equipped with a home-built laser heating stage. For reactivity studies, an electron ionization quadrupole mass spectrometer was used. Images were recorded using the gaseous secondary electron detector.

Results

As hydrogen and oxygen are adsorbed and react to form water, the surface periodically transitions between a highly active metallic state and a less active oxidized state. Changes in the oxidation state of the surface result in a change in the secondary electron yield and are detected as brightness variations. In the case of reactions carried out on polycrystalline nickel foils, a dependence of the reactivity on the grain orientation is observed, as well as spillover coupling at grain boundaries and a complex, spiral-like pattern of propagating reaction fronts on some of the grains. Superimposed on the grain dependent surface dynamics are collective oscillations associated with reaction induced variations in gas phase composition. By varying the oxygen flow or temperature, i.e., one of the key control parameters, we are able to systematically follow the transition of the system from a steady state to oscillatory, and ultimately chaotic behavior. Notably, bifurcations are observed, marking shifts in the system's behavior. Switching from a polycrystalline foil to single crystals removes coupling effects due to grains with different activity and shows the formation of intriguing spiral waves under otherwise steady state conditions. Our results reveal the complexity of simple reactions and provide valuable insights into the most relevant coupling mechanisms. It furthermore demonstrates that catalysis cannot be understood based on ex-situ studies.

Conclusion

On the polycrystalline Ni foil, oscillatory behavior between oxidized and reduced states correlates with significant changes in catalytic activity. The reactivity is influenced by the orientation of the

surface grains. In contrast, the single crystal (100) Ni surface exhibits initial oscillations that stabilize into spiral-like reaction fronts. Unlike the transient patterns observed on the polycrystalline foil, these spirals are persistent. The stability is attributed to the absence of neighboring grain interactions which typically introduce complexities and destabilize reaction fronts on polycrystalline surfaces.

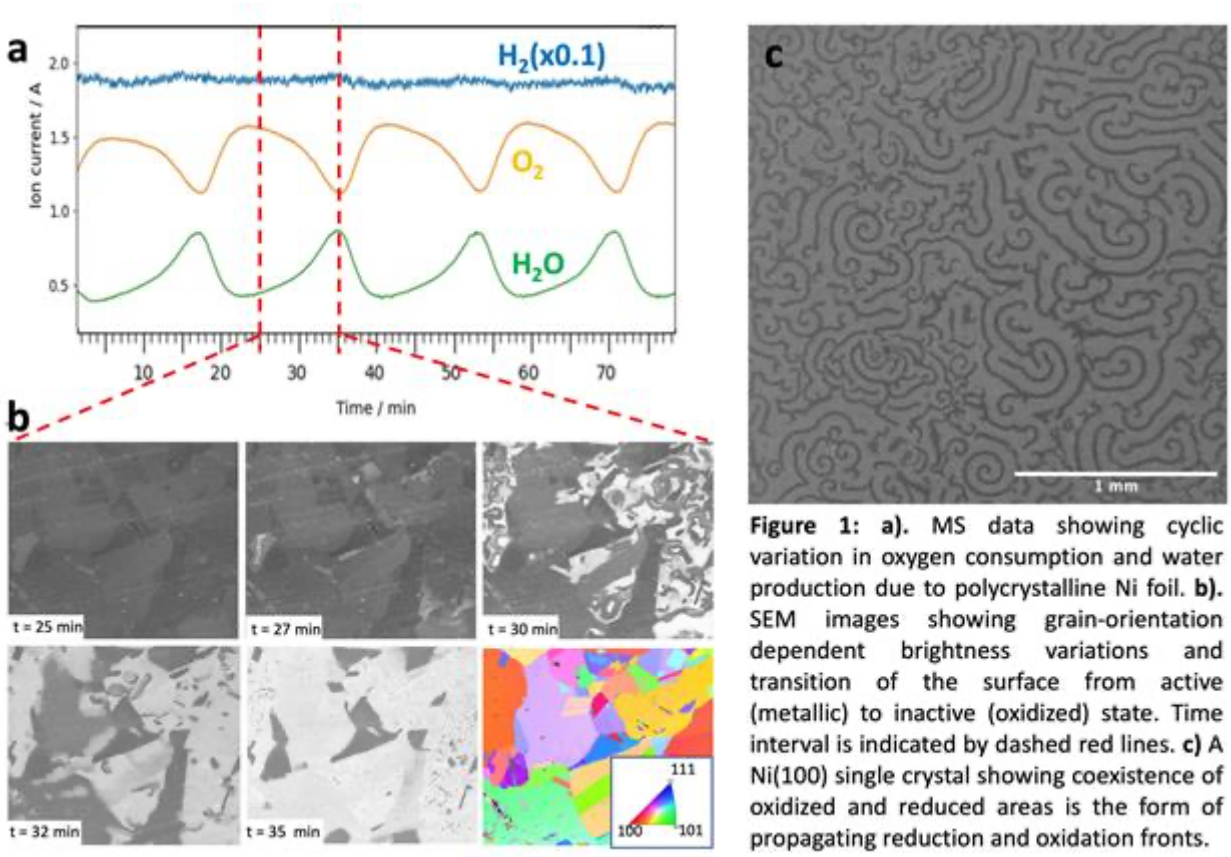

Figure 1: a). MS data showing cyclic variation in oxygen consumption and water production due to polycrystalline Ni foil. **b).** SEM images showing grain-orientation dependent brightness variations and transition of the surface from active (metallic) to inactive (oxidized) state. Time interval is indicated by dashed red lines. **c)** A Ni(100) single crystal showing coexistence of oxidized and reduced areas is the form of propagating reduction and oxidation fronts.

Keywords:

Operando SEM, Oscillations, Dynamic Catalyst

Reference:

[1] Barroo, C., Wang, Z.J., Schlögl, R., Willinger, M.G. Imaging the dynamics of catalysed surface reactions by in situ scanning electron microscopy. Nature catalysis 3, 30-39 (2020).
[2] Hansen, T.W., Willinger, M.G. From atomistic to collective dynamics: Bridging gaps in gas-phase electron microscopy for catalysis. MRS Bulletin 48, 842–851 (2023).
[3] Kurtjanek, Z., Sheintuch, M., Lussz, D. Surface State and Kinetic Oscillations in the Oxidation of Hydrogen on Nickel. Journal of Catalysis 66, 11-27(1980).

938

In-situ observation and analysis of Ni-based catalysts for dry reforming of methane

Dr. Ayako Hashimoto[1,2], Mr. Yutain Han[1,2]
[1]National Institute for Materials Science, Tsukuba, Japan, [2]University of Tsukuba, Tsukuba, Japan

Poster Group 2

Background incl. aims

Global warming is getting a tremendous issue because of the large release of greenhouse gases such as carbon dioxide (CO_2), methane (CH_4) and so forth. Catalyst is one of promising solutions for global warming to reduce the greenhouse gases. Dry reforming of methane (DRM, $CH_4 + CO_2 \rightarrow 2H_2 + 2CO$) is a powerful reaction utilizing the two greenhouse gases. Ni-based catalysts are useful owing to their high catalytic activities and lower cost compared with noble metals. However, they are easily deactivated via carbon formation during RDM reactions, which is referred to as coking by generation from side reactions. While improvements in catalytic activities have been reported so far [1-3], coking and catalytic deactivation have been not fully studied yet. In this work, structural and chemical changes of Ni nanoparticles during DRM process were investigated using in-situ scanning transmission electron microscopy (STEM) with electron energy-loss spectroscopy (EELS) analysis.

Methods

Ni nanoparticles supported Al_2O_3 catalyst (Ni/Al_2O_3) powders were prepared with different mass ratios of 5 and 10 wt% through the impregnation method. Al_2O_3 powders were dissolved with $Ni(NO_3)_2{\cdot}6H_2O$ into ethanol. After the remaining ethanol was evaporated at 80 °C, the powders were heated in H_2 gas at 600 °C for 6 h to reduce the oxidized Ni. The prepared Ni/Al_2O_3 catalysts were observed in the DRM mixture gas conditions (50% CO_2 and 50% CH_4) with pressure of 0.3 ~ 10 Pa and then, were gradually heated at 150 - 450 °C. In comparison, they were also observed in pure CH_4 gas.

For in-situ observations, our previously developed gas environment heating specimen holder system was used [4]. The Ni/Al_2O_3 powders were dispersed on a Si-based heater chip (E-chip, Protochips, USA), which was arranged in the specimen room at the tip of the specimen holder connecting to the heater controller outside of an electron microscope column. The chip was sandwiched between the two orifice plates to create a differential pumping effect leading to a higher environmental pressure in the specimen room. The powders were observed through a double aberration-corrected electron microscope (JEM-ARM200F, JEOL, Japan) operating at an accelerating voltage of 200 kV. In addition, ex-situ experiments were conducted compared with in-situ ones to examine electron irradiation damages.

Results

The TEM and STEM observations of the prepared Ni/Al_2O_3 powders show the Ni nanoparticles with the size of 5 to 50 nm were uniformly dispersed on the Al_2O_3 support powders. After the ex-situ experiment in the DRM gas (10 Pa) at 450°C for 6 h, the powders were covered with thick carbon films due to coking. During in-situ observation at 550°C after ~15 min of elevating temperature, the similar carbon films were also observed on the Ni nanoparticles. This comparison demonstrated that the in-situ observation had little electron irradiation effects on the structures and reaction phenomena. The carbon deposition was observed even at 350°C in the DRM gas, although the amount of carbon was much less than that in the pure CH_4 gas condition.

Next, the chemical bonding and valence state of the Ni nanoparticles on the Al_2O_3 supports were measured under the DRM conditions by in-situ EELS. Before the DRM gas flowing, the Ni nanoparticles were mainly metallic Ni. But after the gas flowing, most of the nanoparticles changed from Ni to oxidated Ni depending on temperature. Some Ni nanoparticles were oxidized at over 450°C and then reduced at over 550°C in the DRM gas. In addition, structural changes of the Ni nanoparticles were also observed with the oxidation and reduction reactions.

Conclusions

We observed the Ni nanoparticles on the Al_2O_3 supports through in-situ STEM and EELS to elucidate actual phenomena occurring on the Ni/Al_2O_3 catalysts under the DRM conditions. Carbon deposition on the Ni nanoparticles was observed even the in-situ observations. Furthermore, the change in the chemical bonding and valence state of the Ni nanoparticles were also measured on some Al_2O_3 supports depending on elevating temperature through in-situ EELS.

Keywords:

in-situ observation, catalytic materials, nanoparticles

Reference:

[1] M.C.J. Bradford, and M.A. Vannice, Applied Catalysis A: General 142 (1996) 73–96.
[2] P. Ferreira-Aparicio et al., Applied Catalysis A General 170 (1998) 177–187.
[3] Y. Cui et al., Applied Catalysis A: General 318 (2007) 79-88.
[4] A, Hashimoto et al., Microscopy 70 (2021) 545-549.

943

Advanced approaches for the analysis of micro- to nano-quartz particles using SEM, ESEM, FIB-SEM, SBF-SEM

Martin Olbert[1], Vilém Neděla[1], Josef Jirák[1], Jiří Hudec[1]
[1]Environmental electron microscopy group, Institute of Scientific Instruments of the CAS, v.v.i., Brno, Czech Republic

Poster Group 2

Background incl. aims
Quartz micro- to nano-particles are used in a wide variety of industries, especially in the semiconductor industry, optics, as a filler for epoxy resins, etc.. During the preparation of these particles, it is essential to know and control one of the crucial parameters - the particle size distribution (PSD). The production process itself significantly affects the PSD as well as other morphological characteristics. The shape, texture, and size distribution of the particles have a significant impact on the material's mechanical strength, density, electrical properties, and thermal properties. Various methods are used to evaluate PSD. This paper discusses laser diffraction (LD), and microscopy methods: Scanning Electron Microscopy (SEM), Environmental Scanning Electron Microscopy (ESEM), Focused Ion Beam Scanning Electron Microscopy (FIB-SEM) and Serial Block-Face Scanning Electron Microscopy (SBF-SEM). The applications, sample preparation requirements, advantages and accuracy of PSD analysis for the above methods are compared and discussed. The study focuses on ESEM as an interesting, useful and cost-effective technique with many advantages for the study of quartz micro- to nano-particles.

Methods
Quartz powder was first measured using LD. For SEM and ESEM imaging, a non-commercial ESEM AQUASEM II was used. The samples were observed in vacuum and in water vapor at 200 Pa, at 2 magnifications to cover all particle sizes, and using three different types of detectors to detect backscattered and secondary electrons. The particles embedded in the resin were observed using high-resolution ESEM QUANTA 650 FEG at a water vapor pressure of 200 Pa equipped with a Gaseous Secondary Electron Detector. Sub-nanometer particles were observed with high magnification and under pressure of 200 Pa. A procedure has been developed for particle analysis using the Mountains SEM 9 Expert software. Next, the particles embedded in the resin were analyzed by FIB-SEM Tescan Amber. From the resin cube, layers with a thickness of 100 nm were successively sputtered with a Ga+ beam. The last method was SBF-SEM, where layers were sequentially cut from a 1x1x1 mm resin cube using a ConnectomX ultramicrotome in a Tescan Clara UHR SEM microscope.

Results
The result of particle analysis by LD is a plot of the cumulative distribution function of particle sizes. The size parameter is the equivalent spherical diameter. Comparisons were made between SEM/ESEM analyses of the particles, as well as between the powders themselves and their embedding in resin. Our results confirm that the ESEM provides accurate shape and size characterization of quartz particles at vapor pressures in the order of hundreds of Pa and working distances in the low mm range, regardless of the type of detector used. These conclusions were confirmed by the analysis of smaller particles (0.5 - 2 µm). ESEM has also enabled the identification and analysis of particles tens of nm in size. Images acquired with FIB-SEM were processed with 2 software. ORS Dragonfly provided an advanced view of the incorporation of particles embedded in resin. The second, IP-SDK, allowed precise distribution and annotation of individual particles, which allowed accurate statistical evaluation of their distribution, sphericity, volume, aspect ratio, etc.

Images obtained using the SBF-SEM method showed that during the cutting of each layer, the particles were disintegrating, breaking off, and being pulled out, preventing proper particle analysis.

Conclusions

LD is very fast, efficient and widespread method of particle analysis over a large size range. Its disadvantage is the impossibility to know the real morphology of the particles. SEM and ESEM are able to image not only the powder particles but also the particles embedded in the resin, making it possible to fully control the production and use of these particles in other products, which is their great advantage. The ability of SEM and ESEM to image the real morphology and shape of the particles also allows quantification of other morphological parameters, and provide information on the exact shape of the particles. ESEM is a full-fledged and innovative particle analysis tool, and brings a number of advantages, such as a significant reduction in sample charging, thus avoiding the formation of image artifacts that distort the resulting statistics. The potential risk of microscope damage due to contamination of released particles is also significantly reduced. It allows imaging of non-conducting particles without prior modification, and another important advantage is the ability to reveal structural details of even sub-micrometer sized particles. FIB-SEM is one of the most modern, and very advanced tools that allows the measurement of 3D morphological properties of particles, in particular their spatial distribution. However, it is crucial to choose the correct particle labelling procedures, as the accuracy of the resulting distribution depends on this. ORS Dragonfly is a great imaging tool, while IP-SDK provides better statistical evaluation capabilities. SBF- SEM proved to be unsuitable for this type of sample due to the high hardness of the resin.

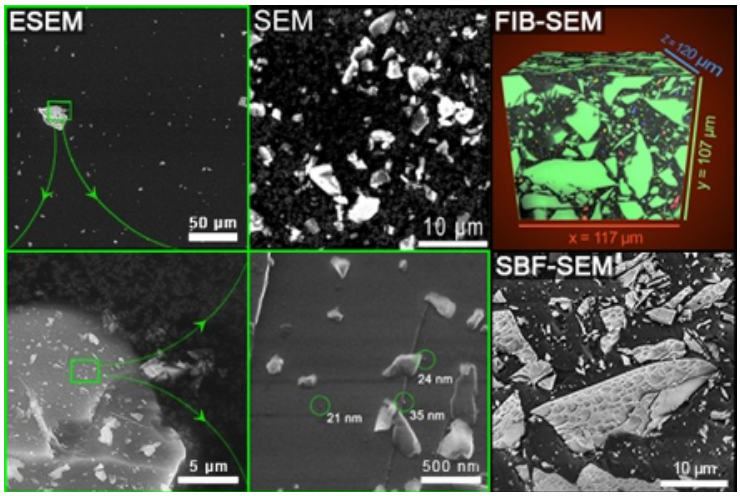

Keywords:

particle-size distribution, ESEM, SBF-SEM, FIB-SEM

Reference:

J. Götze, R. Möckel, Quartz: Deposits, Mineralogy and Analytics, Springer Berlin Heidelberg, 2012, https://doi.org/10.1007/978-3-642-22161-3.

G.B. Basim, M. Khalili, Particle size analysis on wide size distribution powders; effect of sampling and characterization technique, Adv. Powder Technol. 26 (2015) 200–207, https://doi.org/10.1016/j.apt.2014.09.009.

M. Olbert, V. Neděla, J. Jirák, J. Hudec, Size and shape analysis of micro- to nano-particles of quartz powders using advanced electron microscopy and laser diffraction methods, Powder Technology. 433 (2024), https://doi.org/10.1016/j.powtec.2023.119250.

961

Chemical and morphological stability study of copper oxide nanocubes in controlled and non-controlled atmospheres

Irene Piedra[1], Ramon Manzorro[1], M. Jose Guerra[1], Jose J. Calvino[1], Miguel Lopez-Haro[1], Ana B. Hungria[1]
[1]Departamento de Ciencias de los Materiales e Ingeniería Metalúrgica y Química Inorgánica, Facultad de Ciencias, Universidad de Cádiz, Campus Río San Pedro S/N, Puerto Real, 11510 Cádiz, Spain, Cádiz, Puerto Real, Spain

Poster Group 2

Background
Cu-based formulations are high-prospect catalysts for their remarkable performance in environmental reactions and their role as a substitute for expensive noble metals. Depending on the reaction of interest, Cu-based catalysts are exposed to different oxidizing/reducing environments, in a temperature regime that may span over 200-800ºC1. Temperature-programmed experiments under H2 or O2 atmospheres have shown that copper phases are susceptible to release or capture oxygen, changing its oxidation state from Cu0 to Cu2+. These variations are concomitant with structural, chemical, and morphological modifications 2.
In relation with the gas-catalyst interaction, each exposed crystallographic facet may exhibit a singular ability to generate/annihilate oxygen vacancies3, and, therefore, a specific reactivity. The diverse and irregular surface of Cu-based nanoparticles hinder a direct relationship between the observed performance and their surface termination. The use of nanoparticles with controlled morphology and well-defined facets4, such as nanocubes, is proving to be a promising approach to address this complexity because it provides particles with homogeneous and explicit facets, facilitating the investigation of the H2/O2 interaction with copper phases and its chemical and structural consequences. To this end, we propose to synthesize CuOx nanocubes and characterize them by means of HR-TEM and EELS after application of different reducing/oxidizing thermal treatments. It will be paid careful attention to aspects such as their oxidation state, crystallographic homogeneity and stability.

Methods
The structural, chemical and morphological evolution of copper oxide nanocubes synthesized in our laboratory using very dilute solutions of Cu(NO3)2.3H2O, NaOH and ascorbic acid5 have been investigated after exposing the catalysts to oxidizing/reducing atmospheres at different temperatures. We have employed a FEI Talos F200X electron microscope operating at 200kV, capable of both transmission and scanning/transmission (TEM/STEM) modes and equipped with a Gatan Continuum Electron Energy Loss Spectrometer (EELS). The Cu-L2,3 white line EELS signals have been the primary focus of this study towards the determination of the oxidation state, processed using DigitalMicrograph software. More specifically the spatial distribution of CuOx phases have been determined with the Multiple Lineal Least Squares (MLLS) method. High quality Cu0, Cu1+ and Cu2+ references have been previously registered to perform the fitting. The EELS data have been complemented with the analysis of HR-TEM images, extracting the copper phase maps from the Fourier periodicities.

Results
STEM-HAADF images of the as prepared samples unveil the success of the synthesis, with particles exhibiting a cubic morphology spanning over 30 and 60 nm in size. The crystallographic analysis carried out by HR-TEM allowed us to confirm the presence of Cu2O phase (Figure a-b). In addition, a zoomed image of the {100} faces reveals a rough surface assembled by low-dimension facets (Figure

c). Aberration-corrected electron microscopy characterization will be used to better define this type of nanofacets.
To confirm the oxidation state of these systems, we conducted EELS analysis. The Cu-L2,3 EELS signal confirmed the presence of Cu2O, in agreement with the results obtained by HR-TEM. Prior to assessing the potential impact of different gas atmospheres on the initial state, we evaluated its stability over time. Thus, the morphology and Cu-L2,3 EELS features have been tracked after 1, 2 and 3 weeks (Figure d, e and f respectively). The evolution shows a progressive deterioration of the cubes, with areas exhibiting undefined morphologies which increase over time. These regions displayed Cu2+, indicating a transformation to CuO. Consequently, the samples are prone to capture O2 from air, triggering the destruction of the cubes. In contrast, when oxidation treatment was controlled in a muffle oven at 300ºC, the sample exhibited a hollow structure while preserving its morphology.
The pristine Cu2O nanocubes were also submitted to H2 at 100 and 150ºC. The reduction at 100ºC slightly altered the morphology, forming small nanoparticles on the surface of the nanocubes. However, at 150ºC, the HAADF images indicated sintering of the cubes, resulting in large (over 500 nm) aggregates, hindering a proper characterization.
An in-depth characterization is required to obtain the fine details ascribe to these thermal treatments. The implementation of Machine Learning routine to process HR-TEM images will provide a spatial distribution of each phase which will help determining the crystallography of the surface at the nanoscale.

Conclusion

In summary, the structural analysis highlights the morphological changes of Cu2O nanocubes under different oxidation conditions, with uncontrolled atmospheres leading to progressive oxidation while controlled treatments maintain morphology with a hollow structure. Further investigations are necessary to fully elucidate these phenomena. Additionally, observations in H2 atmosphere indicate a temperature-dependent morphological changes. Efforts to enhance accuracy in copper oxidation state studies through advanced methodologies are underway, promising deeper insights into nanomaterial behaviour.

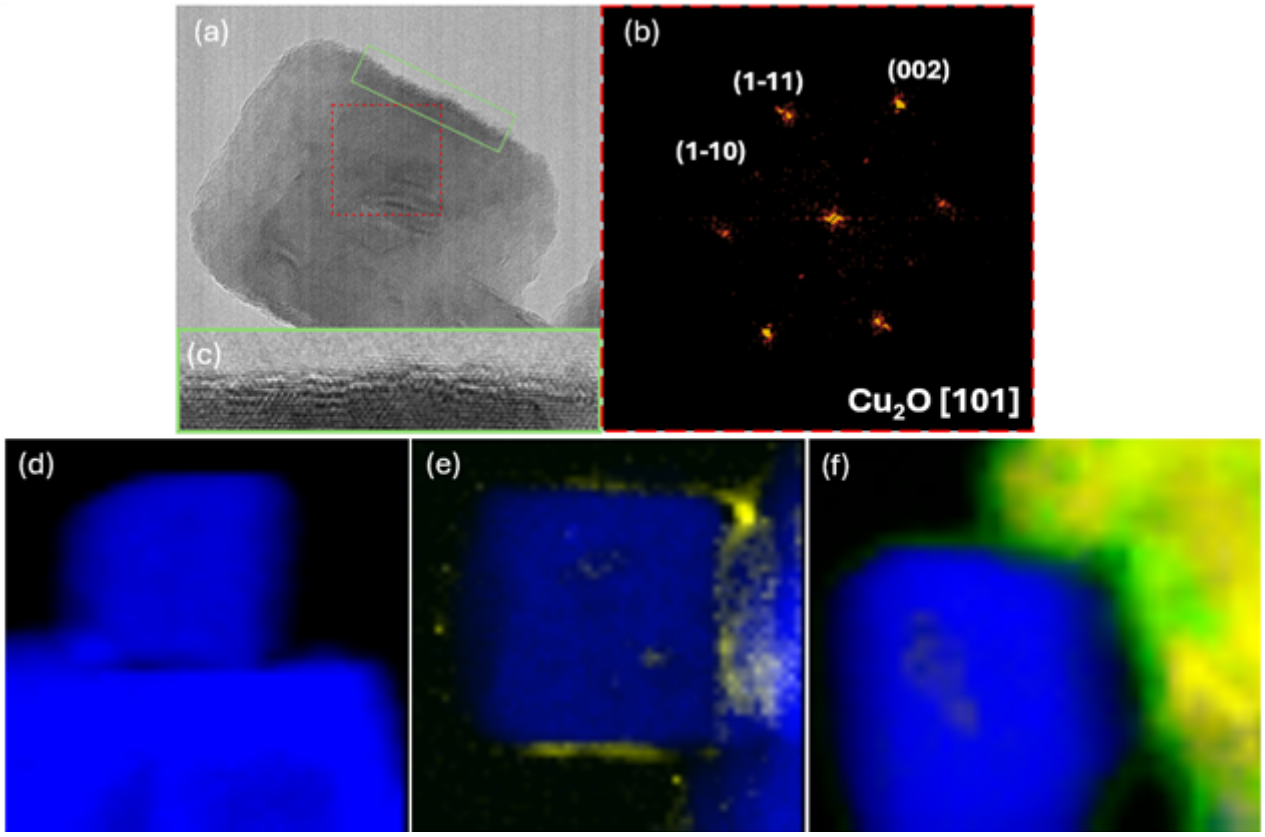

Keywords:

Copper oxide, nanocubes, EELS, HR-TEM

Reference:

1. Gawande, M. B. et al. Cu and Cu-Based Nanoparticles: Synthesis and Applications in Catalysis. Chemical Reviews vol. 116 Preprint at https://doi.org/10.1021/acs.chemrev.5b00482 (2016).
2. Huang, T. J. & Tsai, D. H. CO oxidation behavior of copper and copper oxides. Catal Letters 87, (2003).
3. Tinoco, M. et al. Critical influence of nanofaceting on the preparation and performance of supported gold catalysts. ACS Catal 5, (2015).
4. Trovarelli, A. & Llorca, J. Ceria Catalysts at Nanoscale: How Do Crystal Shapes Shape Catalysis? ACS Catalysis vol. 7 Preprint at https://doi.org/10.1021/acscatal.7b01246 (2017).
5. Hong, B. De & Lee, C. L. Specific activities of rhombic dodecahedral, octahedral, and cubic Cu2O nanocrystals as glucose oxidation catalysts. Chemical Engineering Journal 382, (2020).

975

Phase-controlled formation of NixPy catalyst using environmental TEM for potential application in CO2 reduction

Dr. Kshipra Sharma[1,2], Mr. Tianyi Hu[1,2], Prof. Kimberly A. Dick[1,2]
[1]Centre for Analysis and Synthesis, Lund University, Lund, Sweden, [2]Nanolund, Lund University, Lund, Sweden

Poster Group 2

Background:
The urgent need to mitigate climate change has driven intensive research into efficient strategies for reducing CO2 emission and potentially removing them from the atmosphere. Carbon capture and storage represents a promising approach, together with conversion of CO2 produced in industrial processes and from the environment into useful products and fuels via CO2 reduction reactions. Earth-abundant transition metal phosphides, i.e. nickel-phosphide (NixPy) catalysts, offer several advantages, including, cost- effectiveness, switchable selectivity for a range of reaction products, phase-dependent catalytic activity and potential for facilitating CO2 transformation into value-added products for renewable energy [1–3]. However, the development of this system as a tunable catalyst for CO2 reduction reactions is in its early stages, requiring a comprehensive understanding of synthesis processes to attain control over phases, size, shape/facets, and catalytic activities. Structural evolution that occurs during reactions are still largely unknown, and the relationship between facet structure and product selectivity remains poorly understood. This study aims to investigate the phase-controlled formation dynamics of nickel phosphide nanoparticles and their stabilities at higher temperatures using dedicated in-situ transmission electron microscopy (TEM) coupled with chemical vapor deposition (CVD) system.

Method:
The experiments were conducted using environmental transmission electron microscopy (ETEM) combined with a customized gas handling system. Size-selected nickel nanoparticles (10-30nm) were deposited onto micro-electro-mechanical system (MEMS) heating chips by an aerosol-phase fabrication method. These nanoparticles were then exposed to PH3 gas inside the TEM at appropriate temperatures up to 700°C to transform them into nickel-phosphides. Phase transformation of the nanoparticles was induced by changing the reaction parameters such as reaction temperature and PH3 gas flow inside TEM. The dynamic processes were followed by high-speed high-resolution imaging (up to 300 fps) during gas exposure. Structural information was obtained using power spectra of acquired high-resolution images, while composition was monitored by energy dispersive X-ray spectroscopy. The gas composition inside the microscope was monitored by an integrated residual gas analyzer.

Result:
Our Preliminary results focus on the formation dynamics of phase-controlled nickel phosphide nanoparticles. We investigated the role of reaction parameters, such as phosphene gas flow and heating temperature, on the phase transformation of nanoparticles. Two distinct phases were achieved with varying PH3 flow and temperature. Lower PH3 flow (0.3 sccm) at 300°C resulted in Ni2P phase formation, while higher PH3 concentration at elevated temperatures led to Ni5P4 phase formation. Intermediate experimental conditions, such as higher PH3 flow at lower temperature, resulted in a mixture of Ni2P and Ni5P4 phase particles. All the phases showed high thermal stability. These findings suggest that higher PH3 flow at elevated temperatures favors the incorporation of more phosphorus into the nickel phosphide nanoparticles. According to literature, both phases Ni2P

and Ni5P4 are interesting for catalytic activity for hydrogen evolution reaction [4] and CO2 reduction [2], respectively.

Conclusion:
This work demonstrates an in-situ solid-gas phase strategy for synthesizing nickel phosphide nanoparticles with controlled phase by varying PH3 gas flows and reaction temperatures. Such insights are critical for designing phase-engineered NixPy catalyst for sustainable CO2 conversion technologies, offering significant implications for addressing global climate challenges. The next step in this work would be to investigate these phases for CO2 reduction and to monitor the structure evaluations occur during the catalytic reactions.

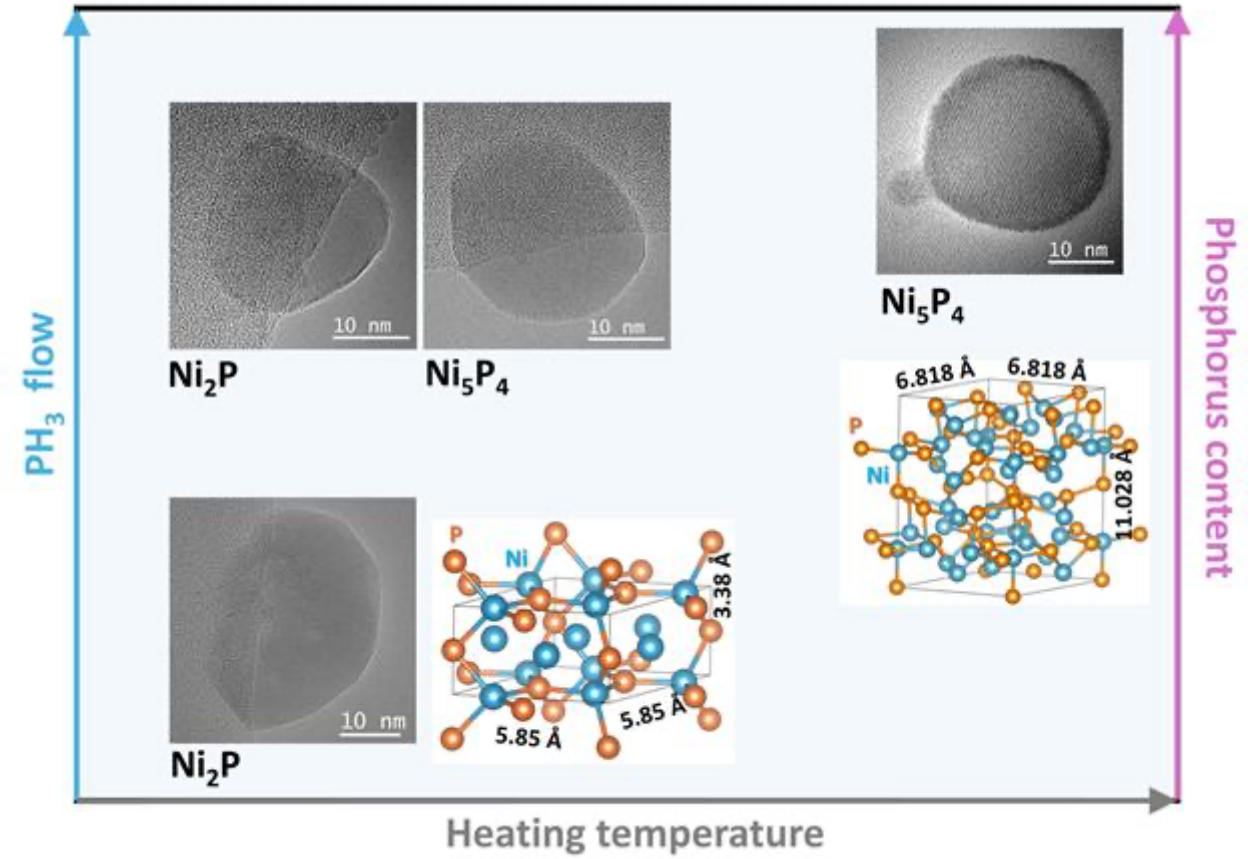

Keywords:

Nickel phosphide, Phase engineering, In-situ

Reference:

1. Zhang Q, Pastor-Pérez L, Villora-Pico JJ, et al. Ni-Phosphide catalysts as versatile systems for gas-phase CO2 conversion: Impact of the support and evidences of structure-sensitivity. Fuel. 2022;323:124301. doi:10.1016/j.fuel.2022.124301
2. Guharoy U, Ramirez Reina T, Olsson E, Gu S, Cai Q. Theoretical Insights of Ni2P (0001) Surface toward Its Potential Applicability in CO2 Conversion via Dry Reforming of Methane. ACS Catal. 2019;9(4):3487-3497. doi:10.1021/acscatal.8b04423
3. González-Castaño M, le Saché E, Berry C, et al. Nickel Phosphide Catalysts as Efficient Systems for CO2 Upgrading via Dry Reforming of Methane. Catalysts. 2021;11(4):446. doi:10.3390/catal11040446
4. Yang Y, Lin X, Li Y, et al. Insights into the Origin of High Activity of Ni5P4(0001) for Hydrogen Evolution Reaction. J Phys Chem C. 2023;127(11):5385-5394. doi:10.1021/acs.jpcc.3c00238

1012

A validation methodology for size and shape measurement of nanoplastics by transmission electron microscopy

Charlotte Wouters[1], Denrich Morales[1], Khariklia Tsilikas[1], Eveline Verleysen[1], Jan Mast[1]
[1]Trace Elements and Nanomaterials, Sciensano, Brussels, Belgium

Poster Group 2

Background incl. aims
The spread of plastics in the environment has led to the formation of microplastics (MPs) and even smaller nanoplastics (NPs) through processes such as aging, degradation, and fragmentation. While significant research has focused on quantification and understanding the potential harmful effects of larger MPs [1], characterizing NPs proves to be challenging, especially within complex matrices [2]. A comprehensive physicochemical characterization is however imperative, especially for evaluating their potential toxicological impacts. In this study, we establish a foundational framework for such measurements by validating a transmission electron microscopy (TEM)-based approach, in the context of the European project PlasticTrace [3]. This validation encompasses all analysis steps, from sample preparation to image analysis, focusing on reference materials composed of polystyrene nanoplastics. By establishing the full measurement uncertainty balance, we aim to determine the accuracy, precision and reliability of NP size and shape characterization by TEM.

Methods
The method is validated supporting on the Nanosphere size standards 3060A (60 ± 4 nm), 3200A (202 ± 4 nm) and 3500A (510 ± 7 nm), purchased from Thermo Fisher Scientific. They are part of a series of polystyrene micro/nanospheres with certified mean diameters traceable to the Standard Meter through the National Institute of Standards and Technology (NIST). The sample preparation consists of optimally diluting the colloidal sample suspension and bringing it on an Alcian blue pre-treated TEM grid. For each material, 15 different TEM specimens are prepared and imaged on 5 different days (3 per day). For each specimen, 10 images are recorded systematically and randomly over the grid surface. Each series of 10 images is analyzed using the ParticleSizer software in ImageJ. The intermediate precision of the quantitative TEM measurement is evaluated using a top-down approach [4] combining the uncertainty related to repeatability (within day) and uncertainty related to day-to-day variations (between day) obtained by ANOVA analysis. Adding the uncertainty related to calibration of the microscope and to trueness, allows to estimate the total combined and expanded uncertainty for the mean, mode and percentiles of parameters including the minimum and maximum Feret diameter (Fmin & Fmax), the equivalent circle diameter (ECD), the maximum inscribed circle diameter (MICD) and the aspect ratio (AR).

Results
Material stability was pertained throughout the validation study and homogeneous distribution of particles on the grid was achieved for all materials. Material 3060A is polydisperse with particle sizes ranging from 10 nm to 70 nm. Materials 3200A and 3500A are more uniform in size, however, a small fraction of particles (<2%) have a significantly larger or smaller diameter. STEM-EDX was performed to verify that all particles have the same elemental composition and thus belong to the polystyrene sample. The intermediate precision obtained is similar for all size parameters. It ranges from 1.1-6.7%, 0.7-1.5% and 0.3-0.7% for materials 3060A, 3200A and 3500A, respectively. The highest values correspond to the d10 percentile and the lowest values to the d75 or d90 perecentiles due to left skewedness of the size histograms (see graphic). The intermediate precision is highest for material 3060A due to the higher degree of polydispersity. For the AR, the intermediate precision is below 1% for all materials and measurands. The main source of uncertainty is related to the trueness

uncertainty for all materials. To assess the accuracy of our approach, a comparison with the certified size values (see Methods section) is required [5]. Specific information on how the certified diameter was obtained is lacking, however, we assume it corresponds to the mean ECD of the material. The values and expanded uncertainties we obtained for the mean ECD are 51±4 nm, 198±7 nm and 518±13 nm, for the three materials respectively. Based on a comparison with the certified values, we conclude that the two largest materials are accurately measured, however the smallest material presents a significant difference with respect to the reference value. Since the mode of the distribution is closer to the reference value of 60 nm, a difference in analysis algorithm e.g. leading to exclusion of a fraction of the smaller particles, might be at the origin of this discrepancy. We see indeed that for material 3060A, the outcome of the validation study is less robust against variations in image analysis settings. However, to make a final conclusion on the trueness of our approach, more detailed information on the certification of the materials is required.

Conclusion

This study establishes a robust methodology for the validation of TEM-based measurements on reference materials of polystyrene nanoplastics. By evaluating the measurement uncertainties associated with size and shape analysis, considerable precision is achieved, however, ensuring trueness can be challenging and requires detailed information on the reported certified diameters. These findings underscore the importance of ongoing refinement and harmonization in analysis algorithms to enhance the accuracy of nanoplastic characterization.

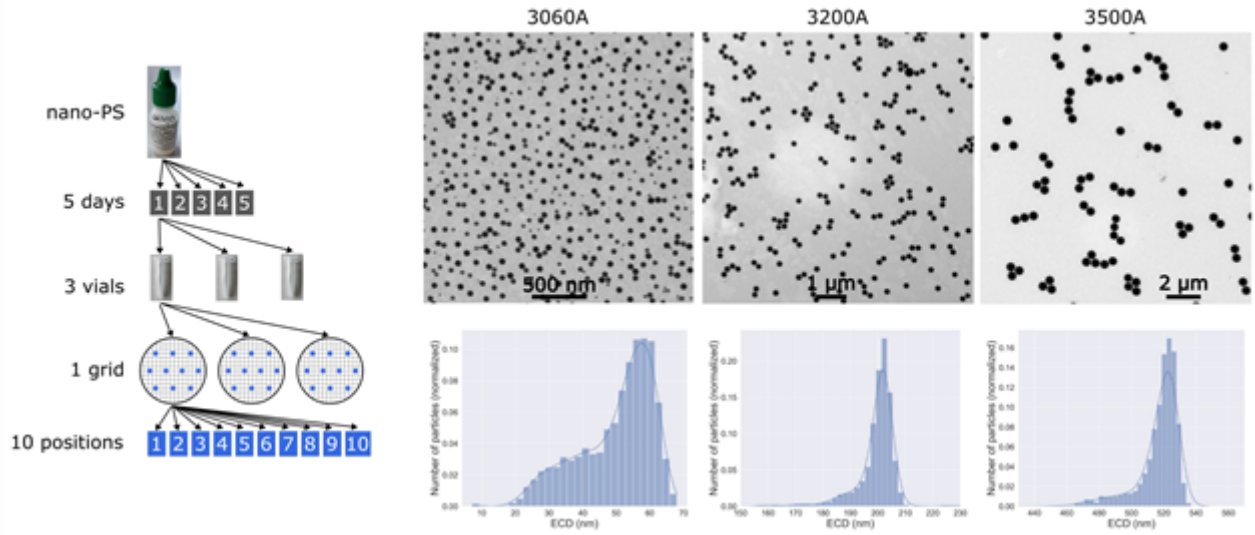

Keywords:

Nanoplastics, TEM, validation study, metrology

Reference:

[1] C. Pironti et al. “Microplastics in the Environment: Intake through the Food Web, Human Exposure and Toxicological Effects,” Toxics 9, 9 (2021) doi: 10.3390/toxics9090224.

[2] M. J. Huber et al., “Physicochemical characterization and quantification of nanoplastics: applicability, limitations and complementarity of batch and fractionation methods,” Anal Bioanal Chem 415, 15 (2023) doi: 10.1007/s00216-023-04689-5.

[3] “PlasticTrace – Tracing Micro and NanoPlastics in Food and Environment.” [Online]. Available: https://plastictrace.eu/

[4] Analytical Methods Committee, “Uncertainty of measurement: implications of its use in analytical science,” Analyst 120, 9 (1995) doi: 10.1039/AN9952002303.

[5] T. P. J. Linsinger, “Application Note 1: Comparison of a measurement result with the certified value,” Geel, Belgium, 2010.

1017

IN-SITU SYNTHESIS OF FexPy NANOPARTICLES

PhD student Azemina Kraina[1,2], Tianyi Hu[1,2], Pau Ternero[2,3], Professor Kimberly A. Dick[1,2]
[1]Centre for Analysis and Synthesis, Lund University, Lund, Sweden, [2]NanoLund, Lund University, Lund, Sweden, [3]Solid State Physics, Lund University, Lund, Sweden

Poster Group 2

Background incl. aims
Iron phosphide is an earth abundant material with several applications, such as an electrocatalyst for the hydrogen evolution reaction (HER) and the oxygen evolution reaction (OER). Water-splitting as a way of producing hydrogen gas is essential to explore due to its low carbon footprint, and using earth abundant catalysts such as iron phosphide is preferred due to being inexpensive, active, and electrochemically stable (1). Therefore, it is of interest to explore methods to manufacture iron phosphide and aim to achieve perfect crystallinity in combination with tuning the different crystalline phases, since they exhibit different catalytic activity. With an environmental transmission electron microscope (ETEM) it is possible to reveal the mechanism of the gas synthesis at an atomic scale in-situ.

Methods
The iron nanoparticles used are created by using spark ablation in a spark discharge generator and deposited on MEMS chips allowing for heating. The ETEM, Hitachi HF-3300S, interfaced with a metal organic chemical vapor deposition (MOCVD) system is the instrument used and the gases induced are PH_3 and H_2. Energy dispersive X-ray (EDX) spectroscopy is used for elemental information and enabled by the SDD X-MaxN 80T detector. Post-experiment data analysis is performed by utilizing FFT spectra obtained from the high-resolution TEM (HRTEM) images and videos from the Gatan OneView IS camera.

Results
By tuning gas flows and temperature synthesis of different iron phosphide phases were observed directly, currently the phases found are Fe_2P and FeP. The transformation into iron phosphide is nearly instantaneous when PH_3 enters the system, however by using dilution with H_2 it is possible to somewhat slow down the process. It also appears that using pure versus oxidized iron nanoparticles still seems to produce iron phosphide. Moreover, there have been observations of a transformation from FeP to Fe_2P by increasing temperature. Fe_2P has been proven to be very stable in various gaseous and temperature conditions, as well as in air.

Conclusions
Different phases of iron phosphide have been synthesized in the ETEM and dynamics of phase transformations have been investigated. The transition between phases has been observed, as well, indicating that it might be possible to realize phase engineering on iron phosphides even after phosphorus has entered the particles. Our future work will aim towards studying the transformation to iron phosphide further, exploring and characterizing the possible phases and achieving selection of crystal structure in a more controlled manner. By finding a reliable way of creating phases it can pave the way for comparing different phases and for example their catalytic activities in a fair way.

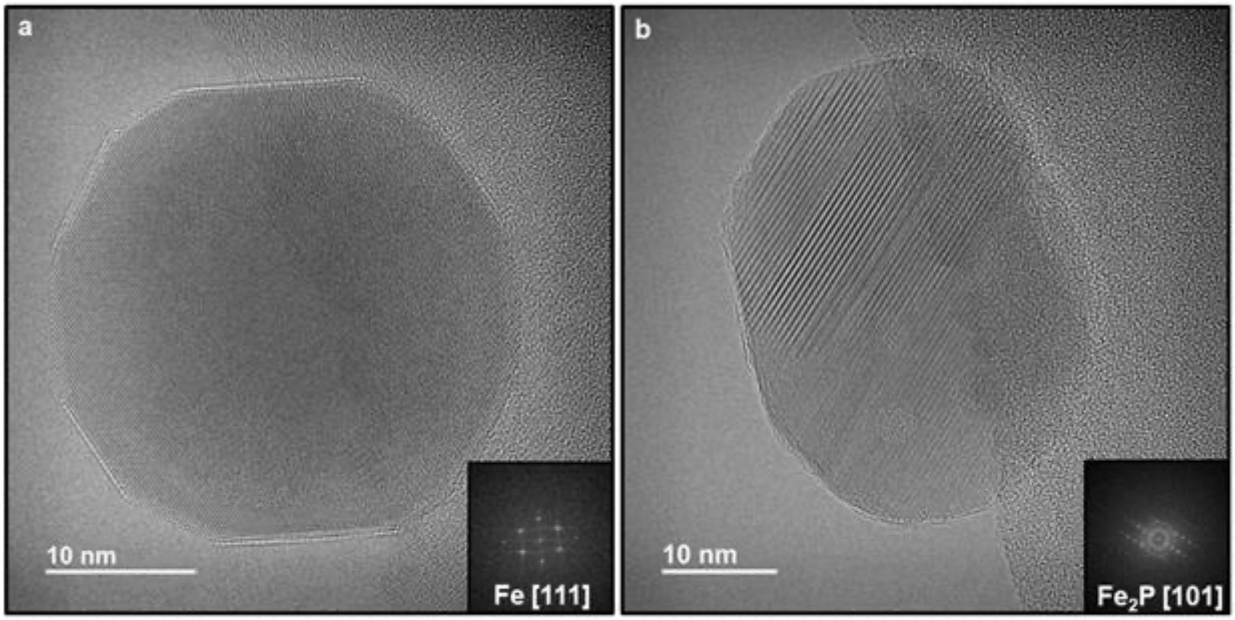

Keywords:

ETEM, Iron Phosphide, nanoparticles, in-situ

Reference:

(1) Xu. S. et.al. J. Mater. Chem. A, 2020,8, 19729-19745

1036

Assessing feasibility of detecting photogenerated charge carriers in photocatalysts via transmission electron microscopy: simulation study

Monia Runge Nielsen[1,2], Shima Kadkhodazadeh[1,2], Michael S. Seifner[1,2]
[1]Nanolab - National Centre for Nano Fabrication and Characterization, Technical University of Denmark, Kongens Lyngby, Denmark, [2]NanoPhoton - Center for Nanophotonics, Technical University of Denmark, Kongens Lyngby, Denmark

Poster Group 2

Background
In the face of global energy and climate crises, the necessity for sustainable solutions has never been more pressing. Photocatalysts, which use sunlight to drive chemical transformations, offer hope in this quest. Among their many applications, one of the most promising lies in the conversion of carbon dioxide (CO2) into fuels, presenting a dual opportunity for reducing atmospheric CO2 levels and generating sustainable energy.1 However, the effectiveness of photocatalysts depends on the complex interaction of light absorption, charge carrier dynamics, and catalytic activity, particularly in the context of poorly understood steps such as charge carrier accumulation.1-3

Methods
Taking advantage of the fact that the accumulation of charge carriers in photocatalyst will induce local alterations in the atomic structure affecting parameters such as nuclear charge, atomic/ionic radius, and chemical bonding.3 These alterations, potentially originating from selective reduction of cations at a specific nanocrystal (NC) active surface facet,4 can manifest as local phase shift variations in transmission electron microscope (TEM) images. The goal of this study is to identify visible light-induced phase shift variations by extracting phase images from reconstructed exit wave functions corresponding to specific NC surface facets under various conditions. Advanced image simulations will provide valuable insights into the detectability of photogenerated charge carriers in TEM experiments.

Results
In this study, ab initio Transmission Electron Microscopy (abTEM) simulations5 was employed to assess the feasibility of detecting photogenerated charge carriers at the interface of photocatalysts under light irradiation, in the TEM. By creating a model photocatalytic system comprising facet engineered NCs, where photons are absorbed on the active facet during reaction, leading to the accumulation of photogenerated charge carriers. Simulating the structural and electronic properties of these photocatalysts under illumination, we aim to elucidate whether charge carrier accumulation at the interface is detectable in the TEM. I will present both high resolution TEM (HRTEM) and integrated differential phase contrast STEM (iDPC-STEM) imaging techniques and assess whether they are sufficiently sensitive to detect the potential difference arising from the slight change in nuclear charge.

Conclusion
This simulation study provides a crucial insight on the sensitivity of TEM techniques to subtle changes in potential and chemical reactivity induced by photogenerated charge carriers, providing insights into the feasibility of using TEM for monitoring photocatalytic reactions. This serves as a crucial step towards using advanced microscopy techniques for probing the dynamics of photocatalysis at the nanoscale, ultimately facilitating the design and optimization of efficient photocatalytic systems for renewable energy generation and addressing environmental issues.

Keywords:

Photocatalyst, charge carriers, abTEM simulations

Reference:

[1] J. Albero, Y. Peng, and H. García, Photocatalytic CO2 Reduction to C2+ Products. ACS Catal. 10 (2020) 5734– 5749, DOI: 10.1021/acscatal.0c00478.
[2] S. Socrar, S. Yoriya, H. Lee, C.A. Grimes and S.P. Feng, A review of recent progress in gas phase CO2 reduction and suggestions on future advancement, Materials Today Chemistry 16 (2020) 100264_1-22, DOI: 10.1016/j.mtchem2020.100264.
[3] J. Wu, Y. Yuang, W. Ye, and Y. Li, CO2 Reduction: From the Electrochemical to Photochemical approach, Adv. Sci. 4 (2017) 1700194_1-29, DOI: 10.1002/advs201700194.
[4] S. Bai, L. Wang, Z. Li and Y. Xiong, Facet-Engineered Surface and Interface Design of Photocatalytic Materials, Adv. Sci. 4 (2017) 1600216_1-26, DOI: 10.1002/advs201600216.
[5] J. Madsen and T. Susi, The abTEM code: transmission electron microscopy from first principles. Open Research Europe 1 (2021) 13015.

1059

Investigation of self-assembly dynamics of magnetic nanoparticles in liquid phase by transmission electron microscopy

Dr Malika Khelfallah[1], Dr Claire Carvallo[2], Dr Amélie Juhin[2], Dr Govind Ummethala[1], Dr Amir Tavabi[1], Peng-Han Lu[1], Dr Thibaud Denneulin[1], Prof. Dr Rafal Dunin-Borkowski[1]
[1]Ernst Ruska-Centre for Microscopy and Spectroscopy with Electrons, Forschungszentrum Jülich GmbH, Jülich, Germany, [2]Institut de Minéralogie, de Physique des Matériaux et de Cosmochimie, Sorbonne Université, MNHN, CNRS, UMR 7590, Paris, France

Poster Group 2

Background incl. aims
Magnetic fluids, colloidal suspensions of magnetic nanoparticles (MNPs), exhibit intriguing self-assembly behaviors that are essential for numerous applications in biomedical, engineering, and artistic fields. Despite numerous simulations, experimental insights into the nanoscale self-assembly process in liquid phases remain scarce. The present study aims to address this deficit by employing advanced transmission electron microscopy (TEM) techniques to elucidate the intricate relationship between the self-assembly phenomena and the magnetic properties in magnetic fluids, in particular in those composed of iron oxide nanoparticles.
Methods
Our investigation involves a multi-scale approach using state-of-the-art TEM methods. First, in-situ observations of magnetic field-induced chaining are conducted using liquid cells, allowing real-time visualization of the self-assembly dynamics. Subsequently, advanced characterization techniques will be employed. These include off-axis electron holography to analyze the magnetic and structural properties of MNP assemblies, and precession-assisted 4D-STEM for orientation mapping. Quantitative measurements of magnetic property distributions based on first-order reversal curve (FORC) diagrams obtained by electron holography will also be performed. With a special focus on electron holography data, the development of software tools for automated data acquisition and analysis is described.
Results
Preliminary results show the successful characterization of self-assembly processes by cryo-TEM. The formation of diverse structures such as chains, rings and networks is demonstrated. Statistical analysis shows excellent agreement between experimental observations and Monte Carlo simulations. Electron holography measured on several assemblies suggests a competition between magnetic dipolar interactions and magnetic anisotropy energy, which deeply affects our understanding of the self-assembly process. In addition, we were able to establish a relationship between macroscopic magnetometry and nanoscale structural organization by combining experimental and simulated FORC diagrams. This is a promising approach for the measurement of magnetic nanostructures with different geometries and chemical compositions.
Conclusion
In summary, our study demonstrates the ability of advanced electron microscopy techniques to resolve the intricate dynamics of self-assembly processes in magnetic fluids. By studying magnetic interactions and structural organization at the nanoscale, our results provide insights that can aid in the efficient design and optimization of magnetic fluid-based technologies. In addition, the development of software tools for data acquisition and analysis offers potential improvements in the accessibility and applicability of advanced TEM methods in the study of magnetic nanomaterials.

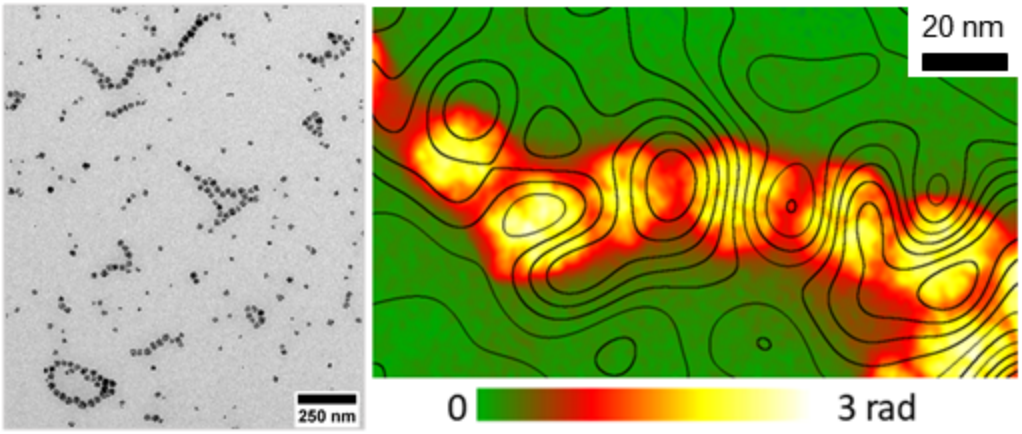

Keywords:

Magnetic fluid, holography, FORC diagrams

Reference:

M. Klokkenburg, C. Vonk, E. M. Claesson, J. D. Meeldijk, B. H. Erné, and A. P. Philipse, “Direct Imaging of Zero-Field Dipolar Structures in Colloidal Dispersions of Synthetic Magnetite,” J. Am. Chem. Soc., vol. 126, no. 51, pp. 16706–16707, Dec. 2004, doi: 10.1021/ja0456252.
S. S. Kantorovich, A. O. Ivanov, L. Rovigatti, J. M. Tavares, and F. Sciortino, “Temperature-induced structural transitions in self-assembling magnetic nanocolloids,” Phys. Chem. Chem. Phys., vol. 17, no. 25, pp. 16601–16608, 2015, doi: 10.1039/C5CP01558H.
M. Khelfallah. Magnetic properties of ferrofluids of self-assembled nano-magnets. Materials Science [cond-mat.mtrl-sci]. Sorbonne Université, 2023. English. ⟨NNT : 2023SORUS502⟩. ⟨tel-04457283⟩
M.Khelfallah, C. Carvallo, V. Dupuis, S. Neveu, D. Taverna, Y. Guyodo, J.-M. Guigner, E. Bertuit, L. Michot, W. Baaziz, O. Ersen, I. M. Andersen, E. Snoeck, C. Gatel and A. Juhin, “Structural and magnetic properties of ferrofluids composed of self-assembled cobalt ferrite nanoflowers: a multi-scale investigation”, 2024, submitted.

1109

Physical and chemical parameters determining the formation of gold sp-metal (Al, Ga, In, Pb) nanoalloys

Prof Patrizia Canton[1], Prof Vincenzo Amendola[2], Dr Vito Coviello[2], Dr Daniel Forrer[3]
[1]Department of Molecular Sciences and Nanosystems, University Ca' Foscari of Venice, Venezia, Italy, [2]Department of Chemical Sciences, University of Padova, Padova, Italy, [3]CNR– ICMATE, Padova, Italy

Poster Group 2

Background incl. aims.
Alloying is a key step towards the fabrication of advanced nanomaterials with multiple and unique properties demanded by the most innovative nanotechnology solutions. In particular, the interest in Au nanoalloys is expected to increase with the capabilities in tailoring and modelling new compounds, such as bimetallic NPs containing the sp-metals, which have appealing plasmonic and electronic properties for a wide range of applications in optics, catalysis, nanomedicine, sensing and quantum devices. However, for these systems little is known about the thermodynamic and synthetic factors leading to successful alloying at the nanoscale.

Methods.
Laser ablation in Liquid (LAL) is currently one of the reference techniques for the green and straightforward preparation of colloids of nanoalloys with conventional (e.g. Au-Ag, Au-Cu) or unconventional composition (e.g. immiscible elements such as Au-Fe, Ag-Fe, Ag-Co, Au-Co); LAL has, in addition, several advantages such as being a green, low-cost and self-standing process.
In this work, Au-M nanoalloys, with M = Al, Ga, In, or Pb, have been synthesized by LAL using anhydrous (acetone) and not-anhydrous (ethanol) liquid environments to delve deeper in the key parameters leading to the successful alloying in the typical operating conditions of LAL.
Electron Microscopy Techniques, SAED, NBD and HREM, have been applied to the study of the synthesized systems together with a multiparametric analysis that was performed considering the mixing enthalpy from DFT calculations and other alloying descriptors like the Hume-Rothery parameters.

Results.
The series of prepared four alloy nanosystems (Au-Al, Au-Ga, Au-In, and Au-Pb) by laser ablation in liquid (LAL) has the purpose to move along the 13th group for studying the effect on the products composition, structure and morphology. In case of Al, Ga, In, and Pb, these are either miscible with Au at some proportions or form intermetallic phases, but they also form stable oxides with a strongly negative standard formation enthalpy. Therefore, oxidation and passivation at the surface of NPs, as well as segregation due to oxidation of the sp metal during the synthesis, may occur. To confirm that the sp metals are alloyed with gold and identify the alloy phase among the various possibilities (substitutional SS, intermetallic compound, or phase-segregated), the XRD patterns of the ten dried colloids were collected and the phases were identified through the Rietveld refinement. In all samples, at least one substitutional alloy or intermetallic phase was detected, confirming the presence of the nanoalloys. The composition of each Au sp metal alloy was different in anhydrous acetone and in ethanol. It is worth noting that the NPs obtained by LAL have a relatively broad size distribution; hence, the composition obtained from the XRD analysis is the average composition of the sample, and it does not give information about the possibility that the chemical composition changes with the size of the NPs. Therefore, alloying was also assessed at the nanoscale using SAED, NBD and HRTEM (see Figure) on the samples obtained in anhydrous acetone, which are those with the highest fraction of Au–sp metal phases. HRTEM analysis evidenced the polycrystalline structure of the NPs, which is also systematically observed in single-element metal particles obtained by LAL.

Consequently, the SAED patterns on groups of NPs are rich in reflections coming from different crystalline domains, even inside the same particle. Nonetheless, it was possible to identify the reflections of the various Au–sp metal alloys previously identified using XRD analysis, where there is no ambiguity about the discrimination from the pure Au FCC reflections. This includes the AlAu4 phase with space group P213, the Au7Ga2 phase with space group P-62m, and reflections compatible with both the Au3In phase with space group Pmmn and the Au9In4 phase with space group P-43m. In the case of the Au–Pb sample, the very low abundance of the alloy compared to that of pure Au and hydrocerussite does not allow for the unambiguous identification of the Au2Pb phase in the SAED and NBD patterns, but it was possible to find a match with HRTEM of a single Au–Pb NP, exhibiting the interplanar distance and the Hanning masked FFT pattern of the Au2Pb phase with space group Fd-3m. Overall, the NBD and HRTEM results, along with the Hanning masked FFT patterns on selected nanometric regions, further confirmed, at the single NP level, all results obtained by SAED on groups of NPs and by XRD on the powder samples.

Conclusion.

The physical and chemical parameters determining the formation of gold–sp metal nanoalloys were studied as a function of the sp metal period, moving from Al to Ga, In and Pb, and under real synthetic conditions involved in the nanosecond laser ablation of bimetallic targets in two different liquid environments (anhydrous acetone and ethanol). The successful formation of Au nanoalloys with sp metals has been demonstrated in most cases and the LAL is confirmed to be a versatile approach for the production of innovative nanoalloys, provided that appropriate synthesis parameters are adopted. Especially relevant is the oxidizing capability of the solvent which must be balanced with the tendency of the metals to undergo oxidation, to avoid phase segregation and byproduct formation. The physical and chemical parameters leading to the formation of alloyed versus phase segregated NPs were analyzed systematically. Good agreement with the typical rules for alloying is found only in the absence of remarkable chemical interactions with the metals; otherwise, the tendency to undergo oxidation prevails. These findings lead to an immediate and deeper understanding of the phenomena that affect the composition of nanoalloys under real physical synthetic conditions. This will provide a crucial support for guiding the realization of next-generation multifunctional metallic nanostructures with remarkable applicative potential in optics, catalysis, nanomedicine, sensing and quantum devices.

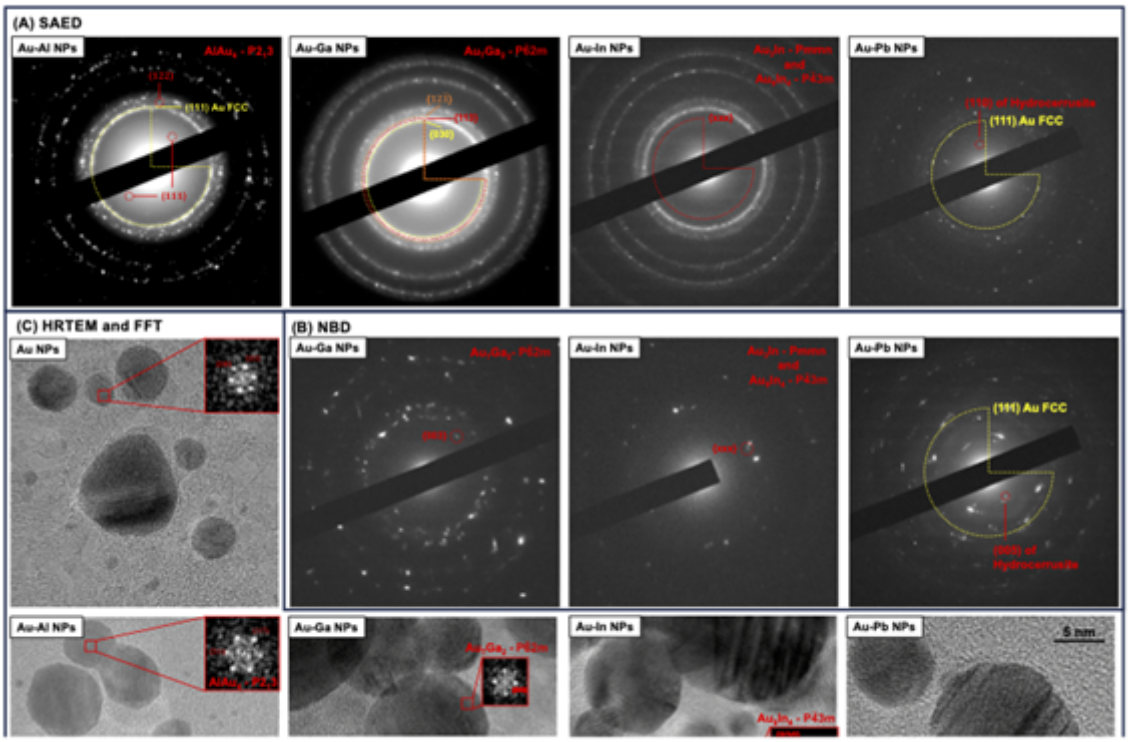

Keywords:

nano-alloying, Laser Ablation, NBD, SAED

Reference:

1) R. Ferrando, J. Jellinek and R. L. Johnston, Chem. Rev., 2008, 108, 845–910.
2) K. Loza, M. Heggen and M. Epple, Adv. Funct. Mater., 2020, 30, 1909260
3) V. Coviello, D. Forrer, P. Canton, V. Amendola Nanoscale, 2024,16, 4745-4759

1129

Tungsten nanoparticles generated in an atmospheric pressure plasma jet

Dr. Martin Müller[1], Maren Dworschak[2], Prof. Jan Benedikt[2], Prof. Lorenz Kienle[1]
[1]Faculty of Engineering, Kiel University, Kiel, Germany, [2]Faculty of Mathematics and Natural Sciences, Kiel University, Kiel, Germany

Poster Group 2

Background

Atmospheric pressure plasma sources have proven to be a cost and space efficient technology for the preparation of various nanostructures. However, synthesis of high melting point metal nanoparticles remains an ongoing challenge. In this work, tungsten nanoparticles are synthesized by the HelixJet atmospheric pressure plasma source using a tungsten wire as a source material and an oxygen free argon plasma. This offers the opportunity to fabricate a wide range of nanoparticles in terms of particle size, morphology and chemical composition in a single preparation step.

Methods

Tungsten nanoparticles were synthesized in an atmospheric pressure plasma jet (APPJ) with helix electrodes (HelixJet) and a metal wire inserted into the plasma. The metal wire was heated by the interaction with the plasma. The vaporized material is carried in the gas stream and condensates to form nanoparticle nuclei. The synthesized nanoparticles were measured with a commercial scanning mobility particle sizer (SMPS) spectrometer. The morphology and the crystal structure of the resulting particles were analyzed by bright field transmission electron microscopy (TEM) and selected area electron diffraction (SAED). Energy dispersive X-ray spectroscopy (EDX) combined with scanning TEM was used to gain local information on the chemical composition of the particles.

Results

TEM along with SAED and EDX showed monocrystalline tungsten nanoparticles with an average size of 14 nm, consisting of beta-tungsten with a thin oxygen-rich layer on the surface. The composition of such particles was studied with EDX profiling and analyzed using a so called sub-shell approach revealing that the core of the particle is composed of pure tungsten while the approximately 1.5nm surface layer has a tungsten to oxygen ratio of around 1:9. When increasing the plasma power, the average size of the nanoparticles also increased. The weakest plasma power used led to nanoparticles of average size of 12 nm. As the working gas flow rate increased, the time spent by the nanoparticles in the plasma decreased and the resulting size decreased. For the highest flow rates, when the residence time dropped to 0.4 s, the resulting particles had a thick oxide layer on the surface, while for the lowest flow rates with residence times above 1.8 s, the resulting particles were composed mainly of alpha-tungsten. Nanoparticles agglomerate into clusters, which are then measured by SMPS. The resulting size spectrum was fitted and individual peaks were sequentially assigned to agglomerates with increasing number of particles. It turns out that the SMPS measures the mobility of agglomerates as if they were larger particles than their actual size given by the sum of individual volumes or masses of particles in the agglomerate, making them to appear significantly larger.

Conclusion

Synthesis of monocrystalline tungsten nanoparticles with an average size as low as 12 nm and with a fairly uniform distribution has been shown. The HelixJet APPJ gives the possibility to prepare nanoparticles of high melting point materials and due to its versatility allows to prepare particles with complex morphology (alloys, oxides, core shells).

Keywords:

Tungsten nanoparticles, Atmospheric plasma

1132

Morphology evolution and phase transition of $Co(OH)_2$ and Co_3O_4 investigated with STEM-tomography and in-situ XRD

Olivia Kaya Gerds[1,2,3], Lars Fahl Lundegaard[3], Hanne Falsig[3], Christian Danvand Damsgaard[1,2,4], Lars Pilsgaard Hansen[3]
[1]Center for Visualizing Catalytic Processes (VISION), Department of Physics, Technical University of Denmark, Kgs. Lyngby, Denmark, [2]Surface Physics and Catalysis, Department of Physics, Technical University of Denmark, Kgs. Lyngby, Denmark, [3]Topsoe A/S, Kgs. Lyngby, Denmark, [4]National Center for Nano Fabrication and Characterization, Technical University of Denmark, Kgs. Lyngby, Denmark

Poster Group 2

Background incl. aims
Transition metal hydroxides ($TM(OH)_2$) have garnered significant attention in research due to their diverse applications in the energy and environmental sectors. These hydroxides exhibit promising capabilities in catalysis, supercapacitors, and battery materials [1-3]. For instance, cobalt hydroxides ($Co(OH)_2$) can decompose to form cobalt oxides (e.g., Co_3O_4), which are materials known for their applications as catalysts in the Fisher-Tropsch process, water splitting, and N2O decomposition [1,4].

Catalytic processes typically occur at elevated temperatures. Understanding the morphological changes and phase transitions of Co_3O_4 upon heating is crucial for controlling its properties in various applications, including those listed above. Furthermore, studies suggest that besides particle size and morphology, the distribution of exposed facets in Co_3O_4 plays a role in the catalyst's activity during N_2O decomposition [4].

In this work, a visualization of the morphological evolution of Co_3O_4 crystals synthesized by calcination of $Co(OH)_2$ at different temperatures is carried out through ex-situ (S)TEM imaging of samples. Furthermore, the facet distribution of a Co_3O_4 particle, revealing the concentration of exposed surfaces, is determined and visualized in 3D by combining STEM-HAADF electron tomography (ET) and high-resolution TEM.

Methods
In an in-situ XRD experiment, the precursor $Co(OH)_2$ underwent calcination to 1200°C in steps of 25°C in synthetic air (20%O_2), mapping the crystal-size evolution of Co_3O_4 and its phase transitions. For visualization of the sample morphologies by electron microscopy, several Co_3O_4 samples were prepared separately by calcining $Co(OH)_2$ at varying temperatures. The choice of temperatures was based on the in-situ XRD experiment.

Transmission electron microscopy was carried out using a probe-corrected Spectra 200 (S)TEM (Thermo Fischer Scientific), operated at 200 kV in scanning mode (STEM), or in parallel beam mode (TEM) for high-resolution imaging. Electron tomography tilt series were acquired in scanning mode using the high-angle annular dark field detector (STEM-HAADF) and a low convergence angle of 5.6 mrad for enhanced depth-of-field [5]. The tilt-series, recorded from +70 to -70 degrees in 2-degree intervals, were reconstructed into a tomogram with voxel size $(0.43\ nm)^3$ using fiducial marker tracking (10nm) and weighted back projection (WBP) in Inspect3D v.4.5. The crystallographic orientation of the reconstruction was determined from additional high-resolution TEM images. Finally, the facet distribution of the 3D reconstructed Co_3O_4 particle was evaluated from a 3D printed model of the reconstructed volume, by identifying the facets.

Results

The decomposition of $Co(OH)_2$ in synthetic air to form Co_3O_4 initiated at 150°C. As the calcination process continued, the mean crystal size of Co_3O_4, as measured by XRD, gradually increased from about 10 nm to 500 nm, indicating sintering. The maximum sintering rate was observed around 850°C, right before an abrupt full phase transition into CoO, which occurred between 875°C and 900°C. Upon cooling, the CoO phase fully transformed back to a Co_3O_4 structure with an average crystallite size (XRD) of ~150 nm. (S)TEM images confirm the presence of both large and small Co_3O_4 nanocrystals in the residual sample.

STEM imaging reveals that the cobalt spinel samples, calcined at 350°C, 450°C, and 550°C, are present in a pseudo-morph structure, resembling the overall shape of the hydroxide precursor, across all three samples. This morphology can be characterized as monocrystalline mesoporous nanograin sheets. While the sheet morphology is consistent across all three samples, an increase in the size of both the grains and pores is observed with increasing calcination temperature.

STEM images of a sample calcined at a high sintering rate (850°C), revealed large particles which appear to be partly faceted. One particle was reconstructed in 3D, revealing clear facets with the (100) facet being predominantly present, followed by (111) and (110). 24% of the surface could not be identified due to rounding, suggesting that the facet formation was not fully completed or equilibrated. This observation was supported by a 50-hour XRD experiment which showed that the mean crystal size of Co_3O_4 initially converges after several hours at 850°C, revealing that the 1-hour heated sample was captured in a dynamic sintering process.

Conclusion

By utilizing electron microscopy – specifically tomography – we were able to observe the morphological changes of Co_3O_4 synthesized by calcination of $Co(OH)_2$ at various temperatures. The Co_3O_4 samples exhibited a sheet-like monocrystalline mesoporous nanograin structure at 350°C and underwent drastic morphological changes as the material sintered to form large particles at higher temperatures. The shape and facet distribution of a Co_3O_4 crystal (calcined at 850°C for 1 hour) were determined using electron tomography combined with high-resolution TEM imaging, revealing the (100) facet as predominantly present, followed by (111) and (110). This approach provides valuable insights into the complex transformation processes (e.g., sintering) occurring in catalytic processes.

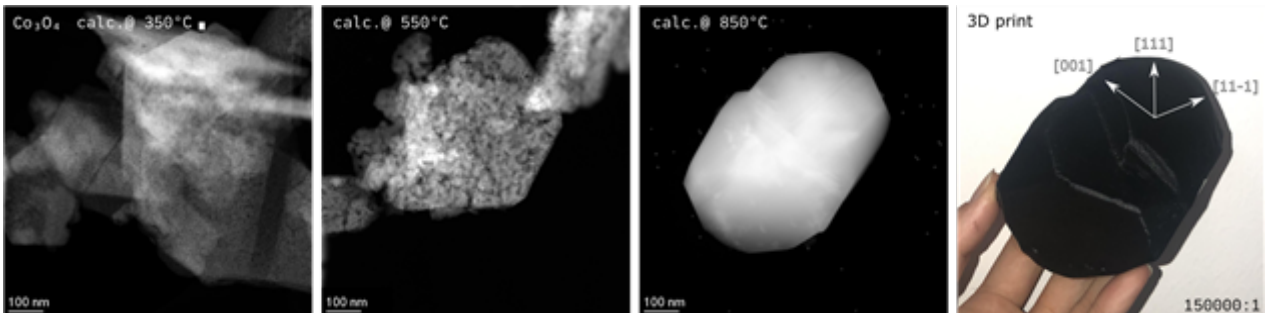

Keywords:

Co_3O_4, morphology, sintering, facet distribution

Reference:

Sun, T. et al. Chem. Eng. J. 390, 124591 (2020)
Ma, H. et al. ACS Appl. Mater. Interfaces 8 (2016)
Seo, J.H. et al. J Anal Sci Technol 14, 31 (2023).
Li, M. et al. Catal. Today 376, 177 (2021)
Bals, S. et al. Angew Chem Int Ed 53, 10600 (2014)

1135

Synthesis and Characterization of Ultrathin Unconventional Mixed 2H-HCP/FCC Phase Au Nanowire

Dr. Abhijit Roy[1,2], Dr. Raul Arenal[1,2,3]
[1]Laboratorio de Microscopías Avanzadas (LMA), Universidad de Zaragoza, ZARAGOZA, SPAIN, [2]Instituto de Nanociencia y Materiales de Aragón (INMA), CSIC-Universidad de Zaragoza, ZARAGOZA, SPAIN, [3]ARAID Foundation Zaragoza , Zaragoza, Spain

Poster Group 2

Background incl. aims
Crystal structure engineering enables the cultivation of noble metal nanostructures featuring unique crystal phases, showcasing innovative optical, catalytic, and electronic characteristics. Variations in atomic stacking sequences within these nanostructures are termed polymorphs, often showcasing distinct properties and functionalities despite being of the same material. The crystal structure of nanocrystals is frequently influenced by synthesis conditions such as reaction temperature, surfactants, precursor properties and gas environment. Polytypism, evidenced by the coexistence of several phases within a single nanostructure, defines this phenomenon. Compared to the typical stacking arrangement of "ABC" along the [111] fcc direction in fcc gold, the 4H/2H gold structure exhibits a stacking sequence of "ABCB/AB" along the [001] 4H/2H direction. 1,2
Ultrathin gold nanowires (NWs) with a diameter of approximately 2 nanometers hold significant interest for both nanoscience research and nanotechnology applications. Due to their high surface area and quantum-confined dimensions, these nanowires exhibit fascinating properties such as quantum conductance and ballistic conduction.3 The synthesis of high-quality, single-crystalline ultrathin gold NWs is essential for accurate physical property measurements and further application exploration. Recent reports have surfaced, highlighting successful advancements in the synthesis of these ultrathin gold NWs. However, reports on the synthesis and characterization of ultrathin 2H/4H Au nanowire is still very limited and a detailed structural and optical study of this nanostructure is nedded to be examined closely.1,2,4,5

Methods
In a typical synthesis process, 4.08 mg gold chloride hydrate (HauCl4, H2O) were dissolved into a mixture of 220 µL of oleylamine, 3.54 mL hexane and 250 µL of 1,2-dichloropropane, in a 20 mL glass vial. The solution was shaken for complete dissolution of HauCl4. Next, 80 mL de-ionized water is added into a 500 mL beaker, which was heated to 58°C. The glass vial is kept on the beaker for 16h and after that the solution is centrifuged at 5000 rpm for 2 minutes to filter the residue. The residue was further washed using hexane 3 times. For TEM characterization the Au nanowire solution in hexane was drop-casted on a C coated Cu grid. The HRTEM, selected area diffraction (SAD) were done in an image corrected FEI TECNAI F-30 operated at 300 kV. HRSTEM, energy dispersive X-ray spectroscopy (EDS) were carried out in a probe-corrected FEI TITAN TEM equipped with high-brightness gun and an Oxford Instruments Ultim X-MaxN 100TLE detector for EDS measurements.

Results
We have observed uniform formation of ultrathin Au nanowire. The diameter of the nanowire is between 1.9 nm – 2.3 nm and the length varies between 50nm to 300 nm. The EDS meaurement on them clearly shows the naowires are indeed Au. HRTEM measurement shows formation of 2H-HCP phase mostly on the top of the nanowire and a mixed 2H/HCP and FCC phase in the middle portion as observed form the IFFT image also. A detailed study on the structural evolution of this nanostructure upon electron beam irradiation will be prersented in this work.

Conclusion

We have done successful synthesis of ultrathin Au nanowire consisting of mixed 2H-HCP/FCC phase. Interestingly the nanowire contains bead like structure as observed from the HRSTEM and HRTEM images and they are observed to be very much sensitive to the electron beam.

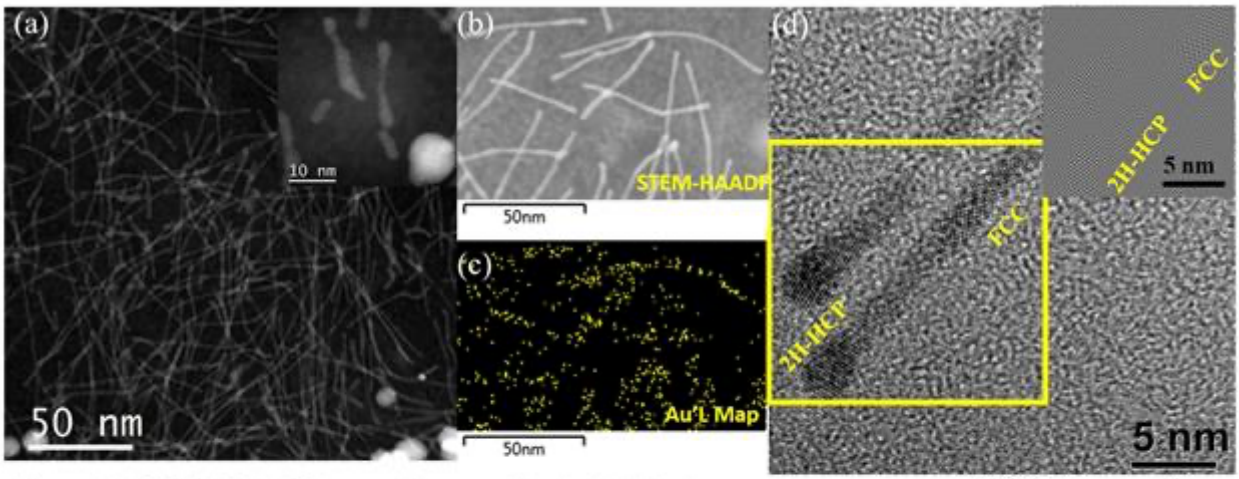

Figure. (a) STEM-HAADF image of uncoventional ultrathin Au nanowire. Inset shows HRSTEM image of two ultrathin nanowire. (b) and (c) shows the HAADF-STEM and Au-L Map of the Au nanowire (d) shows HRTEM image of two ultrathin Au nanowire showing distinct presence of 2H-HCP and FCC region in the nanostructure. Inset shows the inverse fast Fourier transform image of the region marked by yellow square.

Keywords:

Au nanostructure, 4H/2H-HCP Au, Nanowire

Reference:

Reference:

1. Q. Wang, et. Al. J. Mater. Chem. A, 2019, 7, 23812.
2. Q. Li, et. Al. J.Am.Chem.Soc.2018, 140, 15783−15790.
3. L. M. Lacroix et. Al. J. Am. Chem. Soc. 2014, 136, 13075-13077
4. Z. Fan. et. Al. Nat. Comm. 2015, 6, 7684.
5. Z. Fan. et. Al. Nat. Comm. 2020, 11, 3293.

Funding : Research supported by the Spanish MICIU (PID2019-104739GB-100/AEI/10.13039/501100011033), the Government of Aragon (DGA) through the project E13_23R and by the European Union's Horizon Europe research and innovation programme under the Marie Sklodowska-Curie grant agreement No 101109165.

1139

Studying nano-catalysts degradation with an identical location STEM approach

Dr. Francisco Ruiz Zepeda[1], Lazar Bijelić[1], Armin Hrnjić[1], Ana Rebeka Kamšek[1], Dr Andraž Pavlišič[1], Dr Marjan Bele[1], Dr Primož Jovanovič[1], Dr. Matija Gatalo[1], Dr Milutin Smiljanić[1], Prof. Nejc Hodnik[1]
[1]National Institute of Chemistry, Ljubljana, Slovenia

Poster Group 2

The local structure and morphology of a material is usually modified when submitted to an electro-catalytic process depending on the cycling and potential used. One way to learn more about the effects happening on the material is by using identical location, that is, examining a specific region of interest of the material before and after the electrochemical process takes place. In this work, we show different examples using identical location analytical scanning transmission electron microscopy (IL-STEM) to track specific changes of the material by observing before and after states. In this way, it is possible to study degradation mechanisms directly in the region of interest. Since some of the changes are occurring at the atomic level, understanding them can shed some light on the structural-properties relationship, including the metal support interaction. Most of the analyses shown in this work correspond to Pt-based nanoparticles typically employed in fuel cells and electrolysers that have been submitted to a particular electrochemical cycling protocol. The structural and morphological information gathered from the initial and after states suggests the occurrence of dissolution from specific atomic columns and atomic sites as well as redeposition for different columns and sites. These observations can lead to the conclusion that certain facets may be affected more than others, or in other cases, as it will be shown, to reveal how the support interacts with the catalysts. In this regard, the analysis of regions that suffered modifications can give us certain clues on how degradation started or evolved. Hence, the incorporation of advanced electron microscopy analytical techniques coupled with electro-chemistry experiments can provide crucial insights for a better catalyst design, including stability and durability.

Aknowledgements:
Authors would like to thank the European Research Council (ERC) Starting Grant 123STABLE (Grant agreement ID: 852208).

Keywords:

Nanoparticles, Catalysis, Identical location STEM,

1141

TEM structural analysis of photocatalytically active mesoporous single crystalline LaTiO2N particles

Dr. Mont. Jakub Zalesak[1], MSc. Jakob Praxmair[1], MSc. Julian Hörndl[1], Univ.-Prof. Simone Pokrant[1]
[1]Chemistry and Physics of Materials, University of Salzburg, Salzburg, Austria

Poster Group 2

Background incl. aims

Single crystalline mesoporous oxynitride particles have been studied as prospective catalysts in solar hydrogen-generating devices [1]. Both, photocatalytic and photoelectrochemical applications benefit from the high active surface area of catalytic particles in combination with good charge-transport properties [2]. A suitable combination of desired properties is achieved in the case of large mesoporous LaTiO2N single crystalline particles (up to 1 µm). The absence of grain boundaries reduces charge carrier recombination while at the same time their porosity results in increased surface area [3][4]. LaTiO2N mesoporous particles are obtained by transforming La2Ti2O7 particles in a thermal ammonolysis process. In this contribution, we focus on a structural description of pore formation and pore arrangement concerning the LaTiO2N orthorhombic lattice.

Methods

The photocatalytically active mesoporous single-crystalline LaTiO2N particles were synthesised via a thermal ammonolysis process La2Ti2O7 + 2 NH3 ⇌ 2 LaTiO2N + 3 H2O, T > 900 °C.
A dual beam microscope Thermo Fisher Scientific Helios 5 FX was used for SEM imaging (immersion mode, in-lens detector, 3 kV, 100 pA) and orientation-specific preparation of electron transparent samples. Chunks of mesoporous particles were lifted out and transferred onto a compustage holder. The thinning was performed at ion accelerating voltage ranging from 30 to 2 kV and beam current ranging from 2 nA to 25 pA. During the thinning process, the sample was aligned using α and β tilts of the compustage holder in combination with a pixilated 4D STEM detector.
TEM/STEM analyses were performed using a JEOL F200 cold FEG microscope operated at an accelerating voltage of 200 kV. For the STEM-EELS analyses, CEOS CEFID energy filter equipped with a Tvips XF 416 CMOS camera was used. Tomograms were obtained by performing tilt series with a step width of 2° from −54° to 78° in STEM HAADF mode. For tomography, a 200 mesh copper grid coated with a continuous carbon thin film (Plano GmbH) was used. The 3D reconstruction was carried out with ImageJ and the 3D representation with the Amira software (Thermo Fisher Scientific).

Results

The topotactic thermal ammonolysis process conserves the overall size of the particles while at the same time creating a network of both closed and opened pores. Closed volume porosity was estimated to 12% based on a STEM tomography reconstruction. The orientation and arrangement of the pores were compared to the orientation of the crystal. TEM images in combination with SAD patterns show long axes of the pores (ranging from 20-60 nm) oriented along the [001] and [010] directions of the orthorhombic LaTiO2N Imma structure (ICSD-168551). The EELS data was recorded over closed pores and the surrounding matrix. The nitrogen K-eddge (402 eV) shows a higher content of nitrogen in the closed pores. This suggests the presence of entrapped nitrogen gas in the mesoporous structure.

Conclusions

Micrometer-sized mesoporous LaTiO2N particles were prepared by an ammonolysis process from La2Ti2O7 particles. The structural arrangement of the pores was analysed using TEM and STEM

tomography techniques. The pores have their long axes oriented along the [001] and [010] lattice directions. The closed pores have a volume fraction of 12% and contain encapsulated nitrogen gas.

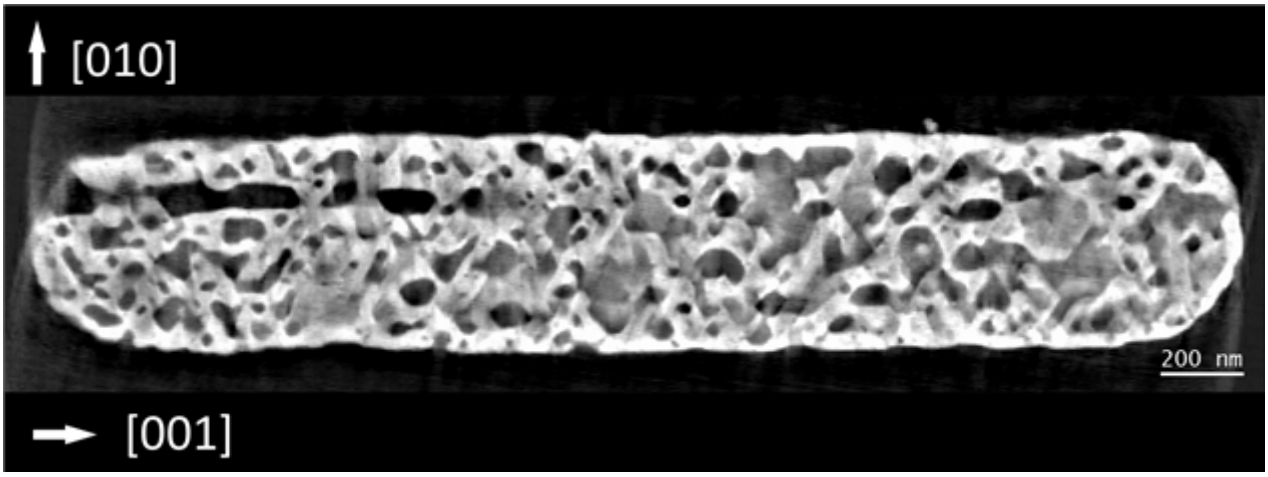

Keywords:

TEM, 2N, Mesoporous, Photocatalysis

Reference:

[1] A. E. Maegli, S. Pokrant, T. Hisatomi, M. Trottmann, K. Domen, and A. Weidenkaff, "Enhancement of photocatalytic water oxidation by the morphological control of LaTiO2N and cobalt oxide catalysts," Journal of Physical Chemistry C, vol. 118, no. 30, pp. 16344–16351, Jul. 2014, doi: 10.1021/JP4084162/SUPPL_FILE/JP4084162_SI_001.PDF.

[2] T. Hisatomi, J. Kubota, and K. Domen, "Recent advances in semiconductors for photocatalytic and photoelectrochemical water splitting," Chem Soc Rev, vol. 43, no. 22, pp. 7520–7535, Oct. 2014, doi: 10.1039/C3CS60378D.

[3] S. Pokrant, S. Dilger, and S. Landsmann, "Morphology and mesopores in photoelectrochemically active LaTiO2N single crystals," J Mater Res, vol. 31, no. 11, pp. 1574–1579, Jun. 2016, doi: 10.1557/JMR.2016.9.

[4] V. Werner, G. A. Zickler, and S. Pokrant, "Morphological design of LaTiO2N particles by topotactic growth mechanisms for photocatalytic applications," Progress in Solid State Chemistry, vol. 73, p. 100442, Mar. 2024, doi: 10.1016/J.PROGSOLIDSTCHEM.2024.100442

1228

Heterogeneous dissolution of Au nanoparticles under constant electrochemical potential as observed via in-situ liquid-cell TEM

Dr. Sorour Semsari Parapari[1], Layrton José Souza da Silva[1,2], Miguel Bernal[3], Daniel Torres[3], Dr. Miran Čeh[1,2], Dr. Kristina Žužek[1,2], Dr. Jon Ustarroz[3,4], Dr. Sašo Šturm[1,2]
[1]Jožef Stefan Institute, Department for Nanostructured Materials, Ljubljana, Slovenia, [2]Jožef Stefan International Postgraduate School, Ljubljana, Slovenia, [3]ChemSIN, Université libre de Bruxelles , Brussels, Belgium, [4]Electrochemical and Surface Engineering (SURF), Vrije Universiteit Brussel, Brussels, Belgium

Poster Group 1

Background incl. aims
Better synthesis control of nanostructured catalysts and their durability in electrochemical systems can be achieved by an in-depth understanding of the electrochemical deposition and dissolution processes. Electrodeposition and electrodissolution studies of nanomaterials are conventionally investigated over large specimen areas. The thermodynamics and kinetics of both NP nucleation and dissolution are affected by the specific surface interactions between NPs and substrate, which depend on the heterogeneous substrate's chemical, structural, and morphological properties. Although some high-sensitivity electrochemical techniques allow recording electrochemical signals of the growth or dissolution of single NPs, a direct visualization of these processes at high-spatial resolution can provide invaluable information on the underlying mechanisms. Recently developed liquid-cell transmission electron microscopy (LC-TEM) holders allow in-situ study of materials reactions on a nanoscale. Such specialized holders contain liquid cells that can withhold the liquid in a confined environment, allowing the imaging and spectroscopy of samples in the reaction media. Combining the capabilities of LC-TEM holders with micro-size electrodes printed on a chip enables us to study dynamic phenomena during electrochemical reactions. In this work, we have employed the LC-TEM to directly visualize the dynamic dissolution of electrodeposited gold nanoparticles (NPs) on an electrode and tap into the durability and stability of Au electrocatalysts. Combining the in-situ electrochemical LC-TEM, ex-situ nano-scale, and macro-scale measurements provided a unique perspective on the interaction between the metallic particles and the substrate during the electrochemical process [1,2].

Methods
The in-situ EC-LTEM experiments were performed using a JEOL JEM 2100 TEM at a 200 kV accelerating voltage in the bright-field mode. Experimental images and videos were recorded at the standard illumination conditions for real-time imaging with controlled electron beam damage effects. The electrochemical measurements in the TEM were carried out using a Protochips Poseidon 500 liquid holder, which allows observation of dynamic electrochemical processes in the liquid. The electrodeposition process of Au NPs was conducted from 1 mM HAuCl4 + 0.1 M NaCl solution in ultrapure deionized water. The electrochemical dissolution of these Au nanoparticles was observed under a constant applied potential during a potentiostatic regime at 1.5 V vs Pt pseudo reference.

Results
The in-situ electrochemical deposition of Au NPs from the HAuCl4 electrolyte resulted in fairly homogeneous particles of around 20 nm in size. The real-time observation of the dynamic electrochemical dissolution of these particles revealed that these Au NPs were dissolved heterogeneously and consecutively (one after another) during anodic polarization in a time span of more than 30 seconds. Moreover, it was shown that Au NPs form a core-shell structure, with the shells being more resistant to the dissolution process.

Conclusions

The unprecedented combination of in-situ electrochemical LC-TEM and the macro-scale experiments revealed important information from the electrochemical deposition and dissolution of supported metal NPs. This approach opens up new opportunities for the rational design of functional nanostructured materials for catalytic applications and for evaluating their durability under electrochemical polarization from the perspective of their resistance to electrochemical dissolution.

Keywords:

In-situ liquid-cell TEM, electrochemical dissolution

Reference:

1 Bernal, Miguel, et al. "A microscopic view on the electrochemical deposition and dissolution of Au with scanning electrochemical cell microscopy–Part I." Electrochimica Acta 445 (2023): 142023.
2 Bernal, Miguel, et al. "A microscopic view on the electrochemical deposition and dissolution of Au with scanning electrochemical cell microscopy–Part II: Potentiostatic dissolution and correlation with in-situ EC-TEM." Electrochimica Acta 492 (2024): 144302.
3 The authors acknowledge the support from the Fonds Wetenschappelijk Onderzoek in Vlaanderen (FWO, contract G0C3121N), and The Slovenian Research Agency through the national program P2-0084, the Z2-50057, J7-4636, and J2-4433 ARIS projects, and the ARRS-FWO bilateral project N1-0196.

1255

Observation of spontaneous fluctuations in product selectivity of the acetylene hydrogenation reaction in operando TEM

Dr. Christian Rohner[1], Mr Eugen Stotz[1], Dr. Alexander Steigert[2], Dr. Daniel Amkreutz[2], Prof. Dr. Rutger Schlatmann[2], Prof. Dr. Beatriz Roldan Cuenya[1], PD Dr Thomas Lunkenbein[1]
[1]Fritz Haber Institute of the Max Planck Society, Berlin, Germany, [2]Helmholtz-Zentrum Berlin für Materialien und Energie, Berlin, Germany

Poster Group 1

Background incl. aims
The selective hydrogenation of acetylene to ethylene is an important step in the purification of feed streams for the production of polyethylene.¹ A key finding from Teschner et al. describes the beneficial influence of subsurface C species on the selectivity of the reaction.² In that study, spontaneous fluctuations of the product selectivity were also observed under adiabatic conditions. The aim of our ongoing study is the detection of dynamic motifs and structural changes, which govern the occurrence of the fluctuations in the product selectivity. Specifically, we focus on the detection and elucidation of the role of transient and non-transient C species, as mediator for the catalytic performance.

Methods
In the framework of the CATLAB project, the development of thin film catalysts are conducted using existing preparation tools previously employed for thin film photovoltaics. Using a sputter deposition technique results in open networks of aggregated nanocrystals of the catalyst metals of interest, termed laterally condensed catalysts (LCCs). In this fashion, nominally 3nm thick Pd or Pd₆₀Au₄₀ alloy LCCs were deposited on DENS Solutions climate chips (SiNx windows). Using a home built gas-feeding station coupled to a quadrupole mass spectrometer, the reaction and product composition can be followed in real-time.³ Simultaneously, the structural parameters of the LCC are observed by TEM, electron diffraction (ED), and pair distribution function analysis of ED (ePDF).⁴

Results
To the best of our knowledge, the (semi)-hydrogenation of acetylene has not been observed in an operando TEM study prior to our experiments. A surprising result of our first experiment conducted at 150 °C was the observation of the aforementioned fluctuations in selectiviy and activity. and, second, that the product composition did not change, when the chip temperature was reduced to 20 °C (Figure 1). The observation of the fluctuations was confirmed by a second experiment conducted entirely at RT, while the absence of any product formation or fluctuations was confirmed in a blind experiment conducted with the empty operando cell. The high rate of conversion at RT exemplifies the exceptionally high activity of the LCC. However, this also indicates that catalyst material present in the non-heated and non-observable areas of the operando cell may have a significant contribution to the signal detected by the MS. Further, the results of supporting operando TEM experiments are discussed. These show the high potential of the ePDF method for operando measurements on nanocrystalline and amorphous catalysts in showing the formation/decomposition of the beta-PdH phase, and the measurement of crystalline domain growth, sintering and dewetting of the LCC.

Conclusion
In conclusion, the LCC seems to present itself as a highly promising platform for operando TEM, as its preparation is highly reproducible, the particle distribution very homogeneous, the metal layer very thin, and due to the high activity in the acetylene hydrogenation reaction, the product detection is

facile. So far, we could not detect structural changes that correlate with the fluctuations in the MS data. However, this raises the question about how local the origins of these effects are. Our future experiments aim to limit the sputter-deposited LCC to the heatable and observable region of the operando chip by using a specifically designed sputter mask.
Caption to Figure 1. Mass spectroscopy of the acetylene hydrogenation reaction showing spontaneous fluctuations observed in an operando TEM experiment. A Plot of the heater chip temperature and measured heater power (top), together with partial pressures of the relevant educts and products detected by QMS (bottom). B Calculated rel. selectivity (top) and activity (bottom) for the ethylene formation.

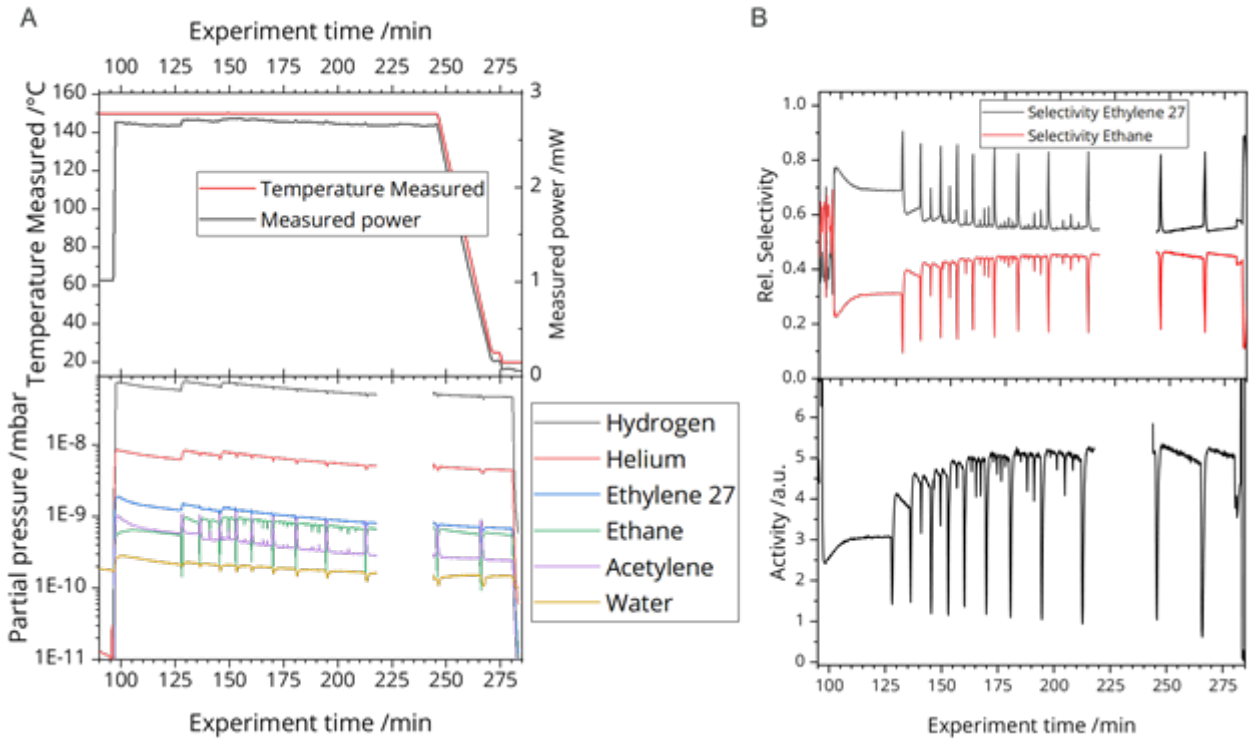

Keywords:

Operando, catalysis, ePDF, acetylene hydrogenation

Reference:

¹ A. Borodzinski, G.C. Bond Catalysis Reviews 2006, 48 (02), 91-144. (DOI: 10.1080/01614940500364909)
² D. Teschner et al. Science 2008, 320 (5872), 86-89. (DOI: 10.1126/science.1155200)
³ M. Plodinec et al. Microscopy and Microanalysis 2020, 26, 220–228. (DOI: 10.1017/S143192762000015X)
⁴ C. Rohner et al. Microscopy and Microanalysis 2023, 29, 1566–1578. (DOI: 10.1093/micmic/ozad087)

1259

Insights into the mechanisms of silver phase formation vial electrochemical liquid-cell TEM

Msc. Layrton José Souza Da Silva[1,2], Dr. Sorour Semsari Parapari[1], Monica Parpal Giménez[3], Mohammed El Marini[3], Prof. Dr. Jon Ustarroz[3,4], Prof. Dr. Sašo Šturm[1,2,5]
[1]Department for Nanostructured Materials, Jožef Stefan Institute, Ljubljana, Slovenia, [2]Jožef Stefan International Postgraduate School, Ljubljana, Slovenia, [3]ChemSIN – Chemistry of Surfaces, Interfaces and Nanomaterials, Université Libre de Bruxelles (ULB), , Brussels, Belgium, [4]SURF – Research Group Electrochemical and Surface Engineering, Vrije Universiteit Brussels, Brussels, Belgium, [5]Department of Geology, Faculty of Natural Sciences and Engineering, University of Ljubljana, Ljubljana, Slovenia

Poster Group 1

Background incl. aims

Understanding the mechanisms involved in nanoparticle formation, especially at the initial stages, is a significant challenge in materials science. The knowledge of early stages provides essential information regarding design strategies during nanomaterial synthesis1; silver is one such material of interest. This metal is significant for catalysis2 and sensing3 applications. Different silver nanoparticle synthesis strategies were investigated previously through chemical and electrochemical routes. However, there is a lack of comprehensive dynamic knowledge regarding the mechanisms of its reactions in solution. The control of essential parameters such as nanoparticle size, size distribution, and morphology will benefit from proper description and direct observation of nanoscale reactions. In-situ Liquid-Cell Transmission Electron Microscopy (LCTEM) is an experimental microscopy technique that allows observation of these nanoscale processes close to the native environment, directly in the liquid. Electrochemical reactions, in particular, can be studied and imaged using a miniaturized three-electrode electrochemical cell setup MEMS chip. Therefore, in this work, we are employing a correlative methodology for in-situ electrochemical LCTEM experiments to study the electrodeposition of silver nanoparticles.

Methods

The in-situ EC-LCTEM experiments were performed using a JEOL JEM 2100 TEM at a 200 kV accelerating voltage in parallel beam mode. The electrochemical measurements in the TEM were carried out using a Protochips Poseidon 500 liquid holder, which allows observation of dynamic electrochemical processes in the liquid. Cyclic voltammetry (CV) technique was used to obtain the characteristic curve for the electrolyte/electrode deposition system, potential window between -300 mV to 200 mV vs. Pt. A chronoamperometry (CA) experiment at -300 mV vs. Pt was carried out to study the growth of silver nanostructures in liquid. The electrolyte solution containing 2 mM AgNO3 + 50 mM KNO3 in ultrapure deionized water was used for the electrodeposition experiments. The electron beam dose was estimated to be below 1000 e-/A2·s.

Results

The in-situ LCTEM CV measurements pinpointed the peak potentials for nucleation of Silver onto the clean electrode measured at -150 mV vs Pt, and the potentials for reduction and oxidation of Ag, which were measured to be around -60 mV vs Pt and 70 mV vs. Pt. Due to this overpotential value, a potential of -300 mV vs. Pt was selected. The growth of small nuclei was recorded immediately after biasing started. The size of this first nuclei was around 6 nm. The growth rate of these particles was observed to be much higher at the beginning of the experiment due to the higher availability of electrolytes. As the electrolyte was not as available to the particle's growth, diffusion-limited growth of needle-like nanostructures extended from these nuclei shortly after.

Conclusion

The LCTEM technique is a powerful experimental method for probing dynamic chemical processes at the nanoscale. Electrochemical deposition, in particular, exhibits mechanisms that are still unclear and might follow non-classical phase transformation routes. This study allowed us to explain the mechanisms of silver nanostructure's electrochemical nucleation and growth.

Keywords:

In-situ TEM; Liquid-Cell TEM; Electrodeposition

Reference:

1 J. Ustarroz, Curr. Opin. Electrochem. 2020, 19, 144–152.

2 M. Vega-Cartagena, A. Rojas-Pérez, G. S. Colón-Quintana, D. A. Blasini Pérez, A. Peña-Duarte, E. Larios-Rodríguez, M. A. De Jesús, C. R. Cabrera, J. Electroanal. Chem. 2021, 891, 115242.

3 D. V. Yakimchuk, U. V. Prigodich, S. E. Demyanov, J. Ustarroz, H. Terryn, K. Baert, S. A. Khubezhov, D. I. Tishkevich, A. V. Trukhanov, V. Sivakov, E. Y. Kaniukov, Mater. Chem. Phys. 2022, 283, 126016.

1286

SEM and mCT investigations on GDEs with Copper-Nafion coating for carbon dioxide reduction to ethylene

Dr. rer. nat. Lisa Christine Ehle[1], M. Sc. Vera Ubbenjans[2], Dr. rer. nat. Adrian Mikitisin[1], Prof. Dr. rer. nat. Joachim Mayer[1], Dr. Rer. Nat. Lisa Christine Ehle
[1]Central facility for electron microscopy (GFE), RWTH Aachen University, Aachen, Germany,
[2]Chemical Engineering (AVT), RWTH Aachen University, Aachen, Germany

Poster Group 1

Background incl. aims
Replacing conventional high energy consuming chemical syntheses by a carbon-neutral route is in high demand for the future chemical industries. Especially the electrochemical synthesis of ethylene through the reduction of carbon dioxide instead of cracking intermediates of mineral oil at high temperatures allows sustainable value chains with a carbon circular economy [1]. Copper turned out to be the only pure metal that reduces carbon dioxide to products requiring more than two electrons transfers with substantial Faradaic efficiencies like hydrocarbons, aldehydes, and alcohols [2]. In order to prevent agglomeration of nanoparticles and improve adhesion to the substrate material, ionomers like Nafion (perfluorosulfonic acid, PFSA) are added to the ink. The combination of hydrophobic PTFE chains and terminal hydrophilic sulfonic acid groups promotes a homogeneous dispersion of the copper nanoparticles resulting in an overall high chemical activity and serves as a robust binder between the copper nanoparticles and the gas diffusion electrode [3]. However, any variations in the catalyst layers like thickness, porosity, inner network connectivity/tortuosity and conductivity has a significant impact on activity, selectivity and stability of the electrolysis. Therefore, knowledge of the 3-dimensional structure of the catalyst layer is essential for understanding the influence of chosen ink compositions and the resulting morphology of the catalyst layer on the performance of the electrode.
This work investigates the influence of different copper-to-Nafion ratios on the 3-dimensional morphology of the catalyst layer placed on a gas diffusion electrode. SEM panorama images and mCT measurements were used to characterize the homogeneity of the spray coating as well as the network connectivity and tortuosity of copper, Nafion and pores in the catalyst layer.

Methods
Gas diffusion electrodes (GDE) were spray coated with copper-Nafion inks with a loading of 0.5 mg/cm and a Cu:Nafion-ratio of 10 : 1 and 10 : 6, respectively.
SEM data were acquired on a ZEISS Gemini 300, equipped with the EDS detector UltimMax 65 by Oxford Instruments and the software SmartStitch, Version V01.02.13 by ZEISS for generating large panorama images.
Micro-computed tomography measurements (mCT) were acquired with a ZEISS Xradia Versa 620. X-ray voltage was 40 kV, X-ray current was 75.1 mA and the exposure time was 30 s. The field of view was 763.36 x 763.36 µm and the pixel size was 0.7649 µm. The number of total projections was 1201 with a full 360° tomography. The data evaluation was performed with the Dragonfly software, version 2022.2.0.1409 for Windows.

Results
According to the panorama images, the copper-Nafion ratio has a great influence on the morphology of the catalyst layer. Though the loading over the overall GDE is quite homogeneous for both ratios (not shown in this abstract), a higher Nafion content results in huge cracks of the catalyst layer. A higher Nafion content also seems to cause more agglomeration of the copper particles (see Figure 2) compared to the sample with minor Nafion. Additionally, the pore network is finer dispersed for

smaller Nafion contents as the Nafion tends to form a covering layer on the GDE (except for the cracks). A quantification of the copper, Nafion and pores based on the grey scale of the images results in 26% copper, 65% Nafion and 9% pores for a copper-Nafion ratio of 10:1 and in 21% copper, 71% Nafion and 8% pores for a copper-Nafion ratio of 10:6.
In Figure 3 are 3-dimensional mCT images of the samples, which look quite different to the BSE images concerning the homogenity of the catalyst layers. The sample with less Nafion content seems to have an inhomgeneous thickness of the catalyst coating.

Conclusion
The Nafion content significantly changes the morphology of the catalyst layer. Higher Nafion contents result in cracks of the catalyst layer, agglomeration of copper particles and a minor dispersed pores network.

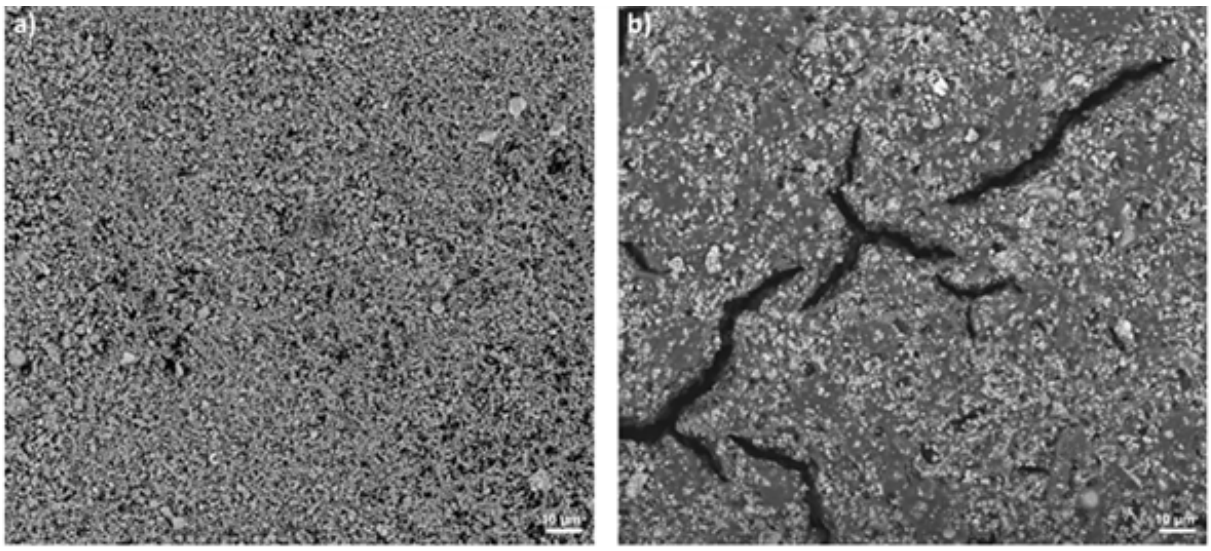

Figure 1: BSE panorama images at 10.000x magnification of a) Cu : Nafion = 10 : 1 and b) Cu : Nafion = 10 : 6.

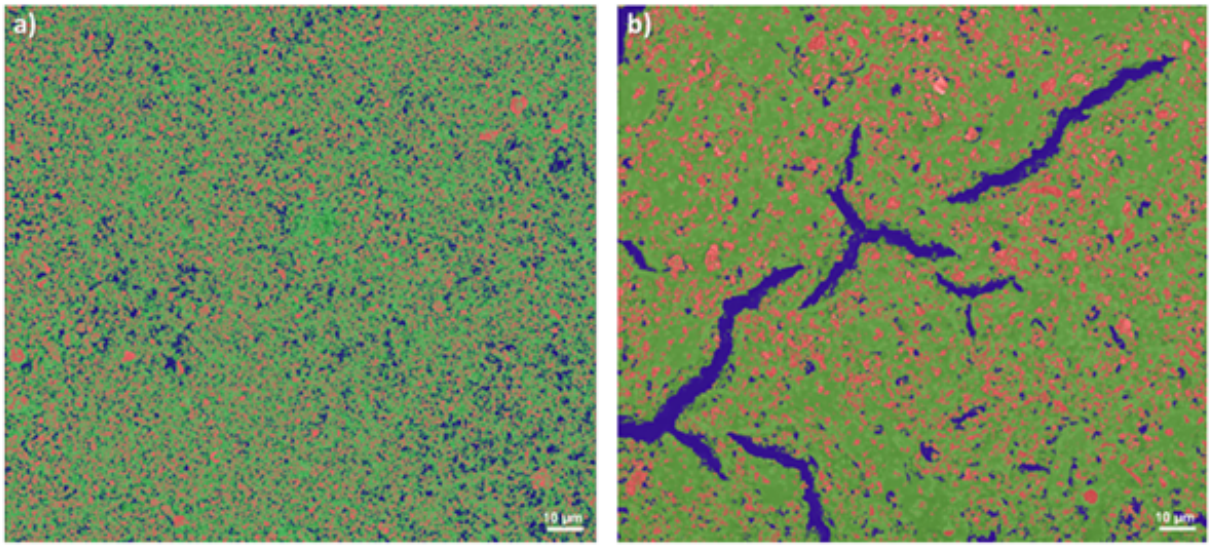

Figure 2: colored BSE panorama images with copper in red, nafion in green and pores (≙ shining through GDE), a) Cu : Nafion = 10 : 1 and b) Cu : Nafion = 10 : 6

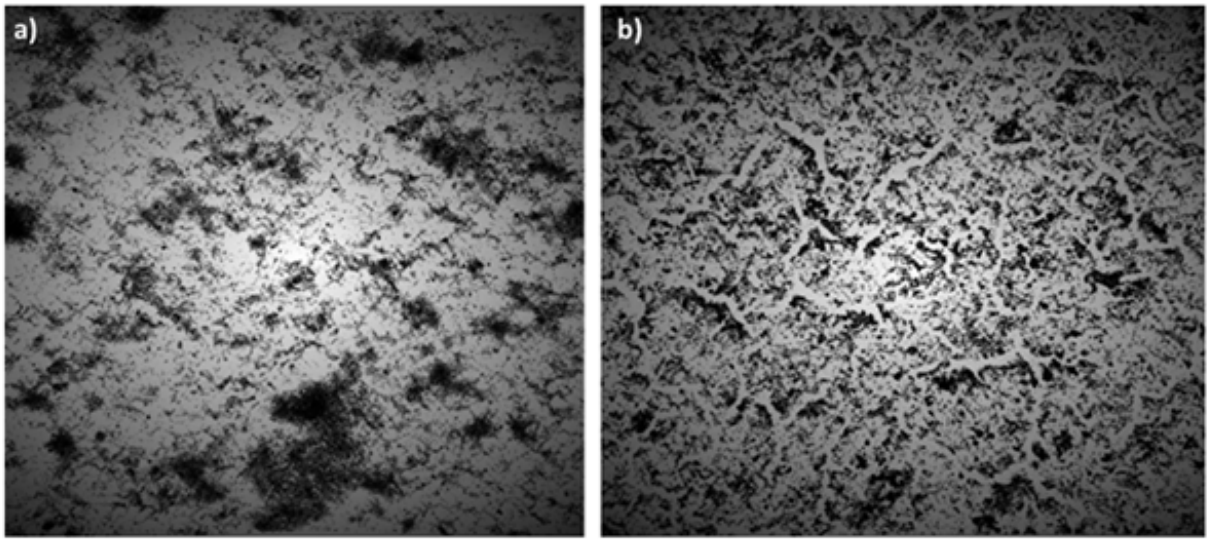

Figure 3: mCT images of sample a) Cu : Nafion = 10 : 1 and b) Cu : Nafion = 10 : 6

Keywords:

mCT, CO2 reduction to ethylene

Reference:

[1] doi: 10.1126/science.aav3506
[2] doi: 10.1021/acs.chemrev.8b00705
[3] doi: 10.1021/acscatal.2c05235

1291

3D Characterization of Pore Structures in Shaped Heterogeneous Catalysts Using FIB-SEM Tomography

Dr. Aram Yoon[1], Dr. Jaejin Kim[2], Dr. Xiaodan Chen[1]
[1]Shell Energy Transition Campus Amsterdam, Amsterdam, Netherlands, [2]Shell Technology Center Houston, Houston, USA

Poster Group 1

Background incl. aims
Heterogeneous catalysts are crucial for industrial chemical processes, with their efficiency relying heavily on physical and chemical properties across multiple scales. Scaling up the application of these catalysts necessitates a comprehensive understanding of their structures for multiscale design, particularly for industrial applications where powdered catalysts are typically pressed into shaped forms, like extrudates. These extrudates form porous medium where mass transport limitations predominantly govern the reactions kinetics, making the characterization of pore size and distribution critical.

Methods
Direct measurement of pore structures in shaped catalysts is challenging due to the local inhomogeneities and the large size of extrudates (several millimeters) compared to the nanoscale pores. Traditional transmission electron microscopy is inadequate due to its destructive sample preparation and thin sample requirement. To address these challenges, we employed a combination of focused ion beam and scanning electron microscope (FIB-SEM) tomography to achieve high-resolution imaging of the pore structures within catalyst extrudates. This approach enabled us to capture detailed images of pores ranging in size from 50 to 100 nanometers. Using Avizo software, we reconstructed the 3-dimensional microstructure of the catalysts, providing a comprehensive view of pore volumes and their connectivity.

Results
The application of FIB-SEM tomography, coupled with advanced 3D reconstruction, enabled accurate characterization of pore structures within the catalyst extrudates. Our results revealed intricate details of the pore distribution and connectivity, essential for understanding mass transport properties. The 3 dimensional images facilitated precise estimation of pore volumes, enhancing our ability to model and predict catalyst performance under various operational conditions.

Conclusion
This study highlights the importance of advanced imaging techniques in catalyst characterization. By accurately mapping the 3D pore structure, we gain a deeper understanding of the relationship between pore geometry and catalyst performance. These insights are crucial for optimizing catalyst design to ensure efficient mass transport and improved catalytic efficiency at larger scales.

Keywords:

Heterogeneous Catalysts, FIB-SEM, 3D Reconstruction

1307

Morphology-Driven Photothermal Efficiency in Nanostructured Semiconductors

Dr. Maibelin Rosales[1], Dr. Raynald Gauvin[2], Dr. Andreina García[3], Dr. Senentxu Lanceros-Méndez[1,4]
[1]BCMaterials, Basque Center for Materials, Applications and Nanostructures, Bilbao, Spain, [2]Mining and Materials Engineering Department, McGill University., Montreal, Canada, [3]Advanced Mining Technology Center (AMTC), Universidad de Chile, Santiago, Chile, [4]IKERBASQUE, Basque Foundation for Science, Bilbao, Spain

Poster Group 1

Nowadays, nanostructured semiconductor design represents outstanding model material systems for examining how the precise morphology manipulation at the nanoscale allows to fine-tuning their electronic structures to boost a plasmonic effect. Recent advances in designing metal-oxide semiconductor-based photocatalysts with photo-chemical/-thermal dual effects to photo-oxidize water contaminants and water-splitting reactions to produce hydrogen have garnered significant interest[1].

So far, in semiconductors, this dual functionality has often been achieved by doping or creating heterojunctions with external photothermal agents[2] such as carbon-based materials, conjugated polymers, and noble metal-based nanoparticles[3]. In this work, we have demonstrated that the precise morphological control of SnO_2 nanostructures promotes electronic structure changes in the material that impact its band structure and induce structural defects, such as oxygen vacancies, that enhance the density of free charge carriers enabling a plasmonic behavior tuning[4]. Under irradiation, this effect confers autarchic photo-thermal capability to the nanomaterial by generating hot carriers that produce local heating, which is then transferred to the surroundings. This increased temperature improves the mobility of photogenerated charge carriers of the semiconductor and molecular collisions in the medium, consequently boosting its photocatalytic efficiency[3].

This synergistic effect of photo-chemical and -thermal processes in a single system represents a novel approach to obtain high-performance photocatalysts. Herein, we focus on SnO_2 nanostructures, precisely engineered with varying morphologies such as nanoparticles, nanorods, nanosheets, and nanoflowers, synthesized via hydrothermal methods using structure-directing agents at different temperatures that allow for control of the shape. The microstructure, size, and morphology of these SnO_2 nanostructures were analyzed by a Thermo Fisher Scientific Tecnai F20 field-emission (scanning) transmission electron microscope (FEG-S/TEM) operated at 200 kV and a Hitachi High-Technologies SU-8000 and SU-8230 field emission scanning electron microscope (FE-SEM) operated at low voltage. Demonstrating the precise control of synthesis parameters enabled the achievement of desired morphologies with different structural dimensionalities from zero-dimensional nanoparticles to three-dimensional nanoflowers.

Optical and electronic properties were investigated using diffuse reflectance (DRS) and photoluminescence (PL) spectroscopies. The optical band gap energies (Ebg) were determined using Tauc's plots, and the obtained Ebg values exhibited a nanomaterial shape-dependent response. PL analysis was to assess the nature of structural defects and how they can affect their electronic band structure by tailoring the morphology. The strong emission peaks observed in the PL spectra were linked to surface and structural defects such as tin interstitials, dangling bonds, and oxygen vacancies (OV), which can introduce localized energy levels within the bandgap, affecting their electronic band structure[4].

Tailoring morphology together with the obtained confinement effect at the nanoscale allowed not only the fine-tuning of the electronic structure of synthesized SnO_2 nanostructures but also control over localized surface plasmon resonance (LSPR), critical for generating high-energy hot carriers and enhancing photothermal conversion[2]. Under blue laser irradiation, the temperature changes in an aqueous medium were evaluated for all nanostructures. Notably, flower-like SnO_2 displayed an increased temperature by up to 14.5°C, attributed to the enhanced local electric field at tips, edges, and corners present in this kind of shape. In parallel, the temperature gradient enhanced the charge carrier transfer, boosting higher reactive oxygen species (ROS) generation, such as hydroxyl radical, which in turn accelerates the photo-oxidation rate[5]. Moreover, under UVA-Vis irradiation, the nanomaterials exhibited remarkable light harvesting and light-to-heat conversion capabilities that significantly enhanced the photocatalytic performance for water pollutant removal and green hydrogen production through a synergistic photo-chemical/thermal effect.

On the other hand, the morphology variation studied through FESEM and HRTEM provided insights into the crystal growth mechanism based on the structural dimensionality of these nanomaterials, ranging from zero- to three-dimension. Furthermore, a potential mechanism as photo-thermo-catalyzers was also proposed. This work and the corresponding findings pave the way for the precise design of nanostructured materials with tailored morphologies for enhanced photocatalytic and photothermal applications, particularly in environmental remediation and sustainable energy production.

Acknowledgements
This study forms part of the Advanced Materials program and was supported by MCIN with funding from European Union NextGenerationEU (PRTR-C17.I1). M.R.V. acknowledges support from the European Union's Horizon Europe research and innovation programme under the Marie Skłodowska-Curie MERLIN (101110470). A.G. thanks National Fund for Scientific and Technological Development (FONDECYT REGULAR 1220088)

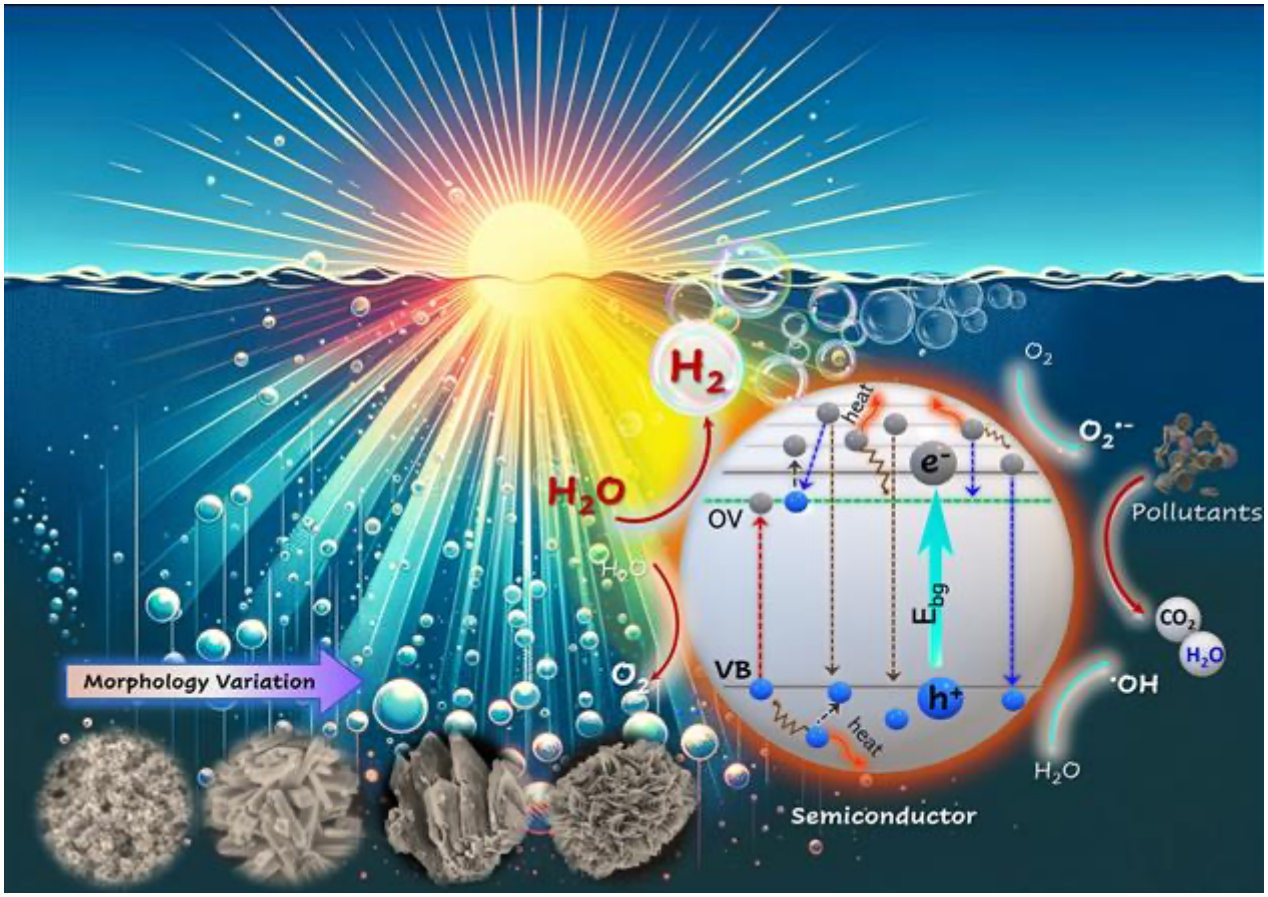

Keywords:

Nanomaterials, morphology, semiconductors, photothermal, photocatalysis

Reference:

1. D. Wang, R. Chen, X. Zhu, et al., Synergetic Photo-Thermo Catalytic Hydrogen Production by Carbon Materials, J Phys Chem Lett, 13 (2022) 1602-1608.
2. N. Zhang, Y. Xiong, Plasmonic semiconductors for advanced artificial photosynthesis, Advanced Sensor and Energy Materials, 2 (2023).
3. X. Cui, Q. Ruan, X. Zhuo, et al., Photothermal Nanomaterials: A Powerful Light-to-Heat Converter, Chem Rev, 123 (2023) 6891-6952.
4. S. Kumar, M. Sharma, R.N. Aljawfi, et al., Tailoring the structural, electronic structure and optical properties of Fe: SnO2 nanoparticles, Journal of Electron Spectroscopy and Related Phenomena, 240 (2020).
5. M. Rosales, T. Zoltan, C. Yadarola, et al., The influence of the morphology of 1D TiO2 nanostructures on photogeneration of reactive oxygen species and enhanced photocatalytic activity, Journal of Molecular Liquids, 281 (2019) 59-69.

1340

Catalytically active MoS2 support for hydrogen generation from seawater

Soohyun Kwon[1], Doctor Ji-Hyung Han[2], Assistant professor Joohyun Lim[1]
[1]Department of Chemistry, Kangwon National University, Chuncheon, Republic of Korea, [2]Jeju Global Research Center, Korea Institute of Energy Research, Jeju, Republic of Korea

Poster Group 1

1. Background incl. aims
Electrocatalytic water splitting is an environmentally sustainable method to produce clean hydrogen but generally demands expensive high-purity water. Thus, direct seawater electrolysis can be attractive, yet it has serious challenges, such as inorganic precipitation and chlorine corrosion, which reduce electrocatalytic activity. Seawater acidification using a bipolar membrane (BPM) has been proposed as a promising approach to mitigate these problems.[1] Meanwhile, Pt is the most active electrocatalyst for the hydrogen evolution reaction (HER), but its high cost limits its use. Therefore, two-dimensional MoS2 has emerged as a potential non-precious metal catalyst. Hybrid electrocatalysts, specifically Pt nanoparticles anchored on MoS2 nanosheets, have also been studied to achieve the required HER activity. However, it has not yet been studied under seawater conditions. Here, we investigate MoS2 nanosheets as a catalytic support in Pt/MoS2/carbon cloth (Pt/MoS2/CC) cathode, focusing on the structure and HER performance under a BPM-based seawater electrolysis system, compared with Pt/CC and MoS2/CC.

2. Methods
2.1. Synthesis of Pt/MoS2/CC
Pt/MoS2/CC was synthesized via the hydrothermal method followed by the sintering under N2 gas.
2.2. Physical and chemical characterization
Field-emission scanning electron microscopy (FE-SEM) was used to examine the morphology of the samples. Field-emission transmission electron microscopy (FE-TEM) was conducted to analyze the morphology and crystal structure of the samples. Energy-dispersive X-ray spectroscopy (EDS) was performed to check the chemical composition of the samples in SEM and TEM. X-ray diffraction (XRD) analysis was applied to determine the crystal structure of the samples. X-ray photoelectron spectroscopy (XPS) was employed to investigate the bond between Pt nanoparticles and MoS2 nanosheets with Pt and Mo oxidation states.
2.3. Electrochemical characterization
Electrochemical measurements were performed using a potentiostat. Linear sweep voltammetry (LSV) was conducted on a three-electrode system in acidic conditions. Chronopotentiometry (CP) was conducted on the BPM-based seawater electrolyzer in simulated seawater.

3. Results
SEM images of Pt/MoS2/CC showed that carbon cloth was entirely covered with dense MoS2 nanosheets, and Pt nanoparticles were attached to MoS2 nanosheets. In addition, Pt nanoparticles were not uniform. XRD patterns confirmed that the crystal structure of MoS2 was maintained after the sintering at 400/450 °C. During HER under a BPM-based seawater electrolysis system, Pt/MoS2/CC cathode showed lower overpotential and higher stability than Pt/CC.

4. Conclusion
Based on the result, MoS2 nanosheets are anticipated to enhance the anchoring strength of Pt nanoparticles, provide additional active sites, and compel the formation of inorganic precipitates, thereby contributing to stable catalytic activity. More details about the structural interaction

between MoS2 nanosheets and Pt nanoparticles, as well as the electrode characteristics of MoS2 in seawater, will be discussed.

Keywords:

Seawater electrolysis, HER, Pt, MoS2

Reference:

[1] J. H. Han, E. Jwa, H. Lee, E. J. Kim, J. Y. Nam, K. S. Hwang, N. Jeong, J. Choi, H. Kim, Y. C. Jeung, T. D. Chung, Chem. Eng. J. 2022, 429, 132383